

UNIVERSITY OF NAPLES FEDERICO II

DEPARTMENT OF STRUCTURES FOR ENGINEERING AND
ARCHITECTURE

PH.D. PROGRAMME IN

STRUCTURAL, GEOTECHNICAL AND SEISMIC ENGINEERING

COORDINATOR PROF. LUCIANO ROSATI

XXIX CYCLE



Romeo Tomeo

Ph.D. THESIS

**SOIL-STRUCTURE INTERACTION EFFECTS ON THE
SEISMIC BEHAVIOUR OF REINFORCED CONCRETE
STRUCTURES**

TUTORS

Prof. Emidio NIGRO
Dr. Antonio BILOTTA

2017

Acknowledgments

Now, at the end of this path, looking back I realize there are many people to whom I must devote a sincere thanks.

Firstly, my tutors: Prof. Emidio Nigro and Dr. Antonio Bilotta, who gave me the opportunity to start this PhD and that always gave me good advices for my research, as well as the possibility of undertaking an experience abroad that has been extremely educational for me and that I will always carry in my heart.

Secondly, I thank all the people I met during my journey at Aristotle University of Thessaloniki.

The professor Dimitris Pitilakis, which allowed me to make great strides in my research activity; Sotiria and Anna, who provided me with essential assistance in learning to use a tough software as OpenSees; Thanos, Stella, Dimitris and all the other guys of the geotechnical section of the department of civil engineering, as well as Alexandra, Nikos and all the other friends I met in Thessaloniki, that made me feel like at home.

I also say thanks to all the colleagues I met during these three years at the Department of Structures for Engineering and Architecture of Naples, with whom I shared my days and some very funny moments.

I say thanks, of course, to my family and to the friends of a lifetime, that are a constant reference point for me.

But most of all, I must say thanks to Donatella, that shared with me all the good and bad moments of the last three years, always giving me her loving support and her attentions. This thesis is dedicated to her.

Romeo Tomeo

Index

List of Figures	I
List of Tables.....	i
1 Introduction	1
1.1 Statement of the problem.....	1
1.2 Literature Review	3
1.3 Scope and objectives of the research.....	20
1.4 Outline of the Thesis.....	22
2 Simplified approaches for evaluating SSI effects on RC structures	23
2.1 Implementation of SSI in American Standards and Guidelines	23
2.1.1 Force Based Procedures	25
2.1.2 Displacement Based Procedures	31
2.1.3 Response Time-History Procedures	34
2.2 Linear Modal Analyses for different RC structures	36
2.2.1 Regular Frame Buildings.....	39
2.2.2 In plane irregular buildings	44
2.2.3 In plane highly irregular buildings.....	45
2.2.4 In elevation irregular buildings	47
2.2.5 Effect of concrete cracking	48
2.2.6 Effect of single footings.....	49
2.3 Non Linear Static Analyses for existing buildings.....	50
2.4 Concluding remarks.....	61
3 Numerical Modelling for Dynamic Analyses	63
3.1 Structural modelling.....	64
3.2 SSI modelling: sub-structures approaches.....	69
3.2.1 Foundations Impedances	71
3.2.2 Beam on Non Linear Winkler Foundation Model	77
3.3 SSI modelling: direct approaches	84
3.3.1 Complete FEM model.....	86

4	Parametric Analyses for the evaluation of SSI effects on Reinforced Concrete Moment Resisting Frames	93
4.1	Reference Structures	94
4.1.1	<i>Buildings designed according to the D.M. 30/05/1972.....</i>	<i>95</i>
4.1.2	<i>Buildings designed according to the D.M. 14/01/2008.....</i>	<i>100</i>
4.2	Soil Classes	105
4.3	Selection of the accelerograms.....	107
4.4	Analyses	110
4.5	Results.....	113
4.5.1	<i>4 Floors Pre-Code building</i>	<i>113</i>
4.5.2	<i>4 Floors Code compliant building.....</i>	<i>120</i>
4.5.3	<i>8 Floors Pre-Code building</i>	<i>123</i>
4.5.4	<i>8 Floors Code compliant building.....</i>	<i>127</i>
4.5.5	<i>Effects of SSI modelling on the estimation of the seismic demand ..</i>	<i>132</i>
4.6	Retrofitting interventions by means of shear walls	140
4.7	Concluding remarks	145
5	Conclusions	155
5.1	Introduction	155
5.2	Main Findings	156
5.3	Limitations and suggestions for future works.....	158
5.4	Suggestions for implementation in seismic design codes.....	159
	References	161
	Annex A	172
	Foundations Impedances	172
	Annex B	177
	Ground Motions.....	177
	Annex C	189
	Parametric Analyses Results	189

List of Figures

Figure 1.1 - Simplified system for inertial interaction problems suggested in <i>Veletsos & Meek</i> (1974).....	4
Figure 1.2 - Foundation stiffness and damping factors for elastic and viscoelastic half-spaces, $\nu = 0.4$ (<i>Veletsos & Verbic</i> , 1973).....	7
Figure 2.1 - Schematic illustration of the shape of the design response spectrum in the NEHRP Recommended Provisions (from NIST GCR 12-917-21)	26
Figure 2.2 - Foundation damping factor (FEMA 2009, ASCE 2010)	29
Figure 2.3 - Schematic illustration of a pushover analysis and development of a pushover curve for a structure with a flexible base (from NIST GCR 12-917-21) ..	31
Figure 2.4 - Ratios of Response Spectra for base slab averaging using the semi-empirical formulations adopted in FEMA 440 (2005)	33
Figure 2.5 - Schematic illustration of a tall building with subterranean levels: (a) complete system; (b) simplified model for service-level earthquake intensity; and (c) simplified foundation model for maximum considered earthquake intensity (from NIST GCR 12-917-21).....	35
Figure 2.6 - Regular frame buildings.....	37
Figure 2.7 - In plane irregular buildings.....	37
Figure 2.8 - In plane highly irregular buildings.....	38
Figure 2.9 - In elevation irregular buildings.....	38
Figure 2.10 - Results for Regular Frame Buildings.....	43
Figure 2.11 - Results for in plan irregular buildings	44
Figure 2.12 - Results for in plan highly irregular buildings	46
Figure 2.13 - Results for in elevation irregular buildings.....	47
Figure 2.14 - Regular buildings: effect of concrete cracking	49
Figure 2.15 - Regular buildings: single footings	50
Figure 2.16 - Reference buildings: a) 4 Floors building, b) 8 Floors building, c) Plan Dimensions.....	51
Figure 2.17 - Existing buildings	54
Figure 2.18 - Capacity Spectrum Method	56
Figure 2.19 - N2 Method	56
Figure 2.20 - Capacity Spectrum Method: Results.....	59
Figure 2.21 - N2 Method: Results	60
Figure 2.22 - Influence of foundation motions on capacity curve.....	61
Figure 3.1 - BeamWithHinges element in OpenSees	65

Figure 3.2 - Fiber sections definition in OpenSees.....	65
Figure 3.3 - Material objects adopted in OpenSees for the representation of the uniaxial stress-strain relationships of the concrete cover and core (left) and for the reinforcement steel (right)	66
Figure 3.4 - Modelling of shear failures (re-adapted from <i>Elwood, 2004</i>).....	68
Figure 3.5 - Substructure approach for the evaluation of SSI effects (<i>Stewart et al., 1998</i>).....	70
Figure 3.6 - Dynamic stiffness modifiers and damping ratios versus dimensionless frequency, for rectangular footings resting on the surface of a homogeneous half-space, with zero hysteretic damping and $\nu = 0.33$: (a) geometry; (b) x-direction; and (c) y-direction (from NIST GCR 12-917-2)	75
Figure 3.7 - Dynamic stiffness modifiers and damping ratios versus dimensionless frequency, for square footings embedded in a homogeneous half-space, with zero hysteretic damping, and $\nu = 0.33$: (a) geometry; and (b) x-direction (y-direction similar) (from NIST GCR 12-917-2)	76
Figure 3.8 - Parallel Material in OpenSees (<i>Mazzoni et al, 2009</i>).....	77
Figure 3.9 - Beam-on-Nonlinear Winkler Foundation (BNWF) model: (a) hypothesized foundation-superstructure system; (b) idealized model; and (c) variable vertical stiffness distribution (<i>Raychowdhury and Hutchinson, 2009</i>)	79
Figure 3.10 - Cyclic response of OpenSees BNWF springs subjected to a sinusoidal displacement: (a) q-z spring (<i>Qzsimple2</i> material model); (b) p-x spring (<i>Pxsimple1</i> material model); and (c) t-x spring (<i>Txsimple1</i> material model) (<i>Raychowdhury and Hutchinson, 2009</i>)	80
Figure 3.11 - Vertical spring distribution used to reproduce total rotational stiffness k_{yy}	82
Figure 3.12 - Schematic illustration of a direct analysis of soil-structure interaction using continuum modelling by finite elements (by NIST CGR 12-917-21)	85
Figure 3.13 - Complete FEM model implemented in OpenSees	87
Figure 3.14 - Rayleigh proportional damping for linear soil profile	88
Figure 3.15 - Hysteretic soil damping definition for elastic soil elements	90
Figure 3.16 - Hyperbolic backbone curve for soil nonlinear shear stress-strain response and piecewise-linear representation in multi-surface plasticity (after <i>Prevost, 1985; Stewart et al., 2008; Parra, 1996</i>).....	91
Figure 4.1 - Plan view of the reference structures	94
Figure 4.2 - 4 Floors Pre-Code building.....	98
Figure 4.3 - 8 Floors Pre-Code building.....	99
Figure 4.4 - Reference spectrum for the design.....	100
Figure 4.5 - 4 Floors Code compliant building	103
Figure 4.6 - 8 Floors Code compliant building	104
Figure 4.7 - Group 1 – Compatibility with the EC8 type 1 spectrum.....	109
Figure 4.8 - Group 2 – Compatibility with the EC8 type 2 spectrum.....	109
Figure 4.9 - Group 3 – Compatibility with the NTC 08 spectrum	109

Figure 4.10 - Complete FEM model: soil grid dimensions for a) 4 floors buildings and b) 8 floors buildings	111
Figure 4.11 - Reference schemes for dynamic analyses.....	112
Figure 4.12 - 4 Floors Pre-Code building – Comparison between Fixed Base Model and Complete FEM model – Group 3 Records	114
Figure 4.13 - Influence of SSI on safety checks at a) Damage Limit State (DLS) and b) Collapse Limit State (CLS)	115
Figure 4.14 - 4 Floors Pre-Code building – Comparison between Fixed Base Model and BNWF model - Group 3 Records	116
Figure 4.15 - 4 Floors Pre-Code building – Comparison between Complete FEM model and BNWF model (average results on 21 signals)	118
Figure 4.16 - 4 Floors Pre-Code building: comparison between Fixed Base Model, Complete FEM model and BNWF model (trend lines).....	119
Figure 4.17 - 4 Floors Code compliant building – Comparison between Fixed Base Model and Complete FEM model – Group 3 Records.....	120
Figure 4.18 - 4 Floors Code compliant building – Comparison between Fixed Base Model and BNWF model - Group 3 Records.....	121
Figure 4.19 - 4 Floors Code compliant building – Comparison between Complete FEM model and BNWF model (average results on 21 signals)	122
Figure 4.20 - 4 Floors Code compliant building: comparison between Fixed Base Model, Complete FEM model and BNWF model (trend lines)	123
Figure 4.21 - 8 Floors Pre-Code building – Comparison between Fixed Base Model and Complete FEM model – Group 3 Records	124
Figure 4.22 - 8 Floors Pre-Code building – Comparison between Fixed Base Model and BNWF model - Group 3 Records	125
Figure 4.23 - 8 Floors Pre-Code building – Comparison between Complete FEM model and BNWF model (average results on 21 signals)	126
Figure 4.24 - 8 Floors Pre-Code building: comparison between Fixed Base Model, Complete FEM model and BNWF model (trend lines).....	127
Figure 4.25 - 8 Floors Code compliant building – Comparison between Fixed Base Model and Complete FEM model – Group 3 Records.....	128
Figure 4.26 - 8 Floors Code compliant building – Soil Type C – Comparison between Fixed Base Model and BNWF model	129
Figure 4.27 - 8 Floors Code compliant building - Comparison between Complete FEM model and BNWF model (average results on 21 signals)	130
Figure 4.28 - 8 Floors Code compliant building - Comparison between Fixed Base Model, Complete FEM model and BNWF model (trend lines)	131
Figure 4.29 - Top acceleration: time history and Fourier Spectrum.....	132
Figure 4.30 – Comparison between free-field motion (FFM) and foundation input motion (FIM).....	134
Figure 4.31 - 4 Floors Pre-Code building: Influence of non-linear soil behaviour modelling.....	135

Figure 4.32 – Soil shear behaviour for “equivalent” linear soil and non-linear soil: soil Type D (soft clay), Group1 - Ground Motion 1, PGA=0.10g	136
Figure 4.34 - BNWF model: influence of P-x springs.....	139
Figure 4.35 - Dual system frame-wall	140
Figure 4.36 - 4 Floors Pre-Code building: retrofitting intervention by means of a shear wall – Comparison between Fixed Base Model and Complete FEM model.....	141
Figure 4.37 - 4 Floors Pre-Code building: retrofitting intervention by means of a shear wall – Comparison between Fixed Base Model and Spring model.....	142
Figure 4.38 - Top acceleration for Fixed Base model and Complete FEM model (linear analysis).....	143
Figure 4.39 - Transfer functions for Fixed Base model and Complete FEM model ...	143
Figure 4.40 - SSI effect for a dual system frame-wall.....	144
Figure 4.41 - Influence of modelling technique on SSI effects	147
Figure 4.42 - Influence of seismic design criteria on SSI effects	148
Figure 4.43 - 4 Floors Pre-Code building: shear behaviour at the floor of maximum IDR	149
Figure 4.44 - 4 Floors Code compliant building: shear behaviour at the floor of maximum IDR.....	150
Figure 4.45 - Influence of structure fundamental period on SSI effects.....	151
Figure 4.46 - Influence of soil type on SSI effects	152
Figure 4.47 - Influence of the selected record on the SSI effects.....	153

Annex B

Figure B. 1 - Group 1 – GM1: Montenegro 15/04/1979	178
Figure B. 2 - Group 1 – GM2: Montenegro (aftershock) 24/05/1979	178
Figure B. 3 - Group 1 – GM3: Campano Lucano 23/11/1980.....	179
Figure B. 4 - Group 1 – GM4: Campano Lucano 23/11/1980.....	179
Figure B. 5 - Group 1 – GM5: South Iceland (aftershock) 21/06/2000.....	180
Figure B. 6 - Group 1 – GM6: South Iceland (aftershock) 21/06/2000.....	180
Figure B. 7 - Group 1 – GM7: South Iceland (aftershock) 21/06/2000.....	181
Figure B. 8 - Group 2 – GM1: Friuli 06/05/1976.....	181
Figure B. 9 - Group 2 – GM2: Friuli (aftershock) 15/09/1976.....	182
Figure B. 10 - Group 2 – GM3: Friuli (aftershock) 15/09/1976.....	182
Figure B. 11 - Group 2 – GM4: Golbasi 05/05/1986	183
Figure B. 12 - Group 2 – GM5: Kozani 13/05/1995	183
Figure B. 13 - Group 2 – GM6: South Iceland 17/06/2000.....	184
Figure B. 14 - Group 2 – GM7: South Iceland (aftershock) 21/06/2000.....	184
Figure B. 15 - Group 3 – GM1: Friuli Earthquake 4th shock 15/09/1976	185
Figure B. 16 - Group 3 – GM2: Friuli Earthquake 4th shock 15/09/1976	185
Figure B. 17 - Group 3 – GM3: Ferruzzano 11/03/1978.....	186
Figure B. 18 - Group 3 – GM4: Irpinia Earthquake 23/11/1980	186
Figure B. 19 - Group 3 – GM5: Irpinia Earthquake 23/11/1980	187
Figure B. 20 - Group 3 – GM6: Val Comino Earthquake 07/05/1984	187

Figure B. 21 - Group 3 – GM7: L'Aquila Mainshock 06/04/2009188

Annex C

Figure C. 1 - 4 Floors Pre-Code – Soil Type C – Fixed Base VS Complete FEM.....190

Figure C. 2 - 4 Floors Pre-Code – Soil Type C – Fixed Base VS BNWF.....191

Figure C. 3 - 4 Floors Pre-Code – Soil Type D – Fixed Base VS Complete FEM192

Figure C. 4 - 4 Floors Pre-Code – Soil Type D – Fixed Base VS BNWF.....193

Figure C. 5 - 4 Floors Code compliant – Soil Type C – Fixed Base VS Complete FEM
.....194

Figure C. 6 - 4 Floors Code compliant – Soil Type C – Fixed Base VS BNWF195

Figure C. 7 - 4 Floors Code compliant – Soil Type D – Fixed Base VS Complete FEM
.....196

Figure C. 8 - 4 Floors Code compliant – Soil Type D – Fixed Base VS BNWF197

Figure C. 9 - 8 Floors Pre-Code – Soil Type C – Fixed Base VS Complete FEM.....198

Figure C. 10 - 8 Floors Pre-Code – Soil Type C – Fixed Base VS BNWF.....199

Figure C. 11 - 8 Floors Pre-Code – Soil Type D – Fixed Base VS Complete FEM ...200

Figure C. 12 - 8 Floors Pre-Code Soil Type D – Fixed Base VS BNWF.....201

Figure C. 13 - 8 Floors Code compliant – Soil Type C – Fixed Base VS Complete
FEM.....202

Figure C. 14 - 8 Floors Code compliant – Soil Type C – Fixed Base VS BNWF203

Figure C. 15 - 8 Floors Code compliant – Soil Type D – Fixed Base VS Complete
FEM.....204

Figure C. 16 - 8 Floors Code compliant – Soil Type D – Fixed Base VS BNWF205

List of Tables

Table 2.1 - Reduction coefficients for shear modulus and shear wave velocity (FEMA 440, 2005).....	28
Table 2.2 - Regular building – Soil Type C – Vibration periods	43
Table 2.3 - Regular building – Soil Type C – Overall Damping.....	43
Table 2.4 - Regular frame buildings: SSI effect on superior modes (soil class C).....	44
Table 2.5 - In plan irregular buildings: SSI effect on superior modes (soil class C)....	45
Table 2.6 - In plan highly irregular buildings: SSI effect on superior modes (soil class C).....	46
Table 2.7 - In elevation irregular buildings: SSI effect on superior modes (soil class C)	48
Table 2.8 - 4 Floors building: structural members	52
Table 2.9 - 8 Floors building: structural members	53
Table 2.10 - Capacity Spectrum Method: Results	59
Table 2.11 - N2 Method – Results.....	60
Table 3.1 - Values of Shear Wave Velocity Reduction factor (FEMA 440, 2005).....	73
Table 4.1 - Reference Structures	95
Table 4.2 - 4 Floors Pre-Code building: columns dimensions	97
Table 4.3 - 8 Floors Pre-Code building: columns dimensions	97
Table 4.4 - Code compliant buildings - Parameter values for material object “Concrete01” in OpenSees.....	102
Table 4.5 - 4 Floors Code compliant building: columns dimensions	105
Table 4.6 - 8 Floors Code compliant building: columns dimensions	105
Table 4.7 - Soil properties	106
Table 4.8 - Values of the soil-structure relative stiffness ($\sigma = V_s T_{\text{fix}} / h$).....	106
Table 4.9 - Group 1: seven accelerograms from the European Strong Motion Database compatibles with the Type 1 spectrum proposed by Eurocode 8	108
Table 4.10 - Group 2: seven accelerograms from the European Strong Motion Database compatibles with the Type 2 spectrum proposed by Eurocode 8	108
Table 4.11 - Group 3: Seven accelerograms from the Italian Accelerometric Archive compatibles with the spectrum proposed by NTC 08	108
Table 4.12 - Soil shear modulus reduction coefficients for the “equivalent” linear soil model and for the non-linear soil model (Ground Motion 1, Group1).....	137

Annex A

Table A. 1 - Elastic Solutions for Static Stiffness of Rigid Footings at the Ground Surface (NIST GCR 12-917-21)	173
Table A. 2 - Embedment Correction Factors for Static Stiffness of Rigid Footings (NIST GCR 12-917-2).....	174
Table A. 3 - Dynamic Stiffness Modifiers and Radiation Damping Ratios for Rigid Footings (NIST GCR 12-917-2).....	175
Table A. 4 - Dynamic Stiffness Modifiers and Radiation Damping Ratios for Embedded Footings (NIST GCR 12-917-2).....	176

1 Introduction

1.1 Statement of the problem

The deformations of a structure during earthquake shaking are affected by interactions between three linked systems: the structure, the foundation, and the soil underlying and surrounding the foundation.

A seismic Soil-Structure Interaction (SSI) analysis evaluates the collective response of these systems to a specified free field ground motion.

Two physical phenomena comprise the mechanisms of interaction between the structure, foundation, and soil (*Stewart et al., 1998*).

The first is known as *Inertial Interaction*. It is due to inertial effects developed in the structure because of its own vibrations resulting in base shear and moment, which, in turn, cause relative displacements between foundation and free field.

The second is known as *Kinematic Interaction* and it is due to the presence of stiff foundation elements on or in soil that will cause foundation motions to deviate from free field motion because of (*Stewart et al, 1998*):

- *Base-Slab Averaging*: the free field motions associated with inclined and/or incoherent wave fields are “averaged” within the footprint area of the base-slab due to the kinematic constraint of essentially rigid-body motion of the slab;
- *Embedment effects*: the reduction of seismic ground motion with depth for embedded foundations;
- *Wave Scattering*: scattering of seismic waves near corners and asperities of the foundation.

The general methods can be categorized as *direct* and *substructure approaches* (Stewart *et al.*, 1998).

In a *direct approach*, soil and structure are included within the same model and analysed in a single step. The soil is often discretized through solid finite elements and the structure through finite beam elements.

Because assumptions of superposition are not required, true nonlinear analyses are possible. However, results from nonlinear analyses can be quite sensitive to poorly defined parameters in the soil constitutive model, and the analyses remain quite expensive from a computational standpoint. Hence, direct SSI analyses are more commonly performed using equivalent linear methods to approximate the effects of soil nonlinearity.

In a *substructure approach*, the SSI problem is broken down into three distinct parts, which are combined to formulate the complete solution. The superposition inherent to this approach requires an assumption of linear soil and structure behaviour.

Three steps in the analysis are required (Stewart *et al.*, 1998):

1. *evaluation of a Foundation Input Motion (FIM)*, which is the motion that would occur on the base-slab if the structure and foundation had no mass (the FIM is dependent on the stiffness and geometry of the foundation and soil; since inertial effects are neglected, the FIM represents the effects of kinematic interaction only);
2. *determination of the impedance function*, that describes the stiffness and damping characteristics of foundation-soil interaction (it should account for the soil stratigraphy and foundation stiffness and geometry, and is computed using equivalent-linear soil properties appropriate for the in situ dynamic shear strains);
3. *dynamic analysis* of the structure supported on a flexible-base represented by the impedance function and subjected to a base excitation consisting of the FIM.

The effects of kinematic and inertial interaction are, thus, described by a complex-valued transfer function relating free field and foundation motions, and

a complex-valued impedance function that quantifies the stiffness and damping characteristics of foundation-soil interaction.

The damping represented by the imaginary part of the impedance function is a consequence of hysteretic damping in the soil and foundation, and radiation of seismic energy away from the foundation through the soil.

Both the transfer and impedance functions are dependent on the finite stiffness and damping characteristics of the soil medium. For the fictional condition of an infinitely stiff soil, the amplitude of the transfer function for translational motion is unity and the phase is zero (i.e. the foundation and free field motions are identical), and the impedance function has infinite real parts and zero imaginary parts. It is of some practical significance that this unrealistic assumption of rigid soil is made when SSI effects are ignored (which is common practice in structural design).

The principal advantage of the substructure approach is its flexibility. Because each step does not depend on the others, the analyst can focus resources on the most significant aspects of the problem.

Analyses of inertial interaction effects predict the variations of first-mode period and damping ratio between the actual “flexible-base” case (which incorporates the flexibility of both the foundation-soil system and the structure) and a fictional “fixed-base” case (which incorporates only the flexibility of the structure).

The flexible-base modal parameters can be used with a free field response spectrum to evaluate design base shear forces for the structure. Hence, these analyses correspond to Steps 2 and 3 of the substructure approach. The analyses for kinematic interaction (Step 1 of the substructure approach) predict frequency-dependent transfer function amplitudes relating foundation and free field motions.

1.2 Literature Review

Soil-structure-interaction (SSI) principles are nowadays implemented in few Standards and Guidelines, mostly American (see Section 2.1).

In these documents, simplified approaches, related to a simple elastic oscillator, are usually referenced for the evaluation of the SSI effects on the seismic behaviour of structures.

These simplified approaches are essentially based on the study of *Veletsos & Meek* (1974) for the evaluation of inertial soil-structure interaction effects.

The reference model of *Veletsos & Meek* is shown in Figure 1.1.

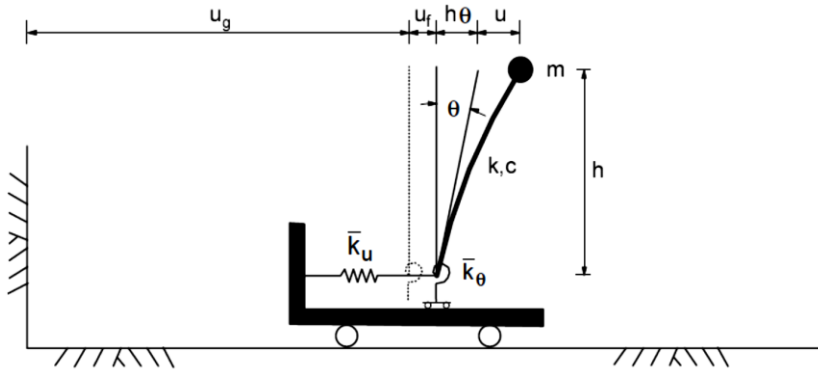


Figure 1.1 - Simplified system for inertial interaction problems suggested in *Veletsos & Meek* (1974)

The system consists of a single degree of freedom structure with height h , mass m , stiffness k , and viscous damping coefficient c .

The base of the structure is allowed to translate relative to the free field an amount u_f and rotate an amount θ . The impedance function is represented by lateral and rotational springs with complex stiffnesses \bar{k}_u and \bar{k}_θ respectively. The imaginary components of the foundation stiffness terms represent the effects of damping.

The simple system in Figure 1.1 can be viewed as a direct model of a single-story building or, more generally, as an approximate model of a multi-mode, multi-story structure which is dominated by first-mode response.

In the latter case, h is interpreted as the distance from the base to the centroid of the inertial forces associated with the first vibration mode.

The impedance function represents the dynamic stiffness and damping characteristics of foundation-soil interaction.

Mathematically, an impedance function is a matrix that relates the forces (e.g. base shear and moment) at the base of the structure to the displacements and rotations of the foundation relative to the free field.

The terms in the impedance function are complex valued and frequency dependent.

When values of impedance parameters at a single frequency must be used, values at the predominant frequency of the soil-structure system are selected.

In the most general case, six degrees of freedom would be necessary for each support point on the foundation. In practice, however, the foundation is often assumed to be rigid, which reduces the total degrees of freedom to six.

When considering the lateral response of a structure on a rigid foundation in a particular direction, as is the case for the model in Figure 1.1, only two impedance terms are generally necessary:

$$\begin{bmatrix} V \\ M \end{bmatrix} = \begin{bmatrix} \bar{k}_u & 0 \\ 0 & \bar{k}_\theta \end{bmatrix} \begin{bmatrix} u_f \\ \theta \end{bmatrix} \quad (1.1)$$

In equation 1.1, off-diagonal terms are neglected, as they are usually small.

It should be noted that vertical excitation and torsion are neglected in the simple impedance function in equation 1.1.

In their work, *Veletsos & Meek* reference to impedance functions for a rigid circular foundation on the surface of a visco-elastic halfspace (*Veletsos and Wei, 1971 and Veletsos and Verbic, 1973*).

This solution accounts for the three-dimensional nature of the problem and the frequency dependence of the stiffness and damping parameters.

In the solution for a rigid disk on a half-space, terms in the impedance function are expressed in the form:

$$\bar{k}_j = k_j(a_0, \nu) + i\omega c_j(a_0, \nu) \quad (1.2)$$

where j denotes either deformation mode u or θ , ω is angular frequency (radians/sec.), a_0 is a dimensionless frequency defined by:

$$a_0 = \frac{\omega r}{V_s} \quad (1.3)$$

with r = foundation radius, V_s = soil shear wave velocity, and ν = soil Poisson ratio.

Foundation radius is computed separately for translational and rotational deformation modes to match the area (A_f) and moment of inertia (I_f) of the actual foundation, as follows:

$$r_1 = \sqrt{\frac{A_f}{\pi}} \quad r_2 = \sqrt[4]{\frac{4I_f}{\pi}} \quad (1.4)$$

The real stiffness and damping of the translational and rotational springs and dashpots are expressed, respectively, by:

$$\begin{aligned} k_u &= \alpha_u K_u & c_u &= \beta_u \frac{K_u r_1}{V_s} \\ k_\theta &= \alpha_\theta K_\theta & c_\theta &= \beta_\theta \frac{K_\theta r_2}{V_s} \end{aligned} \quad (1.5)$$

The quantities α_u , β_u , α_θ , and β_θ are dimensionless parameters expressing the frequency dependence of the results, while K_u and K_θ represent the static stiffness of a disk on a half-space, defined by:

$$\begin{aligned} K_u &= \frac{8}{2-\nu} G r_1 \\ K_\theta &= \frac{8}{3(1-\nu)} G r_2^3 \end{aligned} \quad (1.6)$$

where G = soil dynamic shear modulus.

Presented in Figure 1.2 are the frequency dependent values of α_u , β_u , α_θ , and β_θ for $\nu=0.4$ based on closed form expressions in *Veletsos and Verbic (1973)*.

Values of soil shear stiffness G and hysteretic damping β used in the formulation of impedance functions should be appropriate for the in situ shear strains.

Despite the demonstrated utility of the impedance function formulation by *Veletsos and Verbic*, commonly encountered conditions such as non-uniform soil profiles, embedded, non-circular, or flexible foundations, are not directly modelled by these procedures.

The effects of such conditions on foundation impedance can be approximately simulated with adjustments to the basic solution.

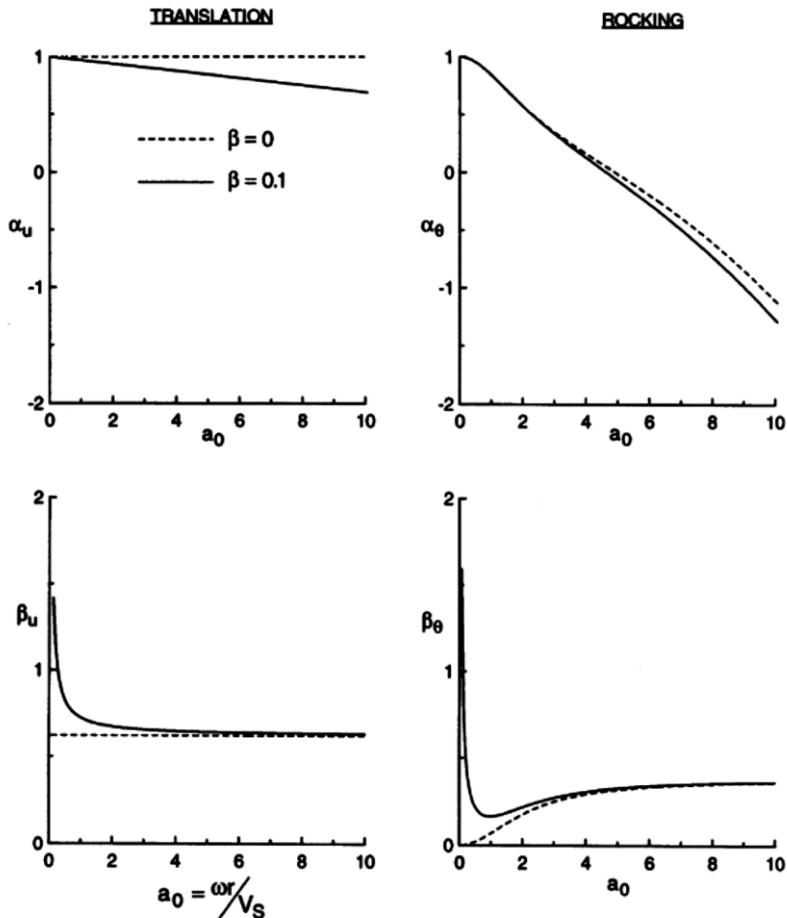


Figure 1.2 - Foundation stiffness and damping factors for elastic and viscoelastic half-spaces, $\nu = 0.4$ (Veletsos & Verbic, 1973)

Non-uniform soil profiles can often be characterized by gradual increases in stiffness with depth, or by a very stiff layer underlying relatively soft, surficial layers.

For profiles having gradual increases in stiffness with depth, *Roesset* (1980) found that using soil properties from a depth of about $0.5r$ gave half-space impedances which reasonably simulated the impedance of the variable profile.

For the case of a finite soil layer overlying a much stiffer material, the key considerations are an increase in the static stiffness and changes in the frequency dependent variations of stiffness and damping (*Kausel, 1974*).

Foundation embedment effects were investigated by *Elsabee and Morray (1977)* for the case of a circular foundation embedded to a depth e into a homogeneous soil layer of depth.

Dobry and Gazetas (1986) reviewed the literature for impedance function solutions for foundations of various shapes including circles and rectangles with aspect ratios of 1 to ∞ . Their results generally confirmed that the use of equivalent circular mats is an acceptable practice for aspect ratios $L/B < 4:1$, with the notable exception of dashpot coefficients in the rocking mode.

The effects of foundation flexibility on impedance functions for surface disk foundations were investigated by *Iguchi and Luco (1982)* for the case of loading applied through a rigid central core, *Liou and Huang (1994)* for the case of thin perimeter walls, and *Riggs and Waas (1985)* for the case of rigid concentric walls.

These studies have generally focused on foundation flexibility effects on rocking impedance; the horizontal impedance of non-rigid and rigid foundations were found to be similar (*Liou and Huang, 1994*).

In 1991 *Gazetas* provided, aiming at encouraging the practicing engineer to make use of the results obtained with state-of-the-art formulations, a complete set of algebraic formulas and dimensionless charts for readily computing the dynamic stiffnesses and damping coefficients of foundations harmonically oscillating on/in a homogeneous half-space.

All possible modes of vibration, a realistic range of Poisson's ratios, and a practically sufficient range of oscillation frequencies are considered in the study.

The foundations have a rigid base-mat of any realistic solid geometric shape. The embedded foundations are prismatic, having a sidewall-soil contact surface with a height that may be only a fraction of the embedment depth.

The solutions of *Gazetas*, as well as those suggested by *Pais and Kausel (1988)* can be found in Annex A.

In their work, *Veletsos and Meek (1974)* found that the maximum seismically induced deformations of the oscillator in Figure 1.1 could be predicted accurately

by an equivalent fixed-base single degree-of-freedom oscillator with period T_{SSI} and damping ratio ξ_{SSI} .

These are referred to as “flexible-base” parameters, as they represent the properties of an oscillator which is allowed to translate and rotate at its base.

The flexible base period is evaluated as:

$$\frac{T_{SSI}}{T} = \sqrt{1 + \frac{k}{k_u} + \frac{kh^2}{k_o}} \quad (1.7)$$

where T is the fixed-base period of the oscillator in Figure 1.1 (i.e. the period that would occur in the absence of base translation or rocking).

The flexible-base damping ratio has contributions from the viscous damping in the structure as well as radiation and hysteretic damping in the foundation.

Jennings and Bielak (1973) and *Veletsos and Nair* (1975) expressed the flexible-base damping as:

$$\xi_{SSI} = \xi_0 + \frac{\xi}{\left(\frac{T_{SSI}}{T}\right)^3} \quad (1.8)$$

where ξ_0 is referred to as the foundation damping factor and represents the damping contributions from foundation-soil interaction (with hysteretic and radiation components). A closed form expression for ξ_0 is presented in *Veletsos and Nair* (1975).

In their study, *Veletsos & Meek* considered, as free field motions, a harmonic motion, a relatively simple pulse-type excitation and an actual earthquake record.

They presented comprehensive response spectra for a range of the parameters defining the problem, and the results were used to assess the accuracy of the simple, approximate method of analysis.

Special attention was given to defining the conditions under which the interaction effect is of sufficient importance to warrant consideration in design.

The main findings of the study are the following.

1. Soil-structure interaction may affect significantly the dynamic response of structures and must, in general, be considered in design.
2. The three most important parameters controlling the interaction phenomenon are (a) the wave parameter, expressed as the ratio:

$$\sigma = \frac{V_s T}{h} \quad (1.9)$$

that is a measure of the relative stiffness between the soil and the structure; (b) the ratio between the height of the structure and the foundation radius, and (c) the relationship of the fixed-base natural frequency of the structure to the frequency regions of the design spectrum.

3. The principal effect of interaction is to reduce the resonant frequency of the structure and to modify its effective damping; the net result may be a reduction or increase in the maximum deformation of the structure;
4. Consideration of soil-structure interaction in a dynamic analysis is warranted only for values of the wave parameter, σ , less than 20.
5. For values of σ less than 20 but more than about 3, the maximum deformation of the structure may be estimated reliably by analysing the system as a single-degree-of-freedom oscillator.

When an earthquake occurs, both the soil and the structural elements can exhibit non-linear behaviour and, in general, the soil reaches the limit of its elastic behaviour before the structural elements.

In the simplified approach proposed by *Veletsos & Meek* the foundation impedance functions are evaluated assuming an elastic half-space, although the same authors suggest using a value of the shear modulus and of the soil damping coherent with in situ shear strains.

This way to consider the non-linear soil behaviour is doubtless rather approximated and more refined modelling techniques are preferable to take into account the non-linear soil behaviour.

A more refined way to take into account the non-linear soil-behaviour is presented by *Pitilakis & Cloteau* (2010), which proposed an equivalent linear sub-structure approximation of the soil–foundation–structure interaction.

Based on the inherent linearity of the approach, the solution of the structural and the soil domain is obtained simultaneously, incorporating the effects of the primary and secondary soil non-linearities.

The proposed approximation is established theoretically and then validated against centrifuge benchmark soil–foundation–structure interaction tests.

It is proved that the equivalent linear substructure approximation can simulate efficiently the effects of the nonlinear soil behaviour on the soil–foundation–structure system under a strong earthquake ground motion.

In *Pitilakis et al.* (2013), an approximate linearization method using the familiar concept of G - γ and D - γ curves for determining the dynamic impedance (stiffness and damping) coefficients of rigid surface footings accounting for nonlinear soil behaviour was proposed.

The method is based on subdivision of the soil mass under the footing into a number of horizontal layers of different shear modulus and damping ratio, compatible with the level of strain imposed by an earthquake motion or a dynamic load. In this way, the original homogeneous or inhomogeneous soil profile is replaced by a layered profile with strain-compatible properties within each layer, which do not vary in the horizontal sense.

The system is solved in the frequency domain by a rigorous boundary-element formulation accounting for the radiation condition at infinity. For a given set of applied loads, characteristic strains are determined in each soil layer and the analysis is repeated in an iterative manner until convergence in material properties is achieved. Both kinematic and inertial interaction can be modelled simultaneously by the method, which thus encompasses primary and secondary material nonlinearity in a single step. The results are presented for a circular footing resting on: (1) a half space made of clay of different plasticity index and (2) a half space made of sand of different density, excited by a suite of recorded earthquake motions. Dimensionless graphs are provided for the variation of foundation stiffness and damping with frequency and excitation level in vertical, swaying, rocking, and torsional oscillations.

In the work of *Saez et al.* (2008), the assessment of the effects of non-linear soil behaviour on the structural seismic demand evaluation was concerned by means of non-linear dynamic analyses, in order to study the role of several parameters on the seismic performance evaluation.

The dynamic analyses were performed for a complete finite element model including soil and structural non-linear behaviour and for a fixed base model at the base of which the free field motion obtained by means of a non-linear 1D wave propagation problem for a soil column.

The study shows that SSI with a non-linear soil model varies significantly the structural response with respect to a fixed base model.

In particular, the authors highlighted that non-linear SSI can increase or decrease the seismic demand depending on the type of the structure, the input motion and the dynamic soil properties and that in general there is an economic justification to take into account the modification effects due to non-linear soil behaviour.

Moreover, the authors emphasized the major challenge to quantify the non-linear SSI effects in seismic demand evaluation: the prediction of an accurate global damping, able to be related to a simpler approach.

Ostadan (2004) emphasized that for a realistic soil-structure interaction (SSI) analysis, material damping in the soils and structural materials as well as the foundation radiation damping should be considered.

However, estimating total system damping is often difficult due to complex interplay of material damping and radiation damping in the dynamic solution.

However, an estimate of total system damping is frequently needed for evaluation of SSI effects and for detailed linear or nonlinear structural analysis in order to develop realistic results.

In his work, *Ostadan* presented a summary of series of parametric studies and proposed an effective approach to estimate system damping for SSI systems.

The accuracy of the method was verified using a model of a large concrete structure on a layered soil site.

The study showed that simple methods currently available to estimate system damping from dynamic structural responses (half-bandwidth, inverse of the peak and damping ratio method) often fail to predict reasonable results for soil-structure systems due to frequency dependency of the foundation stiffness and dashpot parameters and the complex participation of the SSI and structural modes of vibration in the total response.

The paper shows that the response from an impulse load applied to the SSI model yields an accurate estimate of system damping while including the effects of material damping, radiation damping as well as composite effects of numerous structural and SSI modes to the dynamic response of the interest.

Similarly, *Celebi* (2000) underlined that in most cases, when dynamic analyses are performed, critical damping percentages are adopted from rounded empirical values which represent only structural damping. However, radiation damping, as well as other types of damping, can contribute significantly to the overall effective damping.

In his work, two cases of regular buildings that exhibit radiation damping are presented.

Simple methods are used to confirm the radiation damping percentages.

The characteristics of the site, foundation and superstructure of the two buildings are used to show that the radiation damping for such buildings can be substantial and beneficial in assessment of their responses to large earthquakes.

In general, energy dissipation as a means of reducing the seismic response of structures has become a popular topic among researchers and structural engineers who have developed and implemented devices, such as friction dampers, fluid dampers, and isolators, in the retrofit of structures.

In his work, *Crouse* (2001) underlined how a natural source of energy dissipation, generally neglected, is the interaction between a structure, its foundation, and the supporting soil medium and how this interaction can be significant and potentially beneficial in certain situations, resulting in large reductions in seismic response.

It is emphasized that SSI experiments and theoretical calculations using simple models have yielded relatively large modal damping ratios in certain situations for structures such as short-span bridges, offshore concrete gravity platforms, nuclear power plant containments, fuel storage tanks, short to mid-rise buildings, and nuclear waste processing plants.

The author highlighted that, however, the composite modal damping values determined by theoretical models are not necessarily those that should be used in final design, which should consider uncertainties associated with the SSI model

and its parameters, relevant experimental data, and the degree of conservatism desired for the design.

Usually, numerical models implemented for taking into account the SSI assume that no relative movements between the foundation and the soil are allowable.

However, when a structure supported on shallow foundations is subjected to inertial loading due to earthquake ground motion, the foundation may undergo sliding, settling and rocking movements.

If the capacity of the foundation is mobilized, the soil-foundation interface will dissipate significant amounts of vibrational energy, resulting in a reduction in structural force demand. This energy dissipation and force demand reduction may enhance the overall performance of the structure, if potential consequences such as excessive tilting, settlement or bearing failure are accounted for.

Despite this potential benefit, building codes, particularly for new construction, discourage designs that allow foundation capacity mobilization. This lack of acceptance to embrace Soil-Foundation-Structure Interaction (SFSI) as a design inelastic mechanism may stem from the well-founded concern that significant uncertainties exist in characterization of soils. More importantly, the lack of well-calibrated modelling tools, coupled with parameter selection protocols cast in a simplistic fashion are lacking.

In the work of *Raychowdhry* (2008), a numerical model based on the Beam-on-Nonlinear-Winkler-Foundation (BNWF) concept was developed to capture the above mentioned foundation behaviour.

The BNWF model was selected due to its relative simplicity, ease of calibration, and acceptance in engineering practice. The soil-foundation interface is assumed to be an assembly of discrete, nonlinear elements composed of springs, dashpots and gap elements.

Spring backbone curves typically used for modelling soil-pile response are taken as a baseline and further modified for their usefulness in shallow footing modelling. Evaluation of the model and associated parameter selection protocol is conducted using a suite of centrifuge experiments involving square and strip

footings, bridge and building models, static and dynamic loading, sand and clay tests, a range of vertical factors of safety and aspect ratios.

It was observed that the model can reasonably predict experimentally measured footing response in terms of moment, shear, settlement and rotational demands. In addition, the general hysteresis shape of the moment-rotation, settlement-rotation and shear-sliding curves is reasonably captured. However, the model consistently underestimates the sliding demand measured in the experiments, perhaps due to the lack of coupling between the vertical and lateral modes of response. Following the model validation, input parameter sensitivity was investigated using tornado diagram analysis and the First-Order-Second-Moment (FOSM) method. Among the parameters required for the BNWF modelling, the vertical tension capacity and friction angle have the most significant effect on the capability of the model to capture force and displacement demands. The model was then exercised by studying the response of shear wall-foundation and shear wall-frame-foundation systems. The analyses indicated that if reliably quantified and designed, SFSI has great potential for reducing system level seismic forces and inter-story drift demands. It was observed that the energy dissipated in the sliding mode is dominant for stiffer (and shorter) shear-wall structures, while energy dissipated in the rocking mode has a larger relative contribution for taller and higher period structures.

Finally, the proposed model was implemented within the framework of OpenSees (an open source finite element software package developed by the Pacific Earthquake Engineering Research center) to encourage its use within engineering community

In the work of *Harden & Hutchinson (2009)*, numerical results demonstrated that reasonable comparison between the nonlinear Winkler-based approach and experimental response in terms of moment-rotation, settlement-rotation, and shear-sliding displacement can be obtained, given an appropriate selection of model and soil properties, for foundation-structure systems where seismically-induced rocking plays a predominant role in the response.

The influence of soil-structure interaction on the inelastic behaviour of structures was studied, among other authors, by *Avilés (2003, 2004)*, which

investigated the effects of kinematic and inertial SSI on the seismic response of a simple yielding system representative of code-designed buildings.

The concepts developed previously by other authors for interacting elastic systems are extended to include the non-linear behaviour of the structure.

A simple soil–structure system representative of code-designed buildings is investigated. The replacement oscillator approach used in practice to account for the elastic interaction effects is adjusted to consider the inelastic interaction effects.

This is done by means of a non-linear replacement oscillator defined by an effective ductility together with the known effective period and damping of the system for the elastic condition.

The efficiency of the simplified approach is demonstrated by means of extensive numerical evaluations conducted for elastoplastic structures with embedded foundation in a soil layer over elastic bedrock, excited by vertically propagating shear waves.

The results show that kinematic interaction reduces the strength and displacement demands corresponding to inertial interaction only, this reduction being of little practical importance.

Moreover, strength and displacement demands are well predicted by a simplified procedure that provides a convenient extension to the well-known replacement oscillator approach.

The combined effects of foundation flexibility and structural yielding are found to be clearly beneficial for slender structures with natural period somewhat longer than the site period, but quite detrimental if the structure period is shorter than the site period.

In addition, it is shown that there is no clear evidence whether elastic or yielding systems are most influenced by interaction.

Nowadays, in engineering practice the Performance-Based Design (PBD) is commonly used as design approach for new structures or for the vulnerability assessment of existing buildings.

A challenging task is that to implement the SSI principles in this kind of approach.

The works of *Comartin et al.* and *Stewart et al.* (2004) provide useful suggestions on the topic.

In the work of *Comartin et al.* (2004) a review and discussion of simplified inelastic seismic analysis of new and existing buildings are provided.

Moreover, guidelines for applications of selected procedures including their individual strengths, weaknesses and limitations are contained in the work.

In the work of *Stewart et al.* (2004) guidelines for the design of seismic retrofits for existing buildings are presented, taking as reference the performance based design principles as implemented through non-linear static procedures.

In the work it is emphasized that SSI effects are most important at short periods (i.e., T less than approximately 0.5 s) and that three phenomena can contribute to non-linear static procedures.

First, flexibility at the soil-foundation interface, that can be incorporated into nonlinear pushover curves for the structure by means of foundation spring models.

Second, SSI affects demand spectra through the effective system damping, which is the damping ratio for which spectral ordinates should be calculated.

Third, kinematic SSI, that reduces ordinates of the demand spectra.

The paper describes how damping and kinematic SSI effects should be incorporated into the recommended seismic analysis procedures for existing buildings.

It is highlighted that these effects generally decrease the seismic demand relative to what would be used in current practice, which is based on 5% structural damping and equivalent foundation and free field motions. The demand reduction is greatest at short periods.

Concerning the same topic, some additional issues are discussed in the work of *Pitilakis et al.* (2010).

The authors emphasized how PBD is traditionally performed assuming a fixed-base model and applying at the base of the structure the free field soil response in order to calculate the demand spectrum and thus the dynamic response of superstructure.

In the work, SSI is taken into account in the estimation of the demand spectrum at the foundation level.

The dynamic response of the foundation – structure system, in fact, is known to depend on the foundation input motion (FIM), which in turn depends on the interaction of the superstructure with the underlying soil, when subjected to strong ground motion. Consequently, the dynamic response of a flexible foundation differs from the free field soil ground motion and therefore the demand spectrum for the structure will be affected.

A full parametric finite element analysis is conducted in order to elucidate the influence of all the parameters on the FIM, and consequently on the design demand spectra.

Notably, the relative stiffness between the soil and the structure, the slenderness of the structure, the structure-to-foundation mass ratio, as well as the ratio of the predominant excitation to the system frequency are successively altered, so as to clarify their contribution in the modification of the FIM.

In addition, if the superstructure has inelastic behaviour, a pushover analysis is needed in order to estimate the capacity of the structure. It will be also affected by the soil compliance in case of strong seismic excitations.

The work highlights the following issues.

1. The shape of demand spectra and thus the structural response depends on the local geology at the examined site and the frequency domain of earthquake input motion. Generally, the design response spectra, such as those in building codes are smooth in shape. However, response spectra resulting from actual earthquake input motions are irregular and have spikes at the predominant soils periods.

For this reason, the assumption that SFSI effects are in favour of the structure, reducing accelerations and thus the seismic loads that structures should resist during an earthquake it is only a generalization.

SSI seems to be in favour of the structure for predominant response at high period range, reducing the seismic input in terms of accelerations, on the contrary, the acceleration demand increases for structures that respond at low period range.

2. The effects of the SFSI are severe for stiff structures laying on soft soil profiles, structures with large lumped mass, intense earthquake input motions and for high structures, and thus structures with great slenderness.
3. Intense earthquake input motions, cause modification of soils proprieties during shaking. Thereby, the more intense the input motion is, the higher the soils response periods are. This happens because for strong input motions soil behaves further in the inelastic range.
4. The final decision in what cases the SFSI effects should be taken into account during the seismic design of structure depends on the structure–soil– earthquake characteristics.
5. When it is assumed during the analysis that the structure will respond in the inelastic range, the differences from the traditionally used approach may be even more pronounced. In this case, the design values in terms of accelerations are usually lower than the assuming values for elastic structural response, but it is of great importance to have ensured, that the system has the essential available ductility at the critical locations of potential plastic hinging in order to avoid the total collapse of structure.

Conclusions similar to those provided by *Pitilakis & al.* are provided in the earlier work of *Mylonakis & Gazetas* (2000), which re-explored the role of soil-structure interaction (SSI) in the seismic response of structures using recorded motions and theoretical considerations.

The authors highlight how, in modern codes, the idealised design spectra along with the increased fundamental period and effective damping due to SSI lead invariably to reduced forces in the structure.

They show how reality, however, often differs from this view. It is shown that, in certain seismic and soil environments, an increase in the fundamental natural period of a moderately flexible structure due to SSI may have a detrimental effect on the imposed seismic demand in terms of pseudo-spectral acceleration.

In engineering practice, not only SSI effects are in general neglected.

Another physical phenomenon typically neglected in practice is the aging effect.

In the study of *Pitilakis et al.* (2014) the role of both SSI and aging effects on the seismic vulnerability assessment of Reinforced Concrete (RC) buildings was investigated.

The authors consider, among the various aging processes, the chloride-induced corrosion based on probabilistic modelling of corrosion initiation time and corrosion rate.

They consider different corrosion aspects in the analysis, including the loss of reinforcement cross-sectional area, the degradation of concrete cover and the reduction of steel ultimate deformation. In addition the SSI is modelled by applying the direct one-step approach, which accounts simultaneously for inertial and kinematic interactions.

In the study two dimensional incremental dynamic analysis are performed to assess the seismic performance of the initial un-corroded and corroded RC moment resisting frame structures, designed with different seismic code levels. Time-dependent fragility functions are derived for the immediate occupancy and collapse prevention limit states.

The work highlight the overall increase in seismic vulnerability over time due to corrosion and the modification of the expected seismic demand in terms of maximum inter-story drift ratio due to the consideration of SSI and site effects.

1.3 Scope and objectives of the research

In common seismic design practice, the design of a new building or the vulnerability assessment of an existing one is usually performed assuming that the structure is fixed at the base, and assuming that the signal at the base of the same is that evaluated in free field conditions.

This assumption, reasonable for structures founded on stiff soils, can be unrealistic in case of structures founded on soft soils.

Different researches show that SSI cause, with respect to a fixed base configuration, two main effects:

- an increase of the fundamental period of the system, due to deformability of the foundation soil;

-
- an increase of the overall damping, due to the fact that the structures dissipates a great amount of energy of energy in the underlying soil during its vibrations.

Despite an intense scientific production on the topic, the diffusion of soil-structure interaction analyses in the field of civil constructions is nowadays rather limited, mainly because of three reasons:

- the lack, in many countries, of specific code provisions;
- the belief that SSI has a beneficial effect on the structural response and thus it is possible to have an increase of the safety level neglecting it;
- the complexity in performing a rigorous analysis.

In this thesis the three aforementioned issues are faced.

Firstly, a review of the simplified formulations suggested by American Standards and Guidelines for the evaluation of SSI effects is presented. These formulations, calibrated based on the study of the dynamic response of simple single degree of freedom systems, were then validated by means of linear modal analyses performed for different kinds of reinforced concrete structures.

The main objective was to establish in which cases simplified analyses can be performed and in which cases more refined analyses are needed.

Non-Linear Static Analyses (pushover analyses) were then performed for existing reinforced concrete moment resisting frames in order to establish if a reduction of the seismic demand due to SSI can imply a significant impact on the design of seismic retrofitting interventions.

Finally, more refined dynamic analyses were performed in order to:

- validate the results obtained by means of simplified approaches;
- investigate some issues related to a proper modelling of the foundation soil and to the frequency content of the seismic input motion;
- find some criteria to establish in which cases an accurate modelling of the SSI is necessary and in which cases a simplified modelling can be sufficient;
- evaluate if, effectively, soil-structure interaction has always a beneficial effect on the seismic response of reinforced concrete structures.

1.4 Outline of the Thesis

The present thesis is organized into five chapters with the following contents.

In the present chapter (**Chapter 1**), a brief description of the problem and a literature review on the topic of the evaluation of soil-structure interaction effects on the seismic behaviour of structures, with particular emphasis on the work of *Veletsos & Meek*, is presented together with a description of the motivation and of the main objectives of the research.

In **Chapter 2**, a review of the simplified approaches proposed by American Standards for the evaluation of Soil-Structure Interaction effects on the seismic response of buildings is reported.

The results of simplified linear modal analyses performed for different types of reinforced concrete structures are shown and compared with those obtained by means of the simplified approaches mentioned above.

Moreover, the results of Non-Linear Static Analyses performed for existing reinforced concrete moment resisting frames are shown, in order to investigate the influence of SSI on the ratios Capacity/Demand, that can strongly affect the design strategies of retrofiting interventions.

In **Chapter 3**, a description of the possible modelling techniques of soil-structure interaction effects is presented, focusing the attention on the differences between sub-structures approach and direct approaches. Some issues concerning the non-linear modelling of the soil are introduced.

The numerical models implemented in OpenSees for the parametric analyses shown in Chapter 4 are presented.

In **Chapter 4**, the results of parametric analyses performed for 2D reinforced concrete moment resisting frames are shown, after a brief description of all the parameters investigated.

The results of additional analyses performed for a dual system with a shear wall and a frame are also shown in order to highlight some important issues concerning the interaction of deformable soils with this kind of structural system.

Finally, in **Chapter 5**, the main findings and limitations of the work are summarized. Some suggestions for future researches are also provided.

2 Simplified approaches for evaluating SSI effects on RC structures

In the present Chapter, the simplified approaches proposed by American Codes for the evaluation of the Soil-Structure Interaction (SSI) effects are briefly discussed. In particular, the formulations provided by American Standards for the lengthening of the vibration period and for the modification of the overall damping, with respect to a fixed-base system, are introduced. These formulas substantially derives from the work of Veletsos and his co-authors (*Veletsos & Meek 1974, Veletsos & Nair 1975*) and are based on the study of a simple oscillator (see Section 1.2).

To investigate their validity for different kind of reinforced concrete (RC) structures, several modal analysis were performed for structural models (implemented with the software SAP 2000) with elastic springs at the base.

In addition, several Non-Linear Static analyses (Push Over) were performed, with both the N2 and the Capacity Spectrum Method, for RC moment resisting frames (MRF) designed for vertical loads only, with the aim to investigate the influence that SSI can have on the ratios Capacity/Demand for existing buildings.

This ratios, in fact, can strongly affect the strategies adopted in engineering practice for the design of retrofiting interventions for existing buildings

2.1 Implementation of SSI in American Standards and Guidelines

Soil-structure interaction provisions exist in the following American engineering standards and design guidelines:

- ATC-40, *Seismic Evaluation and Retrofit of Concrete Buildings* (ATC, 1996);
- ASCE 4-98, *Seismic Analysis of Safety-Related Nuclear Structures and Commentary* (ASCE, 1998);
- FEMA 450, *NEHRP recommended provisions for seismic regulations for new buildings and other structures and Commentary* (FEMA, 2003);
- FEMA 440, *Improvement of Nonlinear Static Seismic Analysis Procedures* (FEMA, 2005);
- ASCE/SEI 41-06, *Seismic Rehabilitation of Existing Buildings* (ASCE, 2007);
- FEMA P-750, *NEHRP Recommended Seismic Provisions for New Buildings and Other Structures* (FEMA, 2009);
- ASCE/SEI 7-10, *Minimum Design Loads for Buildings and Other Structures* (ASCE, 2010);
- PEER Report No. 2010/05, *Guidelines for Performance-Based Seismic Design of Tall Buildings* (PEER, 2010).

Despite the availability of these resources, SSI is seldom considered in design practice. This is partially due to challenges in understanding, learning, and implementing fundamental SSI principles, but also in the way SSI provisions are codified in seismic design provisions. In general, accounting for SSI is handled through optional procedures, some of which can only reduce base shear demands. Under such conditions, ignoring SSI is not only easier, it is conservative.

However, there is a growing interest in considering SSI, as a result of the increased awareness about the relevance of its effects on the seismic response of structures. This has been driven principally by seismic retrofit projects in which SSI analysis is used to gain a deeper insight into structural performance and to improve accuracy in the analytical simulation of important structural response quantities.

The following sections briefly describe the implementation of SSI procedures in currently available engineering standards and guidelines.

2.1.1 Force Based Procedures

Implementation of soil-structure interaction into the equivalent lateral force procedure for seismic design is specified in ASCE/SEI 7-10 and in the *NEHRP Recommended Provisions* (FEMA 450, FEMA P-750).

The seismic base shear not considering SSI effects is defined as:

$$V = C_s \bar{W} \quad (2.1)$$

where C_s is a seismic coefficient, taken as the design response spectral ordinate, at building period T , normalized by the acceleration of gravity, g , and \bar{W} is the effective seismic weight of the structure (taken as 70% of the total weight).

ASCE/SEI 7-10 and *NEHRP Recommended Provisions* neglect kinematic interaction effects but account for inertial interaction effects related to period lengthening and damping ratio.

The change in base shear is calculated as:

$$\Delta V = \left[C_s - \bar{C}_s \left(\frac{0.05}{\beta_0} \right)^{0.4} \right] \bar{W} \quad (2.2)$$

and is related to the change in seismic coefficient (or spectral acceleration).

The \bar{C}_s term in Equation 2.2 represents the seismic coefficient obtained from the design spectrum at an elongated period, T_{SSI} .

The term $(0.05/\beta_0)^{0.4}$ represents the reduction in spectral ordinate associated with a change in damping from the fixed-base structural damping value of $\beta_i = 0.05$, to the flexible-base value of β_0 .

It is important to note that in ASCE/SEI 7-10 and *NEHRP Recommended Provisions* the shape of the design spectrum (see Figure 2.1) coupled with the requirement that β_0 must exceed β_i , ensures that utilizing SSI will always reduce base shear.

Modification of design base shear for SSI effects in equivalent lateral force procedures has a potentially significant shortcoming. There is no link between base shear reduction factors intended to represent structural ductility and soil-structure interaction.

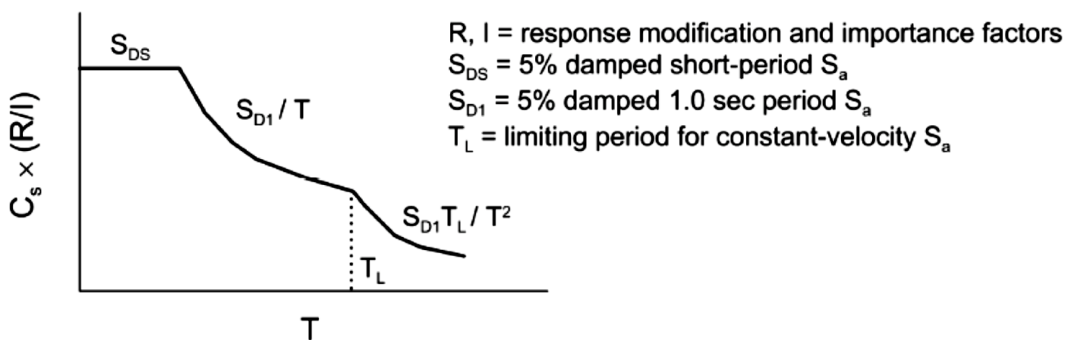


Figure 2.1 - Schematic illustration of the shape of the design response spectrum in the NEHRP Recommended Provisions (from NIST GCR 12-917-21)

Crouse (2001) noted that existing ductility factors may already reflect the beneficial effects of soil-structure interaction, and modifying the base shear to account for both SSI and ductility may be un-conservative in some cases.

Accordingly, there is a need to revisit the definition of ductility factors with respect to SSI effects, and define values that represent structural ductility effects alone.

Period lengthening can be calculated using the equation:

$$\frac{T_{SSI}}{T} = \sqrt{1 + \frac{\bar{k}}{K_y} \left(1 + \frac{K_y \bar{h}^2}{K_\theta} \right)} \quad (2.3)$$

where:

- T is the fundamental period of the structure in the fixed-base configuration;
- \bar{k} is the stiffness of the fixed-base structure, defined by the following:

$$\bar{k} = 4\pi^2 \frac{\bar{W}}{(gT^2)} \quad (2.4)$$

- \bar{h} is the effective height of the structure which shall be taken as 0.7 times the total height, h , except that for structures where the gravity load is effectively concentrated at a single level, it shall be taken as the height to that level;

- K_y is the lateral stiffness of the foundation defined as the horizontal force at the level of the foundation necessary to produce a unit deflection at that level, the force and the deflection being measured in the direction in which the structure is analysed;
- K_θ is the rocking stiffness of the foundation defined as the moment necessary to produce a unit average rotation of the foundation, the moment and rotation being measured in the direction in which the structure is analysed;
- g is the acceleration due to gravity.

ASCE/SEI 7-10 does not specify how lateral stiffness, K_y , or rotational stiffness, K_θ , are to be evaluated.

However, the *Commentary to the NEHRP Recommended Provisions* provides some guidance related to circular foundations, but the formulations provided by authors like *Gazetas* (1991) or *Pais and Kausel* (1988) for arbitrary foundation shapes are more useful for practical engineering applications.

According to these formulations, the foundation stiffnesses, K_y and K_θ , shall be computed using soil properties that are compatible with the soil strain levels associated with the design earthquake motion. The average shear modulus, G , for the soils beneath the foundation at large strain levels and the associated shear wave velocity, V_s , needed in these computations shall be determined from Table 2.1 where:

- V_{s0} is the average shear wave velocity for the soils beneath the foundation at small strain levels (10^{-3} percent or less);
- $G_0 = \gamma V_{s0}^2/g$ is the average shear modulus for the soils beneath the foundation at small strain levels;
- γ is the average unit weight of the soils.

Table 2.1 - Reduction coefficients for shear modulus and shear wave velocity (FEMA 440, 2005)

	PGA [g]			
	≤ 0,10	0.15	0.20	≥ 0.30
Value of G/G_0	0.81	0.64	0.49	0.42
Value of V_s/V_{s0}	0.90	0.30	0.70	0.65

As regards the system damping, the following equation can be used:

$$\beta_{SSI} = \beta_f + \frac{\beta_i}{\left(\frac{T_{SSI}}{T}\right)^n} \quad (2.5)$$

with fixed-base structural damping, $\beta_i = 0.05$, and exponent, $n = 3$ (for ideally viscous material damping).

In ASCE/SEI 7-10 and in the *NEHRP Recommended Provisions*, the foundation damping factor, β_f , is taken from a plot like the one shown in Figure 2.2, in which the period lengthening ratio is related to β_f as a function of structure aspect ratio, h/r .

Note that r is an equivalent foundation radius, which is calculated to match the foundation area for squat structures and the foundation moment of inertia for slender structures.

In particular the following expressions can be used for the evaluation of the equivalent foundation radius:

$$\begin{aligned} r = r_a &= \sqrt{\frac{A_0}{\pi}} \quad \text{for } \frac{h}{L_0} \leq 0.5 \\ r = r_m &= \sqrt[4]{\frac{4I_0}{\pi}} \quad \text{for } \frac{h}{L_0} \geq 1.0 \end{aligned} \quad (2.6)$$

where:

- L_0 is the overall length of the side of the foundation in the direction being analysed;
- A_0 is the foundation area;
- I_0 is the foundation moment of inertia around the axis orthogonal to the direction in which the structure is analysed.

For intermediate values of the ratio h/L_0 the radius r can be determined by linear interpolation.

American codes suggest that the value of β_{SSI} shall in no case be taken less than 0.05 or greater than 0.20.

The relationship in Figure 2.2 is calculated from *Veletsos and Nair (1975)*, using the absolute value of the complex valued damping relationship, and including both radiation damping and hysteretic soil damping.

Soil-structure interaction provisions for the equivalent lateral force procedure in ASCE/SEI 7-10 (and the *NEHRP Recommended Provisions*) are written such that base shear demand is only reduced through consideration of SSI. Therefore, ignoring SSI effects in the design process is analytically conservative.

In practice, the beneficial effects of period lengthening and foundation damping are negligible for tall, flexible structures.

Use of SSI procedures yields the most benefit for short-period, stiff structures with stiff, interconnected foundation systems (i.e., mats or interconnected footings) founded on soil.

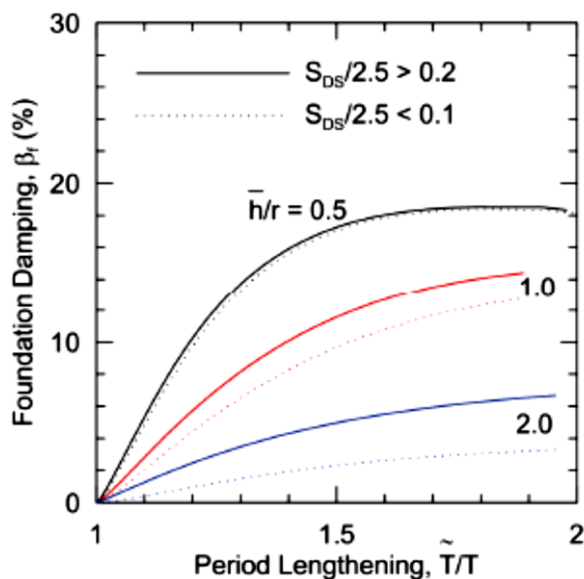


Figure 2.2 - Foundation damping factor (FEMA 2009, ASCE 2010)

Consideration of soil-structure interaction is also permitted when modal response spectrum analysis is used for seismic design. Implementation of SSI in modal response spectrum analysis is similar to the implementation for equivalent lateral force analysis. Period lengthening and modification of damping, however, are only applied in the fundamental lateral mode of response. Higher mode vibration periods and damping ratios are not modified for the effects of SSI.

The principal limitations of force-based procedures in ASCE/SEI 7-10 are:

1. use of simplified spectra that can only result in a decrease in base shear as period lengthens;
2. use of relatively simplified models, applicable to circular foundation geometries, for soil-foundation springs and foundation damping;
3. lack of consideration of kinematic interaction effects on foundation-level ground motions.

These limitations were considered necessary to make the procedures sufficiently simple for broad use in practice.

A potentially important consideration associated with the use of the SSI procedures in Chapter 19 of ASCE/SEI 7-10 is the value of the fixed-base fundamental period, T .

Chapter 12 of ASCE/SEI 7-10 contains approximate methods for evaluation of T , and limiting values, which bias the estimate of T to intentionally produce conservative values of design base shear.

In SSI procedures, T should be taken as the best estimate value of period, without deliberate bias.

Chapter 12 of ASCE/SEI 7-10 (Section 12.13) also contains procedures for incorporation of foundation flexibility (i.e., soil springs) into structural models for linear analysis. The use of an elongated period from Chapter 19 with a structural model containing foundation springs (per Section 12.13) would overestimate the effects of foundation flexibility, so the simultaneous use of both sets of procedures is not permitted in ASCE/SEI 7-10.

2.1.2 Displacement Based Procedures

In displacement-based procedures, system behaviour is represented by a force versus displacement relationship that is calculated through nonlinear static (i.e., Pushover) analyses.

A pushover analysis involves the application of static lateral loads distributed over the height of the structure, and calculation of the resulting displacements in a model of the SSI system. A pushover analysis of a structure with a flexible base is schematically illustrated in Figure 2.3.

The cumulative lateral load resultant, H , is related to a reference displacement, Δ , forming the nonlinear pushover curve. In some applications, the pushover curve is modified to an acceleration-displacement response spectrum (ADRS) by converting H to an equivalent spectral acceleration, and converting Δ to an equivalent spectral displacement (e.g. *Chopra and Goel, 1999; Powell, 2006*). At each point on the pushover curve, the deformations of all components in the structural system are related to the reference displacement.

Powell (2006) describes common ways by which the pushover curve is combined with a design response spectrum to estimate the seismic displacement in a structure.

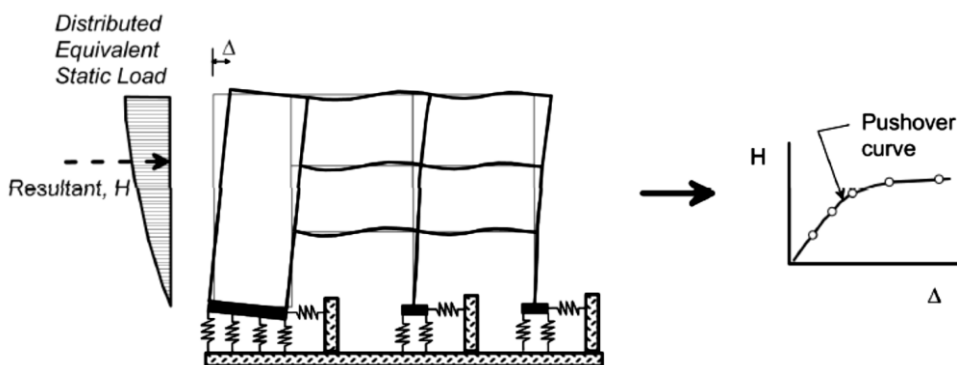


Figure 2.3 - Schematic illustration of a pushover analysis and development of a pushover curve for a structure with a flexible base (from NIST GCR 12-917-21)

Three such methods are known as the *Capacity Spectrum Method* (ATC, 1996), the *Coefficient Method* (FEMA, 1997; FEMA, 2000; and ASCE, 2007), and *Equivalent Linearization* (FEMA, 2005).

Soil-structure interaction is considered in displacement-based analysis procedures through:

1. foundation springs used in the pushover model;
2. reduction of the free field response spectrum for kinematic interaction effects;
3. reduction of the response spectrum for flexible-base damping ratios, β_0 , that are greater than the fixed-base structural damping ratio, β_i .

In general, soil-foundation springs used in pushover analyses are obtained by means of the static stiffness equations provided by *Gazetas* (1991) or by *Pais and Kausel* (1988) neglecting the dynamic stiffness modifiers.

Distributed vertical springs can be evaluated in a manner similar to that described in Section 3.2.2, while horizontal springs are not distributed but are concentrated at the end of the foundation (see Figure 3.11 in Chapter 3).

Kinematic interaction effects are represented in terms of ratios of response spectra (RRS) between the foundation and free field motions. Equations for RRS as a function of period are given for the effects of base slab averaging and embedment are adapted from FEMA 440 as follows:

$$RRS_{bsa} = 1 - \frac{1}{14100} \left(\frac{2(B_e^A \div 0.3048)}{T} \right)^{1.2} \quad T > 1/f_L \quad (2.7)$$

$$RRS_{bsa} = 1 - \frac{1}{14100} \left(2(B_e^A \div 0.3048)f_L \right)^{1.2} \quad T \leq 1/f_L$$

$$RRS_{emb} = \cos \left(\frac{2\pi D}{TV_{sr}} \right) \quad T > 1/f_L \quad (2.8)$$

$$RRS_{emb} = \cos \left(\frac{2\pi Df_L}{V_{sr}} \right) \quad T \leq 1/f_L$$

where V_{sr} is the strain-reduced shear wave velocity evaluated using the reduction factors in Table 2.1. In equations (2.7), the equivalent foundation dimension B_e^A is expressed in units of meters. These equations are a curve-fit of semi-empirical

base-slab averaging transfer functions (see NIST GCR 12-917-21). The resulting RRS curves for base-slab averaging are shown in Figure 2.4.

In FEMA 440, the limiting frequency, f_L , is taken as 5 Hz (period = 0.2 sec).

In FEMA 440, the objective of the damping analysis is to estimate the foundation damping ratio, β_f , which is then combined with the fixed-base structural damping ratio, β_i , to estimate β_0 using equation 2.5 (with $n = 3$).

The principal challenge is to extract β_f from the results of the pushover analysis of the structure in both its fixed-base and flexible-base condition. It is worth to note that foundation flexibility can significantly reduce radiation damping (K_θ) from rotational vibration modes, which is considered in the FEMA 440 procedures.

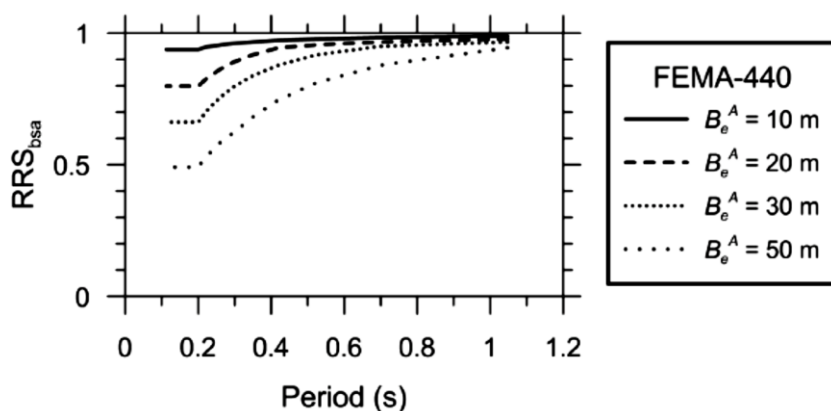


Figure 2.4 - Ratios of Response Spectra for base slab averaging using the semi-empirical formulations adopted in FEMA 440 (2005)

First, the period lengthening ratio at small displacements is estimated using the initial stiffness of capacity diagrams for the fixed-base and flexible-base structures.

Assuming shaking in the y -direction, stiffness K_y is evaluated using, for example, the equations proposed by Gazetas (the dynamic stiffness modifier, α_x , is assumed as unity).

The effective rotational stiffness of the foundation system is then evaluated from a manipulation of equation 2.3 as follows:

$$K_{\theta} = \frac{K_{fixed}^* h^2}{\left(\frac{T_{SSI}}{T}\right)^2 - 1 - \frac{K_{fixed}^*}{K_y}} \quad (2.9)$$

where K_{fixed}^* is the equivalent fixed-base stiffness of the structure evaluated from:

$$K_{fixed}^* = \overline{M} \left(\frac{2\pi}{T}\right)^2 \quad (2.10)$$

Note that dynamic stiffness modifier, α_{θ} , is also taken as unity. The value of K_{θ} estimated from equation 2.9 reflects the stiffness of the foundation structural elements as implemented in the pushover analysis, so no assumptions of foundation rigidity are required.

The next step is to reduce the period lengthening ratio from the small-displacement condition to the large-displacement (i.e., post-yield) condition (with elongated periods). Taking μ as the expected ductility demand for the system (including structure and soil effects), the effective period lengthening in the post-yield state is computed as:

$$\left(\frac{T_{SSI}}{T}\right)_{eff} = \left\{ 1 + \frac{1}{\mu} \left[\left(\frac{T_{SSI}}{T}\right)^2 - 1 \right] \right\}^{0.5} \quad (2.11)$$

This effective period lengthening ratio can then be used with Figure 2.2 to estimate the foundation damping ratio, β_f .

2.1.3 Response Time-History Procedures

Most of the codes listed at the beginning of this chapter (e.g., ATC-40, FEMA 440, FEMA P-750, ASCE/SEI 41-06, and ASCE/SEI 7-10) are silent on the implementation of SSI effects in response history analyses. Similar to ASCE/SEI 7-10, they permit the use of soil springs in principal, but offer no specific guidance on how the springs should be selected or utilized in a response history analysis.

The Pacific Earthquake Engineering Research Center (PEER) Guidelines for Performance-Based Seismic Design of Tall Buildings (PEER, 2010) recommends a response history sub-structure analysis.

However, the specification of input motions and the distribution of springs and dashpots are simplified to streamline response history analysis, as shown in Figure 2.5.

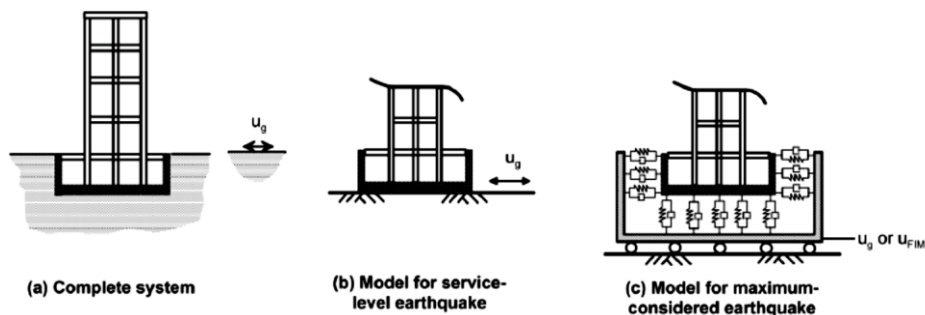


Figure 2.5 - Schematic illustration of a tall building with subterranean levels: (a) complete system; (b) simplified model for service-level earthquake intensity; and (c) simplified foundation model for maximum considered earthquake intensity (from NIST GCR 12-917-21)

Two idealizations of the SSI system are recommended in the PEER Guidelines, depending on the level of earthquake shaking intensity, identified as the: (1) service level earthquake (SLE); and (2) maximum considered earthquake (MCE).

Subterranean levels are modelled in both the SLE and MCE analyses, including the mass, stiffness, and structural capacities of structural elements such as walls, columns, and slabs. Response history analysis for the SLE (Figure 2.5b), is performed with a relatively simple model that omits the surrounding soil and does not include soil springs. Response history analysis for the MCE (Figure 2.5c), is performed with springs and dashpots representing soil-foundation interaction along basement walls and below the base slab. In this case, ground motions are applied to a rigid “bathtub” surrounding the subterranean portions of the structure. In both the SLE and MCE analyses, the motion applied at the base of the model can be either the free field motion (u_g) or the foundation input motion (u_{FIM}). These recommendations are derived largely from the recommendations of *Naeim et al.* (2008).

2.2 Linear Modal Analyses for different RC structures

In order to verify the validity of the simplified formulations suggested by FEMA 450, a sensitivity analysis was performed by means of the software SAP 2000 (*CSI Analysis Reference Manual for SAP2000, ETABS, SAFE and CSiBridge, Computers and Structures Inc., 2013*). In particular, the results obtainable by means of the simplified formulas suggested by FEMA 450 were compared with those obtainable through a simplified modelling of the SSI by means of elastic springs at the base of a certain number of structural models.

In the analyses the influence of the relative soil-structure stiffness and of the ratio between the height of the structure and the plan dimensions of the foundation (\bar{h}/r) was investigated.

It is worth reminding that relative soil-structure stiffness can be expressed as (*Veletsos & Meek, 1974*):

$$\sigma = \frac{V_s T}{\bar{h}} \quad (2.12)$$

in which V_s is the shear wave velocity of the soil, T is the fundamental period of the structure in its fixed base condition and \bar{h} is the effective height of the structure.

As concerns the relative soil-structure stiffness, two different values of the shear wave velocity were assumed for the soil.

In particular:

- $V_s = 800$ m/s (soil type A according to Eurocode 8)
- $V_s = 184$ m/s (soil type C according to Eurocode 8)

As concerns the ratio \bar{h}/r , different heights of the structures were assumed, keeping constant the plan dimensions of the foundation, which was assumed as a mat foundation in all the cases.

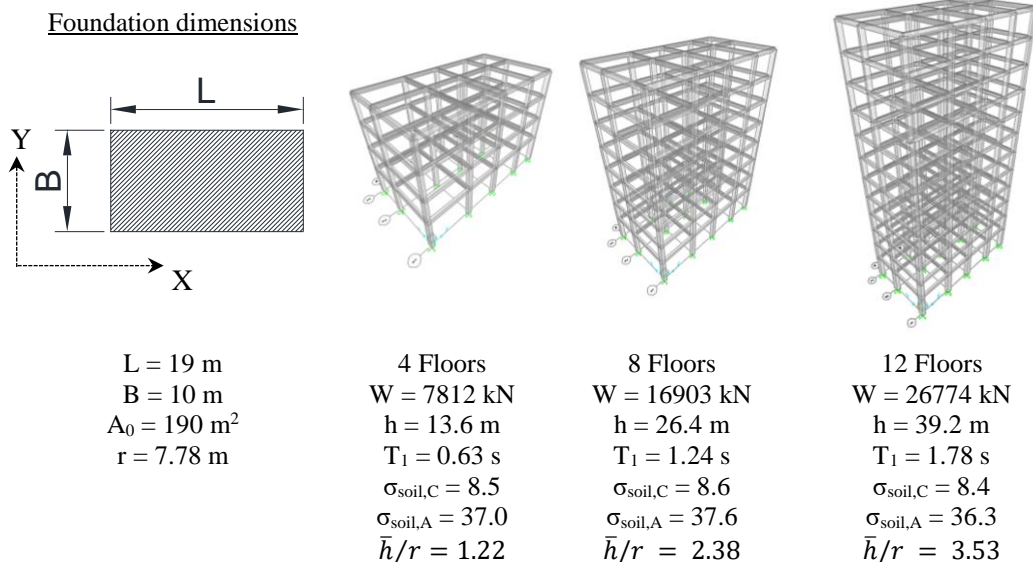


Figure 2.6 - Regular frame buildings

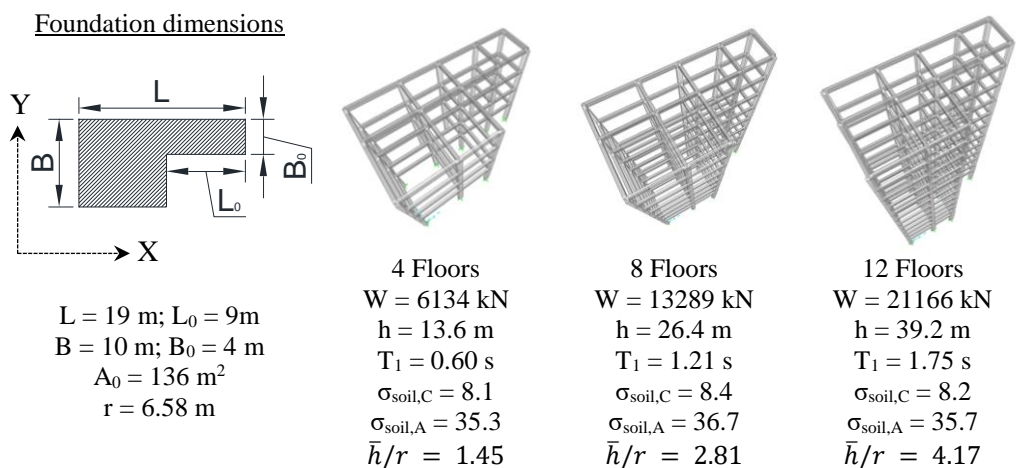


Figure 2.7 - In plane irregular buildings

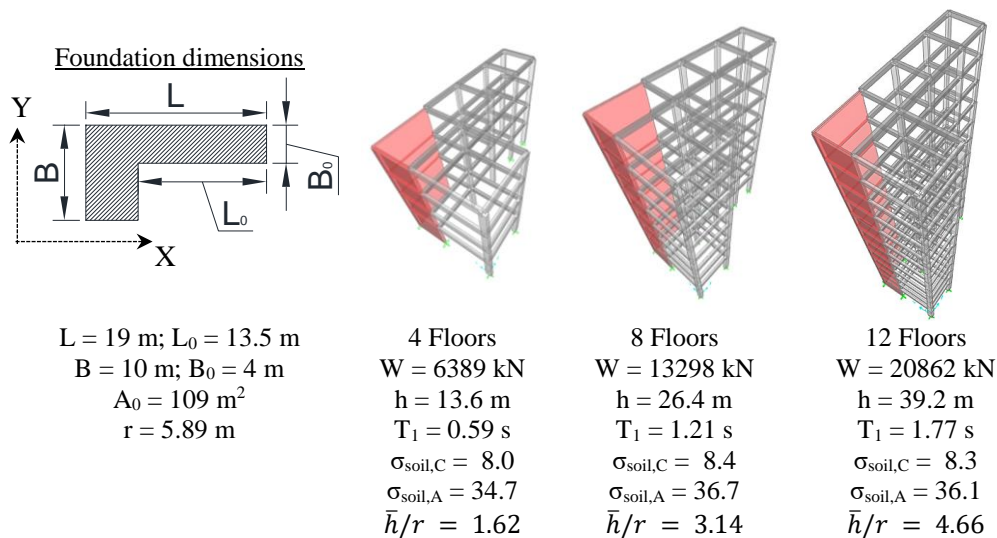


Figure 2.8 - In plane highly irregular buildings

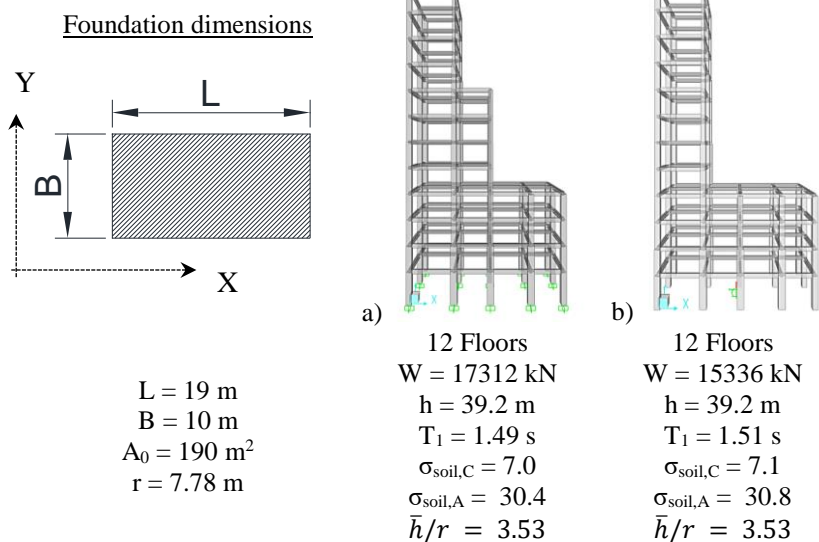


Figure 2.9 - In elevation irregular buildings

From Figure 2.6 to Figure 2.9 all the structures analysed in the study are illustrated, with the indication of:

- the plan dimensions of the mat foundation;
- the total seismic weight of the structure, W ;
- the total height of the structure, h ;
- the value of the first vibration period of the structure on fixed-base, T_1 (obtained through SAP 2000);
- the value of the relative soil-structure stiffness, σ , for the two different soil classes assumed for the study;
- the ratio \bar{h}/r , with \bar{h} assumed equal to $0.7 h$.

It is highlighted that the values of σ were obtained taking into account a reduction of the shear wave velocity of the 30% (PGA = 0.20g).

All the structures were modelled in SAP 2000 assuming that the structural mass at a floor is lumped in the center of gravity of the floor deck (the deck was assumed infinitely rigid in its own plane).

In the next, the calculation performed for the 4 floors frame building of Figure 2.6 is shown in detail.

In the following sections, the results obtained for all the other structural models are briefly illustrated.

2.2.1 Regular Frame Buildings

As shown in Figure 2.6, the four floors building has a total seismic weight of 7812 kN and a height of 13.6 m.

Obtained, by means of SAP 2000, the first two vibration periods of the structure in its fixed-base configuration, equal to $T_1 = 0.63 s$ and $T_2 = 0.57 s$ respectively, it is possible to proceed with the application of the FEMA 450 formulations.

First, the lateral stiffness of the structure is evaluated by means of equation (2.2).

For vibrations in the y direction of the building is obtained:

$$\bar{k}_y = 4\pi^2 \left(\frac{0.7 \cdot 7812}{9.81 \cdot 0.63^2} \right) = 55386 \text{ kN / m}$$

while in the x direction is obtained:

$$\bar{k}_y = 4\pi^2 \left(\frac{0.7 \cdot 7812}{9.81 \cdot 0.57^2} \right) = 67443 \text{ kN / m}$$

For the determination of the foundation's stiffnesses the Commentary FEMA 450-2 was referenced (Section 5.6.2.1.1) in which the following expressions for the calculations of the translational, K_y , and rotational, K_θ , stiffness of the foundation are reported:

$$\begin{aligned} K_y &= \left(\frac{8\alpha_y}{2-\nu} \right) Gr \\ K_\theta &= \left[\frac{8\alpha_\theta}{3(1-\nu)} \right] Gr^3 \end{aligned} \tag{2.13}$$

in which r is an equivalent radius of the foundation, G and ν are the shear modulus and the Poisson's coefficient of the soil, and α_y and α_θ are a-dimensional coefficients depending on the frequency of the seismic excitation.

Neglecting the dependence from frequency of the foundation stiffness it is possible to assume these coefficients equal to the unity.

This assumption can be reasonable for translational stiffness but it is not rigorously correct for the rotational one, for which there is a strong dependence by the frequency.

The formulations provided above, valid for circular foundations, may be applied to mat foundations of arbitrary shapes provided the following changes are made:

- the radius r in the expressions for K_y is replaced by r_a (see equation 2.4), which represents the radius of a disk that has the area, A_o , of the actual foundation;
- the radius r in the expressions for K_θ is replaced by r_m (see equation 2.4), which represents the radius of a disk that has the moment of inertia, I_o , of the actual foundation.

In the examined case, the foundation has an area $A_o = 190 \text{ m}^2$, and:

$$r = r_a = \sqrt{190/3.14} = 7.78 \text{ m}$$

The translational stiffness, equal in both the vibration directions of the building, can be obtained assuming a value of the shear modulus G reduced for the PGA expected to the site and for a value of $\nu = 0.4$ (value suggested by Commentary FEMA 450-2).

For example, for a soil class C ($V_s = 184$ m/s), assuming a unit weight of the soil equal to 14.5 kN/m³ and an expected PGA at the site of $0.20g$, the shear modulus is equal to:

$$G = 0.49 \cdot G_0 = \frac{0.49 \cdot V_s^2 \cdot \gamma}{g} = \frac{0.49 \cdot 184^2 \cdot 14.5}{9.81} = 24417 \text{ kN/m}^2$$

Thus, the translational stiffness is:

$$K_y = K_x = \frac{8Gr_a}{2-\nu} = 949686 \text{ kN/m}$$

As concerns the rotational stiffnesses, it is necessary to evaluate two different values depending on the rocking axis of the foundation.

First, the radius of the foundation is evaluated:

$$r_{mx} = \sqrt[4]{4I_{0,x} / \pi} = 6.70 \text{ m} \quad \text{with} \quad I_{0,x} = L \cdot B^3 / 12 = 1583 \text{ m}^4$$

$$r_{my} = \sqrt[4]{4I_{0,y} / \pi} = 9.24 \text{ m} \quad \text{with} \quad I_{0,y} = B \cdot L^3 / 12 = 5716 \text{ m}^4$$

then the two rotational stiffnesses of the foundation can be defined:

$$K_{\theta,x} = \frac{8Gr_{mx}^3}{3(1-\nu)} = 32661972 \text{ kNm}$$

$$K_{\theta,y} = \frac{8Gr_{my}^3}{3(1-\nu)} = 85540700 \text{ kNm}$$

Finally, the two vibration periods of the system, modified because of SSI, can be evaluated:

$$T_{SSI,1} = T_1 \sqrt{1 + \frac{\bar{k}_y}{K_y} \left(1 + \frac{K_y \bar{h}^2}{K_{\theta,x}} \right)} = 0.69 \text{ s}$$

$$T_{SSI,2} = T_2 \sqrt{1 + \frac{\bar{k}_y}{K_x} \left(1 + \frac{K_x \bar{h}^2}{K_{\theta,y}} \right)} = 0.61 \text{ s}$$

With respect to the fixed-base, increments of 10% and 7% are obtained for the first and second period respectively.

Based on the ratio T_{SS}/T , the modified damping of the system can be calculated through equation (2.3) and Figure 2.2.

For this case, the damping values obtained for the first and second vibration modes are:

$$\beta_1 = 6.7\%$$

$$\beta_2 = 6.2\%$$

with an increment with respect to the usual 5% related to the structural damping only.

In the following Table 2.2 the same results obtained for the 8 and 12 floors buildings are reported.

Moreover, the same tables report the values of the first two periods obtained by means of finite element modelling in SAP 2000.

In particular elastic springs with a stiffness equal to that provided by FEMA 450 were introduced at the base of the FEM models.

These elastic springs were assigned in the center of the foundation after having constrained all the joints at the base of the model by means of a “body” constraint, useful to reproduce the behaviour of an infinitely rigid foundation.

The accordance between the results obtained with the two approaches is very good with differences lower than 3%.

In terms of damping, increasing the ratio \bar{h}/r the modification of the overall damping tends to become negligible.

The same results reported in Table 2.2 are illustrated in Figure 2.10, in which the results obtained for a soil class A are reported, too. It is clear that for very stiff soil, the SSI effects are negligible, in terms of both period and damping.

In addition, in Table 2.4 are reported the first six periods obtained in SAP 2000 in the fixed-base configuration and in the case of elastic spring at the base (calibrated for a soil class C).

It is evident that the SSI tends to influence only the response associated with the first two modes of the structure.

Table 2.2 - Regular building – Soil Type C – Vibration periods

Number of Floors	Fixed Base	FEMA 450	T_{SSI}/T	SAP 2000	T_{SSI}/T
4	$T_1 = 0.63$ s	$T_{SSI,1} = 0.69$ s	1.10	$T_{SSI,1} = 0.71$ s	1.13
	$T_2 = 0.57$ s	$T_{SSI,2} = 0.61$ s	1.07	$T_{SSI,2} = 0.62$ s	1.09
8	$T_1 = 1.24$ s	$T_{SSI,1} = 1.45$ s	1.16	$T_{SSI,1} = 1.47$ s	1.18
	$T_2 = 1.12$ s	$T_{SSI,2} = 1.22$ s	1.09	$T_{SSI,2} = 1.23$ s	1.10
12	$T_1 = 1.78$ s	$T_{SSI,1} = 2.23$ s	1.25	$T_{SSI,1} = 2.25$ s	1.26
	$T_2 = 1.61$ s	$T_{SSI,2} = 1.83$ s	1.13	$T_{SSI,2} = 1.83$ s	1.14

Table 2.3 - Regular building – Soil Type C – Overall Damping

Number of Floors	FEMA 450
4	$\beta_1 = 6.7$ %
	$\beta_2 = 6.2$ %
8	$\beta_1 = 5.7$ %
	$\beta_2 = 5.6$ %
12	$\beta_1 = 5.3$ %
	$\beta_2 = 5.5$ %

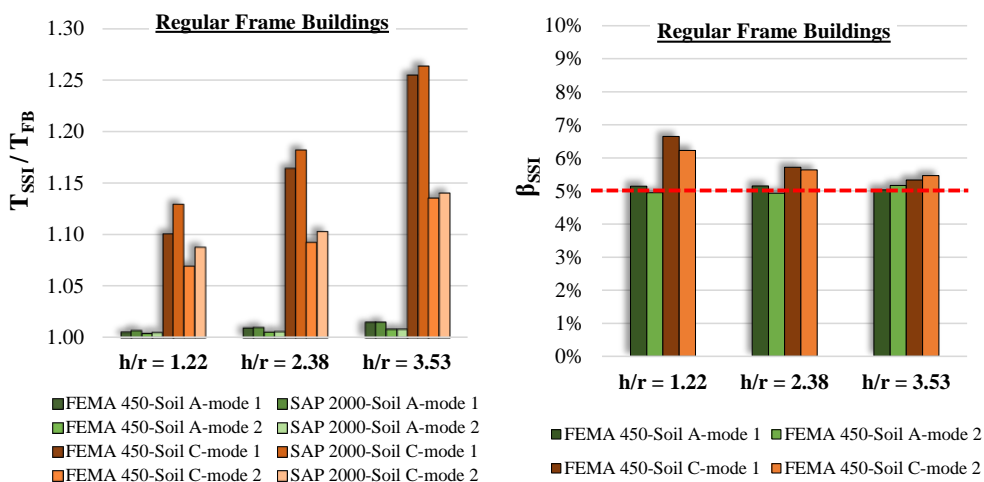


Figure 2.10 - Results for Regular Frame Buildings

Table 2.4 - Regular frame buildings: SSI effect on superior modes (soil class C)

Mode	4 Floors		8 Floors		12 Floors	
	<i>T</i>	<i>T_{SSI}</i>	<i>T</i>	<i>T_{SSI}</i>	<i>T</i>	<i>T_{SSI}</i>
	[s]	[s]	[s]	[s]	[s]	[s]
1	0.63	0.71	1.24	1.47	1.78	2.25
2	0.57	0.62	1.12	1.23	1.61	1.83
3	0.44	0.46	0.88	0.90	1.25	1.27
4	0.20	0.21	0.41	0.42	0.59	0.61
5	0.19	0.20	0.37	0.38	0.56	0.57
6	0.14	0.15	0.29	0.30	0.44	0.45

2.2.2 In plane irregular buildings

Figure 2.11 shows the results obtained for the buildings of Figure 2.7 are shown.

The mass modal percentage related to the first vibration period vary from the 80% (4 floors) to the 70% (12 floors) of the total mass.

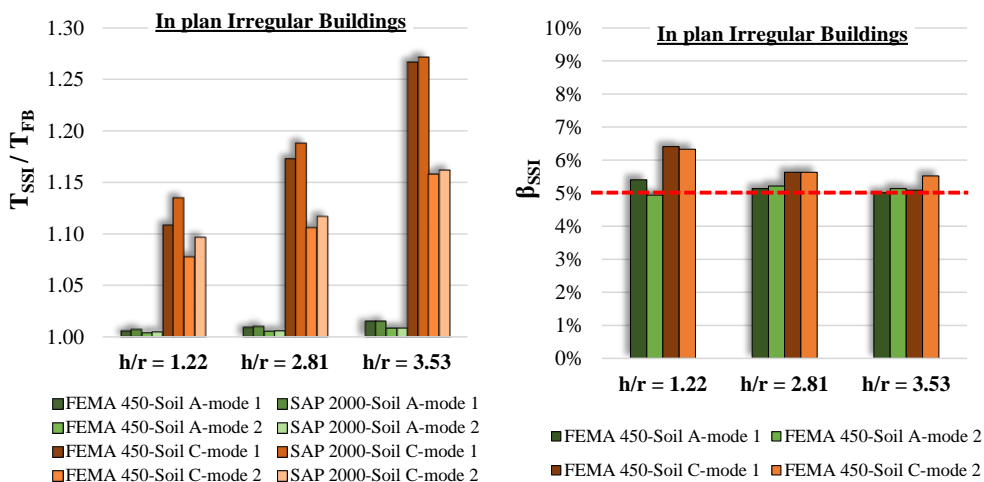


Figure 2.11 - Results for in plan irregular buildings

The ratio T_{SSI}/T increase with the ratio \bar{h}/r and the results obtained by means of FEMA 450 are in good agreement with those obtained by SAP 2000 (differences lower than 2.5% in all the cases).

In terms of overall damping, only in case of 4 floor building founded on soft soil (soil class C) a not negligible increase can be observed (values greater than 6%).

From Table 2.5 can be observed that SSI affects only the first two vibration modes of the structures.

Table 2.5 - In plan irregular buildings: SSI effect on superior modes (soil class C)

Mode	4 Floors		8 Floors		12 Floors	
	T [s]	T_{SSI} [s]	T [s]	T_{SSI} [s]	T [s]	T_{SSI} [s]
1	0.60	0.69	1.21	1.44	1.75	2.23
2	0.55	0.60	1.09	1.22	1.57	1.83
3	0.41	0.43	0.84	0.86	1.20	1.22
4	0.20	0.21	0.40	0.41	0.59	0.60
5	0.18	0.19	0.36	0.37	0.54	0.55
6	0.13	0.14	0.27	0.28	0.41	0.42

2.2.3 In plane highly irregular buildings

In Figure 2.12 the results obtained for the buildings of Figure 2.8 are reported.

The mass modal percentage related to the first vibration period is equal, on average, to the 45% of the total mass.

The accordance between FEMA 450 and SAP 2000 is good on the first vibration period (differences lower than 1%), but there are differences up to the 15% as concerns the evaluation of the second period.

Moreover, increasing the ratio \bar{h}/r , the lengthening ratio of the second period tend to decrease, contrarily to the other cases.

In terms of damping, for both the 4 and 8 floors buildings, it is possible to observe not negligible increases of the damping factor associated to the first mode (6.7% and 5.9% respectively).

For the 4 floor building an increase up to 9.5% of the damping factor can be observed on the second vibration mode.

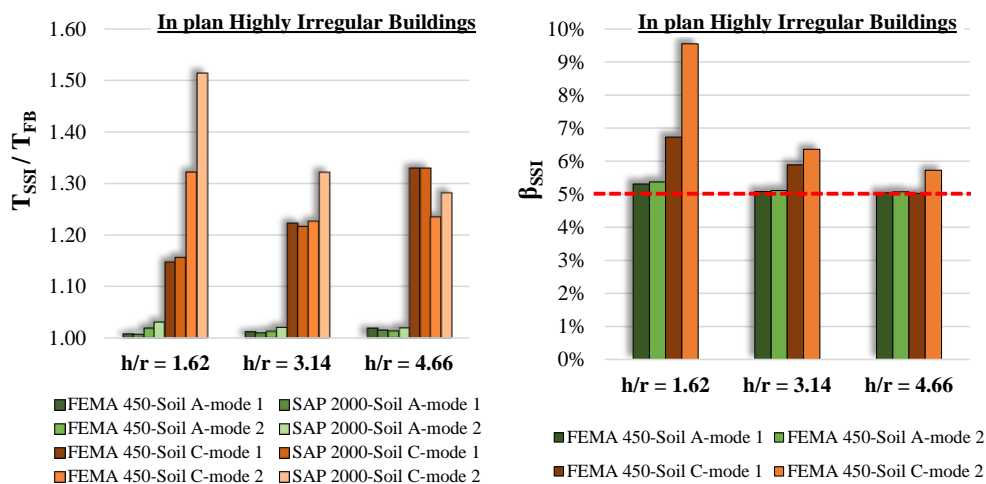


Figure 2.12 - Results for in plan highly irregular buildings

In Table 2.6 the values of the first six period of vibration, obtained by means of SAP 2000, are reported for the fixed-base configuration and with elastic springs at the base.

It can be observed that in this case the SSI affect the superior modes too.

The simplified formulations suggested by FEMA 450 seem not able to capture adequately the SSI effects.

Table 2.6 - In plan highly irregular buildings: SSI effect on superior modes (soil class C)

Mode	4 Floors		8 Floors		12 Floors	
	T [s]	T_{SSI} [s]	T [s]	T_{SSI} [s]	T [s]	T_{SSI} [s]
1	0.59	0.68	1.21	1.47	1.77	2.35
2	0.27	0.40	0.74	0.97	1.27	1.62
3	0.19	0.27	0.39	0.58	0.69	0.98
4	0.12	0.20	0.35	0.40	0.58	0.59
5	0.10	0.11	0.21	0.22	0.32	0.36
6	0.06	0.11	0.17	0.21	0.32	0.33

2.2.4 In elevation irregular buildings

Figure 2.13 reports the results obtained for the structures depicted in Figure 2.9.

The FEMA 450 formulations provide results in good agreement with SAP 2000 on both the first and second vibration period.

It is worth to note that in the case of buildings with a not regular distribution of mass and stiffness along the height of the structure, the FEMA 450 (sections 5.3.4 and 5.8.3.1) suggest calculating the effective weight, \bar{W} , and the effective height of the structure, \bar{h} , by means of relations:

$$\bar{W}_m = \frac{\left(\sum_{i=1}^n w_i \varphi_{i,m} \right)^2}{\sum_{i=1}^n w_i \varphi_{i,m}^2} \quad \bar{h}_m = \frac{\sum_{i=1}^n w_i \varphi_{i,m} h_i}{\sum_{i=1}^n w_i \varphi_{i,m}} \quad (2.14)$$

in which:

- w_i is the seismic weight at the i -th floor;
- $\varphi_{i,m}$ is the displacement at the i -th floor due to the m -th vibration mode of the structure on fixed-base;
- h_i is the distance from foundation level of the mass at the i -th level;

As concerns the damping, can be noted that the differences with respect to the fixed-base are negligible.

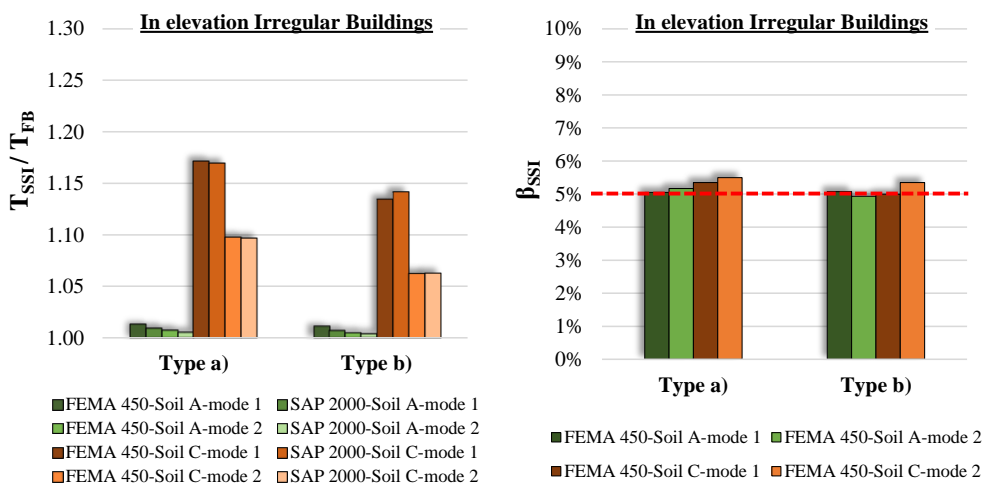


Figure 2.13 - Results for in elevation irregular buildings

The results in Table 2.7 demonstrate that even in this case the SSI affects only the first two vibration modes of the structures.

Table 2.7 - In elevation irregular buildings: SSI effect on superior modes (soil class C)

Mode	Type a)		Type b)	
	T [s]	T_{SSI} [s]	T [s]	T_{SSI} [s]
1	1.49	1.74	1.51	1.72
2	1.30	1.43	1.49	1.58
3	0.68	0.72	0.75	0.76
4	0.58	0.60	0.56	0.59
5	0.54	0.55	0.55	0.57
6	0.40	0.42	0.41	0.45

2.2.5 Effect of concrete cracking

In Figure 2.14 the results obtained for the regular frame buildings (see Figure 2.6) are reported in the case of a 50% reduction in stiffness of the structural elements to take into account the concrete cracking. The results refers to a soil type C (according to EC8) for which the SSI effects are more relevant.

In terms of lengthening of vibration period, a reduction of the ratio T_{SSI}/T can be observed with respect to the case in which the concrete cracking was neglected.

This reduction reach the 11% for the first period and the 6% for the second (8 Floor building).

Because of the reduction in lengthening ratio, the overall damping of the system will have a reduction too with respect to the “un-cracked” model.

This reduction can reach the 12% for the damping associated with the first mode and the 3% for that associated to the second mode (4 floor building).

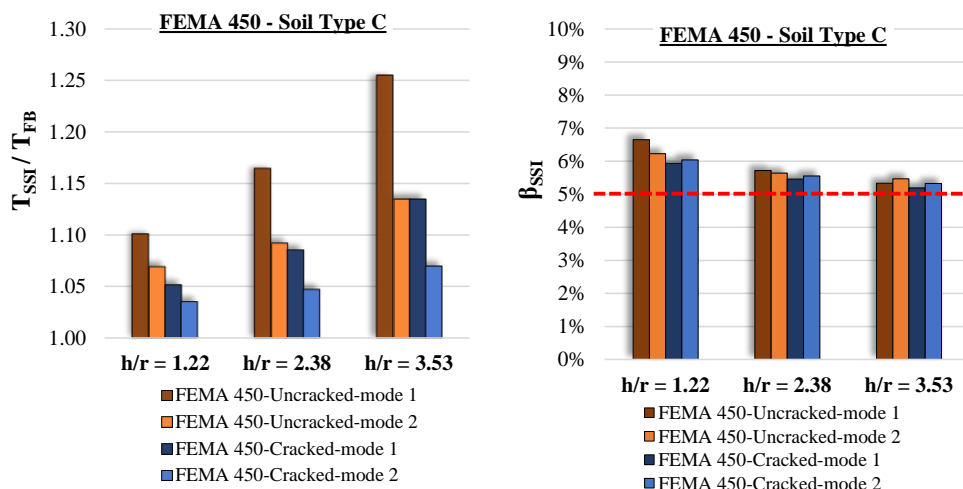


Figure 2.14 - Regular buildings: effect of concrete cracking

2.2.6 Effect of single footings

In Figure 2.15 the results obtained for the buildings of Figure 2.6, but assuming that at the base of the columns there are simple footings (square footings with a side of 2 m) are reported.

The formulae suggested by FEMA 450 for the period are evaluated determining the stiffnesses of the foundation as:

$$\begin{aligned}
 K_y &= \sum k_{yi} \\
 K_\theta &= \sum k_{vi} y_i^2 + \sum k_{\theta i}
 \end{aligned} \tag{2.15}$$

in which k_{yi} , k_{vi} and $k_{\theta i}$ are the horizontal translational, vertical translational and rotational stiffness of the single footing respectively, that can be determined based on literature formulations like those provided by *Gazetas* (see Table A. 1 in Annex A).

The application of equations (2.8) equal to assume an infinitely rigid behaviour of the foundation. This assumption was deliberately not modelled in SAP 2000.

The analyses confirmed the trend observed in the case of mat foundation, with lengthening ratios increasing with the height of the structure, but lower than those obtained for mat foundations, with a maximum value of 1.12 for the 12 floors

building. Even for the overall damping, it is possible to observe lower values than those obtained for a mat foundation (6% for 4 floors building).

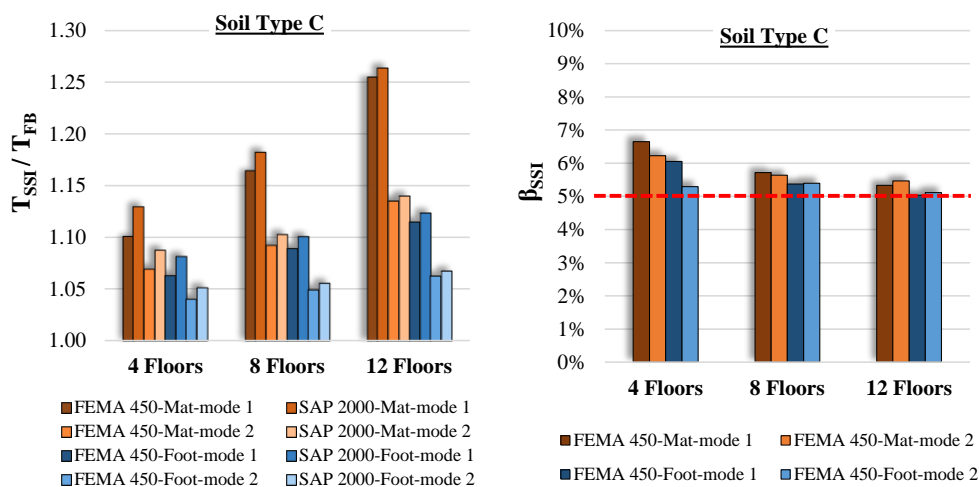


Figure 2.15 - Regular buildings: single footings

2.3 Non Linear Static Analyses for existing buildings

In order to investigate the influence of Soil-Structure Interaction on the ratios Capacity/Demand (C/D), that can strongly affect the design strategies of seismic retrofitting interventions for existing buildings, two moment resisting frames of 4 and 8 floors, designed without any seismic provision, were analysed.

The two buildings, illustrated in Figure 2.16, have some typical features of existing reinforced concrete buildings:

- structural elements designed for vertical loads only and without any resistance's hierarchy rule;
- low dissipative capacity in the nodal zone;
- no linking elements in the orthogonal direction to the main frames;
- single foundation footings (no linking beams).

They have the same geometry in plan, that is shown in Figure 2.16c.

The total floor load was assumed equal to 7.0 kN/m^2 .

The cubic compression resistance of concrete was assumed, for the design, equal to $R_c = 30 \text{ MPa}$.

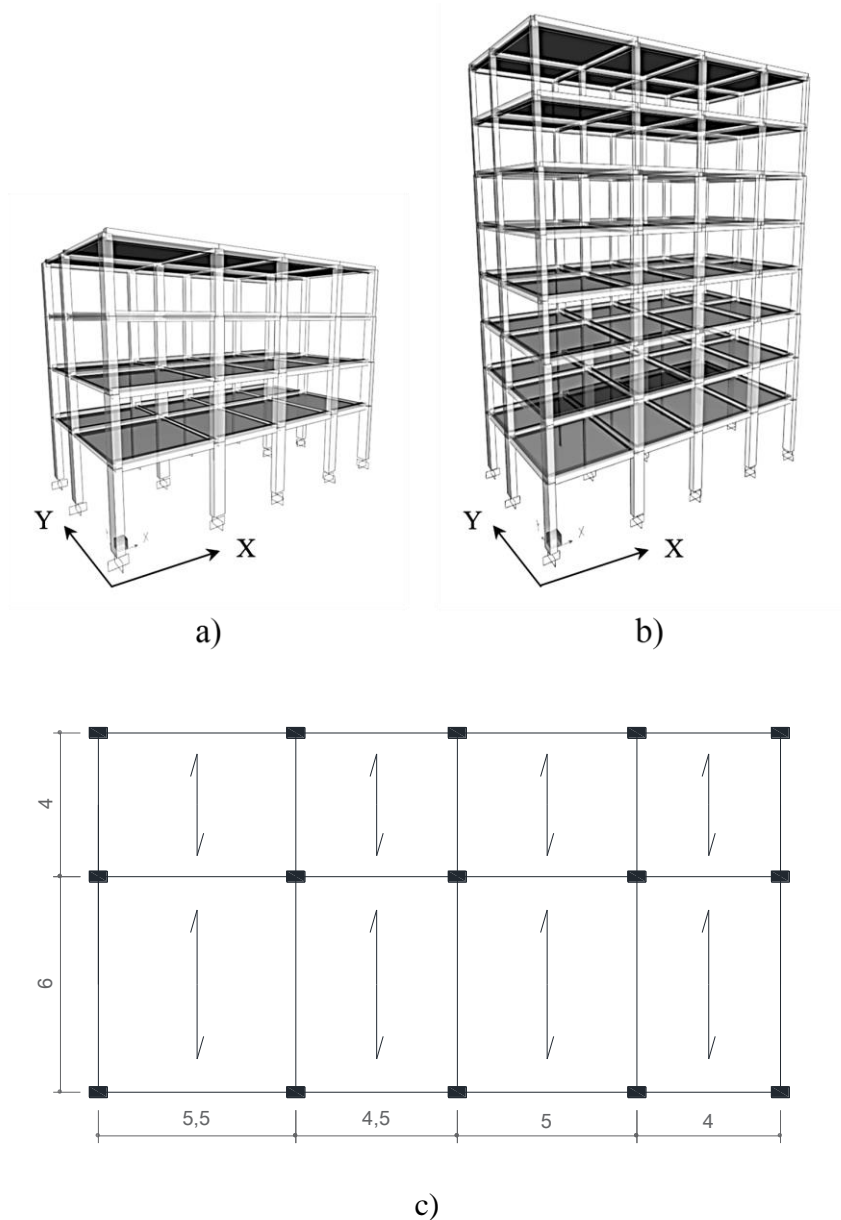


Figure 2.16 - Reference buildings: a) 4 Floors building, b) 8 Floors building, c) Plan Dimensions

The structural elements were designed with elastic calculations based on the allowable stress method, according to what suggested by Italian Ministerial Decree of the 30th of May 1972 (D.M. 1972).

The beams were designed in pure flexure with a value of the allowable compression stress in the concrete of 9.75 MPa, according to the relation:

$$\sigma_{a,c} = 60 + \frac{R_c - 150}{4} \quad (\text{with } R_c \text{ in kg / cm}^2) \quad (2.16)$$

The columns were designed in pure compression with a value of the maximum allowable compression stress in the concrete of 6.825 MPa, equal to the 70% of $\sigma_{a,c}$.

The structural elements have the dimensions reported in Table 2.8 and in

Table 2.9 for the 4 floors building and for the 8 floors building, respectively.

In the tables, the amount of longitudinal reinforcement is reported too, that was established based on the prescriptions of the code. In particular, the longitudinal reinforcements must have an area not lower than 0.6% and not greater than 5% of the concrete area strictly necessary to support the vertical load, based on the allowable stress adopted, and not lower than the 0.3% of the effective area of concrete. In addition, the rebar diameter must be not smaller than 12 mm.

The structural non-linear behaviour was modelled in SAP 2000 following a lumped plasticity approach.

Interacting M2-M3 hinges (*Computers and Structures Inc.*, 2013), defined for an axial load corresponding to that due to vertical loads only, were assigned at the ends of structural members.

Table 2.8 - 4 Floors building: structural members

Floor	Columns / Beams	N _{max} [kN]	B [m]	H [m]	$\sigma / \sigma_{a,c}$ [-]	Reinforcements
1	Columns	876	0.40	0.70	0.46	12 Φ 12 = 1356 mm ²
2	Columns	657	0.40	0.70	0.34	12 Φ 12 = 1356 mm ²
3	Columns	438	0.40	0.60	0.27	10 Φ 12 = 1130 mm ²
4	Columns	219	0.40	0.50	0.16	8 Φ 12 = 904 mm ²
1	Beams	-	0.30	0.50	-	(M-) 4 Φ 20 = 1256 mm ² (M+) 2 Φ 20 = 1256 mm ²
2,3,4	Beams	-	0.30	0.45	-	(M-) 4 Φ 20 = 1256 mm ² (M+) 4 Φ 20 = 1256 mm ²

Table 2.9 - 8 Floors building: structural members

Floor	Columns / Beams	N _{max} [kN]	B [m]	H [m]	σ / σ _{a,c} [-]	Reinforcements
1	Columns	1751	0.40	0.70	0.92	12 Φ16 = 2412 mm ²
2	Columns	1532	0.40	0.70	0.80	12 Φ16 = 2412 mm ²
3	Columns	1313	0.40	0.70	0.69	12 Φ16 = 2412 mm ²
4	Columns	1094	0.30	0.60	0.89	10 Φ14 = 1539 mm ²
5	Columns	876	0.30	0.60	0.71	10 Φ14 = 1539 mm ²
6	Columns	657	0.30	0.60	0.53	10 Φ14 = 1539 mm ²
7	Columns	438	0.30	0.30	0.71	8 Φ12 = 904 mm ²
8	Columns	219	0.30	0.30	0.36	8 Φ12 = 904 mm ²
1	Beams	-	0.30	0.50	-	(M-) 4 Φ20 = 1256 mm ² (M+) 4 Φ20 = 1256 mm ²
2÷8	Beams	-	0.30	0.45	-	(M-) 4 Φ20 = 1256 mm ² (M+) 4 Φ20 = 1256 mm ²

The behaviour of plastic hinges was defined in terms of moment-curvature relation. Thus, a length of plastic hinge was defined, based on the equation (*CEN, 2004*):

$$L_{pl} = 0.1L_v + 0.17h + \frac{0.24d_{bl}f_y}{\sqrt{f_c}} \quad (2.17)$$

where:

- L_v is the shear span of the member;
- h is the height of the section;
- d_{bl} is the average diameter of the longitudinal reinforcements;
- f_c and f_y are the maximum compression stress of concrete and the yielding stress of steel respectively (expressed in MPa).

As concern the materials constitutive laws:

- for concrete a parable-rectangle law was assumed with a maximum deformation equal to 3.5‰ and a maximum compression stress equal to 14.17 MPa (assuming that from tests a compressive strength of 17 MPa was found and assuming a confidence factor equal to 1.2);
- for steel an elasto-perfectly plastic law was assumed with a yielding stress equal to $440/1.2 = 367$ MPa (steel grade FeB 44 k).

The foundations (square single footings of side 2 m for the 4 floors building and 3 m for the 8 floors building) were modelled by means of elastic springs. A set of 6 elastic springs was assigned at each base node of the 1st floor columns.

The foundation stiffnesses were calibrated based on Gazetas formulations (see Table A. 1) for $V_s = 184$ m/s (soil type C according to Eurocode 8) and for a PGA expected at the site of 0.262 g (reduction coefficient = 0.70, see Table 2.1).

In Figure 2.17 the results of preliminary linear modal analyses are shown.

FEMA 450 formulations provide, for the 4 floor building, lower values of the first two vibration periods of the system with respect to those provided by numerical analysis (differences up to 15% in terms of T_{SSI}/T).

This difference is probably related to the greater structural irregularity.

For the 8 floors building, characterized by a lower structural irregularity, the differences are negligible (2% in terms of ratio T_{SSI}/T).

As concerns the damping, the indications obtained for regular buildings were confirmed, with an increase, for the 4 floors building, of damping factor up to 7% for the first mode and up to 6% for the second mode.

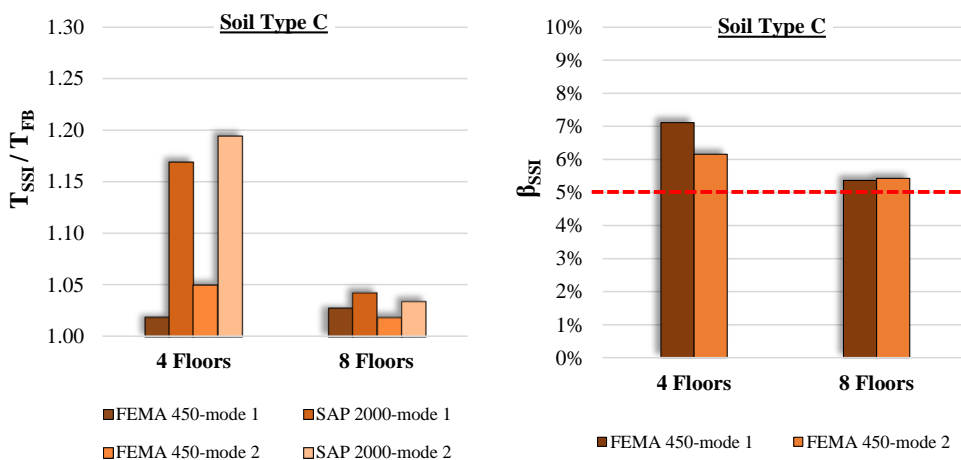


Figure 2.17 - Existing buildings

The non-linear static analyses were performed following both the strategies proposed by the Capacity Spectrum (CSM) Method (FEMA 440 – ATC 40) and by the N2 Method (*Fajfar, 2000*).

The CSM is an iterative procedure in which, once evaluated the capacity curve of the structure and converted it in a capacity spectrum (see Chapter 8 of ATC 40 for more details about procedure), it is compared with the demand spectrum.

The intersection of the two curves determine the Performance Point, based on which it is drawn a bi-linear representation of the capacity curve.

Based on the bi-linear capacity curve, an equivalent viscous damping can be obtained (see Figure 2.18) to reduce the initial elastic demand (obtained for a viscous damping of 5%) and obtain a new performance point. The procedure is repeated until the difference between the demands in terms of spectral displacement obtained in two subsequent iterations does not exceed a certain tolerance (usually 5%).

With the N2 Method, once defined the capacity curve by means of a Push Over analysis and converted it in that of an equivalent SDOF system, it is possible to obtain a bi-linear representation of the same capacity curve (see Figure 2.19).

Based on the capacity curve of the equivalent elasto-plastic SDOF system, it is possible to obtain, under the hypothesis of equal displacement or equal energy, the inelastic demand in terms of spectral displacement.

Concerning the CSM, it is worth to note that, for the buildings under investigation, the capacity curve does not intercept the elastic demand corresponding to a peak ground acceleration equal to 0.262g, so the intersection between demand and capacity can be obtained only by reducing the maximum ground acceleration.

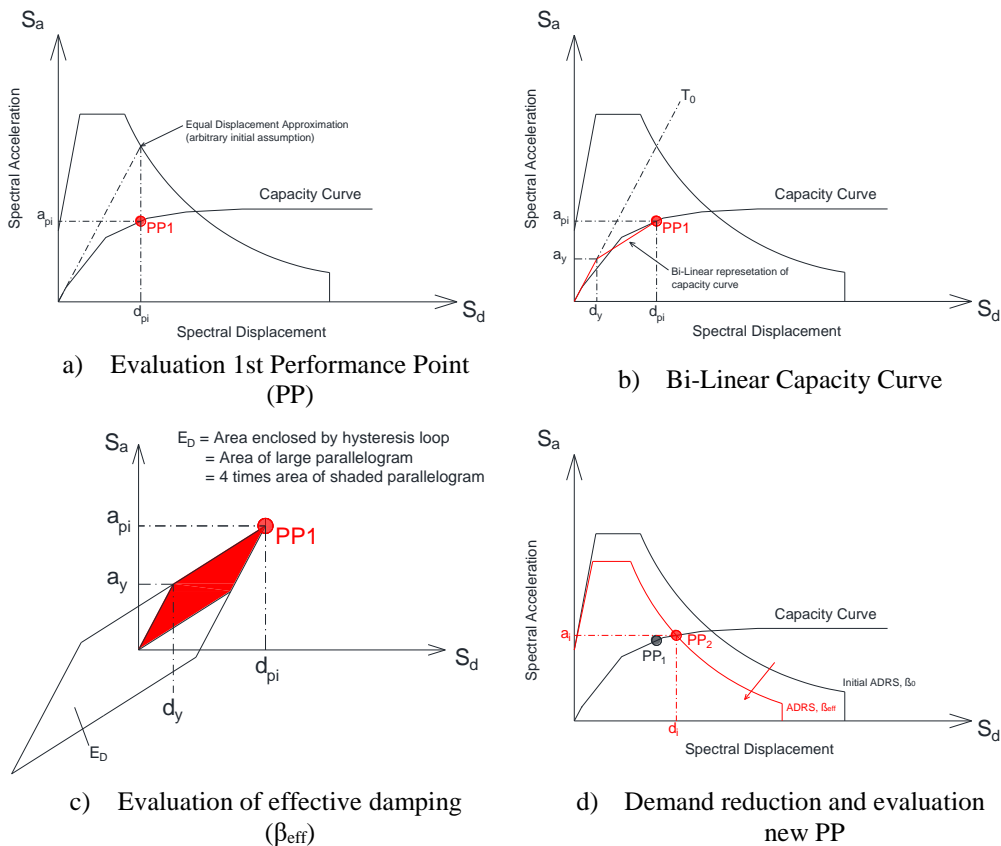


Figure 2.18 - Capacity Spectrum Method

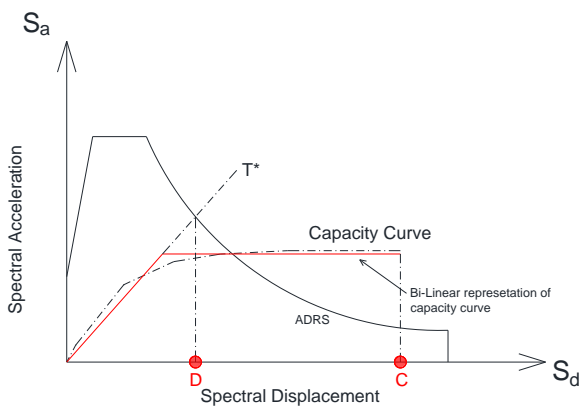


Figure 2.19 - N2 Method

Capacity and Demand are thus expressed in terms of maximum ground acceleration (see Table 2.10).

In the procedure, the demand spectrum was reduced by means of an equivalent viscous damping defined as (see ATC 40, Chapter 8):

$$\begin{aligned}\beta_{eq} &= k\beta_0 + 0.05 && \text{for fixed base system} \\ \beta_{eq} &= k\beta_0 + \frac{0.05}{(T/T)^3} + \beta_f && \text{for flexible base system}\end{aligned}\quad (2.18)$$

where β_0 is the hysteretic damping of the system represented as equivalent viscous damping, calculated as (Chopra, 1995):

$$\beta_0 = \frac{1}{4\pi} \frac{E_D}{E_{s0}} \quad (2.19)$$

where E_D is the energy dissipated by damping and E_{s0} is the maximum strain energy.

E_D is the energy dissipated by the structure in a single cycle of motion, that is, the area enclosed by a single hysteresis loop and can be calculated as (see ATC 40):

$$E_D = 4(a_y d_{pi} - d_y a_{pi}) \quad (2.20)$$

E_{s0} is the maximum strain energy associated with that cycle of motion, that is:

$$E_{s0} = \frac{1}{2} a_{pi} d_{pi} \quad (2.21)$$

Thus, β_0 can be expressed as:

$$\beta_0 = \frac{1}{4\pi} \frac{4(a_y d_{pi} - d_y a_{pi})}{a_{pi} d_{pi} / 2} = \frac{2}{\pi} \frac{a_y d_{pi} - d_y a_{pi}}{a_{pi} d_{pi}} = \frac{0.637(a_y d_{pi} - d_y a_{pi})}{a_{pi} d_{pi}} \quad (2.22)$$

and when β_0 is expressed in percent critical damping:

$$\beta_0 = \frac{63.7(a_y d_{pi} - d_y a_{pi})}{a_{pi} d_{pi}} \quad (2.23)$$

In equations 2.17 a damping modification factors, k , appears, that is a measure of the capacity of the structure to dissipate energy by hysteresis. It depends on the structural behaviour of the building, which in turn depends on the quality of the seismic resisting system and the duration of ground shaking. For existing

buildings with poor seismic details, like those examined in this study, ATC 40 suggest a k value of 0.33.

Figure 2.20 shows the results obtained by means of the application of the CSM.

It can be observed that, as expected, SSI is more beneficial in the case of the 4 floors building, with increase of the ratio C/D , with respect to the fixed-base configuration, of the 29% in the case of analysis in X direction and of 24% for analysis in Y direction.

The analyses performed for the 8 floors building show lower increases of the ratio C/D with respect to the fixed-base configuration (6% for analyses in X direction and 12% for analyses in the Y direction).

Figure 2.21 show the results obtained applying the N2 Method.

The ratios C/D (reported in Table 2.11) are expressed in terms of spectral displacements.

It is worth to note that in this case the demand spectrum was reduced, for flexible-base systems, only based on the damping provided by equation 2.5.

Even in this case SSI affects more the ratios C/D obtained for the 4 floors building with increases, with respect to the fixed-base configuration, of the 34% for analysis in X direction and of 19% for analysis in Y direction.

It is worth to note that in the graphs the displacement reported on the abscissa should be intended as total displacement, therefore inclusive of both the top displacement due to the foundation motions and of the flexural displacement due to the deformability of the structure.

However, it was verified (see Figure 2.22) that the top displacement due to foundation motions is in general negligible (~ 2% of total top displacement) with respect to that due to the structural deformability (~ 98% of total top displacement).

Table 2.10 - Capacity Spectrum Method: Results

Building	Model	Dir.	ζ_{eq} [%]	PGA _D [g]	PGA _C [g]	C/D [-]
4 Floors	Fixed Base	X	16	0.262	0.170	0.65
		Y	12	0.262	0.145	0.55
	With SSI	X	17	0.262	0.220	0.84
		Y	14	0.262	0.180	0.69
8 Floors	Fixed Base	X	10	0.262	0.135	0.52
		Y	13	0.262	0.181	0.69
	With SSI	X	10	0.262	0.145	0.55
		Y	13	0.262	0.202	0.77

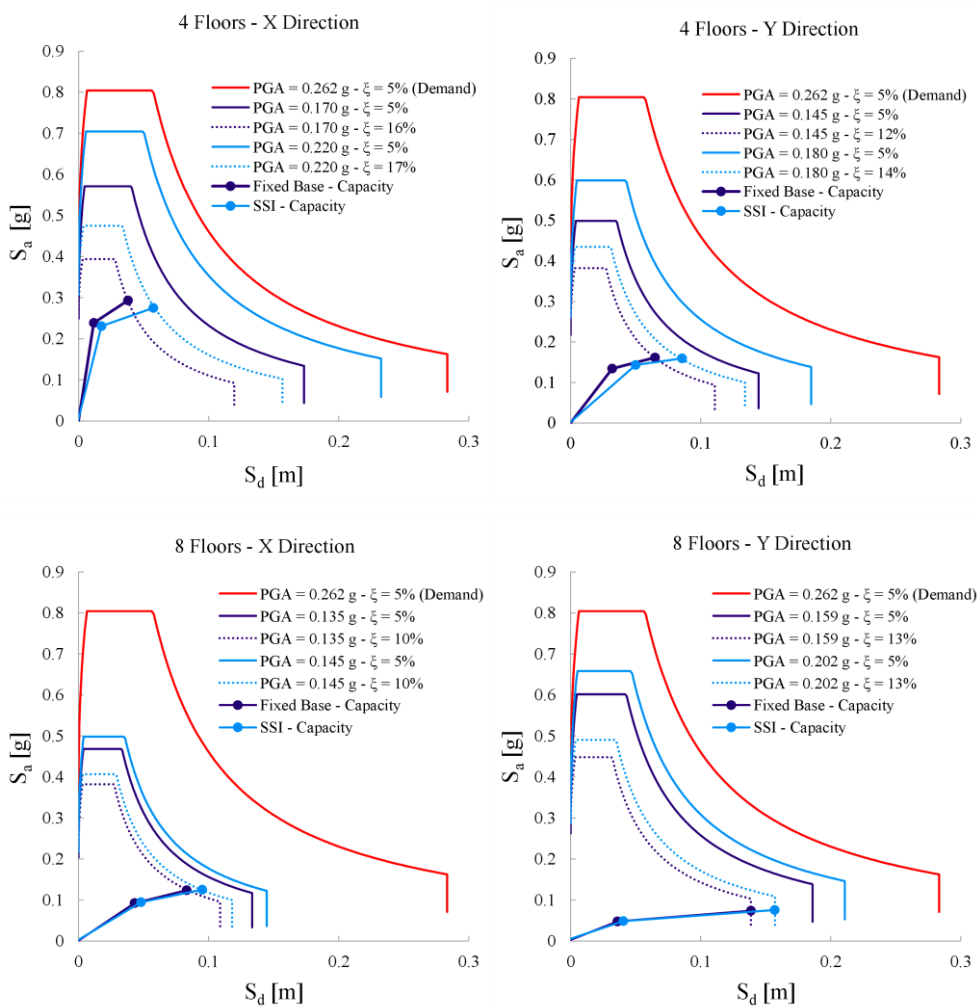


Figure 2.20 - Capacity Spectrum Method: Results

Table 2.11 - N2 Method – Results

Building	Model	Dir.	T* [s]	ξ [%]	S _{dB} [m]	S _{dc} [m]	C/D
4 Floors	Fixed Base	X	0.45	5	0.051	0.041	0.80
		Y	0.98	5	0.105	0.065	0.62
	With SSI	X	0.57	7	0.060	0.064	1.07
		Y	1.17	6	0.116	0.086	0.74
8 Floors	Fixed Base	X	1.38	5	0.149	0.085	0.57
		Y	1.94	5	0.204	0.139	0.68
	With SSI	X	1.44	5	0.155	0.097	0.62
		Y	2.02	5	0.217	0.157	0.73

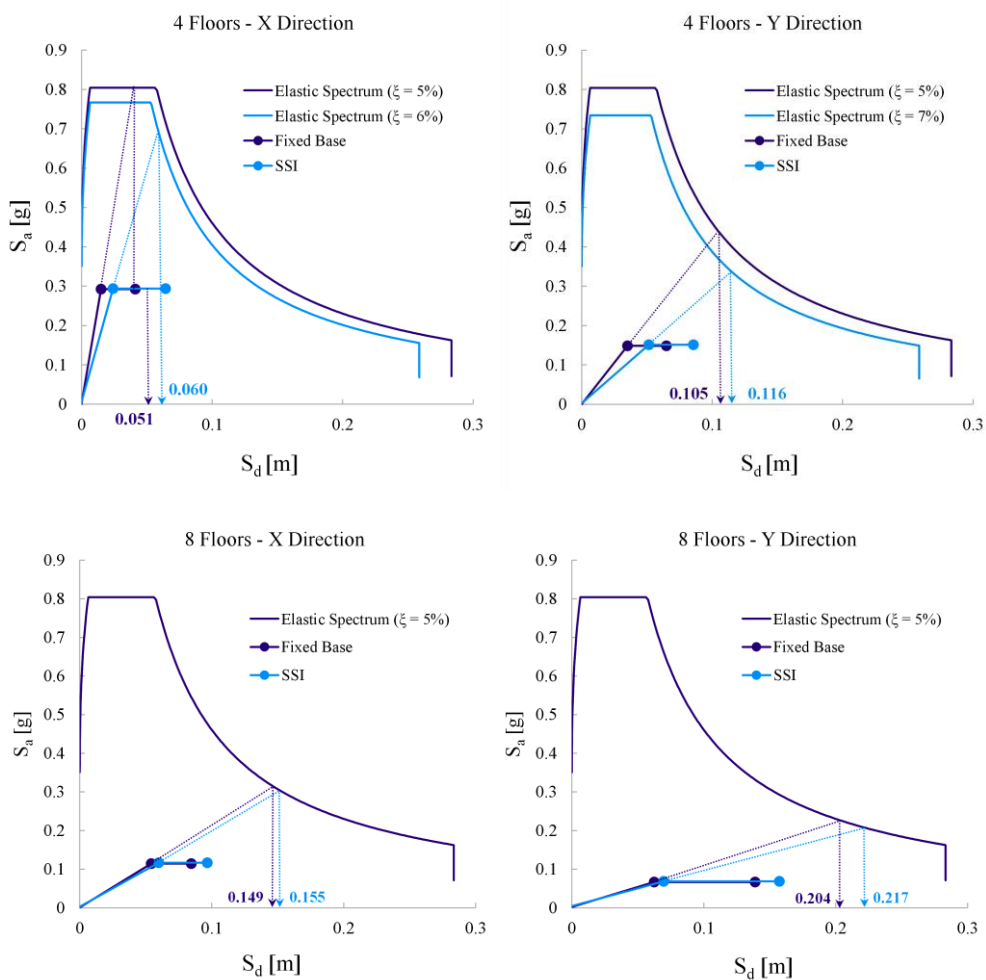


Figure 2.21 - N2 Method: Results

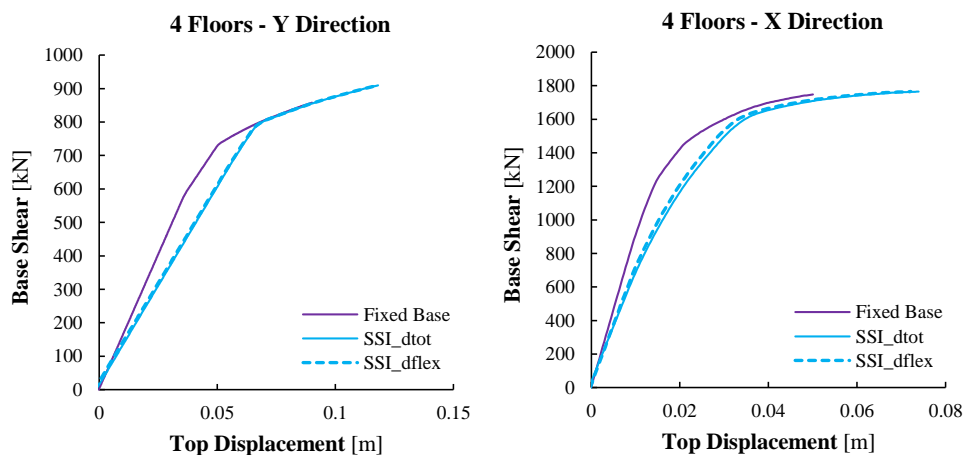


Figure 2.22 - Influence of foundation motions on capacity curve

2.4 Concluding remarks

Aiming to evaluate the influence of:

- the ratio between the height of the structure and the plan dimensions of the foundation;
- the relative soil-structure stiffness

on the entity of soil-structure interaction (SSI) effects, a sensitivity analysis was performed, by means of linear modal analyses, for reinforced concrete structures (regular and not regular) with an increasing number of floors (4, 8, 12) and for two different soil classes (soil class A and C according to Eurocode 8).

In addition, linear modal analyses and non-linear static analyses were performed for two reinforced concrete existing buildings of 4 and 8 floors, designed without seismic provisions, with the aim to evaluate the influence of SSI on the ratios Capacity/Demand (C/D), that can strongly affect the design strategies of seismic retrofitting interventions.

The modal analyses showed that:

- increasing the height of the structure the lengthening of the vibration period tends to increase (up to 30% for 12 floors buildings founded on soft soils);

- for short buildings the period lengthening become less important, but the increase of the damping factor of the system is greater (up to 7%);
- for stiff soils the SSI effects are always negligible;
- concrete cracking, reducing the overall stiffness of the structure, tends to reduce the SSI effects, both in terms of period lengthening and in terms of damping.

Moreover, the simplified formulations provided by FEMA 450 provide estimations of the first two vibration periods lengthening in good agreement, except in the case of very irregular buildings (buildings with shear walls or existing buildings) with those achievable by means of a FEM modelling, with elastic springs, of the SSI effects.

Non-linear static analyses showed that the introduction at the base of a structural model of elastic springs can increase the ratio C/D with respect to a common fixed-base configuration.

This effect seems to be more important for short structures, for which the reduction of the seismic demand due to the increase of the overall damping of the system is added to the reduction of the demand due to the period lengthening.

3 Numerical Modelling for Dynamic Analyses

In the present chapter, the numerical models adopted for dynamic analyses shown in next Chapter 4 are illustrated.

The numerical models were implemented with the OpenSees software (*Mazzoni et al., 2009*), a platform designed around an object-oriented architecture facilitating the use of existing features and the development of new components and modulus, making it particularly attractive to model complex structural or geotechnical systems subjected to static or dynamic loads. An extensive library of material models is available, supporting also a wide range of solution procedures and computation models.

Firstly, the numerical modelling adopted for the reference structures (described in next Chapter 4) is presented.

Secondly, the modelling of the Soil Structure Interaction (SSI) is described.

It is worth reminding that the possible approaches for the modelling of SSI are divided in two big classes:

- the substructure approaches;
- the direct approaches.

In the substructure approaches, the kinematic interaction and the inertial interaction are separately evaluated and their effects are then summed (rigorously only under the hypothesis of linear elastic behaviour of all the components of the system).

In the direct approaches, the soil and the structure are modelled together in a single step to take better into account the interaction between the soil and the

structure. They are obviously more refined but require a high computational effort.

The substructure approaches, which permit to model the presence of the soil in a simplified way by means of springs and dashpots, are usually preferred in engineering practice.

In the present work, both a sub-structure approach and a direct approach were used for numerical analyses.

It is highlighted that in the implemented sub-structures approach, the kinematic interaction was completely neglected, while in the direct approach it was implicitly taken into account.

The type of foundation (shallow foundations resting on the surface of a half-space) assumed for the reference structures anyway guaranteed the coherence between the two modelling approaches.

In this case, in fact, the kinematic interaction effects are always negligible.

3.1 Structural modelling

As concerns the modelling of the reference structures, lumped mass models were adopted, in which the structural mass was concentrated in the nodes of the computational model.

Beams and columns were modelled as '*beamWithHinges*' elements, which consider plasticity to be concentrated over specified hinge lengths at the element ends.

This type of element divides the element in three parts: two hinges at the ends and a linear elastic region in the middle (see Figure 3.1).

The hinges are defined by assigning to each one a previously-defined section and a length of plastic hinge. In the present study, the sections at the end of the structural elements were defined as fiber sections, in which each fiber is associated with a uniaxial stress-strain relationship.

The sectional stress-strain state of the beam-column elements is obtained through the integration of the nonlinear uniaxial stress-strain response of the individual fibers in which the section is subdivided (see Figure 3.2).

This kind of modelling was preferred over other possible techniques for the modelling of non-linear structural behaviour because of the ability of the fiber hinges to take into account the influence of axial load on the flexural behaviour of the columns.

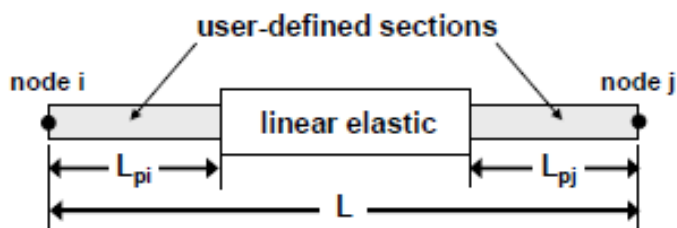


Figure 3.1 - BeamWithHinges element in OpenSees

The uniaxial '*Concrete01*' material was used to construct a uniaxial Kent-Scott-Park concrete material object with degraded linear unloading/reloading stiffness according to the work of Karsan-Jirsa (*Karsan and Jirsa, 1969*) with zero tensile strength. The steel reinforcement was modelled using the uniaxial '*Steel01*' material to represent a uniaxial bilinear steel material with kinematic hardening.

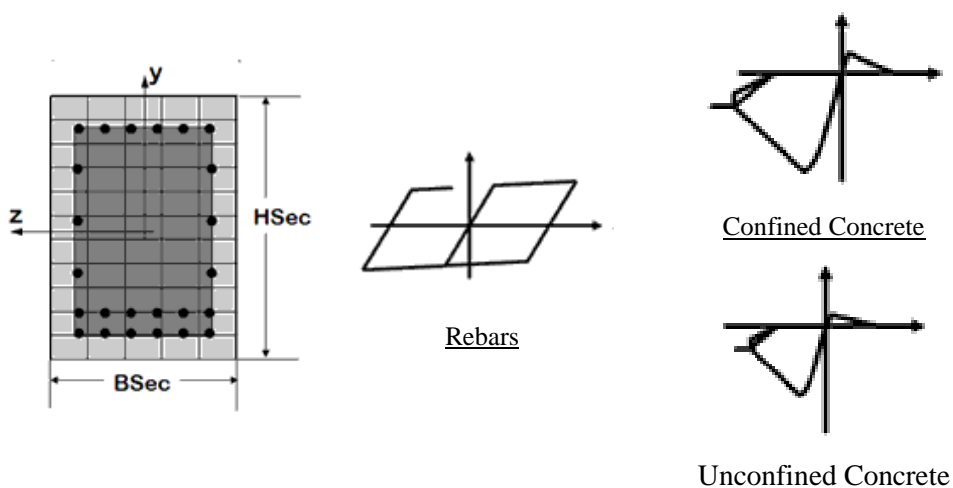


Figure 3.2 - Fiber sections definition in OpenSees

The material objects used for the representation of the stress-strain relationships for concrete (cover and core) and reinforcement steel are shown in Figure 3.3.

The parameters involved in the definition of the concrete material objects are the following:

- the maximum concrete compressive strength f_{pc} ;
- the concrete strain at maximum stress eps_{c0} ;
- the concrete crushing strength f_{pcu} ;
- the strain at ultimate stress eps_U .

In the present study the concrete crushing strength f_{pcu} was taken equal to the maximum concrete compressive strength f_{pc} (parable-rectangle constitutive law for concrete).

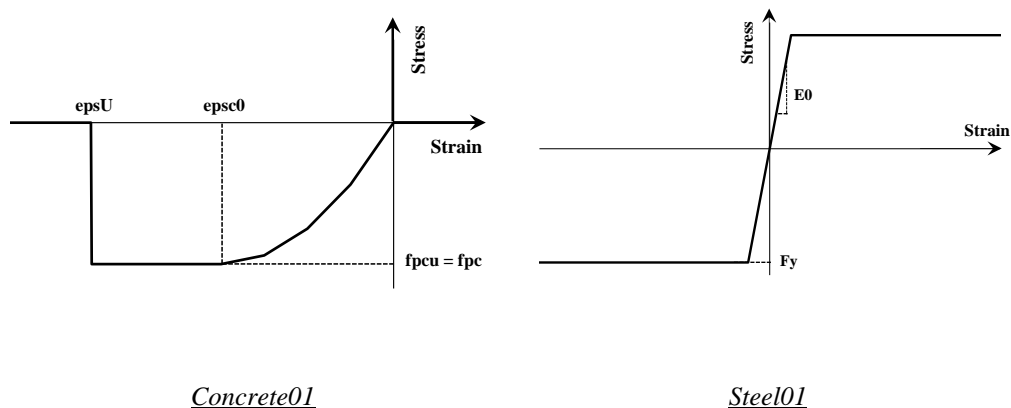


Figure 3.3 - Material objects adopted in OpenSees for the representation of the uniaxial stress-strain relationships of the concrete cover and core (left) and for the reinforcement steel (right)

For the steel material object the main required parameters are the steel yield stress F_y , the initial elastic tangent modulus of steel E_0 and the strain-hardening ratio b (i.e. the ratio between post-yield tangent and initial elastic tangent). In this study the steel modulus was assumed equal to 210000 MPa while and an elastic-perfectly plastic constitutive law was assumed (strain hardening ratio $b=0$).

The yield stress values for the different structural typologies are summarized in Table 4.1 (f_y values).

In the present study the constitutive law for concrete was limited to the value of the strain at ultimate stress (ϵ_{psU}).

The length of the plastic hinges was determined by means of equation 2.17.

In the present study the possible formation of brittle failure mechanisms due to shear was taken into account. This phenomenon is very likely to happen in the case of buildings designed with no seismic provisions, in which no hierarchy shear-flexure rules are respected in the design process and the amount of shear reinforcements is very low (i.e. structural elements designed for vertical loads only).

The modelling of the shear failures was carried out in OpenSees by means of shear springs that work in series with the '*beamWithHinges*' elements.

In particular, the work of *Elwood* (2004) was referenced but re-adapted.

The shear spring in OpenSees is defined by means a '*zero-length element*' and its initial stiffness is defined as:

$$K_v = GA_g / H \quad (3.1)$$

where:

- G is the shear modulus of the material adopted for the beam-column element;
- A_g is the gross section of the element;
- H is the length of the element.

The force-displacement rule of the spring is defined in terms of force-drift between the end nodes of the beam-column element and is described in OpenSees by means of a '*Limit State Material*' (that is a specialization of the '*Hysteretic Material*').

The '*Limit State Material*' in OpenSees allows to define a threshold beyond which the spring has a softening behaviour (a degrading slope and a residual capacity must be defined in the material behaviour).

The threshold in the model suggested by *Elwood* is defined based on a specific value of drift, but in this study it is defined by the shear resistance of the element, defined according to the formulation suggested by *Sezen & Moehle* (2004):

$$V_n = V_c + V_s = k \frac{A_{st} f_{yt} d}{s} + k \left(\frac{0.5 \sqrt{f'_c}}{a/d} \sqrt{1 + \frac{P}{0.5 \sqrt{f'_c} A_g}} \right) 0.8 A_g \quad (\text{MPa}) \quad (3.2)$$

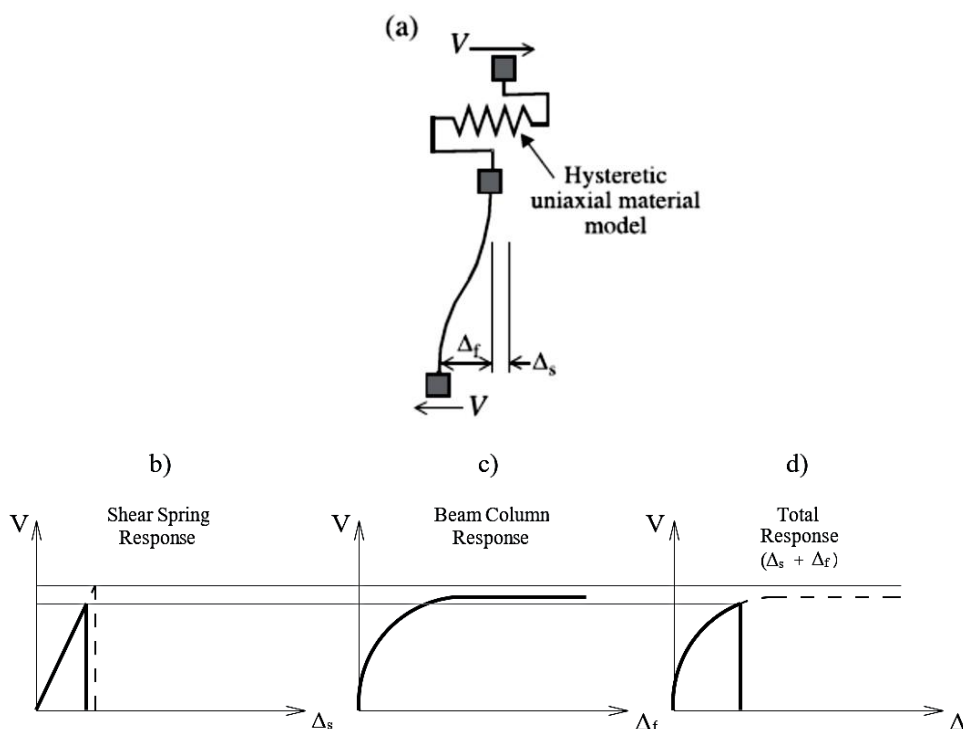


Figure 3.4 - Modelling of shear failures (re-adapted from Elwood, 2004)

In this formulation:

- V_s and V_c are shear contributions assigned to steel and concrete;
- k is a parameter equal to 1.0 for $\mu_\delta \leq 2$, equal to 0.7 for $\mu_\delta \geq 6$, and varies linearly for intermediate μ_δ values (with μ_δ equal to the displacement ductility);
- A_{st} is the area of shear reinforcement parallel to the horizontal shear force;
- s is the spacing between the shear reinforcements;
- f_{yt} is the yield strength of transverse reinforcement;
- d is the effective depth (equal to $0.8h$, with h equal to the section depth parallel to shear force);
- P is the axial compression force;

- f'_c is the concrete compressive strength (MPa);
- A_g is the gross section area;
- a/d is the shear span/effective depth (value limited between 2 and 4).

In the present study, a value of 0.7 was assumed for the k value to take into account in a conservative way of the cyclic degradation of the shear resistance.

Moreover, no residual capacity and an infinite degrading slope were assigned to shear springs, in order to simulate a complete and sudden loss of shear capacity.

Hysteretic damping, which is usually responsible for the dissipation of the majority of energy introduced by the earthquake action, was implicitly taken into account within the nonlinear fiber model formulation of the inelastic frame elements. Additionally, to account for the viscous damping that is mobilized during the dynamic response of the structures (e.g. internal friction in the structural materials, connections, non-structural components etc.) tangent stiffness – proportional damping was assigned with a damping ratio of 5%.

It has been shown (*Priestley and Grant, 2005*) that tangent-stiffness proportional damping is more appropriate for modelling elastic viscous damping in inelastic time-history analyses resulting to a more realistic computation of the elastic damping forces and more reliable estimates of the displacement responses.

P-Delta effects were not considered in the study, since they can be considered negligible according to Italian NTC 08.

3.2 SSI modelling: sub-structures approaches

In a substructure approach, the SSI problem is broken down into three distinct parts which are combined to formulate the complete solution.

The superposition inherent in a substructure approach requires an assumption of linear soil and structure behaviour, although in practice this requirement is often followed only in an equivalent-linear sense.

Referring to Figure 3.5, the three steps in the analysis are as follows.

- 1) Evaluation of a Foundation Input Motion (FIM), which is the motion that would occur on the base-slab if the structure and foundation had no mass. The FIM is dependent on the stiffness and geometry of the foundation and

soil. Since inertial effects are neglected, the FIM represents the effects of kinematic interaction only.

- 2) Determination of the foundation impedances, which describe the stiffness and damping characteristics of foundation-soil interaction. It should account for the soil stratigraphy and foundation stiffness and geometry, and is computed using equivalent-linear soil properties appropriate for the in situ dynamic shear strains.
- 3) Dynamic analysis of the structure supported on a flexible base represented by the impedance function and subjected to a base excitation consisting of the FIM.

The principal advantage of the substructure approach is its versatility. Because each step is independent of the others, the analyst can focus resources on the most significant aspects of the problem.

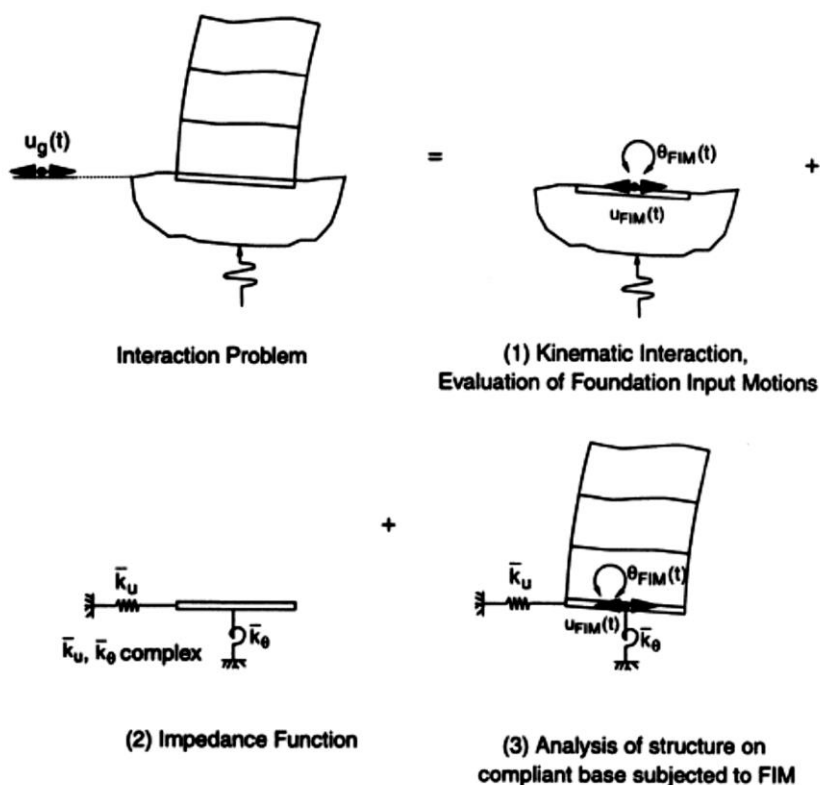


Figure 3.5 - Substructure approach for the evaluation of SSI effects (*Stewart et al., 1998*)

3.2.1 Foundations Impedances

One possible solution for the modelling of the inertial interaction is by means of the foundations impedances, which represent the frequency-dependent stiffness and damping characteristics of soil-foundation interaction.

Classical solutions for the complex valued impedance function can be written as (Luco and Westman, 1971; Veletsos and Wei, 1971):

$$\bar{k}_j = k_j + i\omega c_j \quad (3.1)$$

where \bar{k}_j denotes the complex-valued impedance function; j is an index denoting modes of translational, displacement or rotation; k_j and c_j denote the frequency dependent foundation stiffness and dashpot coefficients, respectively, for mode j ; and ω is the circular frequency (rad/s). A dashpot with coefficient c_j represents the effects of damping associated with soil-foundation interaction. An alternative form to express the impedance is:

$$\bar{k}_j = k_j(1 + 2i\beta_j) \quad (3.2)$$

where:

$$\beta_j = \frac{\omega c_j}{2k_j} \quad (\text{defined for } k_j > 0) \quad (3.3)$$

An advantage of the expression for β_j terms of c_j is that, at resonance of the SSI system, β_j can be interpreted as a fraction of critical damping in the classical sense (Clough and Penzien, 1993). Conversely, a drawback of Equation 3.3 is that, as k_j approaches zero, β_j goes to infinity.

The imaginary part of the complex impedance represents a phase difference between harmonic excitation and response at a given frequency. The phase difference, ϕ_j between force and (lagged) displacement is (Clough and Penzien 1993; Wolf 1985):

$$\phi_j = \tan^{-1}(2\beta_j) \quad (3.4)$$

Angle ϕ_j is also known as a loss angle. For example, if β_j is 10%, peak harmonic displacement will lag peak force by 0.197 radians (11.3 degrees). When β_j goes to infinity, ϕ_j is bounded by $\pi/2$.

Many impedance function solutions are available for rigid circular or rectangular foundations located on the surface of, or embedded within, a uniform, elastic, or visco-elastic half-space. In the case of a rigid rectangular foundation resting on the surface of a half-space with shear wave velocity V_s , *Pais and Kausel (1988)*, *Gazetas (1991)*, and *Mylonakis et al. (2006)* review impedance solutions in the literature and present equations for computing the stiffness and damping terms.

These solutions describe translational stiffness and damping along axes x , y , and z , and rotational stiffness and damping about those axes (denoted xx , yy , and zz). Stiffness is denoted k_j , and is a function of foundation dimensions, soil shear modulus, G , Poisson's ratio of the soil, ν , dynamic stiffness modifiers, α_j , and embedment modifiers, η_j :

$$k_j = K_j \times \alpha_j \times \eta_j$$

$$K_j = GB^m f(B/L, \nu) \quad , \quad \alpha_j = f(B/L, a_0) \quad (3.5)$$

$$\eta_j = f(B/L, D/B, d_w/B, A_w/BL)$$

where K_j is the static foundation stiffness at zero frequency for mode j , and $m = 1$ for translation, and $m = 3$ for rotation.

Shear modulus, G , should reflect the effects of modulus reduction with increasing shear strain amplitude. FEMA 440, for example, provide the information presented in Table 3.1 for adjusting the shear modulus and shear wave velocity for large strain levels based on the PGA expected.

Similar information are reported in *ASCE/SEI 7-10, Minimum Design Loads for Buildings and Other Structures* (ASCE, 2010), and *FEMA P-750, NEHRP Recommended Seismic Provisions for New Buildings and Other Structures* (FEMA, 2009).

Maximum (or small strain) shear modulus, G_0 , can be calculated as $G_0 = V_s^2 \rho$ where V_s is based on geophysical measurements in the field, and ρ is the soil mass density. An average effective value of V_s is generally computed across an effective profile depth, z_p .

Table 3.1 - Values of Shear Wave Velocity Reduction factor (FEMA 440, 2005)

Table 8-1 Approximate Values of Shear Wave Velocity Reduction Factor, n				
<i>Peak Ground Acceleration (PGA)</i>				
	0.10g	0.15g	0.20g	0.30g
n	0.90	0.80	0.70	0.65

Dynamic stiffness modifiers, α_j , are related to the dimensionless frequency a_0 :

$$a_0 = \frac{\omega B}{V_s} \quad (3.6)$$

which has the physical interpretation of being the ratio of B to approximately one sixth of the seismic wavelength for frequency ω .

For time domain analysis, a single frequency ω is usually selected for the purpose of evaluating foundation spring and dashpot coefficients that depend on a_0 . This can be taken as the frequency corresponding to the period associated with the dominant response of the structure.

In most cases, this will be the first-mode, flexible-base period.

Table A. 1 lists expressions for static foundation stiffness, K_j , for three translational and three rotational degrees of freedom for a rigid rectangular footing located at the ground surface. These equations are similar for *Pais and Kausel (1988)*, *Gazetas (1991)*, and *Mylonakis et al. (2006)*.

Embedment of foundations below the ground surface increases static foundation stiffness. Factors, η_j , to increase K_j for the effects of embedment are provided in Table A. 2.

The *Pais and Kausel (1988)* equations are most often used in practice.

The equations by *Gazetas (1991)* and *Mylonakis et al. (2006)* are more general, accounting for embedment effects resulting from gapping between the soil and foundation side walls.

Equations for dynamic stiffness modifiers, α_j , and radiation damping ratios, β_j , for rigid footings located at the ground surface are provided in Table A. 3.

Dynamic stiffness modifiers and radiation damping ratios for embedded footings are provided in Table A. 4.

The frequency dependence of quantities provided in Table A. 3 reflects the effect of condensation of infinite degrees of freedom in soil having mass and associated dynamic effects.

Frequency dependence would disappear for massless soil, as a_0 would become zero (because $V_s \rightarrow 0$) causing $\alpha_j = 1$, and $\beta_j = 0$. Dynamic stiffness modifiers provided in Table A. 4 are insensitive to embedment, so values for embedded foundations are the same as values given in Table A. 3 for footings located at the ground surface (i.e., $\alpha_{j,emb} = \alpha_{j,sur}$).

Figure 3.6 shows the variation in dynamic stiffness modifiers versus frequency for rigid footings located at the ground surface. In the case of translational stiffness, dynamic stiffness modifiers (α_x , α_y) are essentially unity, regardless of frequency or foundation aspect ratio. For rotational stiffness, however, dynamic stiffness modifiers for rocking (α_{xx} , α_{yy}) degrade markedly with frequency, but are relatively insensitive to aspect ratio.

Because soil hysteretic damping, β_s , is taken as zero, Figure 3.6 also shows the variation in radiation damping ratios for translation (β_x , β_y) and rotation (β_{xx} , β_{yy}) versus frequency. Translational radiation damping is only modestly affected by the direction of shaking or the aspect ratio of the foundation. The modest increase of translational damping with aspect ratio is a result of the increased foundation size (i.e., larger wave source).

In contrast, rotational radiation damping is strongly sensitive to the direction of shaking and the aspect ratio of the foundation. Rotational damping is largely controlled by vertical cyclic displacements at the edges of the foundation (without separation between soil and footing). As aspect ratio increases, the ends of the foundation are located further apart, and energy radiating into the soil from each end of the foundation experiences less destructive interference, thus increasing damping.

At low frequencies ($a_0 < 1$ to 2), damping from rotation is generally smaller than damping from translation, although the trend reverses as frequency increases and foundations become relatively oblong. The practical significance of this effect is that translational deformation modes in the foundation, while often relatively unimportant from the perspective of overall structural system flexibility, can be the dominant source of foundation damping. When used to calculate the dashpot coefficient, c_j , the β_j term should be taken as the sum of radiation damping for the appropriate vibration mode and soil hysteretic damping, β_s , provided by a geotechnical engineer.

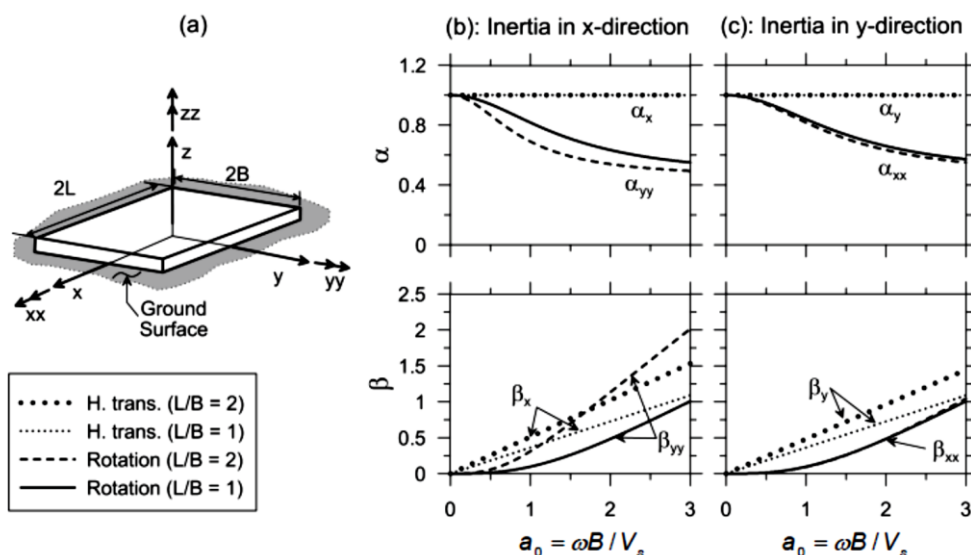


Figure 3.6 - Dynamic stiffness modifiers and damping ratios versus dimensionless frequency, for rectangular footings resting on the surface of a homogeneous half-space, with zero hysteretic damping and $\nu = 0.33$: (a) geometry; (b) x-direction; and (c) y-direction (from NIST GCR 12-917-2)

Figure 3.7 shows the variation in dynamic stiffness modifiers and radiation damping ratios versus frequency for embedded foundations. In equations provided by *Pais and Kausel (1988)*, dynamic stiffness modifiers are unaffected by embedment.

Apsel and Luco (1987), however, found a somewhat different result, indicating some sensitivity to embedment. Moreover, they observed a more rapid

decay in stiffness with frequency for embedded foundations, which is not reflected in the figure.

The elasto-dynamic analyses upon which Figure 3.7 is based assume perfect contact between soil and basement walls. Accordingly, the solutions indicate much higher damping levels than those for shallow foundations (*Gazetas, 1991*).

These damping levels may not be reliable when gaps form between foundations and the adjacent soil, which reduces the potential for radiation damping from basement walls. In studies performed by *Stewart et al. (1999b)*, buildings shaken by earthquakes generally do not exhibit damping levels consistent with such models. As a result, the impedance of embedded foundations can be conservatively estimated from the equations for static stiffness in Table A. 1 and adjusted by dynamic stiffness modifiers for surface foundations from Table A. 3.

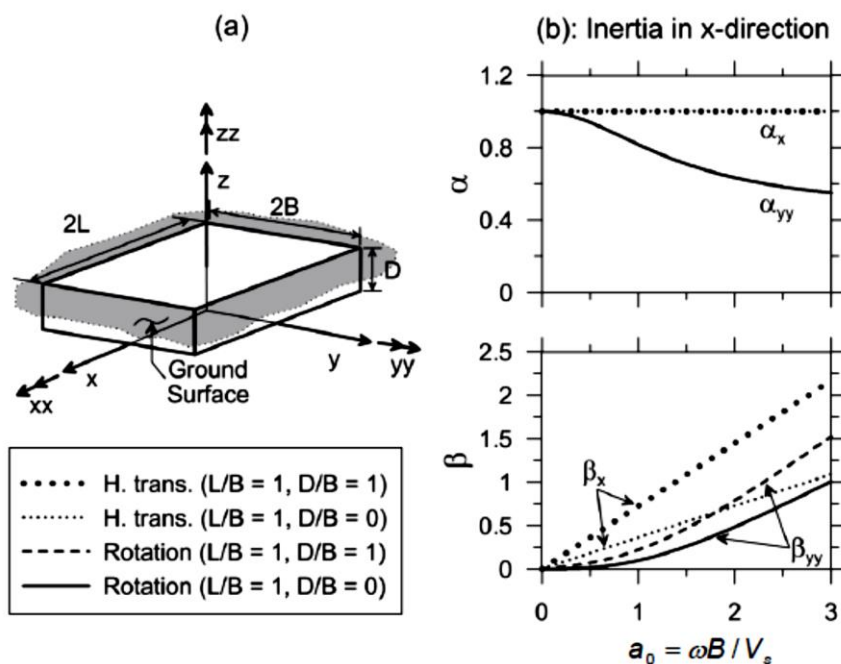


Figure 3.7 - Dynamic stiffness modifiers and damping ratios versus dimensionless frequency, for square footings embedded in a homogeneous half-space, with zero hysteretic damping, and $\nu = 0.33$: (a) geometry; and (b) x-direction (y-direction similar) (from NIST GCR 12-917-2)

In OpenSees the impedances of the foundation can be easily implemented placing in parallel (for each degree of freedom of the foundation) an elastic spring and a viscous dashpot.

The spring and the dashpot can be modelled by means of a zero-length element whose behaviour is defined by an elastic '*Uniaxial*' material and a viscous one that work in parallel by means of a '*Parallel*' material (see Figure 3.8).

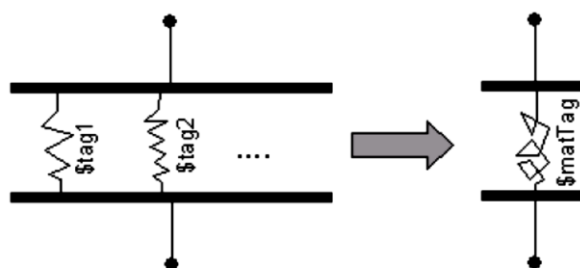


Figure 3.8 - Parallel Material in OpenSees (Mazzoni et al, 2009)

3.2.2 Beam on Non Linear Winkler Foundation Model

Another available technique for modelling the inertial interaction is by means of Beam on Nonlinear Winkler Foundation (BNWF) models.

Key advantages of these models over continuum formulations lies in their ability to describe soil-structure interaction phenomena by one-dimensional nonlinear springs distributed along the soil-foundation interface.

A limitation of the approach relates to its one-dimensional nature. A spring responds only to loads acting parallel to its axis, so loads acting in a perpendicular direction have no effect on the response of the spring. Nevertheless, the BNWF approach is popular because of its simplicity and predictive abilities on a variety of problems.

The BNWF model implemented into OpenSees by *Raychowdhury* and *Hutchinson* (2009) consists of elastic beam-column elements that capture the structural footing behaviour with independent '*zero-length*' soil elements that model the soil-footing behaviour. Currently, it is developed for two-dimensional analysis only. Therefore, the one-dimensional elastic beam-column elements

used for the footing have three degrees-of-freedom per node (i.e., horizontal, vertical, and rotation).

As illustrated in Figure 3.9, one-dimensional uniaxial springs are used to simulate the vertical load displacement behaviour ($q-z$), horizontal passive load-displacement behaviour against the side of a footing ($p-x$), and horizontal shear-sliding behaviour at the base of a footing ($t-x$).

Moment-rotation behaviour is captured by distributing vertical springs along the base of the footing.

The mathematical model of the $q-z$, $p-x$, and $t-x$ nonlinear springs in Figure 3.9 was adapted from a model for pile foundations by *Boulanger et al.* (1999).

Within the OpenSees framework, the materials describing these springs are the '*QzSimple2*', '*PxSimple1*', and '*TxSimple1*' material models, that differ from their parent (pile-calibrated) models ('*QzSimple1*', '*PySimple1*', and '*TzSimple1*') only in the backbone shape parameters.

The material models are based on an arrangement of various linear and nonlinear springs, gap elements, and dashpots. Radiation damping can be accounted for using a dashpot placed in parallel with the elastic component. The backbone curves are thus characterized by a linear-elastic region, followed by an increasingly growing nonlinear region.

The '*QzSimple2*' material has an asymmetric hysteretic response, with a backbone curve defined by an ultimate load on the compression side and a reduced strength in tension to account for the low strength of soil in tension.

The '*PxSimple1*' material is envisioned to capture the passive resistance, associated stiffness, and potential gapping of embedded shallow footings subjected to lateral loads. This material model is characterized by a pinched hysteretic behaviour, which can more suitably account for the phenomena of gapping during unloading on the opposite side of a footing.

The '*TxSimple1*' material is intended to capture the frictional resistance along the base of a shallow foundation. This material is characterized by a high initial stiffness and a broad hysteresis, as anticipated for frictional behaviour associated with foundation sliding.

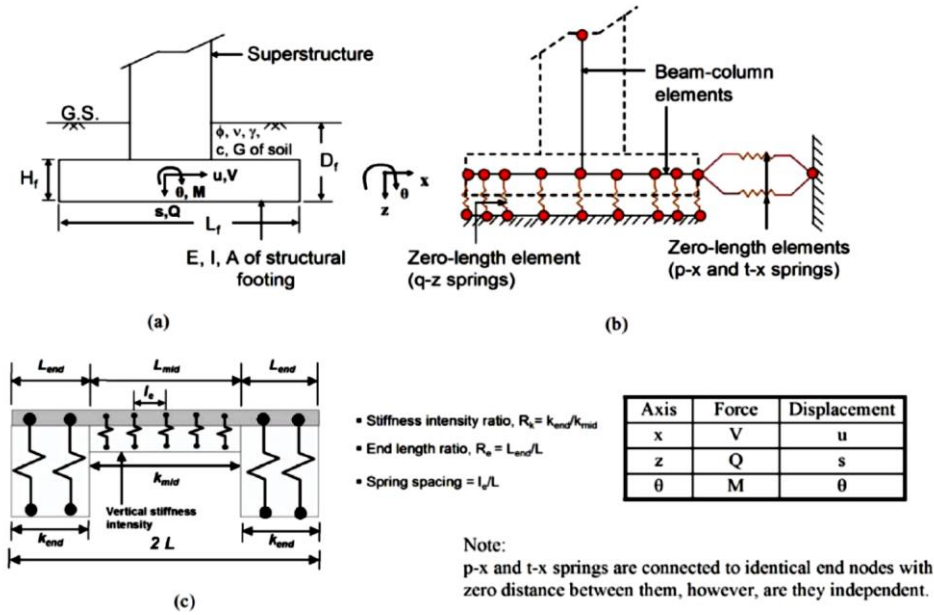


Figure 3.9 - Beam-on-Nonlinear Winkler Foundation (BNWF) model: (a) hypothesized foundation-superstructure system; (b) idealized model; and (c) variable vertical stiffness distribution (Raychowdhury and Hutchinson, 2009)

The functional forms and parameters describing the p - x , t - x , and q - z springs are similar, so only the q - z model is described here. The backbone curve has linear and nonlinear regions. The linear-elastic portion of the backbone curve is described by the initial stiffness k_z :

$$q = k_z s \tag{3.4}$$

where q represents the spring force, and s represents the spring deflection.

The upper limit of the linear elastic region, defined as q_0 , is taken as a fraction of the ultimate load q_{ult} as follows:

$$q_0 = C_r q_{ult} \tag{3.5}$$

where C_r is a parameter specified in OpenSees.

The nonlinear (post-yield) portion of the backbone is described by:

$$q = q_{ult} - (q_{ult} - q_0) \left[\frac{c s_{50}}{c s_{50} + |s - s_0|} \right]^n \quad (\text{for } |s| > s_0) \tag{3.6}$$

where s_{50} is the displacement at which 50% of the ultimate load is mobilized, s_0 is the displacement at load q_0 , and both c and n are constitutive parameters controlling the shape of the post-yield portion of the backbone curve.

The unloading-reloading rules that operate with the backbone curve are relatively simple, generally consisting of the familiar Masing rules (i.e., the shape of the unload and reload portion of the cyclic loop matches twice the backbone curve, *Masing, 1926*).

The drag and gap component is parameterized by a bilinear closure spring in parallel with a nonlinear drag spring. The cyclic response of each of the material models, when subjected to a sinusoidal displacement, is shown in Figure 3.10.

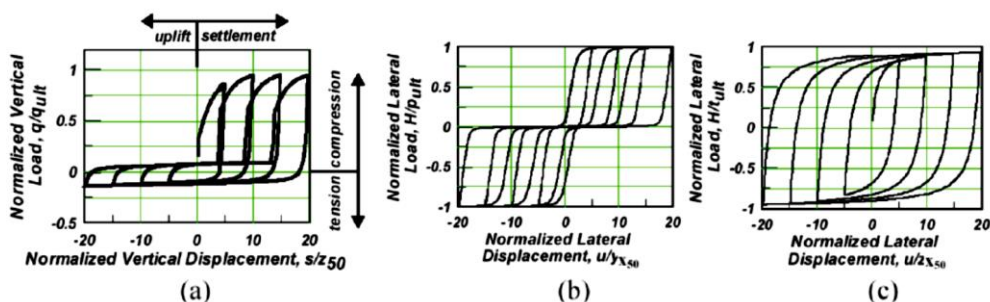


Figure 3.10 - Cyclic response of OpenSees BNWF springs subjected to a sinusoidal displacement: (a) q - z spring ($Qzsimple2$ material model); (b) p - x spring ($Pxsimple1$ material model); and (c) t - x spring ($Txsimple1$ material model) (*Raychowdhury and Hutchinson, 2009*)

User-defined parameters for the q - z element can be synthesized based on two physical parameters obtained from the results of a typical high-quality geotechnical site investigation (i.e., bearing capacity, q_{ult} , and elastic stiffness, k_z) and several parameters defining the details of the elements described above.

These parameters are:

- radiation damping;
- tension capacity (ratio of tension capacity to bearing capacity with typical selected values of 0 to 0.10 as suggested in *Boulangier et al., 1999*);
- distribution and magnitude of vertical stiffness;
- spring spacing;

– shape parameters.

For vertical ‘*QzSimple2*’ springs, the ultimate bearing capacity is calculated based on bearing capacity equation after *Terzaghi* (1943):

$$q_{ult} = cN_c F_{cs} F_{cd} F_{ci} + \gamma D_f N_q F_{qs} F_{qd} F_{qi} + 0.5\gamma B N_\gamma F_{\gamma s} F_{\gamma d} F_{\gamma i} \quad (3.7)$$

where q_{ult} = ultimate bearing capacity per unit area of footing, c = cohesion, γ = unit weight of soil, D_f = depth of embedment, B = width of footing; N_c , N_q and N_γ are bearing capacity factors, F_{cs} , F_{qs} and $F_{\gamma s}$ are shape factors, F_{cd} , F_{qd} and $F_{\gamma d}$ are depth factors and F_{ci} , F_{qi} and $F_{\gamma i}$ are inclination factors.

The bearing capacity factors along with depth, shape and inclination factors are calculated after *Meyerhof* (1963).

For the ‘*PySimple2*’ material, the ultimate lateral load capacity is determined as the total passive resisting force acting on the front side of the embedded footing.

For homogeneous backfill against the footing, the passive resisting force can be calculated using a linearly varying pressure distribution resulting in the following expression:

$$p_{ult} = 0.5\gamma K_p D_f^2 \quad (3.8)$$

where p_{ult} = passive earth pressure per unit length of footing, γ = unit weight of soil, D_f = depth of embedment, K_p = passive earth pressure coefficient are calculated using *Coulomb* (1776).

For the ‘*TzSimple2*’ material, the lateral capacity is the total sliding resistance.

The frictional resistance is determined using the general equation for shear strength of footing soil interface after considering a reasonable base friction angle between soil and the footing base.

The equation used to calculate the sliding capacity is:

$$t_{ult} = W_g \tan \delta + A_b c \quad (3.9)$$

where t_{ult} = frictional resistance per unit area of foundation, W_g = weight on the foundation from the structure, δ = angle of friction between foundation and soil, which typically varies from $1/3\varphi$ to $2/3\varphi$ (with φ = friction angle of the soil), A_b = the area of the base of footing in contact with the soil.

The vertical and lateral stiffness are calculated using expressions given by *Gazetas* (see Table A. 1 in Annex A). The rotational stiffness of the foundation is accounted implicitly for the differential movement of the vertical springs.

As illustrated in Figure 3.9 and Figure 3.11, two parameters are necessary to account for the distribution and magnitude of the vertical stiffness along the length of a footing:

1. the stiffness intensity ratio, R_k (where, $R_k = K_{end} / K_{mid}$);
2. the end length ratio, R_e (where, $R_e = L_{end} / 2L$).

A variable stiffness distribution along the length is used to force the distributed BNWF spring model to match the overall rotational stiffness.

Usually, in fact, the vertical stiffness of the distributed springs is obtained multiplying the vertical stiffness intensity (obtained normalizing the vertical translational impedance by the foundation area):

$$k_z^i = \frac{k_z}{4BL} \quad (3.10)$$

for a reasonable tributary area.

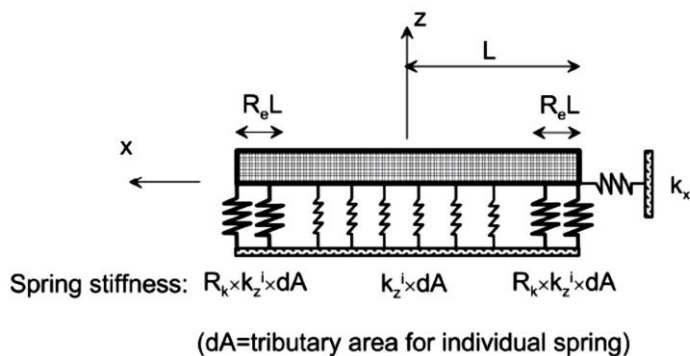


Figure 3.11 - Vertical spring distribution used to reproduce total rotational stiffness k_{yy}

If this approach were used across the entire length, the vertical stiffness of the foundation would be reproduced, but the rotational stiffness would generally be underestimated. This occurs because the vertical soil reaction is not uniform, and tends to increase near the edges of the foundation.

To correct for underestimation of rotational stiffness, to the strips along the foundation edge (of length $R_e 2L$) are assigned stiffer springs. When combined with springs in the interior, the total rotational stiffness of the foundation is reproduced.

The expressions that can be used to calculate the coefficient R_k are:

$$R_{k,yy} = \frac{\left(\frac{3k_{yy}}{4k_z^i BL^3} \right) - (1 - R_e)^3}{1 - (1 - R_e)^3} \quad (\text{for rocking around } yy \text{ axis})$$

$$R_{k,xx} = \frac{\left(\frac{3k_{xx}}{4k_z^i BL^3} \right) - (1 - R_e)^3}{1 - (1 - R_e)^3} \quad (\text{for rocking around } xx \text{ axis})$$
(3.11)

that were derived by matching the moment produced by the springs for a unit foundation rotation to the rotational stiffness k_{yy} or k_{xx} .

This correction for rotational stiffness, however, does not preserve the original vertical stiffness k_z . This is considered an acceptable approximation, in general, because rocking is the more critical foundation vibration mode in most structures.

As noted for the vertical stiffness, even for vertical damping the use of a constant dashpot intensity c_z^i :

$$c_z^i = \frac{c_z}{4BL} \quad (3.12)$$

would overestimate radiation damping from rocking. This occurs because translational vibration modes (including vertical translation) are much more effective radiation damping sources than rocking modes.

To correct for overestimation of rotational damping, the relative stiffness intensities and distribution are used (based on the stiffness factor R_k and end length ratio R_e), but dashpot intensities over the full length and width of the foundation are scaled down by a factor, R_c , computed as:

$$R_{c,yy} = \frac{\frac{3c_{yy}}{4c_z^i BL^3}}{R_{k,yy}(1-(1-R_e)^3) + (1-R_e)^3} \quad (\text{for rocking around yy axis})$$

$$R_{c,xx} = \frac{\frac{3c_{xx}}{4c_z^i BL^3}}{R_{k,xx}(1-(1-R_e)^3) + (1-R_e)^3} \quad (\text{for rocking around xx axis})$$
(3.13)

Use of the above procedures for modifying vertical spring impedances will reproduce the theoretical rotational stiffness and damping through distributed vertical springs and dashpots.

For what concerns the end region (L_{end}), ATC-40, *Seismic Evaluation and Retrofit of Concrete Buildings* (ATC, 1996) suggests the use of $L_{end} = B/6$ from each end of the footing.

This expression of end length ratio is independent of the footing aspect ratio while *Harden and Hutchinson* (2009) suggest an expression that is a function of the footing aspect ratio.

The spring spacing is input by the user as a fraction of the footing half-length L ($S = l_e/L$), where l_e is the non-normalized spring spacing. A maximum element length equal to 8% of the footing half-length (i.e., a minimum number of 25 springs along the full length of the footing) is recommended to provide numerical stability and reasonable accuracy.

The shape parameters (C_r , c , n) are hard-wired into the OpenSees implementation of the material models, meaning that they are not specified by users. The recommended values are soil-type dependent, and were developed based on comparisons of model predictions to test data as described by *Raychowdhury and Hutchinson* (2008).

3.3 SSI modelling: direct approaches

In a *direct analysis*, soil and structure are included within the same model and analyzed as a complete system.

As schematically depicted in Figure 3.12, the soil is often represented as a continuum (e.g., finite elements) along with foundation and structural elements, transmitting boundaries at the limits of the soil mesh, and interface elements at the edges of the foundation.

Evaluation of site response using wave propagation analysis through the soil is important to this approach. Such analyses are most often performed using an equivalent linear representation of soil properties in finite element, finite difference, or boundary element numerical formulations (*Wolf, 1985; Lysmer et al., 1999*).

Direct analyses can take into account all the SSI effects, but incorporation of kinematic interaction is challenging because it requires specification of spatially variable input motions in three dimensions.

Because direct solution of the SSI problem is difficult from a computational standpoint, especially when the system is geometrically complex or contains significant nonlinearities in the soil or structural materials, it is rarely used in practice.

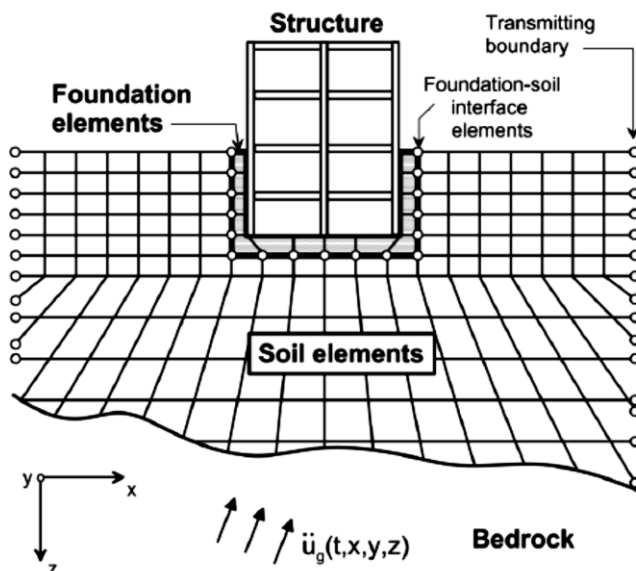


Figure 3.12 - Schematic illustration of a direct analysis of soil-structure interaction using continuum modelling by finite elements (by NIST CGR 12-917-21)

3.3.1 Complete FEM model

With the aim to compare the results obtainable by means of a modelling of the SSI with a substructure approach and with a direct approach, a complete FEM model was implemented in OpenSees.

In the OpenSees model, a homogeneous soil deposit with a bedrock lying at the depth of 30 m beneath the ground surface is modelled in two-dimensions using the plane strain formulation of the ‘quad’ element.

To account for the finite rigidity of the bedrock ($V_{s,bedrock} = 1000$ m/s), a Lysmer-Kuhlemeyer (*Lysmer and Kuhlemeyer, 1969*) dashpot is incorporated at the base of the soil profile.

The dashpot is defined based on the viscous ‘Uniaxial’ material model and the ‘zeroLength’ element formulation, to connect two previously defined nodes. This material model requires a single input, the dashpot coefficient c that is defined according to *Joyner and Chen (1975)* as the product:

$$c = \rho_{bedrock} V_{bedrock} A_{soil} \quad (3.14)$$

where ρ_{soil} is the mass density, $V_{bedrock}$ is the shear wave velocity of the underlying bedrock and A_{soil} is the base area of the soil profile in order to maintain proportional results for any horizontal element size.

The out-of-plane thickness of the quad elements is set equal to $3B$, with B equal to the width of the foundation footings.

This assumption is made in order to reproduce with the Complete FEM model the initial elastic stiffness of a system in which the SSI is modelled by means of foundation impedances.

The nodes placed at the same depth on the two opposite lateral boundaries are tied together in order to achieve a simple shear deformation pattern of the soil profile (*Zienkiewicz et al., 1988*), while the nodes at the base of the soil deposit are restrained against vertical translation and constrained to have the same displacement in the horizontal direction.

Full contact between soil and structures nodes is assumed, forbidding thus any relative movement between the structure and the soil (i.e. no detachment or sliding are allowed). The connection is achieved by applying common nodes and

appropriate constrains (to ensure equal displacement) for both the soil and the structure's foundation.

For sake of simplicity, the foundations are modelled as elastic beam-column elements of infinite rigidity.

The soil profile is excited at the base by a horizontal force time history, which is proportional (through the dashpot coefficient) to the known velocity time history of the ground motion (*Joyner and Chen, 1975; Lysmer, 1978*).

The dimensions of the soil grid were chosen to ensure free field and “quasi transparent” condition at the boundaries (*Pitilakis et al., 2014*).

The dimensions of the soil elements were set based upon the concept of resolving the propagation of the shear waves at or below a particular frequency allowing an adequate number of elements to fit within the wavelength of the chosen shear wave. This ensures that the mesh is refined enough to capture satisfactorily the propagating waves (*Pitilakis et al. 2014*).

Considering a maximum frequency of interest of 10Hz for the analyses, the dimensions of the soil elements were set equal to 1.0 m x 1.0 m.

In Figure 3.13 the Complete FEM model implemented in OpenSees is briefly illustrated.

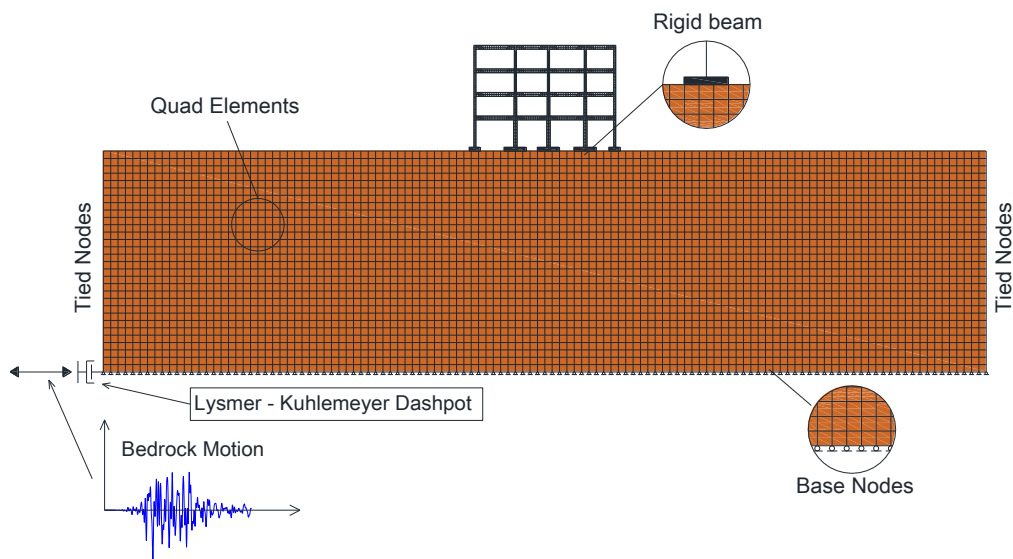


Figure 3.13 - Complete FEM model implemented in OpenSees

As concerns the soil constitutive model, the soil nonlinearity was incorporated in the model in two different ways:

- 1) by means of elastic-isotropic material with an elastic modulus properly reduced to take into account the shear strain amplitude (see Table 3.1) and viscous damping employed in the frequency-dependent Rayleigh form (Rayleigh and Lindsay, 1945);
- 2) by means of an advanced constitutive model implemented in OpenSees, the ‘*PressureIndependentMultiYield*’ material.

The first kind of modelling is preferred because it facilitates dynamic analyses, although the damping in the soil is of hysteretic type and frequency independent.

In this case, the damping matrix is built as a linear combination of the mass and stiffness matrices (Chopra, 2001):

$$[C] = \alpha[M] + \beta[K] \quad (3.15)$$

where α is the mass proportional damping constant, and β is the stiffness proportional damping constant. Figure 3.14 illustrates schematically the damping as a function of the frequency corresponding to the adopted soil profile.

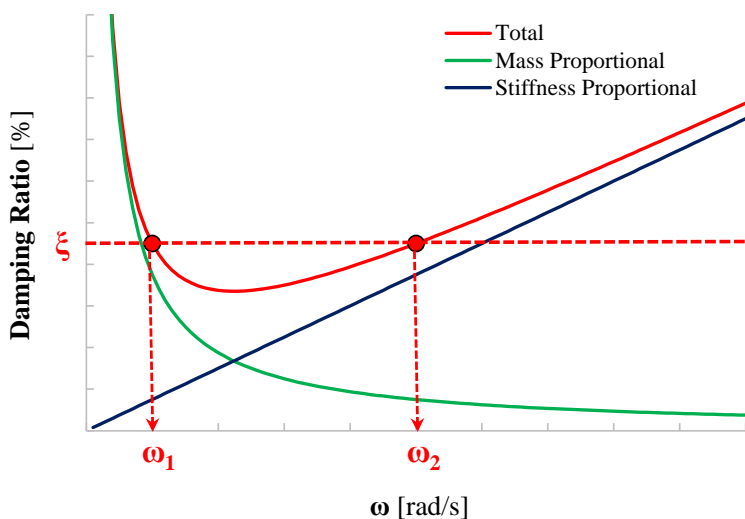


Figure 3.14 - Rayleigh proportional damping for linear soil profile

The selection of the frequencies f_1 and f_2 (ω_1 and ω_2) is made in order the resulting damping curve to simulate an almost constant damping at the frequency

range of interest. In particular the frequency range of interest is defined based on the predominant frequencies of the soil deposit, f_1 and $f_2 = 5f_1$ (Kwok *et al.*, 2007). This range includes the model's natural frequencies and the predominant frequencies of the input motions.

Assuming constant damping for both modes ζ , the damping parameters are finally given by the following expressions:

$$\alpha = 2\xi \left(\frac{\omega_1 \omega_2}{\omega_1 + \omega_2} \right); \beta = 2\xi \left(\frac{1}{\omega_1 + \omega_2} \right) \quad (3.16)$$

where ω_1 and ω_2 are the natural (cyclic) frequencies of the modes.

The damping ratio ξ is determined, given an appropriate reduction curve of the shear modulus for the soil and an expected value of the PGA at the site, on the basis of the shear strain level corresponding to the shear modulus reduction factor provided by FEMA 440 (see Table 3.1) as shown in Figure 3.15. In the present work, the reduction curves provided by *Darendeli* (2001) for a confining pressure $p'_0 = 1 \text{ atm}$ were used.

The '*PressureIndependentMultiYield*' follows the concept of multi-yield surface (nested-surface) plasticity (*Iwan*, 1967; *Prevost*, 1985; *Mroz*, 1967; *Yang*, 2000) where each yield surface is defined in the deviatoric stress space as (*Elgamal*, 1992; *Gu et al.*, 2009):

$$f = \left\{ \frac{3}{2} \left((\tau - \alpha) : (\tau - \alpha) \right) \right\}^{\frac{1}{2}} - K = 0 \quad (3.17)$$

where τ = the deviatoric stress tensor; α = the back-stress tensor referring to the center of the yield surface $f = 0$ and K = the size of the yield surface defining the region of constant plastic shear modulus. For non-pressure sensitive cohesive soil material, the yield surfaces are of the Von Mises type.

The nonlinear shear stress-strain response of the soil is described by the hyperbolic backbone curve (*Gu et al.*, 2009) as:

$$\tau = \frac{G\gamma}{1 + \frac{\gamma}{\gamma_r}} \quad (3.18)$$

where τ = the octahedral shear stress; γ = the octahedral shear strain; G = the low-strain shear modulus and γ_r = a reference shear strain defined as:

$$\gamma_r = \frac{\gamma_{max} \tau_{max}}{G\gamma_{max} - \tau_{max}} \tag{3.19}$$

where τ_{max} is the shear strength corresponding to the shear strain γ_{max} .

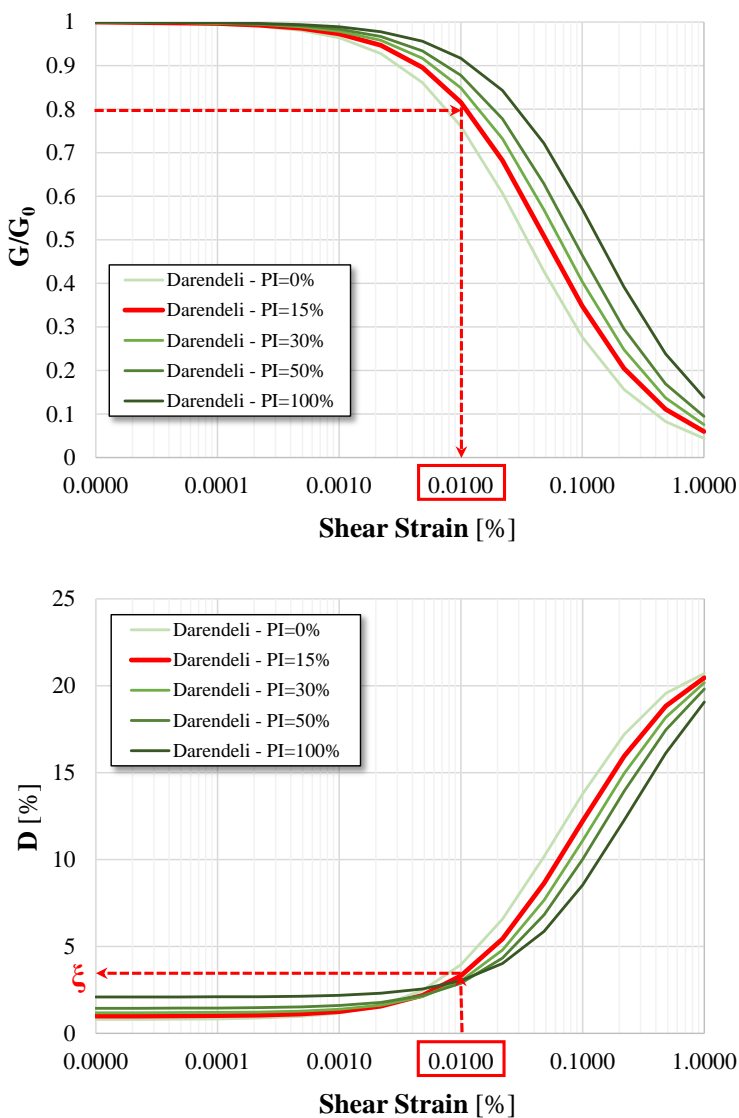


Figure 3.15 - Hysteretic soil damping definition for elastic soil elements

Within the multi-surface plasticity framework the yield surfaces define regions of constant shear moduli in the stress space and are utilized to represent the hyperbolic backbone curve through a piecewise linear representation. As depicted in Figure 3.16 each linear segment represents the domain of a yield surface f_m with shear modulus H_m for $m=1,2,\dots,NYS$ with NYS denoting the total number of yield surfaces (*Stewart et al., 2008*).

The outermost yield surface f_{NYS} , which corresponds to the peak shear strength τ_{max} , represents the failure surface and corresponds to zero shear modulus H_{NYS} .

The yield surface, the hardening law and the flow rule constitute the key components of the applied pressure-independent multi yield surface incremental plasticity model (*Kramer and Elgamal, 2001; Parra, 1996; Yang and Elgamal, 2008*).

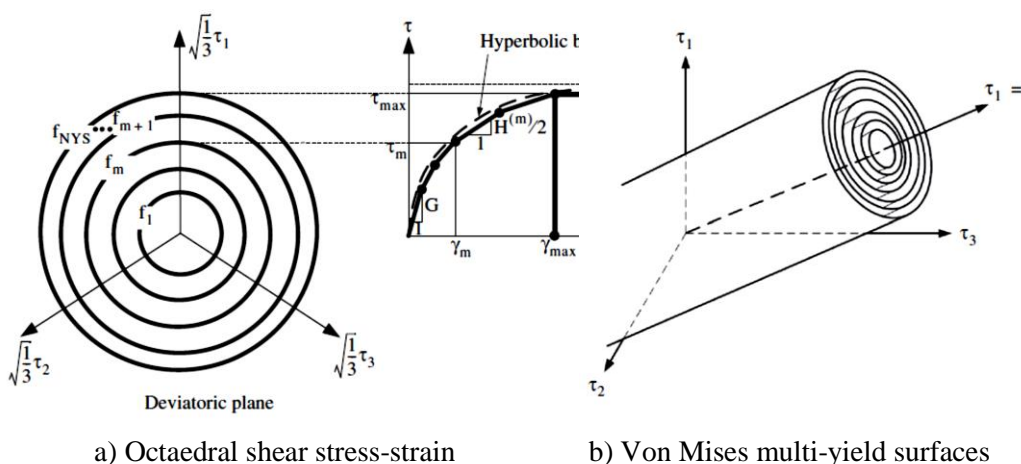


Figure 3.16 - Hyperbolic backbone curve for soil nonlinear shear stress-strain response and piecewise-linear representation in multi-surface plasticity (after *Prevost, 1985; Stewart et al., 2008; Parra, 1996*)

During the static analysis phase the material behaviour is linear elastic. In the subsequent dynamic (fast rate) loading phase, the stress-strain response is turned to elastic-plastic following the multi-surface plasticity concept, with Von Mises yield surfaces, an associative flow rule and a kinematic hardening law (*Prevost,*

1985) employed to capture the Masing hysteretic cyclic response behaviour (*Masing, 1926*).

User-defined backbone curves were defined calibrating the parameters controlling the shear behaviour of the constitutive model to yield the shear modulus reduction curves provided by *Darendeli (2001)* for clays with different plasticity indices and atmospheric pressure $p'_o = 1$ atm.

The backbone curves were appropriately adjusted to render the undrained shear strength C_u using the following equation (*Yang and Elgamal, 2008*):

$$C_u = \frac{\sqrt{3}\sigma_m}{2} \quad (3.20)$$

where σ_m is the product of the last modulus and strain pair in the defined modulus reduction curve. Since the model considers elastoplastic soil behaviour, a considerable amount of hysteretic energy dissipation is represented by the multi-yield function considering that extensive plastic deformation is expected to occur during ground shaking.

A small amount of mass and stiffness proportional Rayleigh damping was assigned to account for the energy dissipation during the elastic part of the cyclic response, which corresponds to the small-strain damping ratio defined based on the damping ratio curves for clay soil proposed by *Darendeli (2001)*.

4 Parametric Analyses for the evaluation of SSI effects on Reinforced Concrete Moment Resisting Frames

In the present chapter, the results of a parametric study performed with the aim to investigate the effects of the Soil-Structure Interaction (SSI) on the seismic performances of reinforced concrete (RC) moment resisting frames (MRFs) are shown.

The study includes buildings of 4 and 8 floors, designed with or without seismic provisions in order to capture different periods of construction.

The following parameters were varied:

- the modelling technique of the SSI effects;
- the soil type;
- the seismic action.

For what concerns the soil, the different classes suggested by Eurocode 8 were taken as reference. Moreover, as concerns the modelling technique of the SSI effects, both “direct approach” and “sub-structures approach” were considered.

Finally, for what concerns the seismic action, different recorded accelerograms (compatible with the code spectra provided by Eurocode 8 and Italian NTC08) were considered.

Before showing the results of the analyses, a brief description of the structures object of the study is provided, together with an illustration of the different design criteria of the buildings.

In addition, some explanations about the numerical modelling conducted in OpenSees are reported, spanning from the modelling of the structural non-

linearities to the modelling of the SSI effects for both the different approaches considered in the present study.

Finally, the results of the dynamic analyses are shown and commented and, in addition, some findings emerged from some analyses performed for a dual system with a frame and a shear wall are illustrated.

4.1 Reference Structures

Four different 2D RC MRFs were selected as reference structures. They can be considered as inner frames of regular 3D buildings with a plan layout equal to that reported in Figure 4.1.

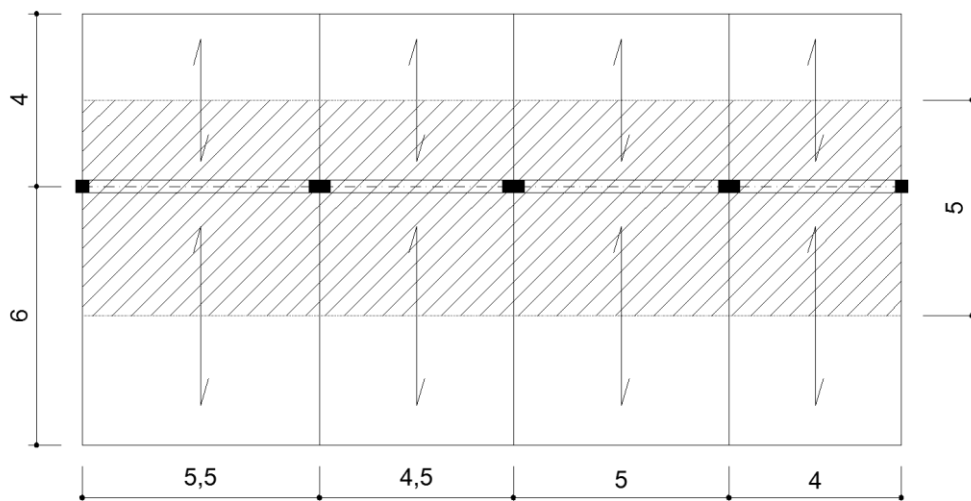


Figure 4.1 - Plan view of the reference structures

The 2D RC MRFs were designed according to different seismic code levels, in order to capture different periods of construction. Two of them have been designed for gravity loads only with no seismic provisions (according to the Italian Ministerial Decree of the 30th of May 1972), while two have been designed with high level of seismic design according to the Italian seismic code NTC 08 (Ministerial Decree of the 14th of January 2008).

Table 4.1 summarizes the main characteristics of the reference structures, namely the total mass, the concrete and steel strength (in the present study unitary

safety factors were assumed) adopted in the models and the fundamental elastic period.

In the following paragraphs, a more detailed description of the selected buildings is shown, including a description of the assumptions made in the design process.

For what not explicitly reported, direct reference to the codes mentioned some lines above can be made.

Table 4.1 - Reference Structures

Building	Total Mass [t]	f_c [MPa]	f_y [MPa]	1st Period [s]
Pre-Code - 4 Floors	290.6	17	380	0.97
Pre-Code - 8 Floors	647.2	17	380	1.14
Code compliant - 4 Floors	292.9	25	450	0.65
Code compliant - 8 Floors	692.8	25	450	0.92

4.1.1 Buildings designed according to the D.M. 30/05/1972

The frame structures designed with no seismic provisions were designed for gravity loads only and with elastic calculations based on the allowable stress method.

The Italian Ministerial Decree of the 30th of May 1972 (D.M. 1972) was taken as a reference for the design process.

For concrete, a characteristic cubic compression resistance equal to $R_{ck} = 25$ MPa was assumed in the design phase, while for steel rebar a tension resistance equal to 380 MPa (steel grade A38) was assumed.

The beams were designed in pure flexure with a value of the allowable compression stress in the concrete of 8.5 MPa, according to the relation:

$$\sigma_{a,c} = 60 + \frac{R_c - 150}{4} \quad \left(\text{with } R_c \text{ in } kg / cm^2 \right) \quad (4.1)$$

The columns were designed in pure compression with a value of the maximum allowable compression stress in the concrete of 5.95 MPa, equal to the 70% of $\sigma_{a,c}$, according to what suggested by the code.

For steel, an allowable tension stress of 190 MPa was assumed, according to what suggested for a steel grade A38.

In Table 4.2 and in Table 4.3 are shown, respectively for the 4 floors and for the 8 floors buildings, the dimensions of columns obtained at the end of the design process.

In the tables the ratio between the vertical stress due to vertical loads (σ) and the allowable compression stress for concrete is reported too.

In the design phase the floor loads were assumed equal to 7.84 kN/m² for the all the floors except for the last one, for which a load of 5.84 kN/m² was considered.

The elevation layouts of the buildings are illustrated in Figure 4.2 and in Figure 4.3, respectively, for the 4 floors and 8 floors buildings, including the section geometries and reinforcing details.

The amount of longitudinal reinforcement was established based on the prescriptions of the code, which requires that longitudinal reinforcement must have an area greater than 0.6% and lower than 5% of the concrete area strictly necessary to support the vertical load, based on the allowable stress adopted, and not lower than the 0.3% of the effective section of concrete.

In addition, the code requires that, for columns, the rebar diameter must be not smaller than 12 mm.

For what concern the transversal reinforcements, it is important to highlight the fact that for vertical loads only, the shear forces in the columns are usually very low: for this reason, the stirrups in the columns of buildings designed with this criterion are often widely spaced.

In D.M. 1972 the following limit for the maximum space between stirrups in the columns must be respected:

$$s_{\max} = \min(15 \cdot \phi_{\text{long}}; 0.25m) \quad (4.2)$$

The dimensions of the simple footings were determined assuming a working stress for the soil of 200 kN/m².

For the four floors building, an area of 3.20m x 1.75m was assumed for internal footings while an area of 1.75m x 1.75 m was assumed for external footings.

The eight floors building has internal footings of area 4.00m x 2.50m and external footings of area of 2.50m x 2.50m.

Table 4.2 - 4 Floors Pre-Code building: columns dimensions

Floor	External / Internal	N [kN]	B [m]	H [m]	$\sigma / \sigma_{a,c}$ [-]
1	External	449	0.30	0.30	0.84
	Internal	817	0.30	0.50	0.91
2	External	330	0.30	0.30	0.62
	Internal	600	0.30	0.40	0.84
3	External	211	0.30	0.30	0.39
	Internal	383	0.30	0.30	0.72
4	External	92	0.30	0.30	0.17
	Internal	167	0.30	0.30	0.31

Table 4.3 - 8 Floors Pre-Code building: columns dimensions

Floor	External / Internal	N [kN]	B [m]	H [m]	$\sigma / \sigma_{a,c}$ [-]
1	External	967	0.40	0.50	0.81
	Internal	1758	0.40	0.80	0.92
2	External	843	0.40	0.50	0.71
	Internal	1532	0.40	0.80	0.80
3	External	718	0.40	0.40	0.75
	Internal	1306	0.40	0.60	0.91
4	External	594	0.40	0.40	0.62
	Internal	1080	0.40	0.60	0.76
5	External	470	0.40	0.40	0.49
	Internal	854	0.40	0.40	0.90
6	External	345	0.40	0.40	0.36
	Internal	628	0.40	0.40	0.66
7	External	221	0.40	0.40	0.23
	Internal	402	0.40	0.40	0.42
8	External	97	0.40	0.40	0.10
	Internal	176	0.40	0.40	0.18

It is highlighted that for the two buildings designed without seismic provisions, no concrete confinement was considered, assuming that stirrups are not effectively closed.

Moreover, the concrete strain at maximum stress, ϵ_{ps0} , was assumed equal to 0.0020 while the strain at ultimate stress ϵ_{psU} was assumed equal to 0.0035 (see Section 3.1).

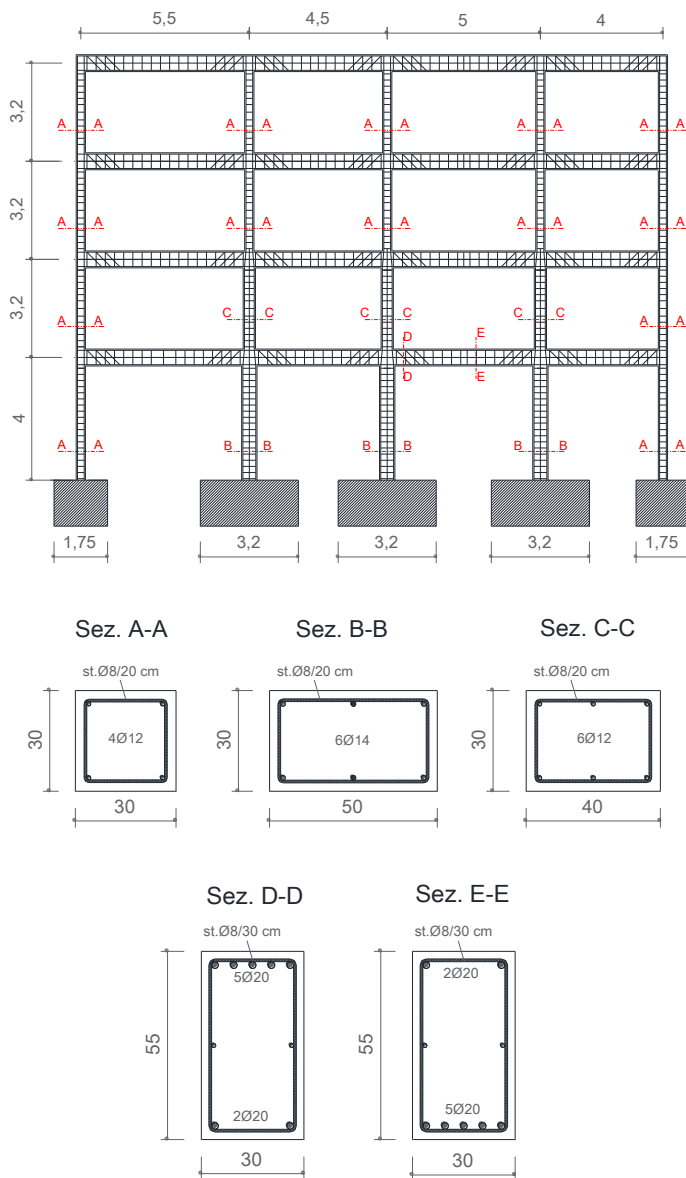


Figure 4.2 - 4 Floors Pre-Code building

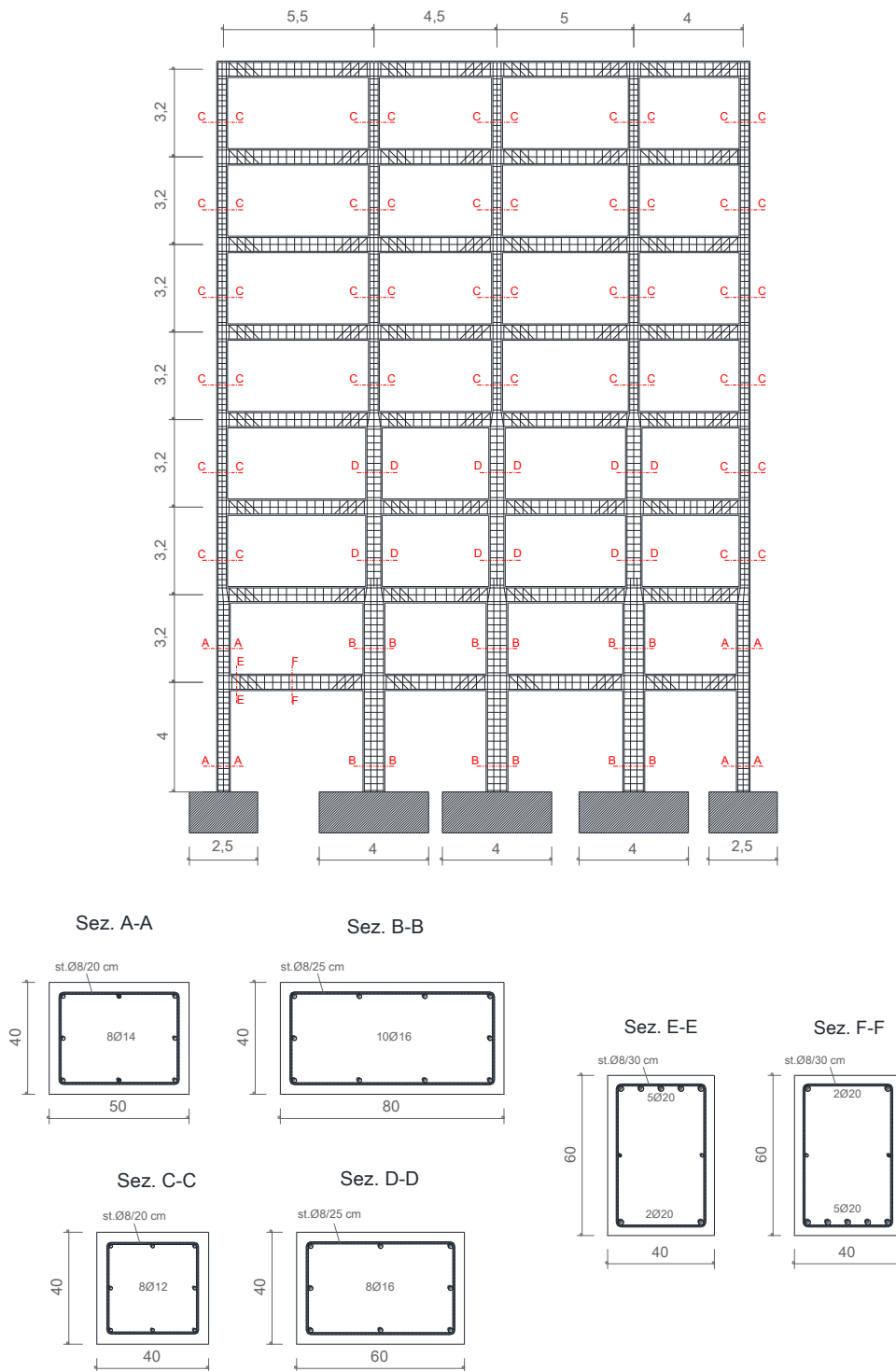


Figure 4.3 - 8 Floors Pre-Code building

4.1.2 Buildings designed according to the D.M. 14/01/2008

The structures were designed taking into account the seismic action through a simplified linear static analysis, assuming as design spectrum the one relative to the municipality of Benevento, sited in the Southern Italy (PGA on bedrock for Life Safety Limit State = 0.257 g).

For what concern the site effects, in the design process a soil type C (according to EC8/NTC08) was assumed (stratigraphic amplification $S_s = 1.35$)

As behaviour factor a value equal to 5.85 was assumed, based on the provisions provided by the code (high ductility class, frame structure with more than one storey and more than one bay).

In Figure 4.4 the design spectrum (elastic and inelastic) adopted for the design of the 4 and 8 floors buildings is shown.

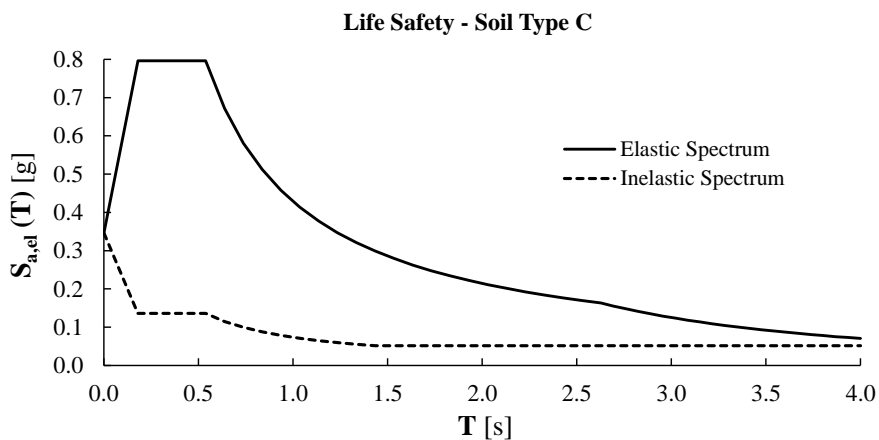


Figure 4.4 - Reference spectrum for the design

In the design process all the rules of the “capacity design” were respected, from the hierarchy beam-column to the hierarchy shear-flexure.

In Figure 4.5 and Figure 4.6, the elevation layouts of the buildings are illustrated respectively for the 4 floors and 8 floors buildings, including the section geometries and reinforcing details.

It is clearly visible the difference in terms of reinforcements details with respect to the buildings designed for vertical loads only, with a far greater amount

of transversal reinforcements in the columns, useful to prevent the formation of brittle mechanisms.

In addition, with respect to the Pre-Code buildings, in this case a continuous foundation (22m x 1.50 m for the 4 floors building, 22m x 3.30 m for the 8 floors building) was assumed, to ensure a rigid behaviour of the foundation, as requested by modern seismic codes.

In Table 4.5 and in Table 4.6 are shown, respectively for the 4 floors and for the eight floors buildings, the dimensions of columns obtained at the end of the design process, with the indication of the ratio (ν) between the vertical load (at the ultimate limit state) on the column and the axial capacity of the same.

The axial capacity was obtained assuming for concrete the design resistance obtained as:

$$f_{cd} = 0.85 f_{ck} / \gamma_c = 0.85 * 25 / 1.5 = 14.17 \text{ MPa} \quad (4.3)$$

as suggested by NTC08.

The vertical loads on the columns were obtained assuming for the floor loads a value equal to 11.36 kN/m² for the all the floors except for the last one, for which a load of 8.36 kN/m² was considered.

In this case, the loads are greater than those considered for the design of the pre-code buildings.

In fact, in this case the loads were amplified by means of partial safety factors to consider the ultimate limit state load combination (1.3 for dead loads and 1.5 for live loads).

Referring to concrete constitutive laws (see Section 3.1) adopted in OpenSees, it is highlighted that, according to Eurocode 8 - part 3:

- a confinement factor (i.e. the ratio of confined to unconfined concrete strength) equal to 1.16 and 1.28 was assumed for 4 floors building and 8 floors building respectively;
- a concrete strain at maximum stress equal to 0.0036 and 0.0048 was assumed for the 4 floors building and 8 floors building, respectively;
- a concrete strain at ultimate stress equal to 0.022 and 0.033 was assumed for the 4 floors building and 8 floors building, respectively.

Table 4.4 summarizes the parameter values of the concrete material object adopted for the two seismically designed buildings.

Table 4.4 - Code compliant buildings - Parameter values for material object “Concrete01” in OpenSees

Floors	Confined / Unconfined	fpc [MPa]	epsc0 [-]	fpcu [MPa]	epsU [-]
4	Unconfined	25	0.0020	25	0.0035
	Confined	29	0.0036	29	0.0220
8	Unconfined	25	0.0020	25	0.0035
	Confined	32	0.0048	32	0.0330

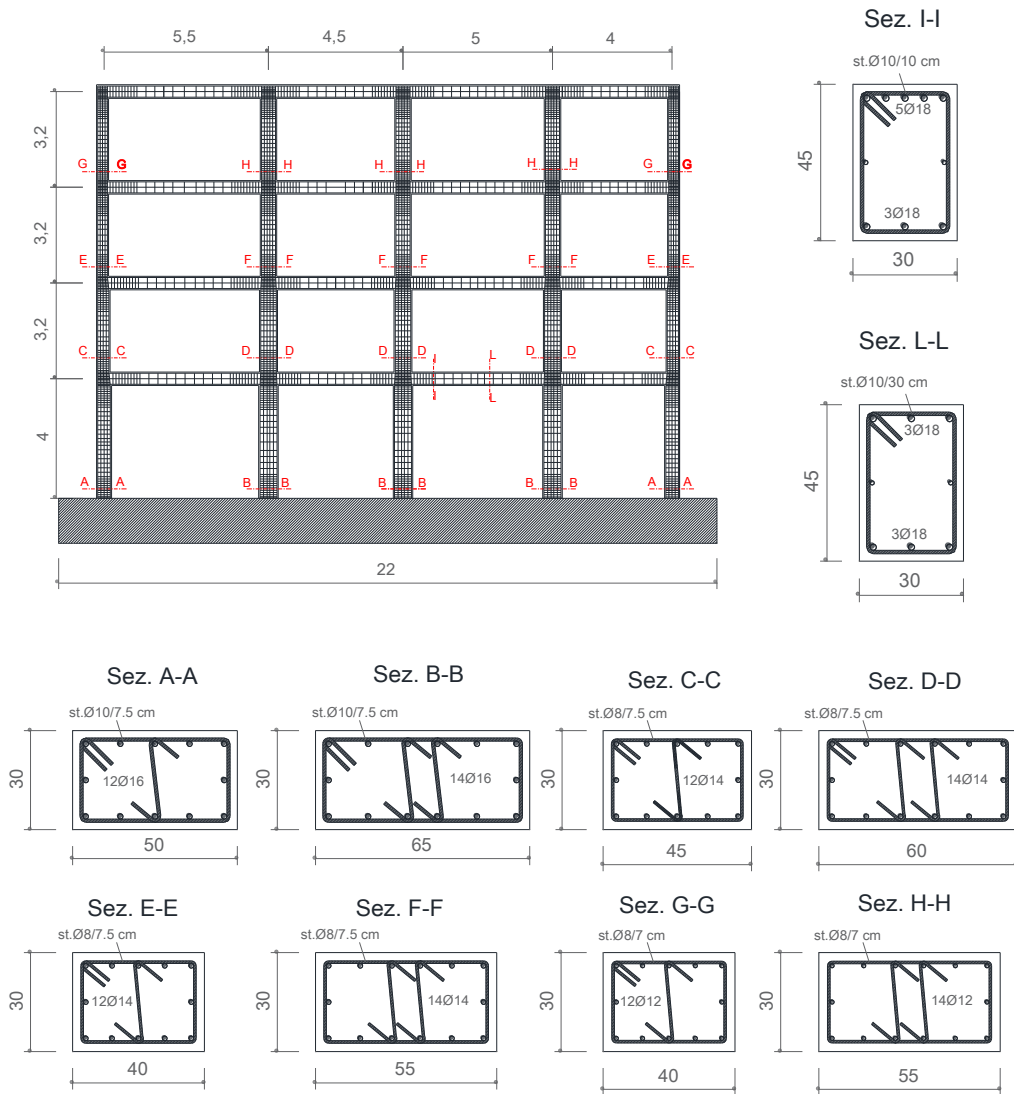


Figure 4.5 - 4 Floors Code compliant building

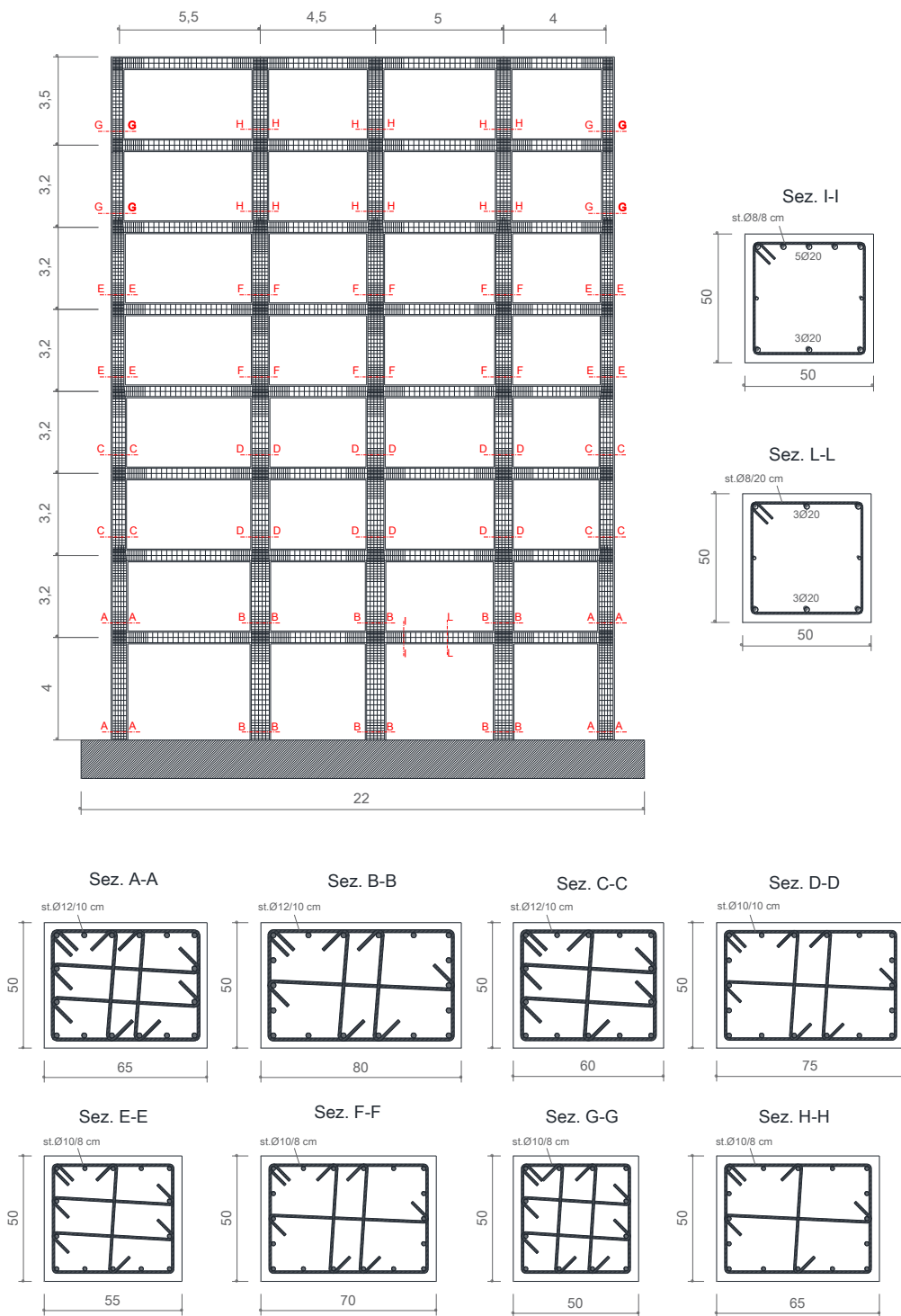


Figure 4.6 - 8 Floors Code compliant building

Table 4.5 - 4 Floors Code compliant building: columns dimensions

Floor	External / Internal	N [kN]	B [m]	H [m]	v [-]
1	External	632	0.30	0.50	0.30
	Internal	1149	0.30	0.65	0.42
2	External	464	0.30	0.45	0.24
	Internal	843	0.30	0.60	0.33
3	External	295	0.30	0.40	0.17
	Internal	537	0.30	0.55	0.23
4	External	127	0.30	0.40	0.07
	Internal	231	0.30	0.55	0.10

Table 4.6 - 8 Floors Code compliant building: columns dimensions

Floor	External / Internal	N [kN]	B [m]	H [m]	v [-]
1	External	1387	0.50	0.65	0.30
	Internal	2522	0.50	0.80	0.45
2	External	1209	0.50	0.65	0.26
	Internal	2197	0.50	0.80	0.39
3	External	1030	0.50	0.60	0.24
	Internal	1873	0.50	0.75	0.35
4	External	851	0.50	0.60	0.20
	Internal	1548	0.50	0.75	0.29
5	External	673	0.50	0.55	0.17
	Internal	1224	0.50	0.70	0.25
6	External	494	0.50	0.55	0.13
	Internal	899	0.50	0.70	0.18
7	External	316	0.50	0.50	0.09
	Internal	574	0.50	0.65	0.12
8	External	137	0.50	0.50	0.04
	Internal	250	0.50	0.65	0.05

4.2 Soil Classes

For what concerns the soil properties, two different soil classes were referenced, according to the soil classes suggested by the EC8.

Considering that SSI can be important for values of the soil-structure relative stiffness, σ , lower than 20 (*Veletsos and Meek, 1978*), and keeping in mind the fundamental periods of the structures under investigations, two types of clays

(soft and medium) were considered in the study, sortable respectively as soil type C and D (according to Eurocode 8).

Table 4.7 summarises the properties of the soils considered in this study with the indication, in particular, of the plasticity index used to choose an appropriate shear modulus reduction curve and a damping curve from those proposed by *Darendeli* (2001) for clays at a confining pressure of $p_o' = 1$ atm.

In Table 4.8 the values of the relative stiffness soil-structure for the different combinations soil-structure analysed are shown.

Table 4.7 - Soil properties

	Soil Type C	Soil Type D
Height of the deposit	30 m	30 m
Type of Soil	Clay	Clay
Plasticity Index	15%	100%
Shear Wave Velocity (V_{s0})	250 m/s	160 m/s
Density (ρ)	2.0 t/m ³	1.6 t/m ³
Cohesion (c)	65 kPa	49 kPa

Table 4.8 - Values of the soil-structure relative stiffness ($\sigma = V_s T_{fix} / h$)

Structure	Soil Type	V_{s0} [m/s]	ρ [t/m ³]	G_0 [kN/m ²]	h [m]	T_{fix} [s]	σ [-]
4 Floors – Pre-Code	C	250	2.0	125000	13.6	0.97	18
	D	160	1.6	40960	13.6	0.97	11
8 Floors – Pre-Code	C	250	2.0	125000	26.4	1.14	11
	D	160	1.6	40960	26.4	1.14	7
4 Floors – Code compliant	C	250	2.0	125000	13.6	0.65	12
	D	160	1.6	40960	13.6	0.65	8
8 Floors – Code compliant	C	250	2.0	125000	26.4	0.92	9
	D	160	1.6	40960	26.4	0.92	6

4.3 Selection of the accelerograms

A set of twenty-one records was used for the dynamic analyses shown in the next sections. In particular, three different sets of seven accelerograms were chosen by means of the software *Rexel* (*Iervolino et al., 2009*).

The first group includes seven accelerometric signals, taken from the European Strong Motion Database, compatible with the type 1 response spectrum provided by Eurocode 8.

The second group consists of seven signals taken from the European Strong Motion Database but compatible with the type 2 response spectrum provided by Eurocode 8.

Finally, the third group consists of seven signals chosen in the Italian Accelerometric Archive and compatible with the response spectrum provided by the Italian D.M. 14/01/2008.

All the records refer to outcrop conditions recorded at site conditions classified as rock according to EC8 (soil type A) with moment magnitude (M_w) and epicentral distance (R) that range between $5.0 < M_w < 7.0$ and $0 < R < 30$ km respectively.

The compatibility with the response spectra mentioned above was checked in the period range from $0.15 \text{ s} < T < 2.0 \text{ s}$.

From Table 4.9 to Table 4.11 the different groups of signals are listed, while in from Figure 4.7 to Figure 4.9 the compatibility of the different sets with the reference spectra is shown.

Before applying the selected outcropping records, the real seismic records are first subjected to baseline correction and filtering. In particular, a Butterworth bandpass 4th order filter type in the frequency range from $f_1 = 0.25$ Hz to $f_2 = 10$ Hz and a linear type baseline correction were applied to all records using *Seismosignal* software (*Seismosoft, Seismosignal 2011*).

Annex B summarizes the acceleration time histories as well as the elastic acceleration response spectra of the seismic records used as input motion.

Table 4.9 - Group 1: seven accelerograms from the European Strong Motion Database compatibles with the Type 1 spectrum proposed by Eurocode 8

Number	Waveform ID	Station ID	Earthquake	Date	M _w	R [km]	PGA [m/s ²]
1	000198xa	ST64	Montenegro	15/04/1979	6.9	21	1.77
2	000234xa	ST68	Montenegro (aftershock)	24/05/1979	6.2	30	0.67
3	000292xa	ST98	Campano Lucano	23/11/1980	6.9	25	0.59
4	000292ya	ST98	Campano Lucano	23/11/1980	6.9	25	0.59
3	006327ya	ST2552	South Iceland (aftershock)	21/06/2000	6.4	24	0.58
4	006333xa	ST2487	South Iceland (aftershock)	21/06/2000	6.4	28	0.20
6	006335xa	ST2557	South Iceland (aftershock)	21/06/2000	6.4	15	1.25

Table 4.10 - Group 2: seven accelerograms from the European Strong Motion Database compatibles with the Type 2 spectrum proposed by Eurocode 8

Number	Waveform ID	Station ID	Earthquake	Date	M _w	R [km]	PGA [m/s ²]
1	000055xa	ST20	Friuli	06/05/1976	6.5	23	3.50
2	000128ya	ST36	Friuli (aftershock)	15/09/1976	6	28	0.69
3	000149xa	ST26	Friuli (aftershock)	15/09/1976	6	12	1.34
4	000410ya	ST161	Golbasi	05/05/1986	6	29	0.54
5	006115ya	ST1320	Kozani	13/05/1995	6.5	17	1.40
6	006265ya	ST2494	South Iceland	17/06/2000	6.5	29	0.56
7	006332xa	ST2483	South Iceland (aftershock)	21/06/2000	6.4	6	5.19

Table 4.11 - Group 3: Seven accelerograms from the Italian Accelerometric Archive compatibles with the spectrum proposed by NTC 08

Number	Waveform ID	Station ID	Earthquake	Date	M _w	R [km]	PGA [m/s ²]
1	IT0103xa	SRC0	Friuli Earthquake 4th shock	15/09/1976	5.9	16	1.29
2	IT0103ya	SRC0	Friuli Earthquake 4th shock	15/09/1976	5.9	16	2.45
3	IT0126xa	FRR	Ferruzzano	11/03/1978	5.2	9	0.72
4	IT0164xa	ALT	Irpinia Earthquake	23/11/1980	6.9	24	0.55
5	IT0169ya	BSC	Irpinia Earthquake	23/11/1980	6.9	28	0.81
6	IT0270xa	PNT	Val Comino Earthquake	07/05/1984	5.9	27	0.63
7	IT0809xa	GSG	L'Aquila Mainshock	06/04/2009	6.3	23	0.29

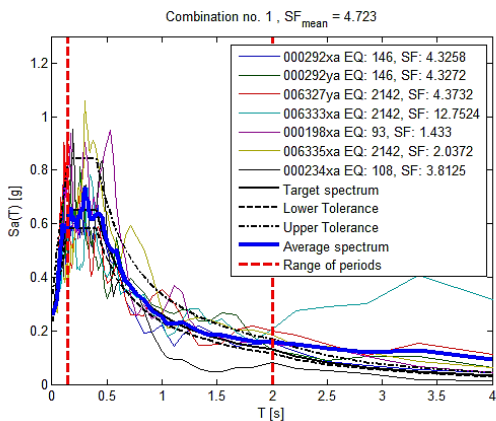


Figure 4.7 - Group 1 – Compatibility with the EC8 type 1 spectrum

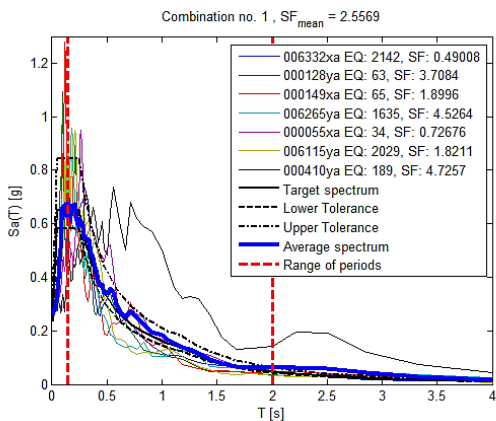


Figure 4.8 - Group 2 – Compatibility with the EC8 type 2 spectrum

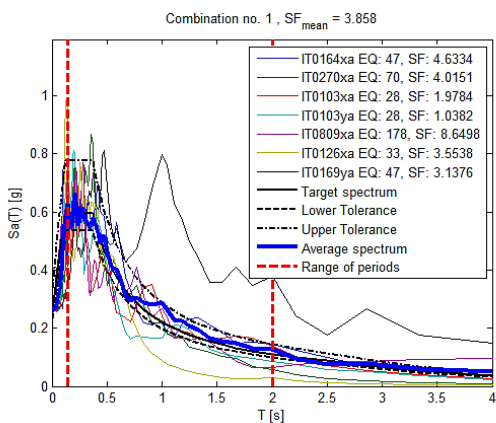


Figure 4.9 - Group 3 – Compatibility with the NTC 08 spectrum

4.4 Analyses

The Non-Linear Time-History (NLTH) analyses were performed for both the cases of fixed-base and flexible-base (i.e. taking into account the Soil-Structure Interaction).

For what concerns the flexible-base models, two different approaches were referenced to model the SSI.

In the first approach the SSI was taken into account by means of a Beam on Non Linear Winkler Foundation (BNWF) model (see Section 3.2.2).

This kind of modelling was preferred over a modelling of the foundation impedances inasmuch the model can implicitly take into account the possible uplift of the foundation. However, this effect was verified to be negligible for the reference structures examined in the study.

The distributed vertical springs and the horizontal spring (see Section 3.2.2), as well as the corresponding radiation damping coefficients, were calibrated based on the *Pais and Kausel* (1988) formulations (see Section 3.2.1) considering the initial shear modulus of the soil.

The horizontal passive load-displacement behaviour against the side of footings was neglected.

This component of the footing response has, in fact, a negligible effect on the structural response in the case of shallow foundations with a small depth of embedment, as shown in the next Section 4.5.5.

In the second approach, the complete system (soil and structure) is modelled in one step.

It is worth to note that, in order to ensure free field and “quasi transparent” condition at the boundaries (see Section 3.3.1) the soil grid adopted for the 4 floors buildings has a total length of 120m with a depth of 30m that includes 3600 four-node quadrilateral elements, whereas for 8 floors buildings the total length and the number of quadrilateral elements increase to 220m and 6600 respectively (see Figure 4.10).

The analyses were performed modelling in a simplified way the non-linear soil behaviour by means of quad elements with elastic isotropic behaviour with

a properly reduced shear modulus and hysteretic damping assigned to soil elements in the Rayleigh form (see Section 3.3.1).

In the next Section 4.5.5, in fact, the results of some analyses performed making reference to a more appropriate modelling of the non-linear soil behaviour by means of the '*PressureIndepenMultiYield*' Material implemented in OpenSees (see Section 3.3.1) are shown.

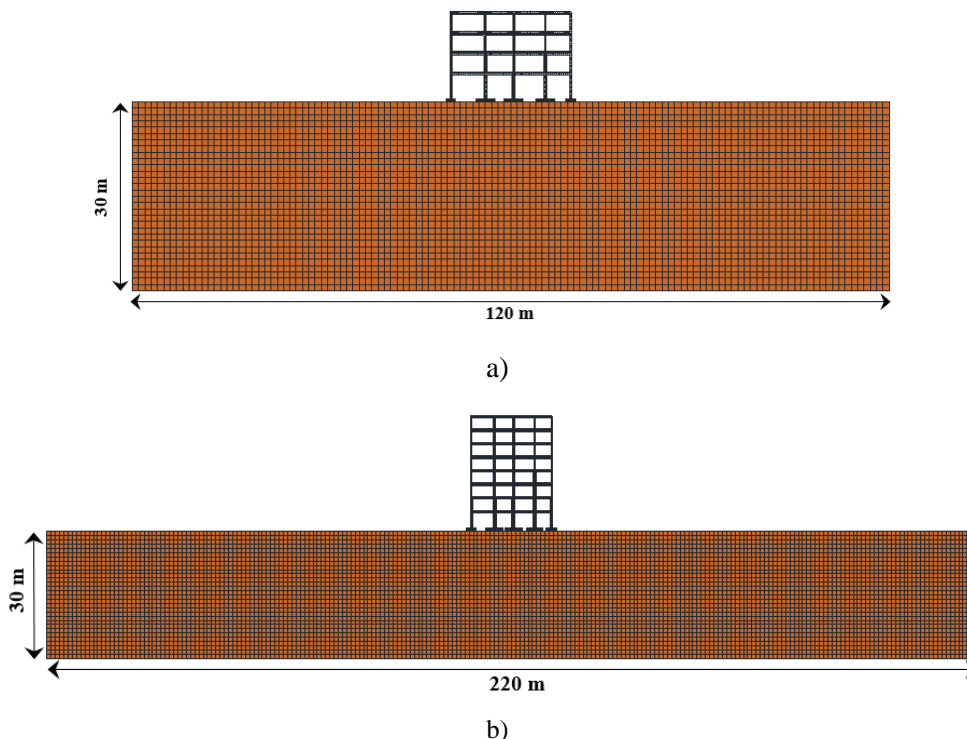


Figure 4.10 - Complete FEM model: soil grid dimensions for a) 4 floors buildings and b) 8 floors buildings

The results show that a simplified modelling of the soil non linearity can be in general acceptable and that the results provided by this kind of modelling are in good agreement with those obtainable through a more refined modelling of the non-linear soil behaviour.

A schematic illustration of the different problems analysed is shown in Figure 4.11.

It is important to note that for the fixed-base model and for the BNWF model the signal applied at the base of the numerical models is the free field motion (FFM) obtained by means of a 1-D wave propagation analysis of a soil column with the same properties and constitutive law adopted in the Complete FEM model.

In all the analyses, the records were scaled to eight different values of peak acceleration at the bedrock, and in particular:

$$0.05 g - 0.075 g - 0.10 g - 0.125 g - 0.15 g - 0.20g - 0.25 g - 0.30 g$$

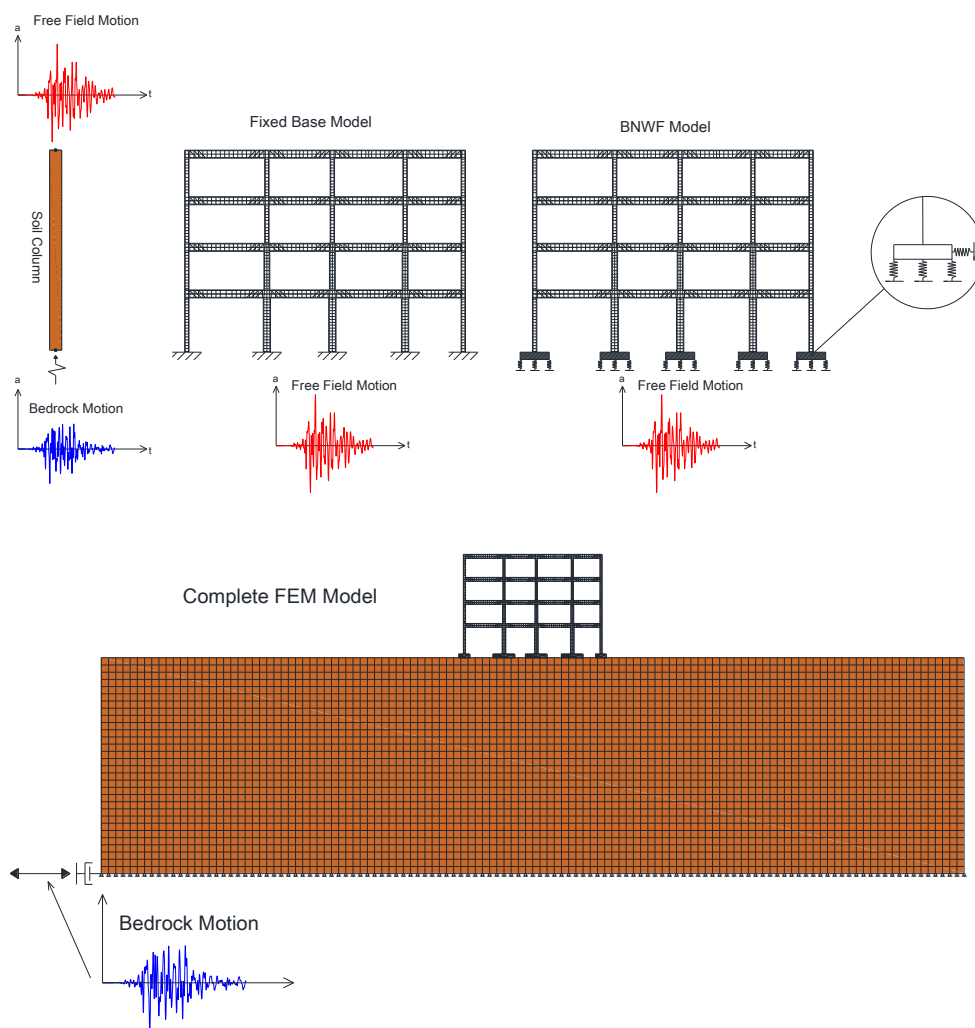


Figure 4.11 - Reference schemes for dynamic analyses

The maximum base shear and the maximum inter-storey drift ratio were chosen as synthetic engineering demand parameters.

Another observation concern the kinematic interaction. In the complete FEM model the kinematic interaction is automatically considered by the numerical model, while in the BNWF model it is neglected.

This assumption is in general accepted in the case of shallow foundations resting on the surface of the half-space.

4.5 Results

In the following sections, the results of the dynamic analyses performed for the reference structures described in the previous sections 4.1.1 and 4.1.2 are presented. Moreover, some remarks related to the influence of the SSI modelling on the estimation of the seismic demand are discussed.

4.5.1 4 Floors Pre-Code building

In Figure 4.12 a comparison of the results obtained for the fixed-base model (blue lines) and for the complete FEM model (red lines) is shown.

The results are those obtained for the Group 3 of records shown in previous Section 4.3.

The same results are shown in Figure 4.14 for the BNWF model (green lines).

The same graphs for all the analyses performed can be find in [Annex C](#).

In the graphs, the single lines refer to the results obtained for one specific record, while the bold lines represent the result obtained as average, given the PGA level, of the results obtained for all the records of the group.

Only the results obtained for PGA levels that did not cause the structural collapse are reported in the graphs. Thus, the number of points at a certain PGA level is not always equal to seven (number of signals for each group).

The average curves were thus stopped to PGA levels for which at least three values of seismic demand were obtained.

As can be noted in Figure 4.12, taking into account the SSI effects by means of a Complete FEM model, it is possible to obtain significant reductions, with respect to a fixed base model, of the seismic demand in terms of both maximum

base shear and maximum inter-storey drift ratio. In particular, reductions up to 17% can be obtained, on average, in terms of maximum base shear and up to 38% in terms of maximum inter-storey drift ratio for a soil type C.

For a soil type D the SSI seems to affect more the seismic demand in terms of maximum inter-storey drift ratio, with reductions in this case up to 36%.

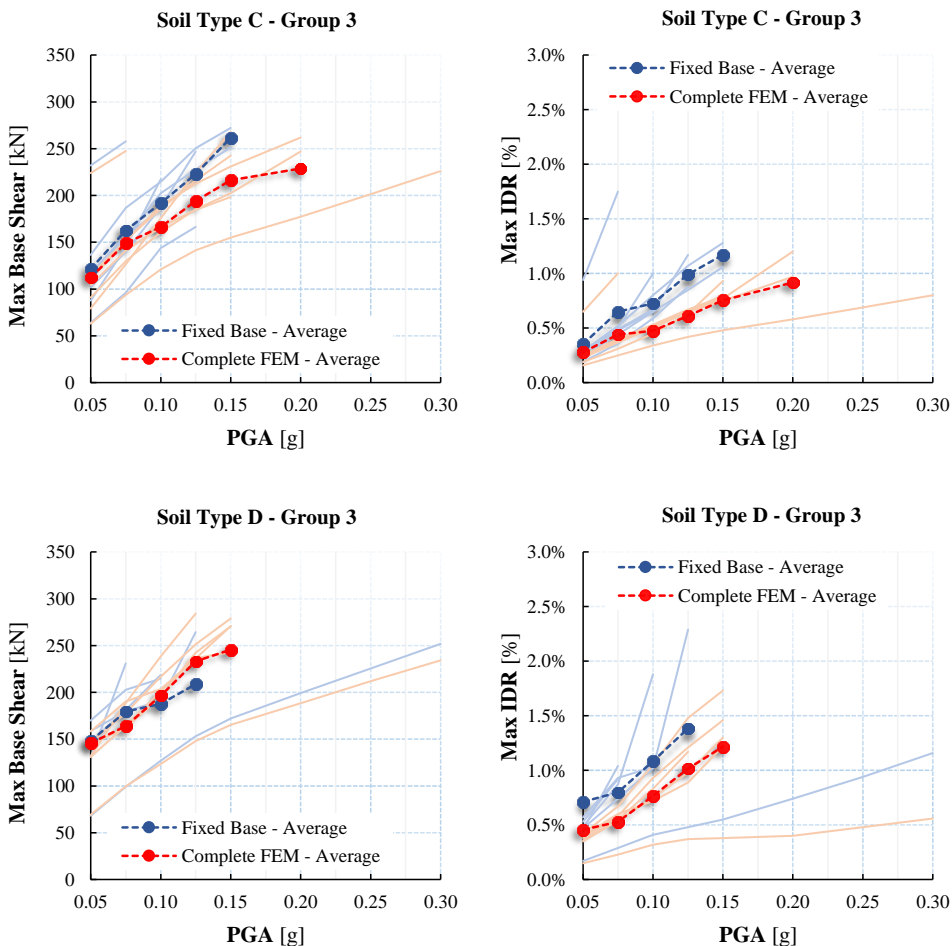


Figure 4.12 - 4 Floors Pre-Code building – Comparison between Fixed Base Model and Complete FEM model – Group 3 Records

The strong reduction of maximum inter-storey drift ratio (IDR) achievable by means of a refined modelling of the SSI effects could have strong impact on the

outcome of safety checks at both the Damage Limit State (DLS) and the Collapse Limit State (CLS).

Usually, in fact, some limit values for the maximum IDR are prescribed by codes for the satisfaction of safety checks.

Italian NTC08, for example, suggests a limit value of 0.5% for the maximum IDR for DLS safety checks.

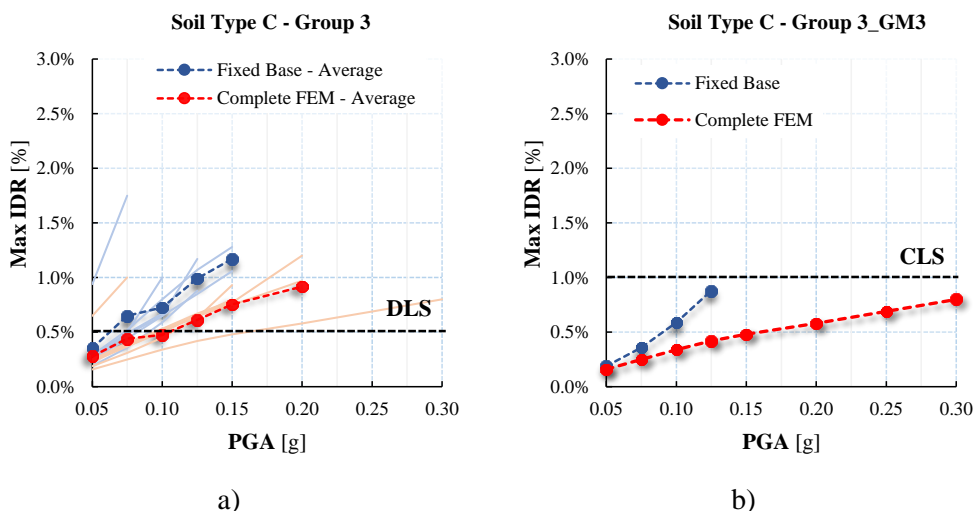


Figure 4.13 - Influence of SSI on safety checks at a) Damage Limit State (DLS) and b) Collapse Limit State (CLS)

As shown in Figure 4.13 a) SSI can lead, for a soil type C, to an increase of the maximum PGA (on bedrock) that the structure is able to withstand without damaging from 0.05g to 0.10g.

However, SSI can have a significant impact even on safety checks at the Collapse Limit State (CLS) too.

Assuming a limit value of 1% for the maximum inter-storey drift ratio, as suggested by *Ghobarah* (2004) for Non-ductile Moment resisting frames, for some signals a strong increase of the maximum PGA that the structure is able to withstand without collapsing can be observed.

In Figure 4.13 b) can be noted that, for a specific record of the group, an increase of the maximum PGA from 0.125 g to 0.30 g can be obtained including the SSI in the numerical modelling by means of a Complete FEM model.

On the contrary, the modelling of SSI by means of a BNWF model seems to produce negligible differences with respect to a fixed-base model, both on the results for a single record and on the average results (see Figure 4.14).

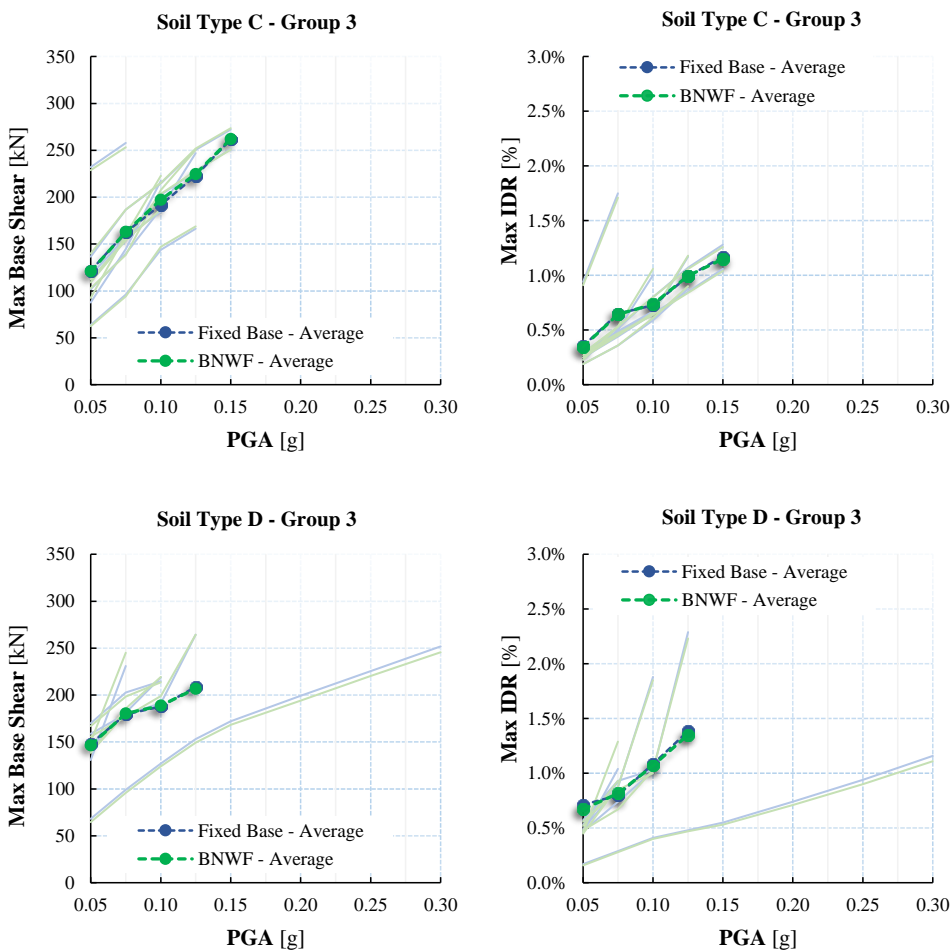


Figure 4.14 - 4 Floors Pre-Code building – Comparison between Fixed Base Model and BNWF model - Group 3 Records

In Figure 4.15 the results (averaged on all the 21 signals) are reported in terms of ratios:

$$\frac{V_{max}^{SSI}}{V_{max}^{FB}} \quad (4.4)$$

$$\frac{IDR_{max}^{SSI}}{IDR_{max}^{FB}}$$

where:

- V_{max}^{SSI} is the maximum base shear obtained for the flexible-base model (Complete FEM model or BNWF model);
- V_{max}^{FB} is the maximum base shear obtained for the fixed-base model;
- IDR_{max}^{SSI} is the maximum inter-storey drift ratio obtained for the flexible-base model;
- IDR_{max}^{FB} is the maximum inter-storey drift ratio obtained for the fixed-base model.

In the graphs, the black squares represent the results obtained through the Complete FEM model while the white circles represent the results obtained through the BNWF model.

It is worth to note that, considering all the 21 records, the modelling of SSI by means of a Complete FEM can lead to reductions of the seismic demand, with respect to a fixed-base model, up to 10% in terms of V_{max} and up to 50% in terms of IDR_{max} .

On the contrary, even considering all the 21 signals, a modelling of SSI effects by means of a BNWF produce negligible differences with respect to a fixed-base model in the evaluation of the seismic demand.

This is probably due to the inadequacy of the BNWF in predicting the sliding demand, which for short structure is the main source of energy dissipation.

As shown by *Raychowdhury* through a comparison of numerical simulations results with the results of experimental tests (*Raychowdhury*, 2008), the model tends to under-estimate the sliding response because of the lack of coupling between vertical and lateral modes of response.

Figure 4.16 shows the trend of all the analyses performed. In this case, on the abscissa, the maximum ground acceleration (i.e. after site effects) is reported.

As can be noted, the influence of SSI effects on the structural response seems to be the same even excluding the site effects.

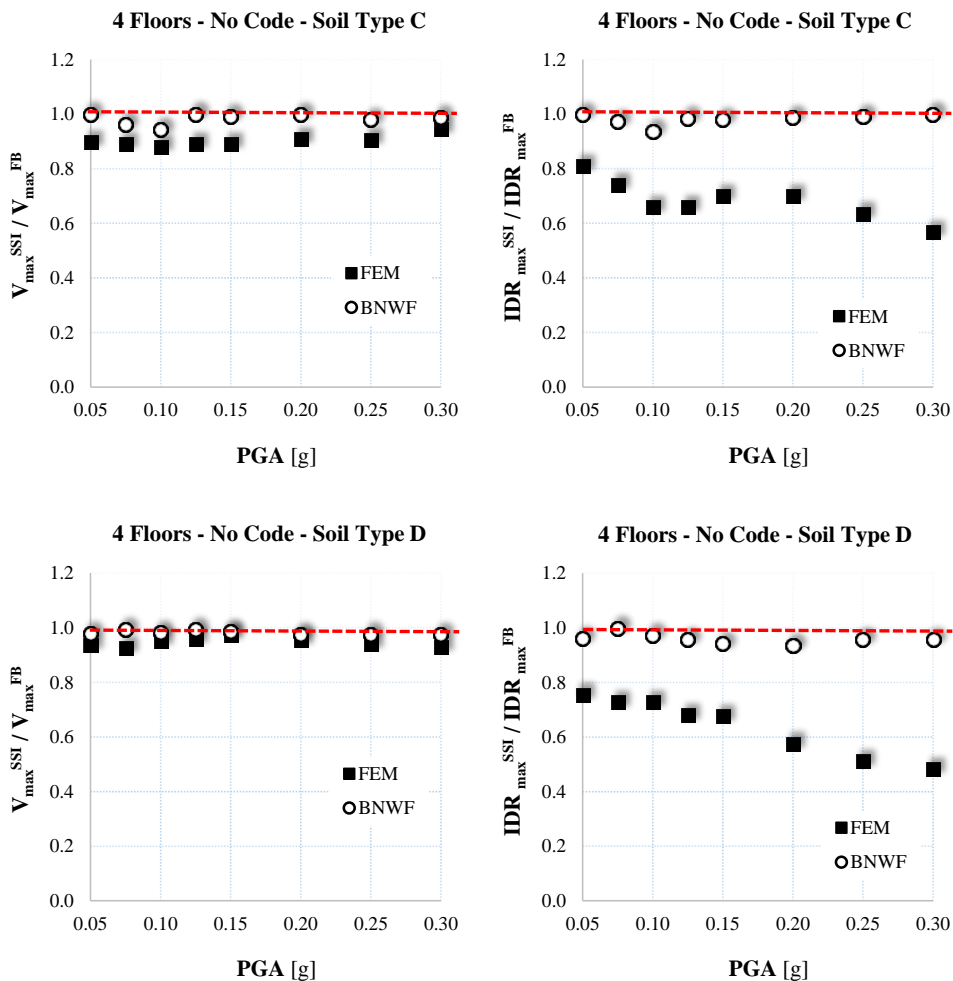


Figure 4.15 - 4 Floors Pre-Code building – Comparison between Complete FEM model and BNWF model (average results on 21 signals)

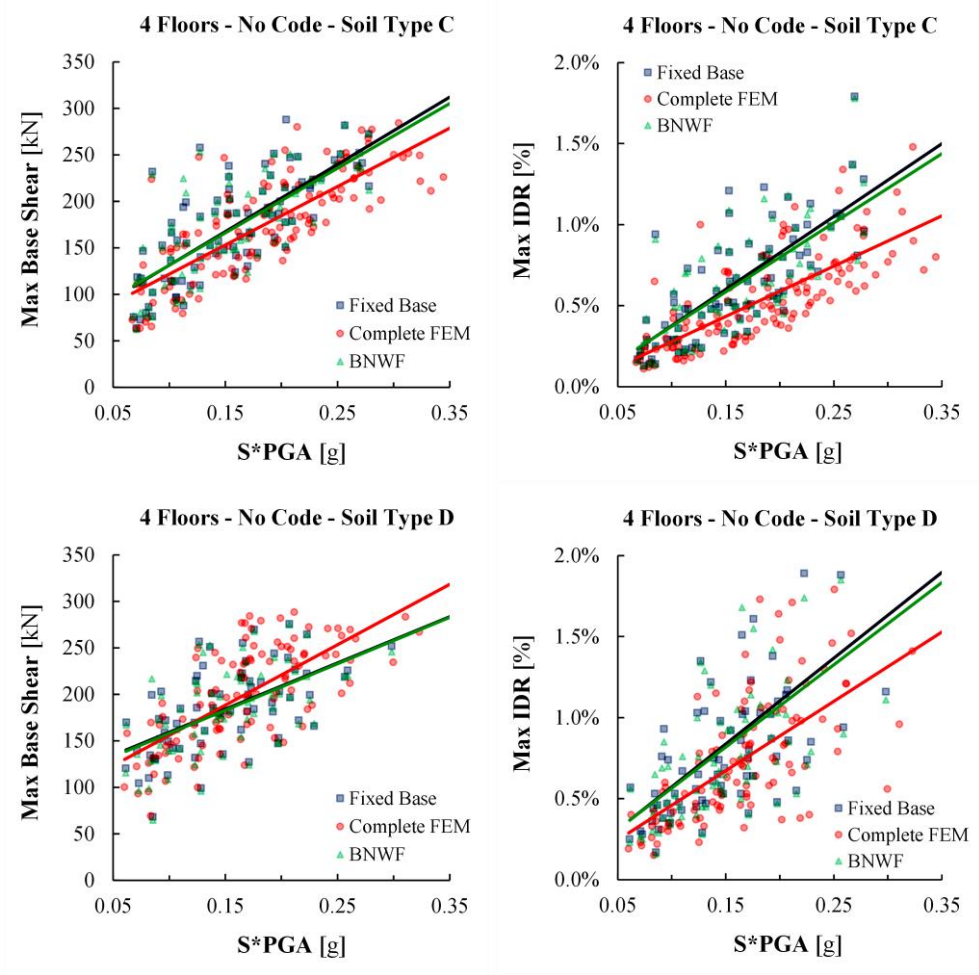


Figure 4.16 - 4 Floors Pre-Code building: comparison between Fixed Base Model, Complete FEM model and BNWF model (trend lines)

4.5.2 4 Floors Code compliant building

In Figure 4.17 the comparison between the results obtained with a fixed base model and with a Complete FEM model is shown.

It is possible to note that in this case the structure is able to withstand, without collapsing, peak ground accelerations up to 0.30g in almost all the cases.

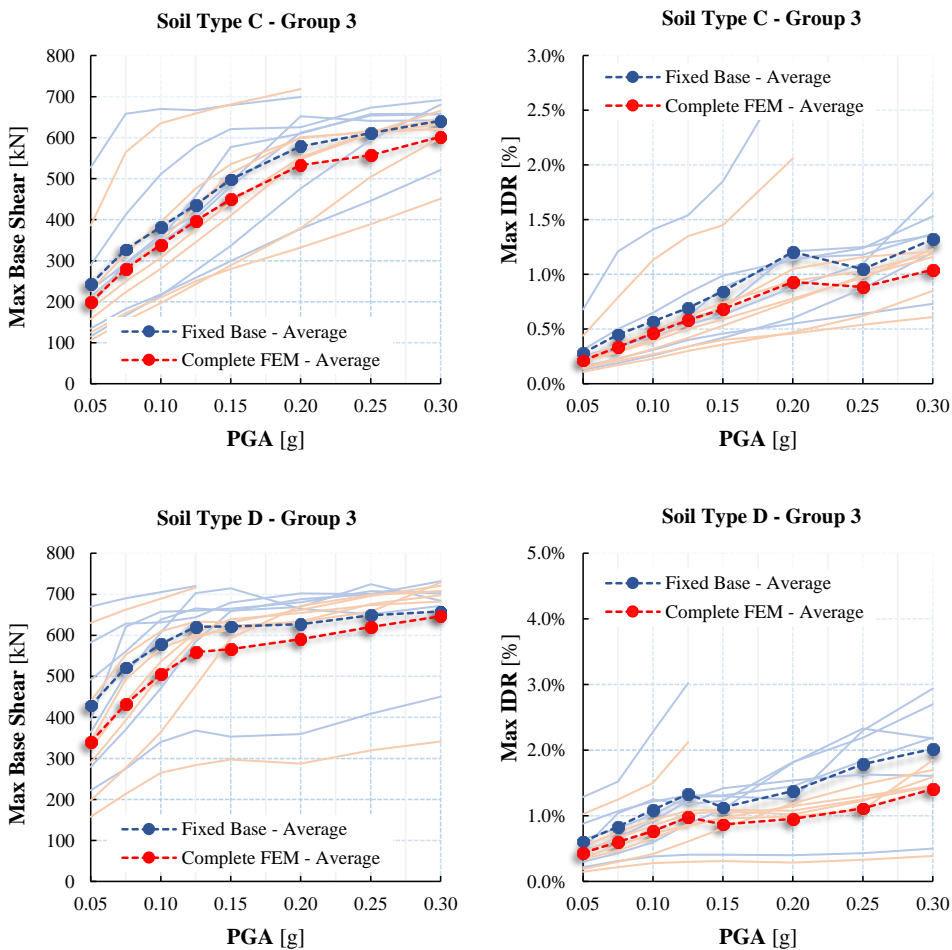


Figure 4.17 - 4 Floors Code compliant building – Comparison between Fixed Base Model and Complete FEM model – Group 3 Records

In this case, through a Complete FEM model, it is possible to obtain, on the group of records, reductions of the seismic demand up to 18% in terms of

maximum base shear and of 25% in terms of maximum inter-storey drift ratio for a soil type C.

For a soil type D, these reductions are of 21% and 38% in terms of maximum base shear and maximum inter-storey drift ratio respectively.

The modelling of SSI with a BNWF model, contrarily, produces no differences in the estimation of the seismic demand with respect to a fixed base model (see Figure 4.18).

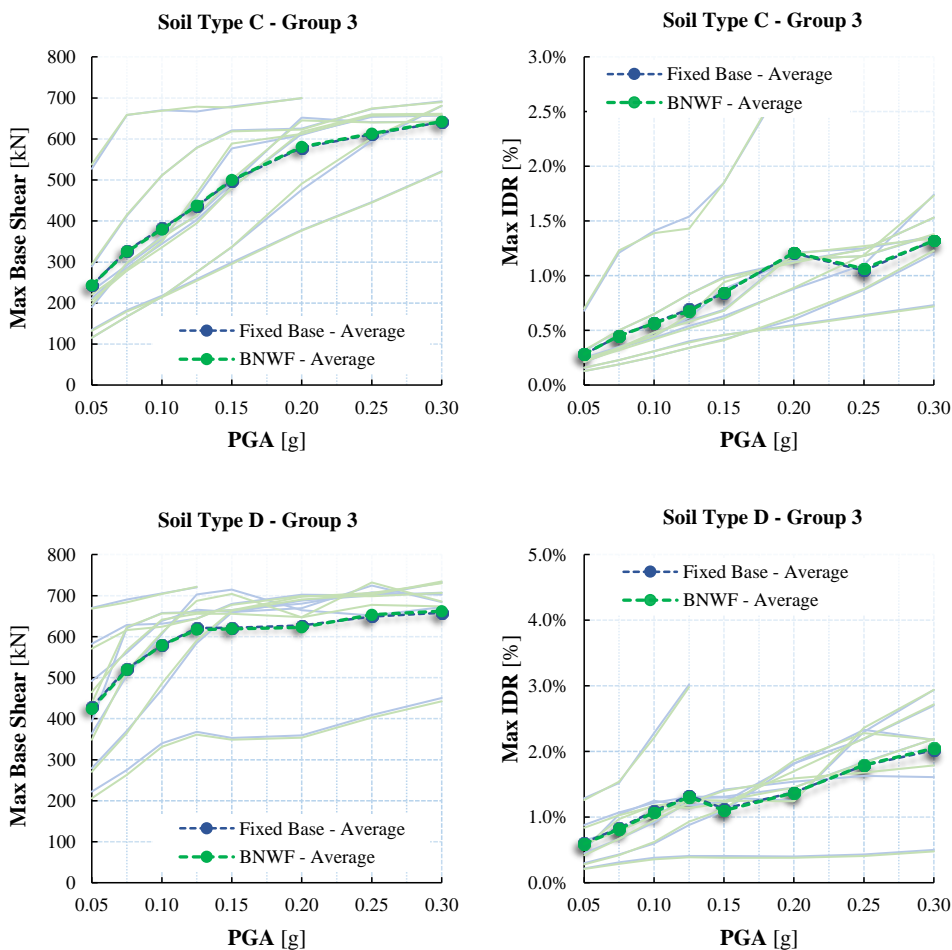


Figure 4.18 - 4 Floors Code compliant building – Comparison between Fixed Base Model and BNWF model - Group 3 Records

Considering all the 21 records (see Figure 4.19), reductions up to 20% in terms of V_{max} and up to 40% in terms of IDR_{max} can be obtained, with respect to a “fixed-base” model, modelling the SSI effects by means of a Complete FEM model.

As for the 4 floors pre-code building, the differences between the results obtained between a fixed-base model and a BNWF model are negligible (see Figure 4.19).

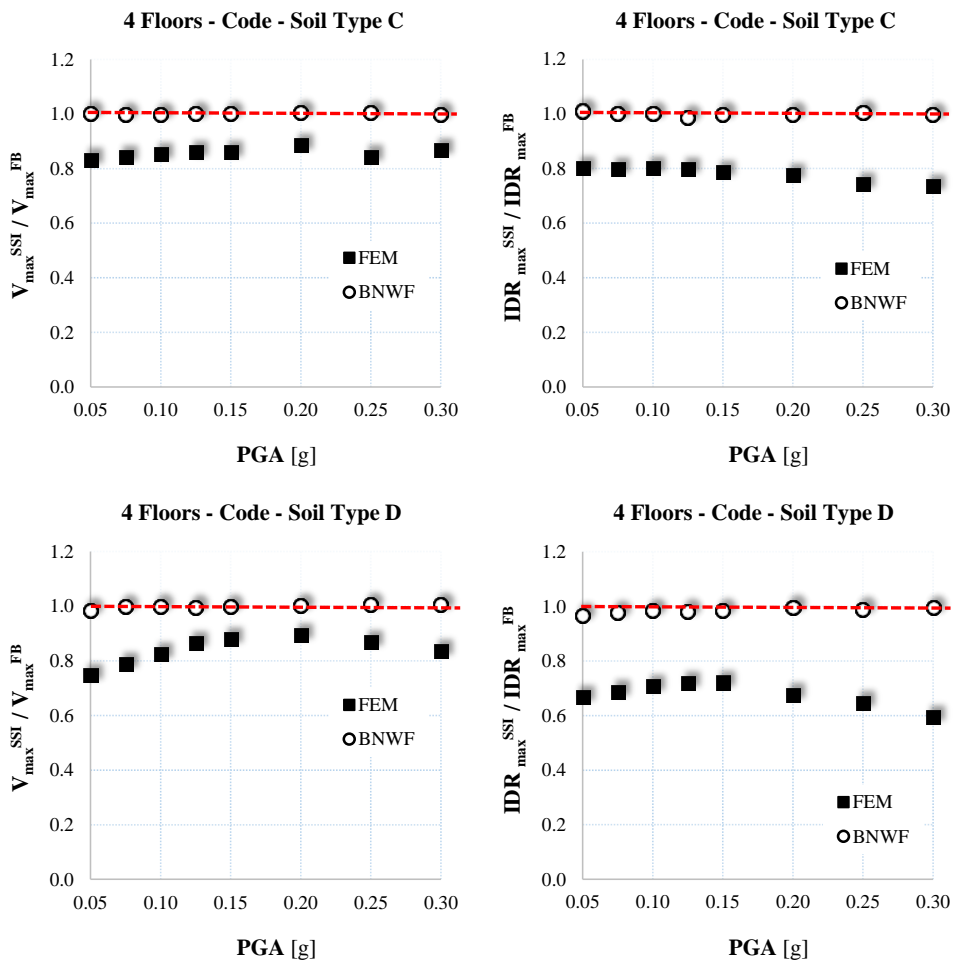


Figure 4.19 - 4 Floors Code compliant building – Comparison between Complete FEM model and BNWF model (average results on 21 signals)

Figure 4.20 confirms the trend of the analyses excluding the site effects.

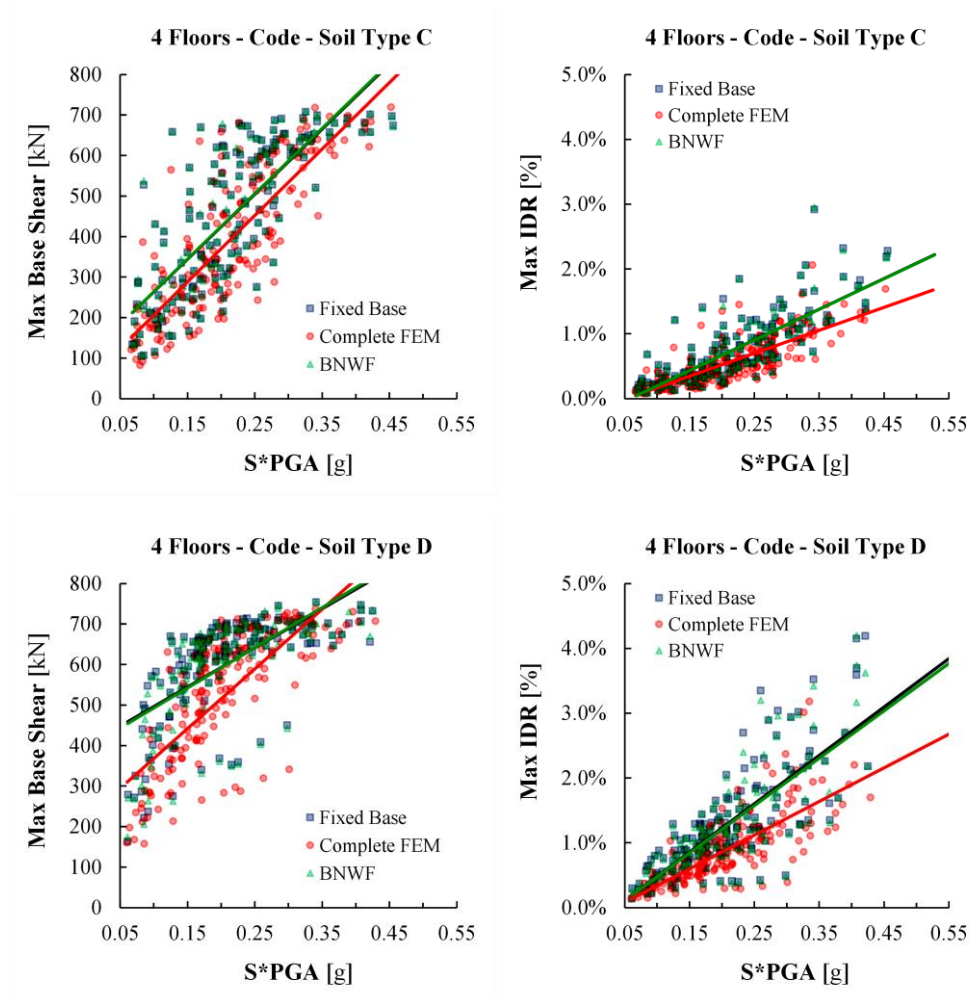


Figure 4.20 - 4 Floors Code compliant building: comparison between Fixed Base Model, Complete FEM model and BNWF model (trend lines)

4.5.3 8 Floors Pre-Code building

In Figure 4.21 the comparison between the results obtained with a fixed base model and with a Complete FEM model is shown for the 8 floors pre-code building.

Considering the single group of records, a modelling of SSI by means of a Complete FEM model can lead to reductions, for a soil type C, of the estimated seismic demand up to 17% and 39% in terms of maximum base shear and maximum inter-storey drift ratio, respectively.

For a soil type D the differences become 12% and 36% in terms of maximum base shear and maximum inter-storey drift ratio respectively.

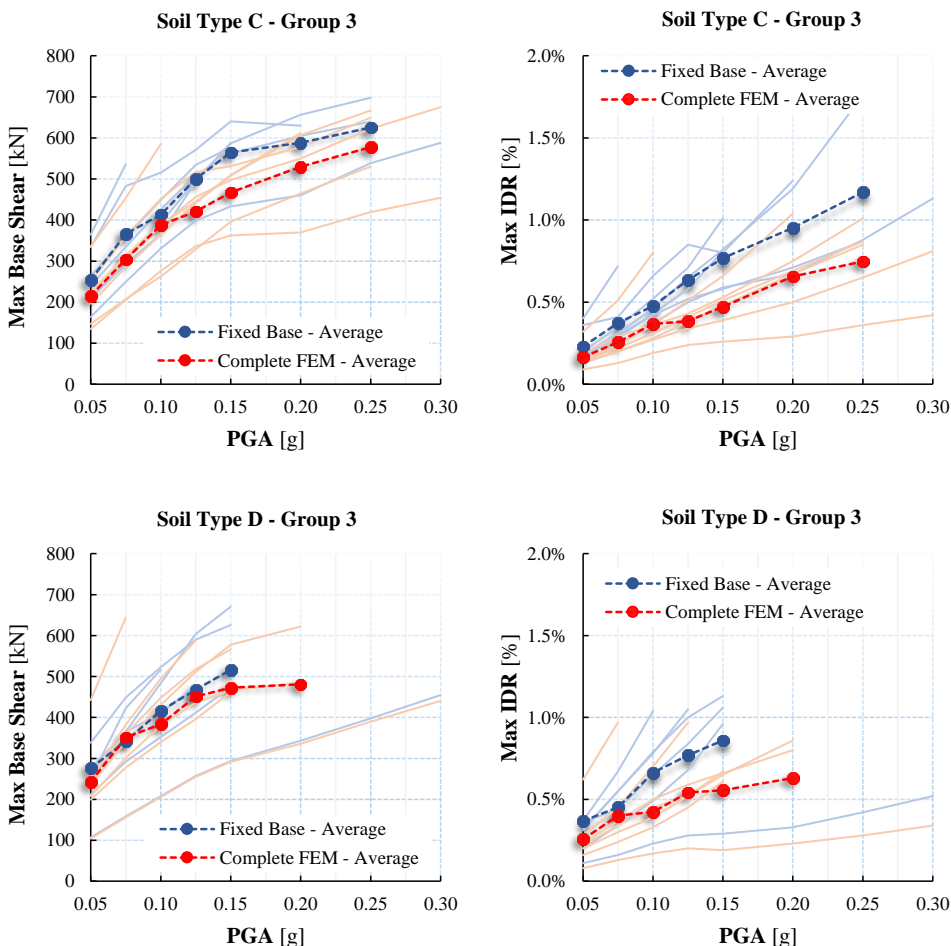


Figure 4.21 - 8 Floors Pre-Code building – Comparison between Fixed Base Model and Complete FEM model – Group 3 Records

Considering a more simplified BNWF model (see Figure 4.22), it is possible to note that for very soft soils (i.e. soil type D) some little reduction of seismic demand can be obtained (6% in terms of maximum base shear and 9% in terms of maximum inter-storey drift ratio).

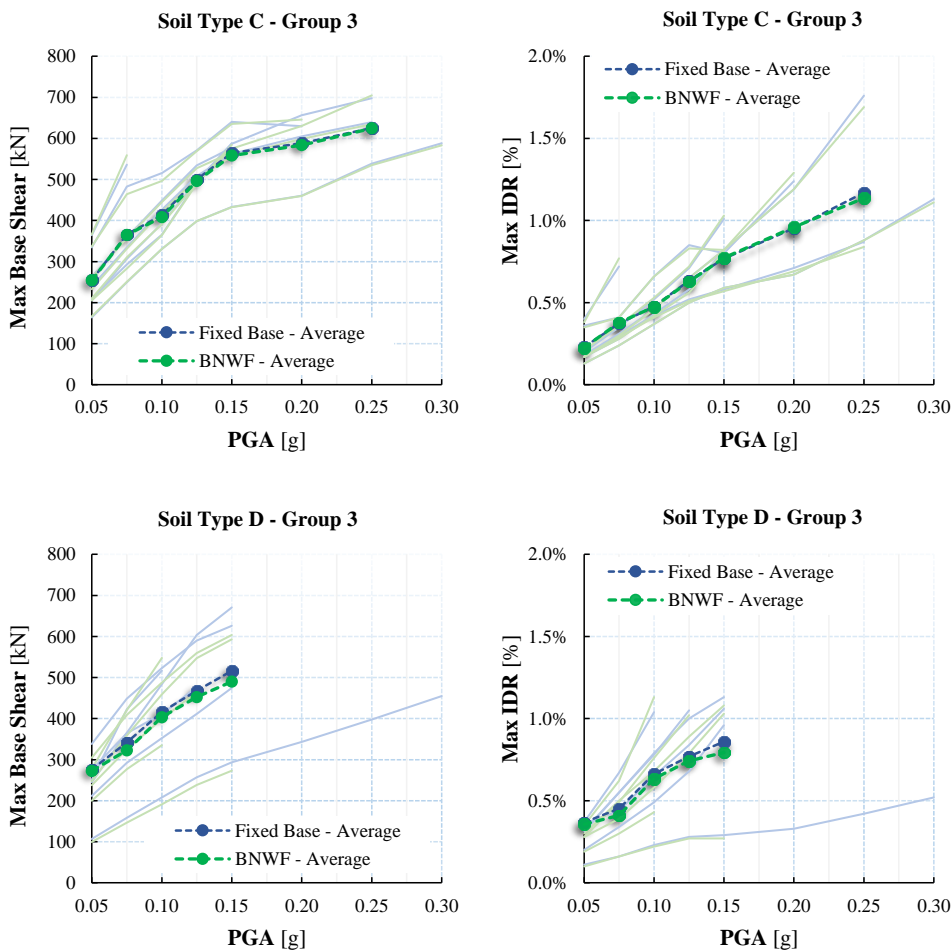


Figure 4.22 - 8 Floors Pre-Code building – Comparison between Fixed Base Model and BNWF model - Group 3 Records

Considering all the 21 records (see Figure 4.23), the average reductions, with respect to “fixed-base” model, can reach the 20% in terms of V_{max} and the 40% in terms of IDR_{max} modelling the SSI effects by means of a Complete FEM model.

A modelling of SSI effects by means of a BNWF can produce reductions up to 20% in terms of both V_{max} and IDR_{max} .

Figure 4.24 confirms the trend of the analyses excluding the site effects.

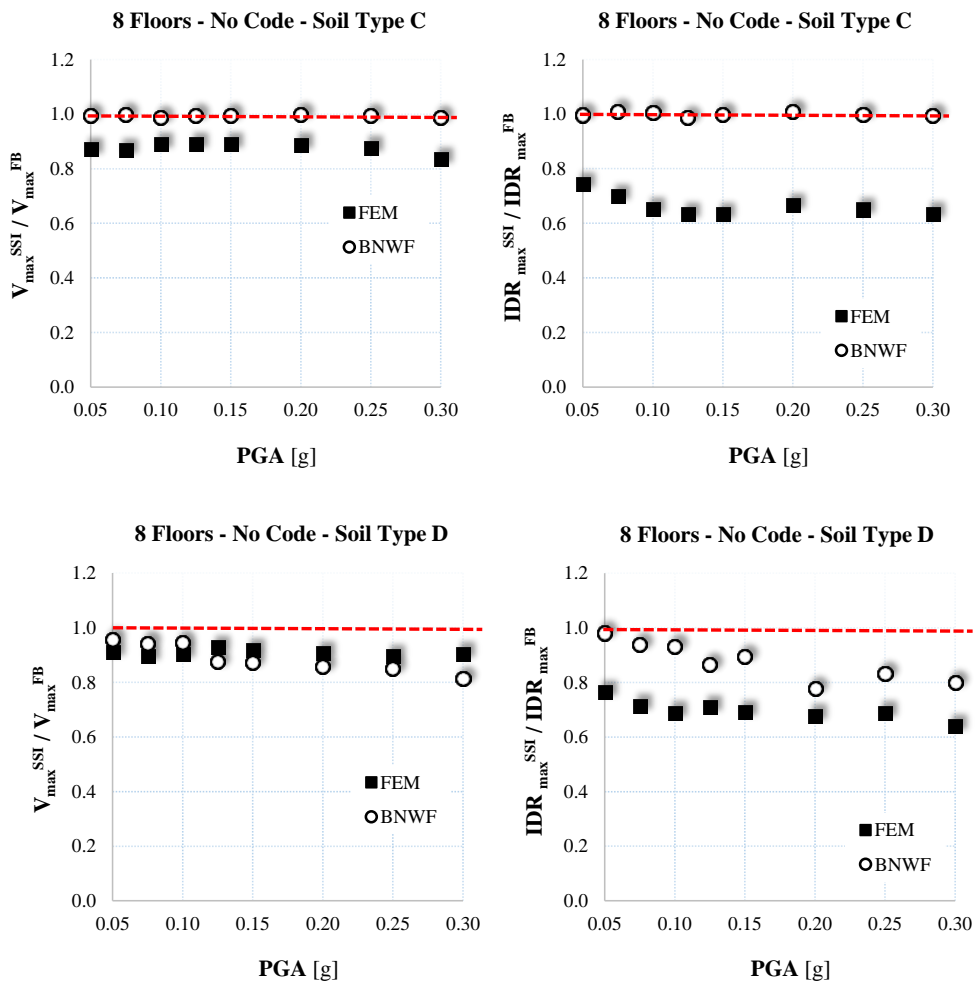


Figure 4.23 - 8 Floors Pre-Code building – Comparison between Complete FEM model and BNWF model (average results on 21 signals)

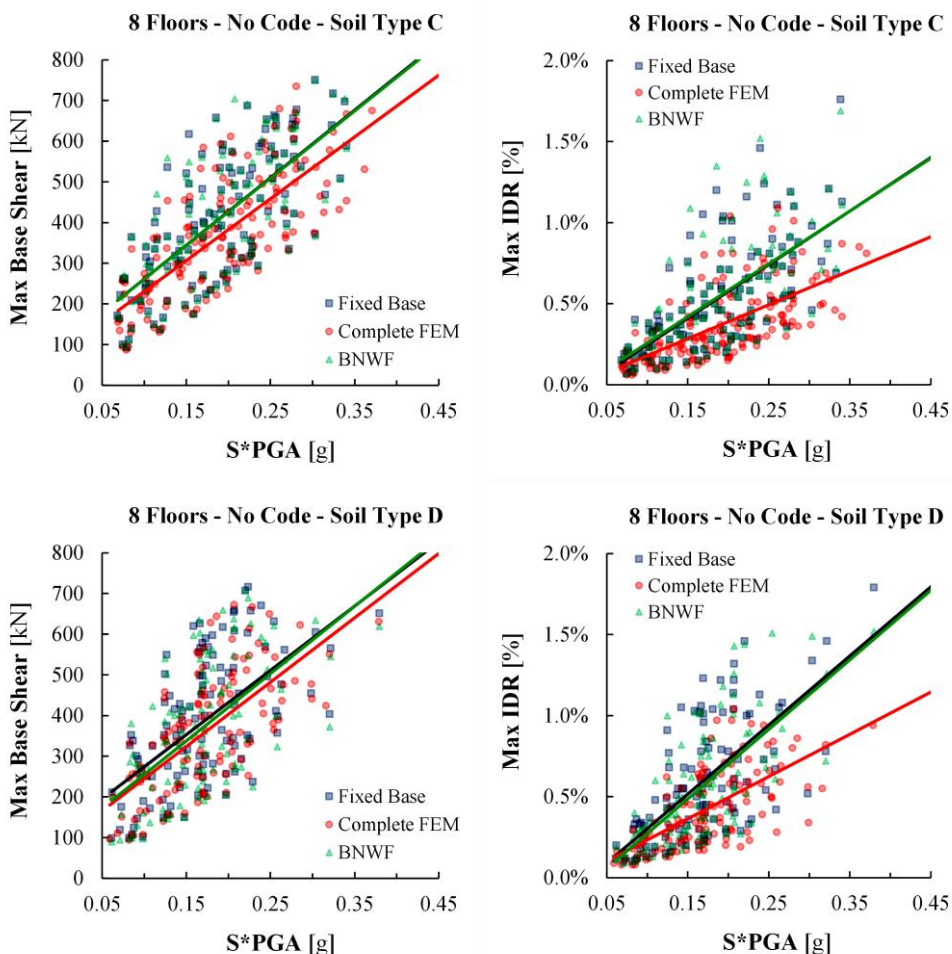


Figure 4.24 - 8 Floors Pre-Code building: comparison between Fixed Base Model, Complete FEM model and BNWF model (trend lines)

4.5.4 8 Floors Code compliant building

In Figure 4.25 the comparison between the results obtained with a fixed base model and with a Complete FEM model is shown for the 8 floors Code compliant building.

Considering the single group of records, a modelling of SSI by means of a Complete FEM model can lead to reductions, for a soil type C, of the estimated seismic demand up to 26% and 36% in terms of maximum base shear and maximum inter-storey drift ratio respectively.

For a soil type D the differences become 21% and 32% in terms of maximum base shear and maximum inter-storey drift ratio respectively.

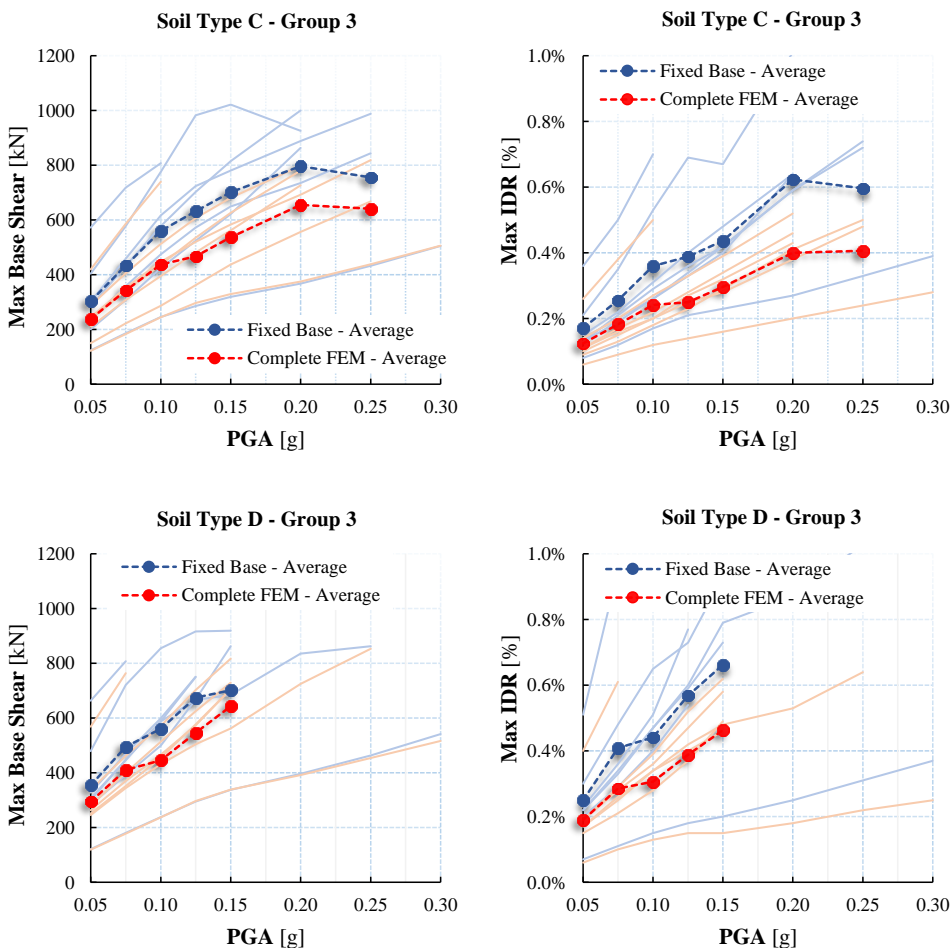


Figure 4.25 - 8 Floors Code compliant building – Comparison between Fixed Base Model and Complete FEM model – Group 3 Records

Considering a more simplified BNWF model (see Figure 4.26), it is possible to note that for a soil type D not negligible reductions of seismic demand can be obtained (9% in terms of maximum base shear and 20% in terms of maximum inter-storey drift ratio).

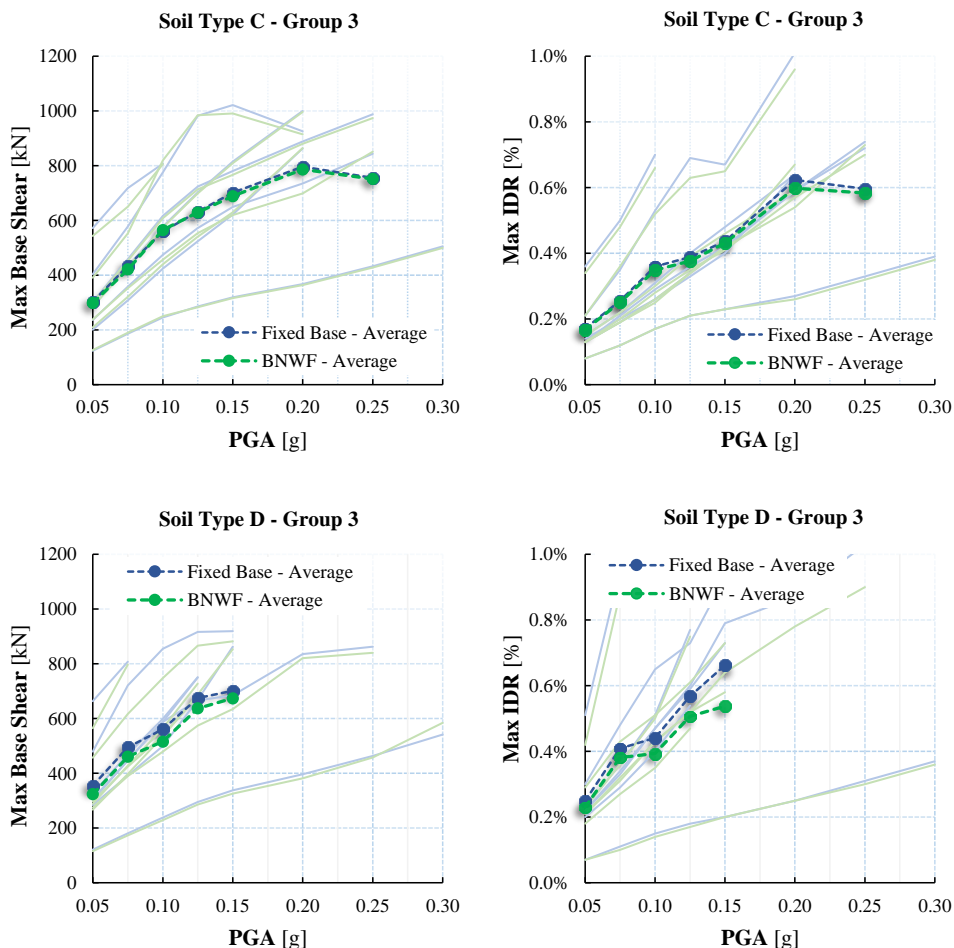


Figure 4.26 - 8 Floors Code compliant building – Soil Type C – Comparison between Fixed Base Model and BNWF model

Considering all the 21 records (see Figure 4.27), the average reductions, with respect to “fixed-base” model, can reach the 20% in terms of V_{max} and the 40% in terms of IDR_{max} modelling the SSI effects by means of a Complete FEM model.

A modelling of SSI effects by means of a BNWF can involve a reduction in the evaluation of the seismic demand up to 10% in terms of maximum base shear and up to 15% in terms of maximum IDR.

Figure 4.28 confirms the trend of the analyses excluding the site effects.

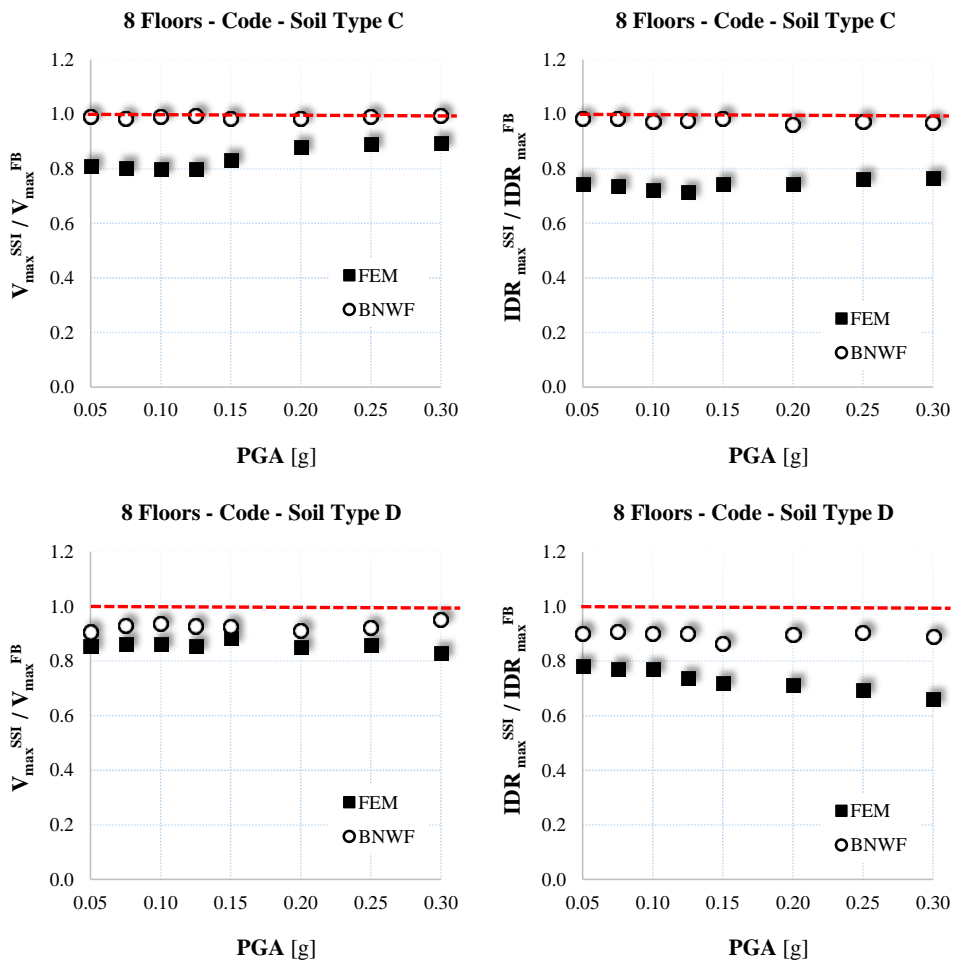


Figure 4.27 - 8 Floors Code compliant building - Comparison between Complete FEM model and BNWF model (average results on 21 signals)

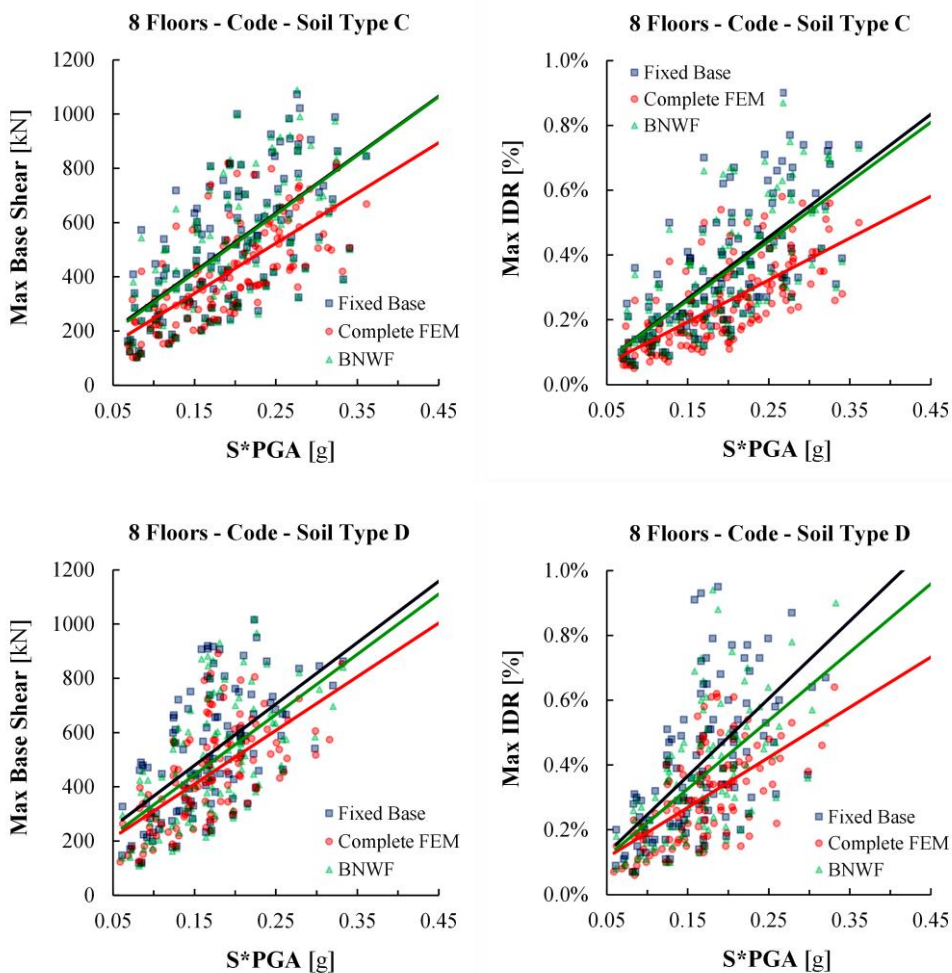


Figure 4.28 - 8 Floors Code compliant building - Comparison between Fixed Base Model, Complete FEM model and BNWF model (trend lines)

4.5.5 Effects of SSI modelling on the estimation of the seismic demand

From the analyses emerged that the influence of SSI effects on the estimation of the seismic structural response strongly depend on the modelling approach.

In particular, the analyses showed that, for almost all the cases analysed, the BNWF model produces negligible differences with respect to a “fixed-base” model in the evaluation of the seismic demand.

These differences become more important when SSI is taken into account by means of a more refined complete FEM model, because of the different characterization of the overall damping of the system.

The difference in predicting the seismic demand between the two modelling approaches of SSI effects can be justified looking at the Fourier Amplitude Spectrum corresponding to the response acceleration of a top node of the structure (see Figure 4.29).

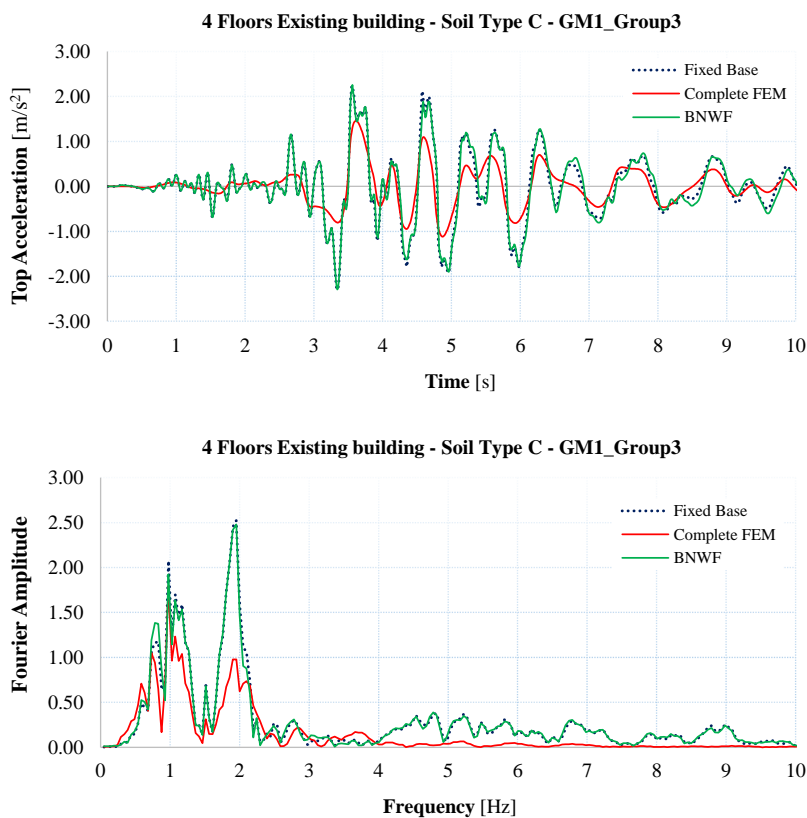


Figure 4.29 - Top acceleration: time history and Fourier Spectrum

It is apparent how in the Complete FEM model the Fourier amplitude is lower, with respect to a BNWF model, on almost all the frequencies of the seismic motion.

This causes a greater damping of the structural response that the BNWF is unable to capture, given the calibration on a specific frequency of the foundation stiffnesses.

In addition can be noted that, especially for 4 floor buildings, the response obtained by means of the BNWF model is basically overlapped to that of the fixed-base model.

This result can be explained referring to the finding provided by *Raychowdhury* (2008) that in his work, from a comparison of numerical simulations results with the results of experimental tests, highlighted the inadequacy of the BNWF in predicting the sliding demand, which is the main source of energy dissipation for short structures.

In the analyses performed with the BNWF model, as stated in Section 4.4, the kinematic interaction was neglected. This assumption was made inasmuch it has generally a negligible effect for shallow foundations (*Stewart et al., 1999*). In order to validate this assumption, in Figure 4.30, a comparison between the free-field motion (FFM) obtained through a 1-D analysis of a soil column and the foundation input motion (FIM) recorded at the base of the foundation in the Complete FEM model is shown. The FIM is that obtained at the base of the 4 floors Code compliant building founded on a soil type D.

The record applied at the bedrock is the first of the Group 1 of records (see Section 4.3) scaled to 0.20g.

As can be noted, the two signals are basically overlapped.

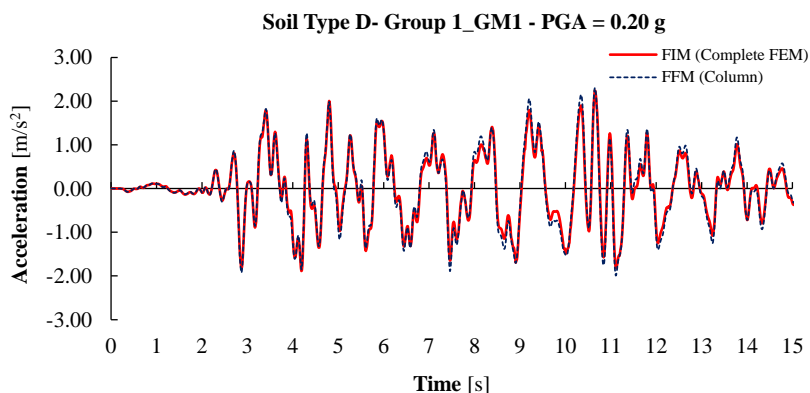


Figure 4.30 – Comparison between free-field motion (FFM) and foundation input motion (FIM)

In all the dynamic analyses performed for the Complete FEM model, the non-linear behaviour of the soil was taken into account in an “equivalent” linear way, properly reducing the shear modulus of the soil (based on the intensity level of the ground motion) and taking into account the dissipative capacity of the soil by means of viscous damping assigned with the Rayleigh formulation.

In Figure 4.31 the results obtained modelling the non-linear soil behaviour by means of the *PressureIndependentMaterial*’ (see Section 3.3.1) implemented in OpenSees are shown and compared with those obtained through a simplified modelling of soil non-linear behaviour.

The analyses were performed only for the 4 Floors pre-code building and for the records of Group 1.

It can be noted that for a soil type C the average results are in very good agreement with those obtained by means of simplified soil model, both in terms of maximum base shear and in terms of maximum inter-storey drift ratio.

For a more soft soil (soil type D) a more appropriate modelling of the non-linear soil behaviour can induce further reductions in terms of maximum base shear (up to 6%) and maximum inter-storey-drift ratio (up to 27%).

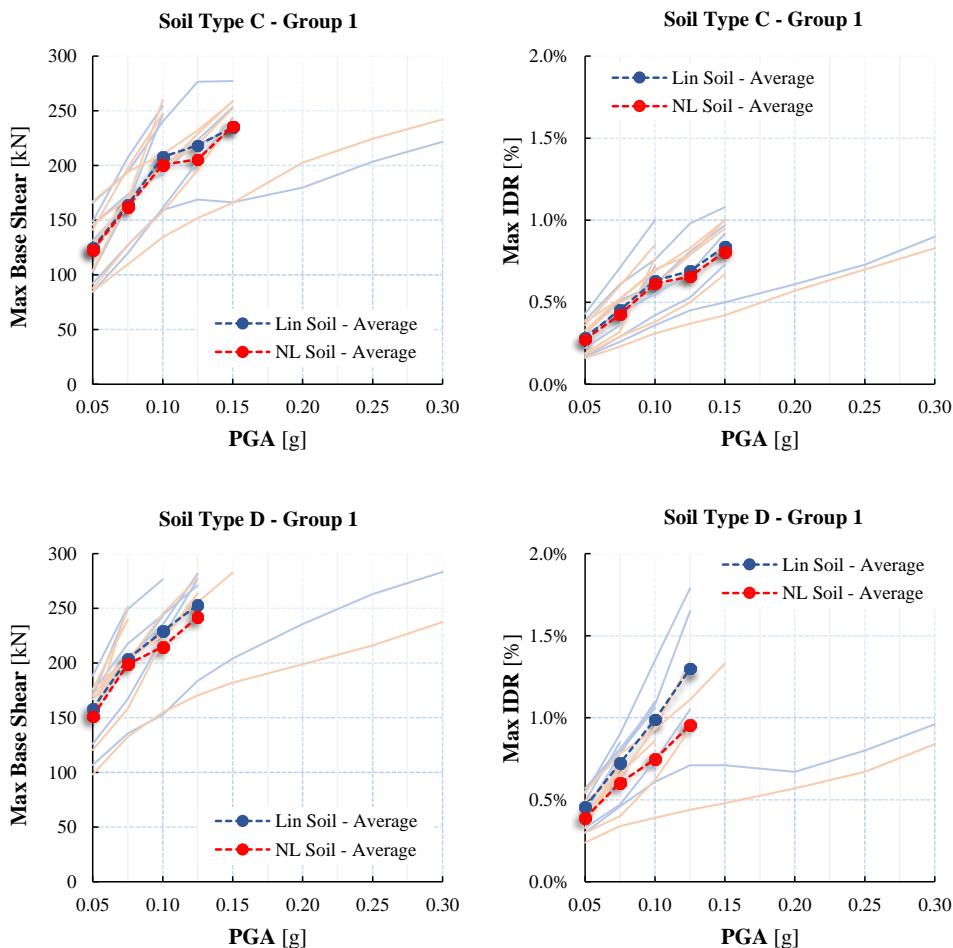


Figure 4.31 - 4 Floors Pre-Code building: Influence of non-linear soil behaviour modelling

A further explanation of the different soil models adopted for the Complete FEM model is shown in Figure 4.32, in which the response in terms of shear behaviour of three different soil elements, placed at different depths (5m, 15m, 30m) below the foundation, is shown.

It can be noted that with the *PressureIndependentMultiYield* material, the soil is able to suffer plastic deformations, which occur, for the particular ground motion considered, especially in the zone near the bedrock. Near the surface, the soil behaves elastically and the stiffness is reasonably captured by means of the “equivalent” linear model of the soil.

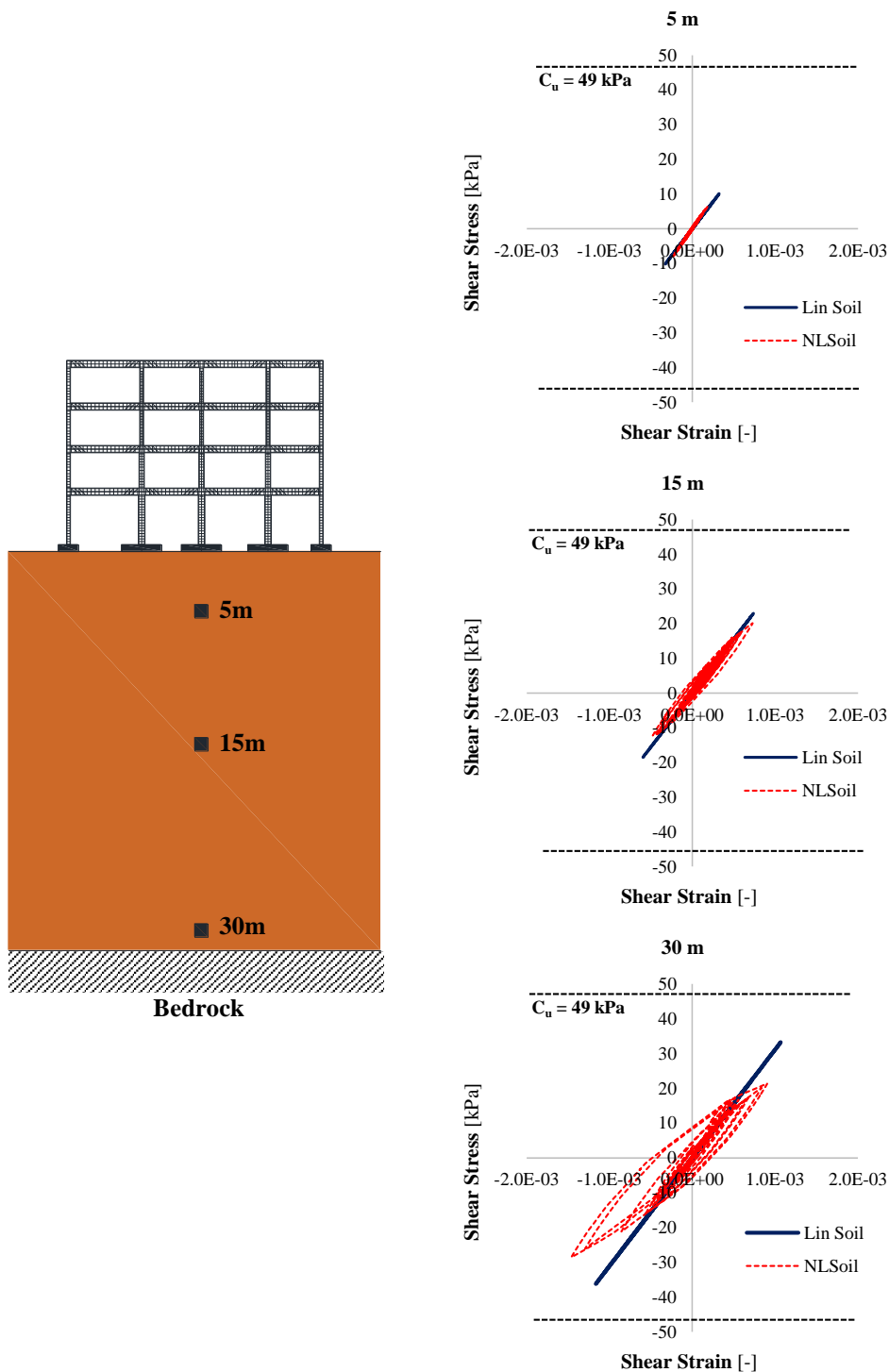


Figure 4.32 – Soil shear behaviour for “equivalent” linear soil and non-linear soil: soil Type D (soft clay), Group1 - Ground Motion 1, PGA=0.10g

In the graphs in Figure 4.32 the shear resistance of the soil is also plotted, which is given by the undrained cohesion of the material ($c_u = 49\text{kPa}$, see Section 4.2), that is the same at all the depths considered. It is worth reminding, indeed, that the material model adopted can be used only to simulate the response of materials whose shear behaviour is insensitive to the confinement change, like clay under undrained loading conditions (see Section 3.3.1).

In Table 4.12, the reduction coefficient of the soil shear modulus assumed for the equivalent linear soil model is compared with that obtained for the rigorous non-linear soil model at different depths in the soil deposit.

Table 4.12 - Soil shear modulus reduction coefficients for the “equivalent” linear soil model and for the non-linear soil model (Ground Motion 1, Group1)

Depth [m]	Soil Type C – 0.15g		Soil Type D – 0.10g	
	Non Linear Soil G/G ₀	Eq. Linear Soil G/G ₀	Non Linear Soil G/G ₀	Eq. Linear Soil G/G ₀
30 m	0.38		0.58	
15 m	0.46	0.64	0.68	0.81
5 m	0.77		0.85	
	Mean = 0.54		Mean = 0.70	

The ratio G/G_0 was obtained, for the non-linear soil model, evaluating G as the ratio between the shear stress and the shear strain at the peak of the hysteresis loop.

The table suggests that a better approximation between the two soil models could be achieved assuming, for the “equivalent” linear soil model, different values of the ratio G/G_0 at different depths or a mean reduction coefficient calibrated on the base of the shear response observed at different depths through a rigorous non-linear soil model (*Stewart et al., 2008*).

However, the values shown in Table 4.12 are related to a specific record and different values could be obtained for a different ground motion.

The great variability related to the ground motion led to the need to choose the soil shear modulus reduction coefficient based on the simplified approach suggested by FEMA 440 (i.e. based on the PGA at the bedrock).

Anyway, it can be noted that near the surface a good agreement between the two coefficients is achieved.

As concerns the BNWF model, it is worth to remember that all the analyses were performed neglecting the horizontal passive load-displacement behaviour against the side of footings (i.e. assuming that foundation rests on the surface of the soil deposit).

In Figure 4.33 some results obtained taking into account the P-x springs (see Section 3.2.2) are shown and compared with those obtained neglecting the horizontal passive behaviour.

The springs were calibrated by assuming that the single footings (of height 1.5 m) are completely surrounded by soil.

As can be noted, the influence of the modelling of P-x springs on the estimation of the seismic demand is negligible for the structures examined.

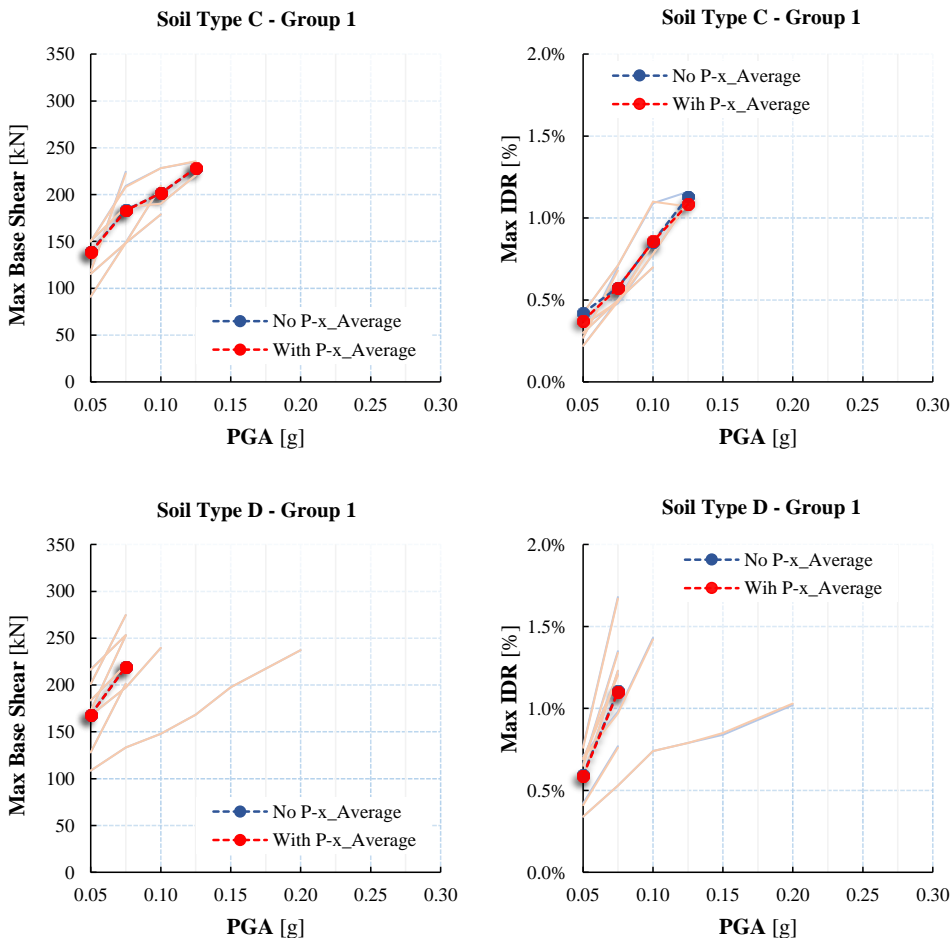


Figure 4.33 - BNWF model: influence of P-x springs

4.6 Retrofitting interventions by means of shear walls

In the next, the results of some analyses performed for the 4 floor pre-code building of previous Section 4.1.1 are shown, assuming that the building is strengthened by means of a shear wall (see Figure 4.34).

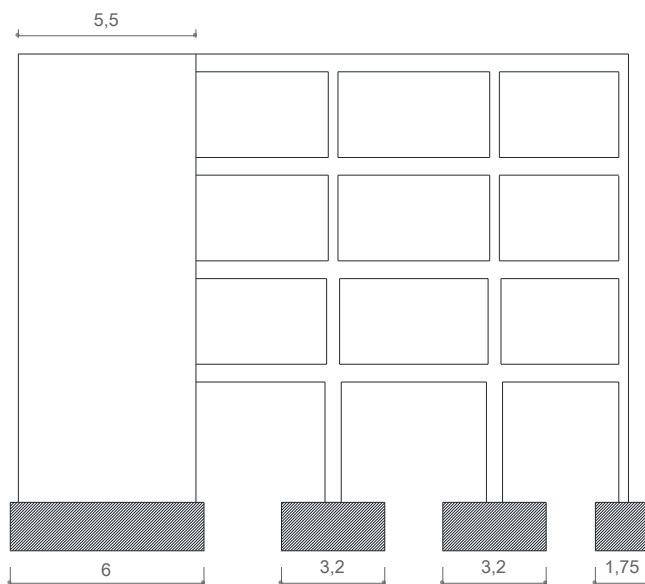


Figure 4.34 - Dual system frame-wall

The wall has a section of 5.5 m x 0.20 m and longitudinal reinforcements of diameter 20 mm.

The footing under the wall has plan dimensions of 6.0 m x 1.5 m.

The wall was modelled by means of a *'beamWithHinges'* element at the first floor and by means of elastic elements at the upper floors.

The non-linear structural behaviour of the wall was taken into account by means of a plastic fiber hinge (see Section 3.1) at the base of the frame element simulating the wall at the first floor. The length of the plastic hinge was assumed equal to $0.3 l_w$, with l_w equal to the height of the section of the wall (as suggested by *Paulay and Priestley, 1991*).

The connection between the beams and the wall was simulated by means of rigid links.

The analyses were performed for:

- a) a fixed base model;
- b) a Complete FEM model;
- c) a model in which SSI is modelled by means of the foundation impedances provided by *Pais & Kausel* (see Section 3.2.1).

In Figure 4.35 the results obtained for the models a) and b) are compared, while in Figure 4.36 the former are compared with those obtained for the model c).

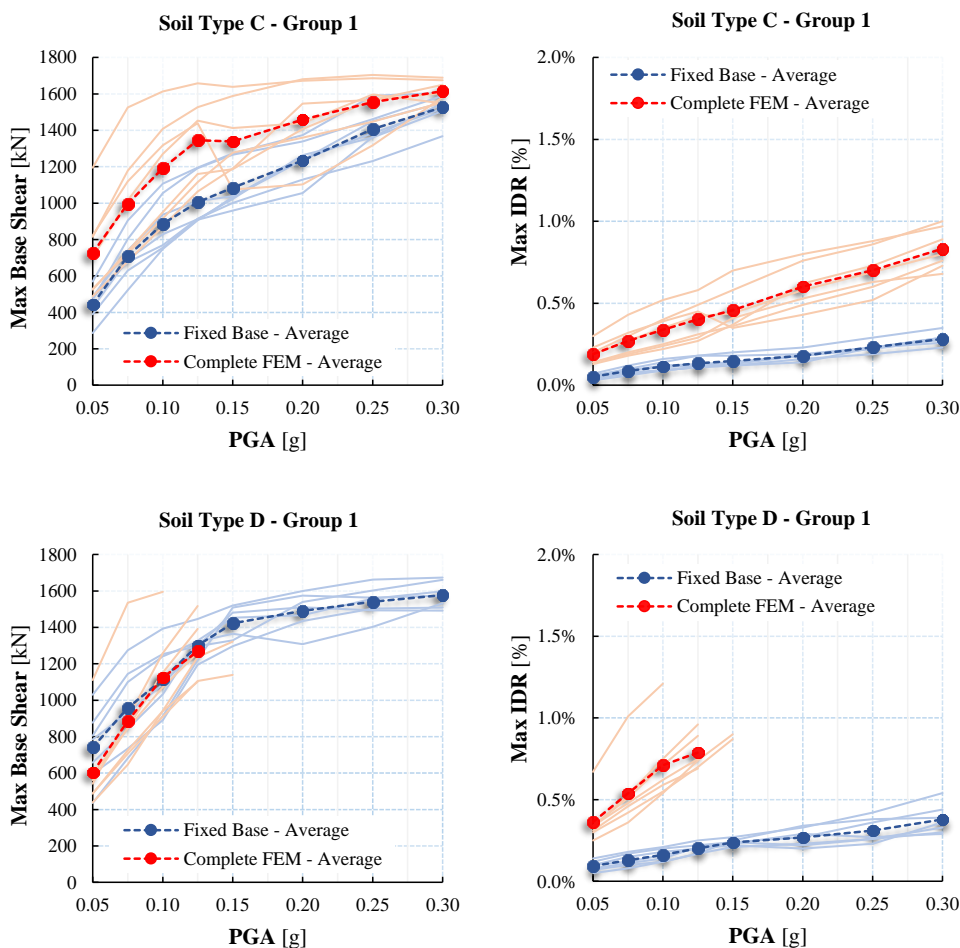


Figure 4.35 - 4 Floors Pre-Code building: retrofitting intervention by means of a shear wall – Comparison between Fixed Base Model and Complete FEM model

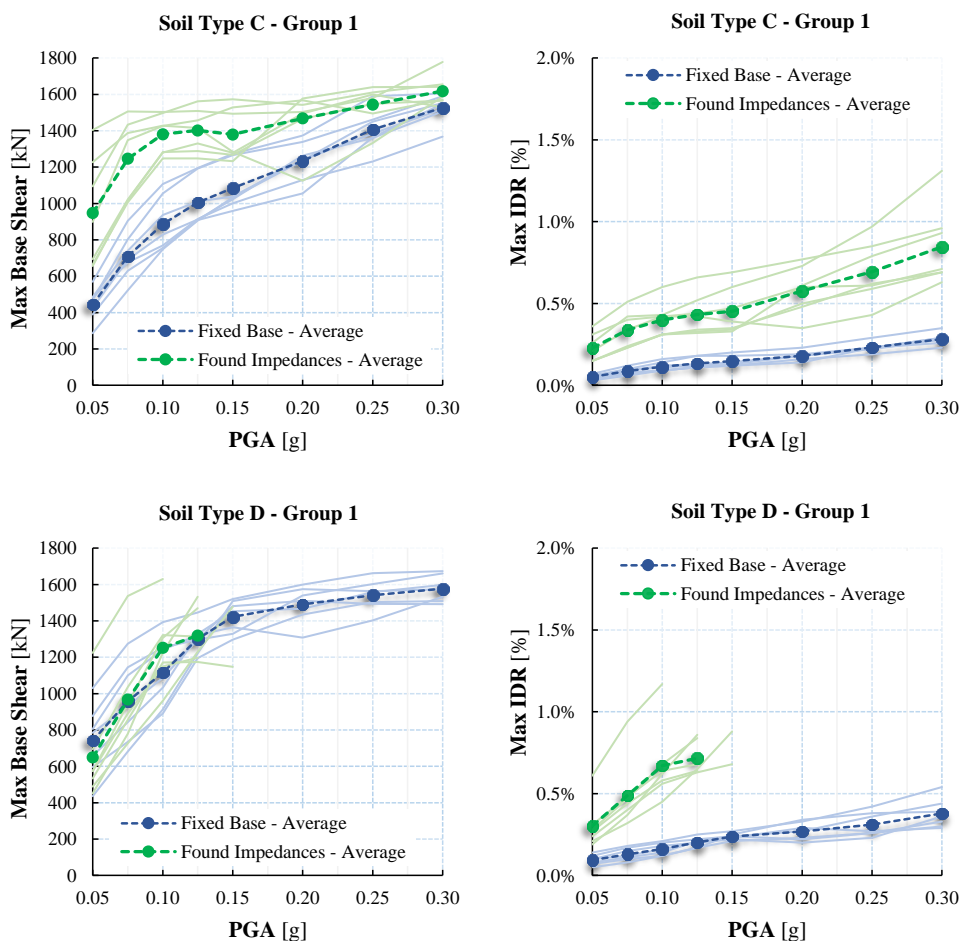


Figure 4.36 - 4 Floors Pre-Code building: retrofitting intervention by means of a shear wall – Comparison between Fixed Base Model and Spring model

The results showed that in this case the modelling of SSI effects could lead to greater estimations of the seismic demand in terms of both maximum base shear and maximum inter-storey drift ratios with respect to a fixed-base model.

In addition, it is possible to note that the results confirm what observed for the frame structures, with the Complete FEM model that predicts lower values of the seismic demand with respect to a model with springs and dashpots at the base.

This is due to the greater damping that the complete FEM model is able to capture with respect to a model in which the SSI is modelled by means of foundation impedances.

Whatever is the modelling approach adopted, the results highlight that a common design procedure of retrofiting interventions based on the assumption of structure fixed at the base can be strongly un-conservative and un-safe.

These results can be explained through some considerations related to easier linear analyses (i.e. analyses performed assuming linear structural behaviour).

In Figure 4.37 the acceleration recorded at the top of the structure is plotted for the fixed base model and for the complete FEM model, assuming a soil type C.

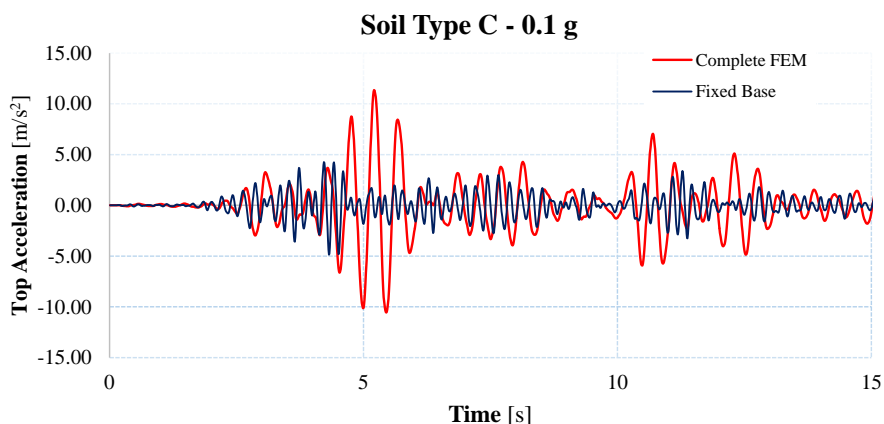


Figure 4.37 - Top acceleration for Fixed Base model and Complete FEM model (linear analysis)

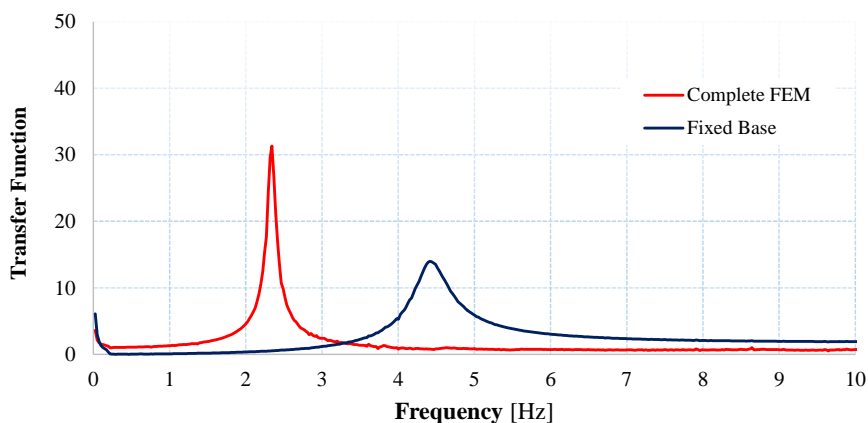


Figure 4.38 - Transfer functions for Fixed Base model and Complete FEM model

Dividing the Fourier spectrum of the top acceleration by that of the free field motion, it is possible to obtain the transfer functions (see Figure 4.38) of the two systems and then the values of the fundamental vibration period.

As can be noted, the initial elastic period of the fixed-base structure is equal to $T = 0.22$ s ($f = 4.55$ Hz) while the modelling of SSI lead to an increase of the fundamental period up to a value of $T = 0.43$ s ($f = 2.34$ Hz).

For stiff structural systems, the fundamental period is usually on the ascending branch of the response spectrum.

In Figure 4.39 the elastic spectrum corresponding to the free field motion is shown. It is apparent that such an increase of period can imply a strong increase of the structural demand.

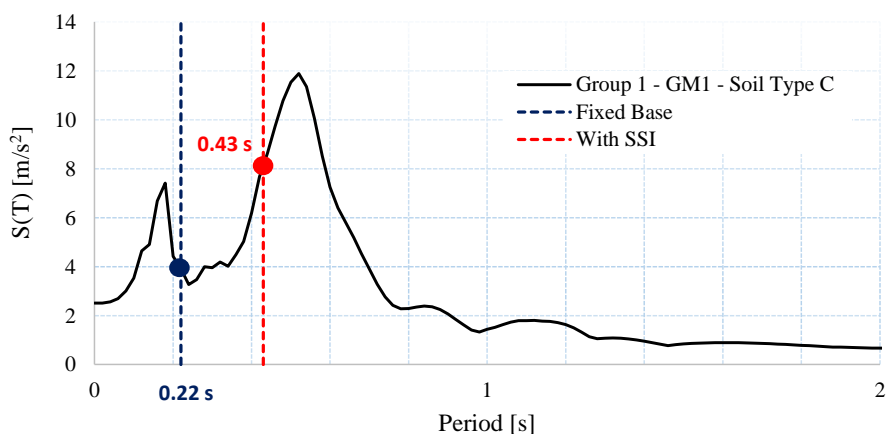


Figure 4.39 - SSI effect for a dual system frame-wall

4.7 Concluding remarks

Soil-Structure Interaction effects on the seismic performances of 2D Reinforced Concrete (RC) Moment Resisting Frames (MRFs) were investigated by means of non-linear dynamic analyses performed with the software OpenSees.

A parametric study was conducted in which the following parameters were varied:

- the modelling technique of the SSI;
- the design criteria of the MRFs;
- the height of the structures;
- the soil properties;
- the signal at the base;
- the intensity of the ground motion.

As concerns the modelling of the SSI, two different techniques suggested in literature were referenced:

- the first is the Beam on Non-linear Winkler Foundation (BNWF) approach, usually preferred in engineering practice for its simplicity and for the reduced computational efforts;
- the second is a Complete FEM approach, in which a direct modelling of both the soil and the structure by means of Finite Elements is achieved.

As concerns the structures, MRFs of 4 and 8 floors designed with or without seismic code provisions were considered.

Two deformable soil deposits (classified as soil types C and D according to Eurocode 8) were chosen in order to obtain significant SSI effects.

The dynamic analyses were performed applying at the base of the model 21 different ground motions, grouped in three different sets of seven records (compatible with the response spectra provided by Eurocode 8 and Italian NTC 08).

Each record was scaled to different values of peak ground acceleration, in order to investigate the structural response from the linear behaviour to the collapse.

In this regard, it is important to highlight that in the present study the possible formation of brittle structural failures was taken into account.

This kind of failures, in fact, can strongly affect the seismic performances of RC MRFs, especially for that designed only for vertical loads.

For all the analyses, the results of the flexible-base models were compared with those obtainable by means of a common fixed-base model excited at the base by the free field motion (i.e. taking into account the site effects).

It is worth to note that for the BNWF model, unlike what happens for the Complete FEM model, the kinematic interaction is not taken into account.

However, the type of foundation assumed for reference structures (i.e. shallow foundations) guarantees the coherence between the two modelling approaches.

The structural response was investigated in terms of two synthetic engineering demand parameters:

- the maximum base shear (V_{max}), that is commonly referenced in the American codes to quantify the SSI effects with respect to the fixed-base case;
- the maximum inter-storey drift ratio (IDR_{max}), that is commonly referenced in literature as a good indicator of the structural damage level.

The major conclusions are resumed below.

1. The *modelling technique* of SSI can significantly affect the estimation of the seismic demand and, in particular, the adoption of a refined Complete FEM model can lead to a reduction in the estimation of the seismic demand, with respect to a fixed base model, up to 50% in terms of IDR_{max} and up to 20% in terms of V_{max} .

On the contrary, a simplified modelling of SSI effects by means of BNWF model can affect the seismic demand only in case of tall buildings (8 floors) founded on very soft soils (maximum reduction of 10% in terms of both V_{max} and IDR_{max}).

The difference between the two modelling approaches can be mainly correlated to the different overall damping captured by the models.

The incapability of the BNWF model to predict accurately the sliding response of the foundation behaviour (Raychowdhury, 2008) lead to underestimating the global damping of the system with respect to a Complete FEM model.

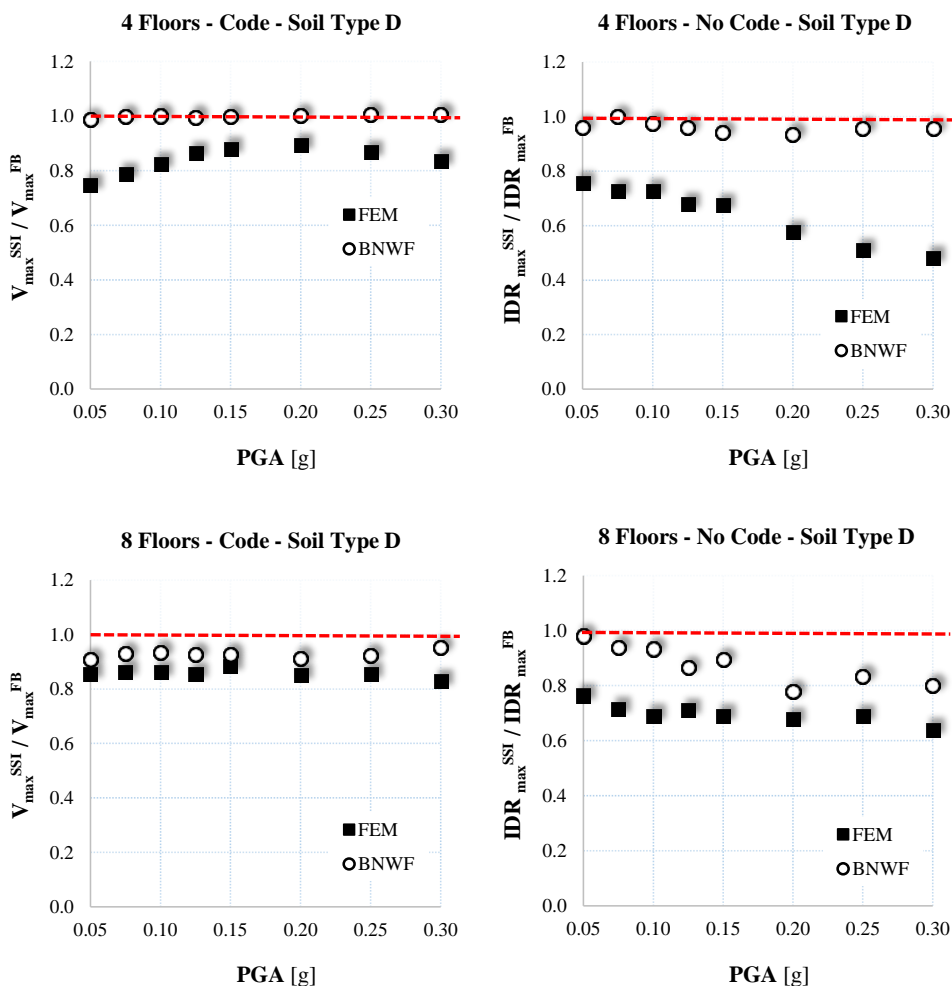


Figure 4.40 - Influence of modelling technique on SSI effects

- As concerns the *seismic design criteria*, it can be noted that for both pre-code and code compliant buildings SSI tends to decrease the structural demand in terms of IDR_{max} more than in terms of V_{max} , particularly for high PGA levels.

Moreover, the reduction in terms of V_{max} is more pronounced for code compliant buildings while the reduction in IDR_{max} is greater for pre-code buildings (as shown in Figure 4.41).

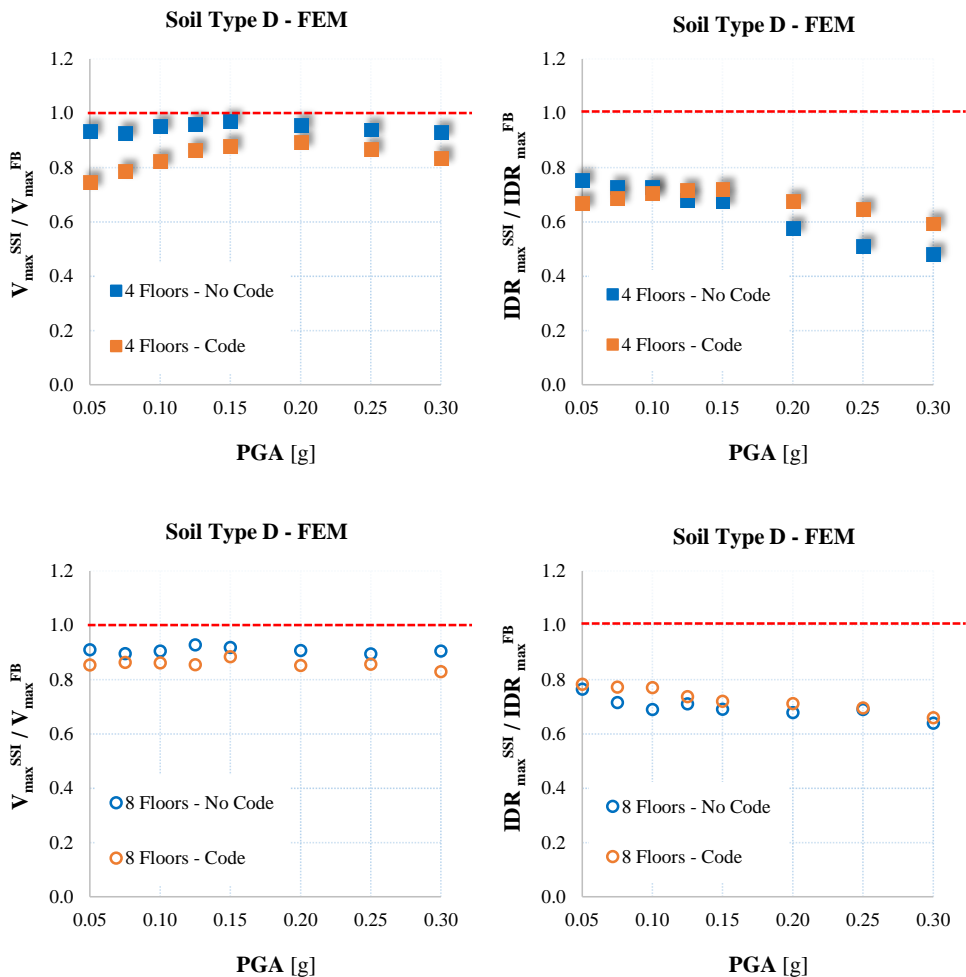


Figure 4.41 - Influence of seismic design criteria on SSI effects

The finding can be explained looking at Figure 4.42 and Figure 4.43 in which, given a particular ground motion, the time history of the response in terms of *IDR-Shear* is plotted for different PGA levels for the 4 floors pre-code and code compliant buildings, respectively. The responses are those recorded, for the fixed base model and for the Complete FEM model, at the floor in which the maximum *IDR* occurs.

It can be noted that, for low PGA values, when no significant yielding of the structural members occur, the reduction of seismic floor accelerations lead to

reductions of the seismic demand that are, especially for the code compliant building, of the same order of magnitude in terms of maximum IDR and shear. Increasing the PGA level, significant yielding of columns occurs and a reduction of floor shear due to SSI can lead to far greater reductions of maximum IDR. For the 4 floors code-compliant building, for example, the reduction of maximum IDR is approximately 9 times the reduction in floor shear for the considered ground motion scaled to a PGA equal to 0.25g.

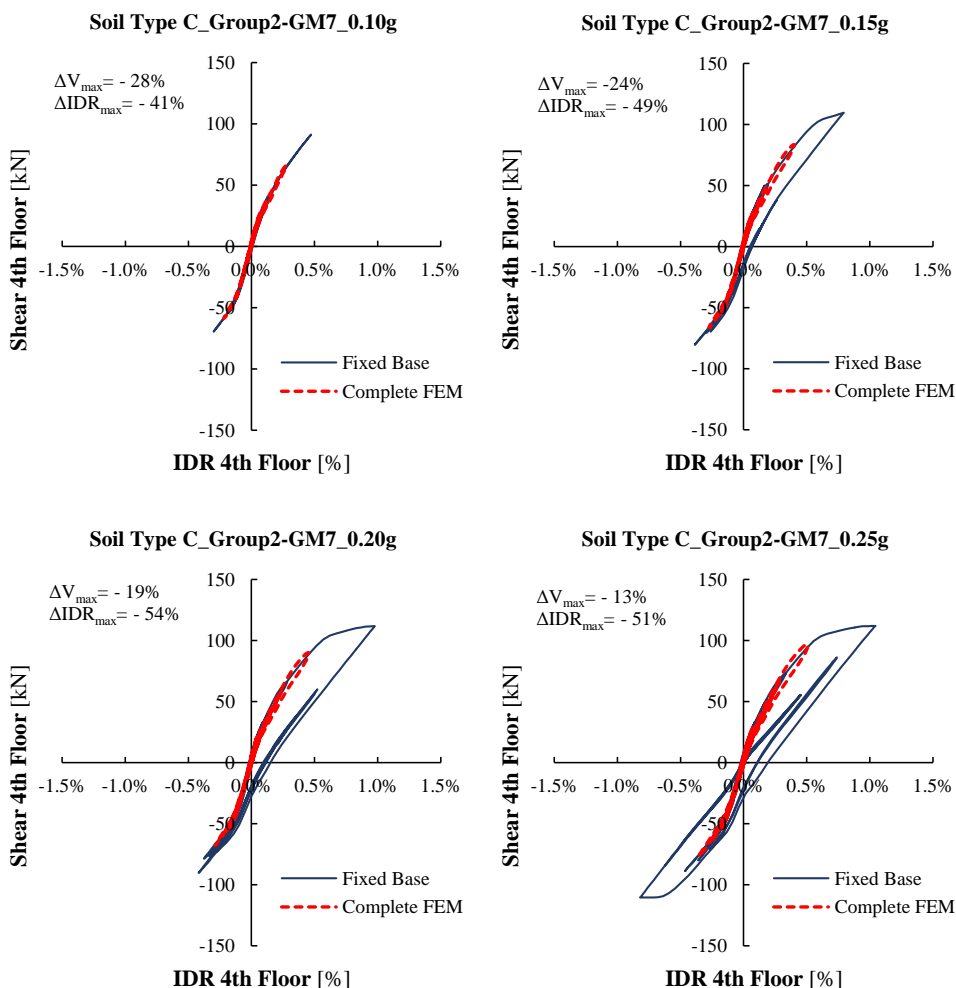


Figure 4.42 - 4 Floors Pre-Code building: shear behaviour at the floor of maximum IDR

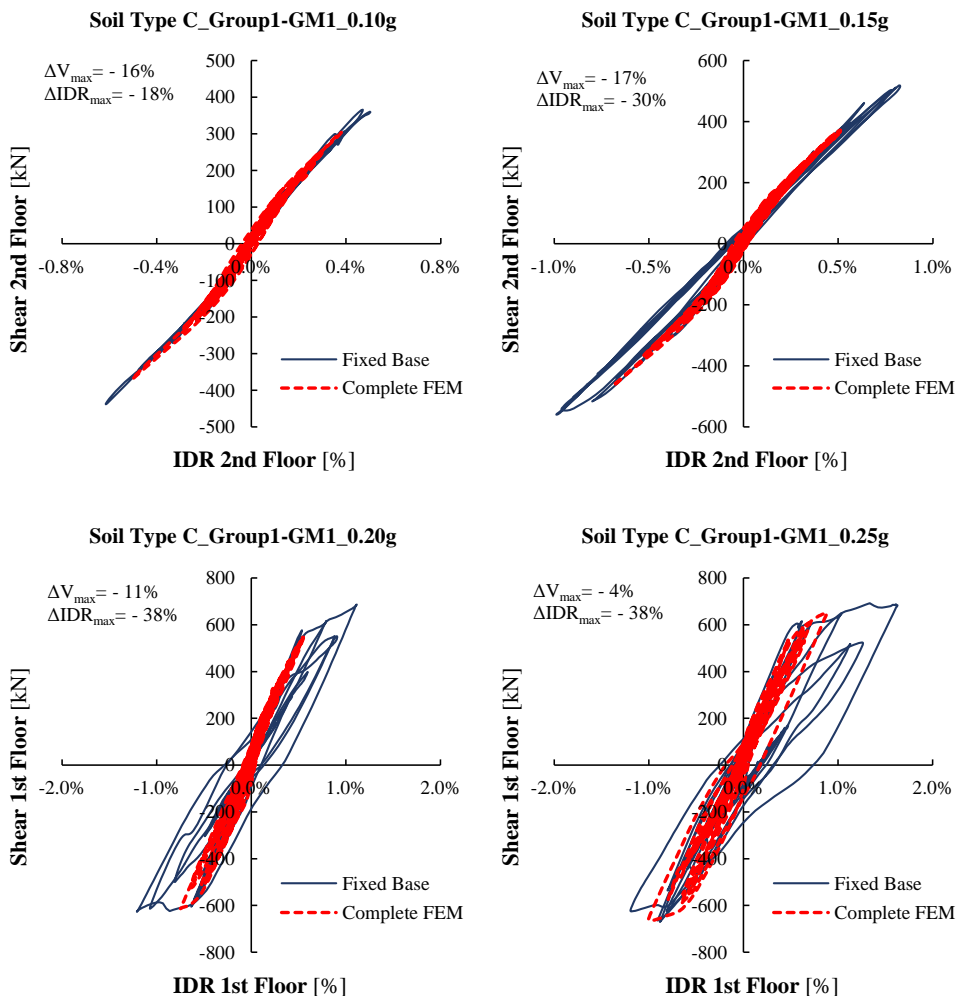


Figure 4.43 - 4 Floors Code compliant building: shear behaviour at the floor of maximum IDR

3. The simplified analyses performed in Chapter 2, in which SSI was modelled by means of elastic springs at the base of linear structural models, showed that the magnitude of SSI effects is in general related to the *fundamental period* of the structure in its fixed base condition. In particular, the modal analyses showed that SSI effects are higher, in terms of period lengthening, for “high-period” structures, while are

greater, in terms of damping increase, in the case of “short-period” structures.

Thus, given a reference spectrum, the combination of the two effects can lead to a certain reduction of the seismic demand with respect to the fixed base configuration. For the 4 and 8 floors code compliant buildings, simplified spectrum-analyses would indicate an equal influence of SSI effects on the seismic response of the two buildings (in particular a reduction of 10% of the pseudo-spectral acceleration can be obtained, with respect to a fixed base model, by means of the simplified procedure).

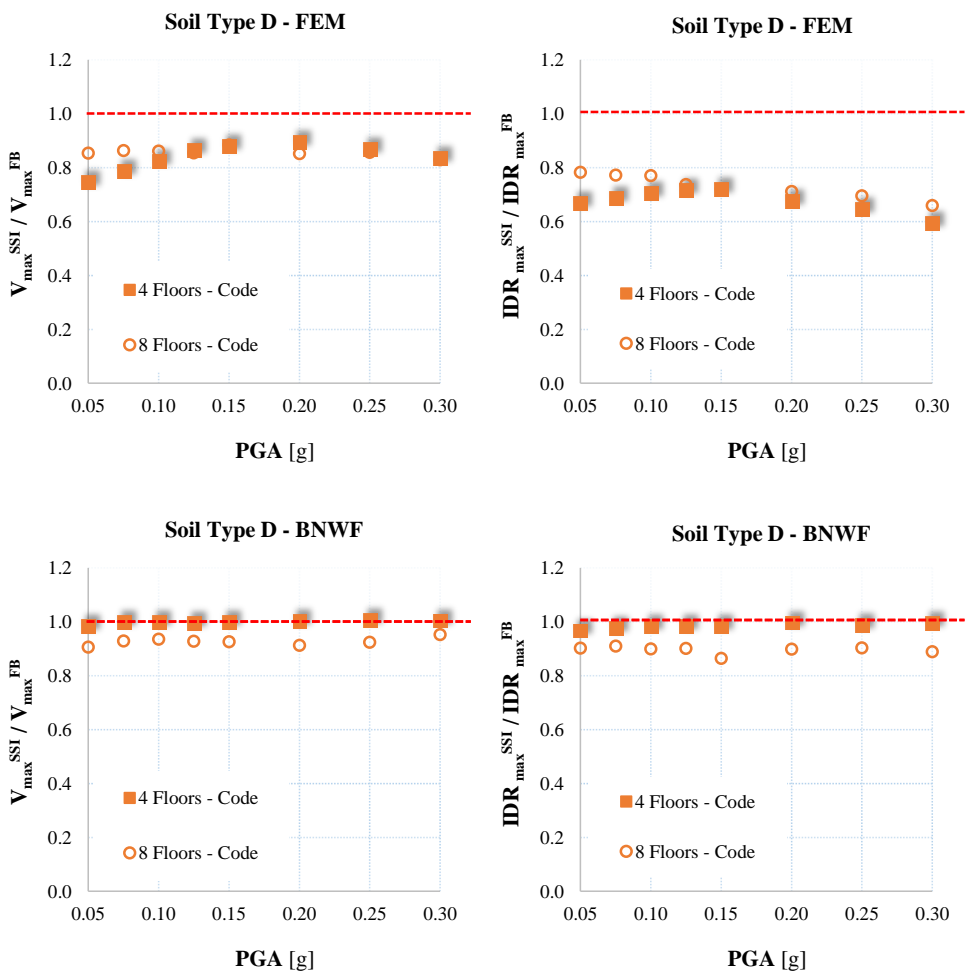


Figure 4.44 - Influence of structure fundamental period on SSI effects

This finding was confirmed by the results of the non-linear time history analyses performed through the Complete FEM model that, however, predict greater reductions of seismic demand with respect to a fixed base model (20% on average in terms of base shear).

On the contrary, a simplified model like the BNWF model, seems to be not adequate in capturing SSI effects in case of “short-period” structures. This finding is probably related to the incapability of the model to predict accurately the sliding response of the foundation behaviour (Raychowdhury, 2008), that for 4 floors building is the main source of energy dissipation.

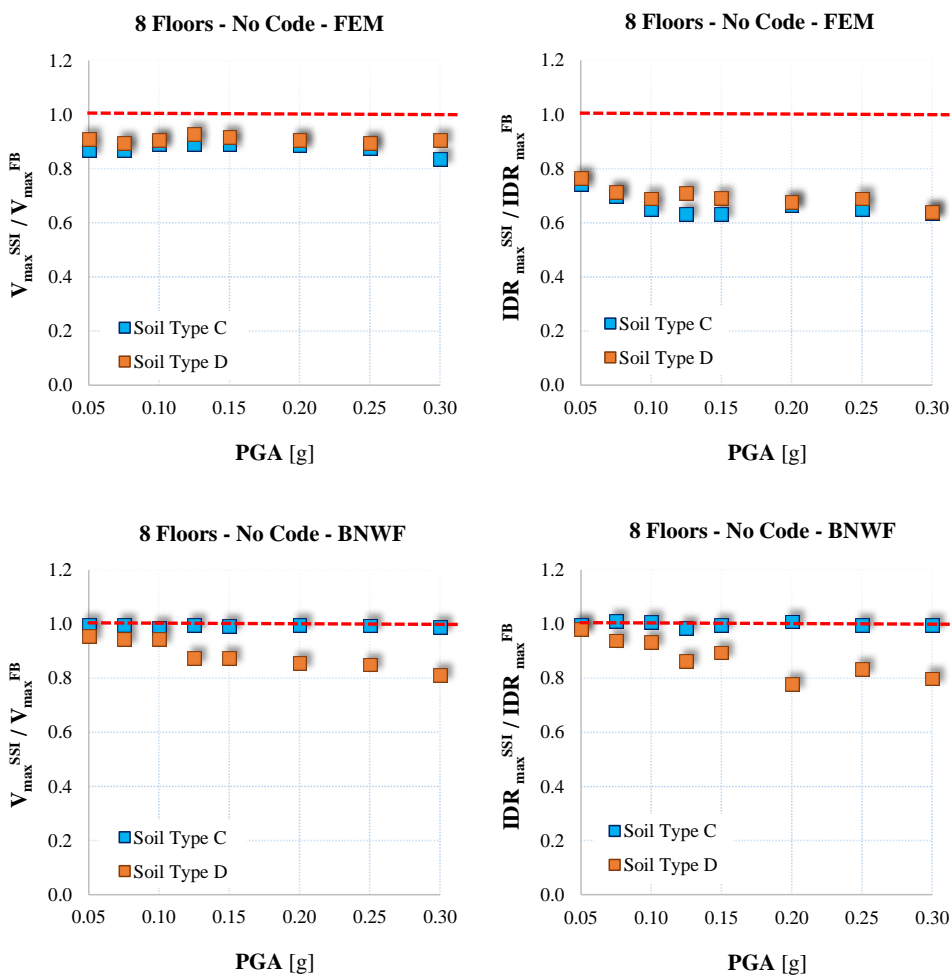


Figure 4.45 - Influence of soil type on SSI effects

4. As concerns the *soil properties* it can be noted that, referring to a Complete FEM model, the SSI effects are not affected by the soil properties assumed for the analyses and only light differences in terms of seismic demand can be appreciated passing from a soil type C to a soil type D.

Referring to a BNWF model, the SSI effects seem to be more affected by the soil properties, with appreciable differences in the estimated seismic demand, with respect to a fixed base model, only in case of very soft soils (soil Type D).

5. As concerns the *signal at the base*, it is worth to note that, in general, a strong dispersion of the structural response can be observed varying the signal at the base, as shown in Figure 4.46 for the 4 Floors code compliant building founded on a soil type C.

In the figure the average curves relative to the Group 3 of records are compared with those obtained for two specific records of the same group.

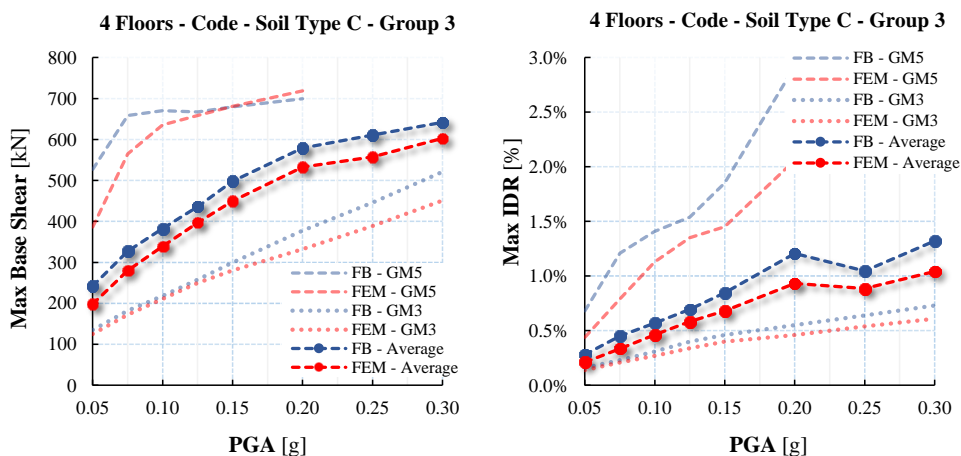


Figure 4.46 - Influence of the selected record on the SSI effects

It can be noted that the dispersion in terms of seismic demand concerns both the fixed base model and the flexible-base models, and is related to the selection of the records, that are in average compatible with a

reference response spectrum, but in some cases present spectral shapes very different to that of the target spectrum.

However, a significant impact of SSI effects can be noted, especially for a Complete FEM model, even on the seismic demand evaluated for a specific record.

6. As concerns the *intensity of the signal*, it is possible to note that increasing the PGA the SSI effects tend to be more important, especially in terms of reduction of IDR_{max} .
7. For the MRFs considered in this study, the elongation of the fundamental period of the system is in general very low, thus the SSI plays on the modification of the structural response more by means of an increase of overall damping.

This effect can be captured only by means of a more refined Complete FEM model.

8. For a more rigid structural system as, for example, a dual system with a frame structure and a shear wall, founded on a soft soil, the modification of the structural response due to the elongation of the fundamental period can become very important.

In addition, for this kind of structures, the first period of the system is on the mounting branch of the response spectrum.

An increase of the fundamental period due to SSI can imply a very high increase of the seismic demand, both in terms of V_{max} and IDR_{max} .

The results underline the need of properly taking into account the SSI in the design of retrofitting interventions that can involve a strong modification of the structural stiffness.

5 Conclusions

5.1 Introduction

In common seismic design practice, the design of a new building or the vulnerability assessment of an existing one is usually performed assuming that the structure is fixed at the base and assuming that the signal at the base is that evaluated in free field conditions.

This assumption, reasonable for structures founded on stiff soils, can be unrealistic in case of structures founded on soft soils.

Different researches show that SSI cause, with respect to a fixed base configuration, two main effects:

- an increase of the fundamental period of the system, due to deformability of the foundation soil;
- an increase of the overall damping, due to the fact that the structure dissipates a great amount of energy in the underlying soil during its vibrations.

Despite an intense scientific production on the topic, the diffusion of soil-structure interaction analyses in the field of civil constructions is nowadays rather limited, mainly because of three reasons:

- the lack, in many countries, of specific code prescriptions;
- the belief that soil-structure interaction has a beneficial effect on the structural response and thus it is possible to have an increase of the safety level neglecting it;
- the complexity in performing a rigorous analysis.

In the thesis these three issues were faced.

In order to validate the simplified formulations suggested by American Standards and Guidelines for the evaluation of SSI effects, a sensitivity analysis

was performed, by means of linear modal analyses, for Reinforced Concrete (RC) structures (regular and not regular) of different heights and founded on stiff or soft soil.

The sensitivity analysis showed that:

- increasing the height of the structure the period lengthening tends to increase (up to 30% for 12 floors buildings founded on soft soils);
- for short buildings the period lengthening become less important, but the increase of the damping factor of the system is greater (up to 7%);
- for stiff soils the SSI effects are always negligible;
- concrete cracking, reducing the overall stiffness of the structure, tends to reduce the SSI effects, both in terms of period lengthening and in terms of damping;
- the simplified formulations provided by FEMA 450 yield estimations of the 1st and 2nd period lengthening in good agreement, except in the case of highly irregular buildings (buildings with shear walls or existing buildings) with those achievable by means of a modelling with elastic springs of the SSI effects.

Non-Linear Static Analyses (Push Over) were then performed for two RC Moment Resisting Frames (MRFs) of 4 and 8 floors designed without seismic provisions, in order to evaluate the influence of SSI effects on the ratios Capacity/Demand (C/D), which can strongly affect the design strategies of seismic retrofitting interventions.

The analyses showed that the introduction at the base of a structural model of elastic springs could increase the ratio C/D with respect to a common fixed-base configuration, especially for 4 floors structures, for which the reduction of seismic demand due to the increase in overall system damping is added to the demand reduction due to period lengthening.

5.2 Main Findings

In order to investigate more accurately the influence of SSI effects on the seismic performances of RC MRFs, as well as deepen the knowledge about some issues related to a proper modelling of the foundation soil and to the frequency content

of the seismic input motion, more refined non-linear dynamic analyses were performed by means of the software OpenSees.

The main findings of the study can be resumed as follows.

1. Based on the modelling approach adopted, the SSI can affect more or less the estimation of the seismic demand with respect to a fixed-base model.
2. The adoption of a Complete FEM model, in which soil and structure are modelled together in one single step, can lead to reductions in the estimation of the seismic demand, with respect to a fixed-base model, up to 50% in terms of maximum inter-storey drift ratio and up to 20% in terms maximum base shear.
3. A simplified modelling of SSI effects by means of a Beam on Non-linear Winkler Foundation (BNWF) model can affect the evaluation of the seismic demand only in case of “high-period” structures founded on very soft soils. Anyway, the reductions in estimations of seismic demand with respect to a fixed-base model (up to 20% in terms of both maximum base shear and maximum inter-storey drift ratio) are lower than those predicted by a Complete FEM model.
4. The difference between the two modelling approaches can be mainly correlated to the different characterization of the overall damping. The BNWF model, in fact, tends to under-estimate the energy dissipation related to the sliding response of the foundation, probably because of the lack of coupling between vertical and lateral modes of response.
5. Usually, in American Standards, SSI is taken into account in a simplified way reducing the global base shear, based on a code spectrum and on the period lengthening; however, the analyses show that SSI affect the structural demand more in terms of maximum inter-storey-drift ratio than in terms of base shear.
6. As concerns the seismic design criteria, the fundamental periods of the structures, the soil properties and the signal, the results showed that, especially adopting a Complete FEM model, it is difficult to find some criteria to establish in which case SSI is more important, at least for the

cases examined in the study. SSI effects, in fact, are related to a complex interplay between the properties of the structure, the soil and the signal.

7. It is worth to note that for the MRFs considered in this study, the elongation of the fundamental period of the system is in general very low, thus SSI affects the modification of the structural response mainly by means of an increase of overall damping, which can be captured only by means of a more refined Complete FEM model.
8. For stiffer structural systems, as dual systems with frames and shear walls, founded on a soft soil, the modification of the structural response due to the elongation of the fundamental period can become very important. For this kind of structures, the first period of the system is often on the mounting branch of the response spectrum. An increase of the fundamental period due to SSI can imply a very high increase of the seismic demand. For this reason, SSI effects should be properly taken into account in the design of retrofitting interventions that can involve a strong modification of the structural stiffness.

5.3 Limitations and suggestions for future works

The present work has certain limitations that should be addressed through additional researches.

In the dynamic analyses performed in Chapter 4 only 2D models were considered. More realistic 3D structural models should be considered for further numerical investigations to take into account the torsional modes of the structural response.

As concerns the soil properties, in the study only uniform deposits of clay soils were referenced. Further numerical analysis should be performed for realistic deposits with different soil layers characterized by different mechanical properties, taking into account sandy soils too.

As concerns the foundation, further numerical investigation should take into account its deformability in order to evaluate its effect on the seismic demand with respect to the case of an infinitely rigid foundation. Moreover, the behaviour of RC structures founded on deep foundations should be investigated. For this

kind of foundation, generally preferred in the case of soils with poor mechanical properties, relevant kinematic interaction effects can affect the structural response.

For dual systems with shear walls, for which significant foundation rocking and uplift is expected, further analyses should be performed by means of a BNWF model. A challenging task could be the implementation of an interface model in a Complete FEM model in order to better simulate the real behaviour of the complex soil-foundation.

In the present study the SSI effects on the seismic structural response of RC structures was investigated by means of both simplified analyses (linear and static non-linear analyses) and more refined dynamic analyses.

An interesting future development could interest the comparison between simplified and rigorous approaches in order to validate the damping percentage that are usually provided by codes through synthetic graphs.

Finally, the analyses performed with both simplified and more refined approaches showed that SSI can have important consequences in terms of reduction of the seismic demand for Moment Resisting Frames.

Detailed analyses should be performed to evaluate the economic save that could be achieved through the consideration of the SSI effects in a retrofitting design procedure.

5.4 Suggestions for implementation in seismic design codes

Based on the results of the simplified and more rigorous analyses performed in this study, some suggestions are provided for the insertion of some indications for taking into account SSI effects in seismic codes.

1. Particular emphasis should be dedicated to a preliminary evaluation of the possible influence of SSI effects on the structural response.

A possible criterion to suggest to practitioners could be the evaluation of the wave parameter suggested by *Veletsos & Meek*, σ (see Section 1.2), in order to establish if potentially SSI can affect the structural response. Generally, for σ values < 20 SSI can potentially affect the structural seismic response.

Moreover, it should be emphasized that for stiff structural systems (i.e. shear walls, dual systems) founded on soft soils a common fixed base model can be strongly un-conservative and provide un-safe estimations of seismic demand.

2. Simplified formulas should be suggested for the evaluation of the fundamental period and of the overall damping of the flexible-base system to use in simplified linear static procedures. Particular emphasis should be placed on the fact that these simplified formulations work well for regular buildings but more precise estimations of the period lengthening are required if the structure is highly irregular.
3. Of course, some references should be provided for the evaluation of the foundation impedances as well as some indications for a proper calibration of springs and dashpots, (i.e. determination of the shear modulus and the hysteretic damping of the soil).
4. It should be highlighted that simplified models with springs and dashpots will be most significant for stiff structural systems, as shear walls or dual systems with shear walls and frames.

For moment resisting frames, especially “short-period” structures, only more rigorous modelling techniques (i.e. direct approaches) will be able to capture SSI effects.

References

- ATC 40 (1996) - Seismic Evaluation and Retrofit of Concrete Buildings, Vol 1.
- Aviles J., Pérez-Rocha L.E. (2003) - *Soil–structure interaction in yielding systems* - Earthquake Engineering and Structural Dynamics, vol. 32, no. 11, pp. 1749–1771.
- Aviles J., Pérez-Rocha L.E. (2005) - *Design concepts for yielding structures on flexible foundation* - Engineering Structures 27, 443–454
- Boulanger, R.W., Curras, C.J., Kutter, B.L., Wilson, D.W., and Abghari, A. (1999) - *Seismic soil-pile-structure interaction experiments and analyses* - Journal Geotechnical and Geoenvironmental Engineering, Vol. 125, pp. 750-759.
- Chopra, A. K. (1995) - *Dynamics of Structures Theory and Applications to Earthquake Engineering* - Prentice-Hall, Inc., Englewood Cliffs, New Jersey.
- Chopra, A.K., Goel, R.K. (1999) - *Capacity-demand-diagram methods based on inelastic design spectrum* - Earthquake Spectra, Vol. 15, No. 4, pp. 637-656.
- Circolare 2 febbraio 2009, n. 617 - *Istruzioni per l'applicazione delle "Nuove norme tecniche per le costruzioni" di cui al D.M. 14 gennaio 2008*
- Clough, R.W., and Penzien, J. (1993) - *Dynamics of Structures* - McGraw Hill, New York.
- Comartin C.D., Aschheim M., Guyader A., Hamburger R., Hanson R., Holmes W., Iwan W., Mahoney M., Miranda E., Moehle J., Rojahn C., Stewart J. (2004) - *A Summary of FEMA 440: Improvement of Nonlinear Static Seismic Analysis Procedures* - 13th World Conference on Earthquake Engineering Vancouver, B.C., Canada, August 1-6, 2004 - Paper No. 1476

- Computers and Structures Inc. (2013) – *CSI Analysis Reference Manual for SAP2000, ETABS, SAFE and CSiBridge*
- Coulomb, C. A. (1776) - *Essai sur une application des règles des maximis et minimis à quelques problèmes de statique relatifs à l'architecture* - Mm. acad. roy. prs. Divers savants, Paris, 3, 38.
- Crouse C.B., McGuire J. (2001) – *Energy Dissipation in Soil-Structure Interaction – Earthquake Spectra*, Vol.17, No.2, May 2001
- Darendeli M. (2001) - *Development of a new family of normalized modulus reduction and material damping curves* - PhD Thesis, University of Texas.
- Decreto del Ministero delle Infrastrutture e dei Trasporti del 14 Gennaio 2008 - *Norme Tecniche per le Costruzioni* - Supplemento Ordinario n. 29 della Gazzetta Ufficiale della Repubblica Italiana del 4 Febbraio 2008.
- Decreto Ministeriale 30 Maggio 1972 – *Norme Tecniche alle quali devono uniformarsi le costruzioni in conglomerato cementizio, normale e precompresso e ad struttura metallica*
- Di Lernia A., Amorosi A., Boldini D. (2015) – *Interazione Dinamica Terreno Struttura: il caso di Lotung* - Incontro Annuale dei Ricercatori di Geotecnica 2015- IARG 2015, June 24-26, 2015 – Cagliari (Italy)
- Dobry, R. and Gazetas, G (1986) - *Dynamic response of arbitrarily shaped foundations* - J. Geotech. Engrg., ASCE, 112(2), 109-135.
- El Ganainy H., El Naggar M.H. (2009) - *Efficient 3D nonlinear Winkler model for shallow foundations* - Soil Dynamics and Earthquake Engineering, 29, 1236–1248
- Elsabee, F. and Morray, J.P. (1977) - *Dynamic behavior of embedded foundations* - Rpt. No. R77-33, Dept. of Civil Engrg., MIT, Cambridge, Mass.
- Elwood K.J, Moehle J.P. (2003) - *Shake Table Tests and Analytical Studies on the Gravity Load Collapse of Reinforced Concrete Frames* - Pacific Earthquake Engineering Research Center, PEER Report 2003/01.

- Elwood K.J. (2004) - *Modelling failures in existing reinforced concrete columns* - Can. J. Civ. Eng. 31: 846–859 (2004)
- Elwood K.J, Moehle J.P. (2008) - *Dynamic collapse analysis for a reinforced concrete frame sustaining shear and axial failures* - Earthquake Engng Struct. Dyn. 2008; 37:991–1012
- EN 1998-1 (2004) - *Eurocode 8: Design of structures for earthquake resistance – Part 1: General rules, seismic actions and rules for buildings*
- EN 1998-5 (2004) (English): *Eurocode 8: Design of structures for earthquake resistance – Part 5: Foundations, retaining structures and geotechnical aspects*
- EN 1998-3 (2005) - *Eurocode 8: Design of structures for earthquake resistance – Part 3: Assessment and retrofitting of buildings*
- Fajfar P., EERI M. (2000) - *A Nonlinear Analysis Method for Performance Based Seismic Design* - Earthquake Spectra, Vol.16, No.3, pp.573-592.
- FEMA 356 (2000) – *Prestandard and Commentary for the seismic rehabilitation of buildings.*
- FEMA 440 (2005) - *Improvement of Nonlinear Static Seismic Analysis Procedures.*
- FEMA 450 (2003) - *NEHRP Recommended Provisions for Seismic Regulations for New Buildings and Other Structures. Part1: Provisions*
- FEMA 450 (2003) - *NEHRP Recommended Provisions for Seismic Regulations for New Buildings and Other Structures. Part2: Commentary*
- Freeman S.A. (2004) - *Review of the Development of the Capacity Spectrum Method* - ISET Journal of Earthquake Technology, Paper No. 438, Vol. 41, No. 1, March 2004, pp. 1-13.

- Gajan S., Hutchinson T.C., Kutter B.L., Raychowdhury P., Ugalde J.A., Stewart J.P. (2008) - *Numerical Models for Analysis and Performance-Based Design of Shallow Foundations Subjected to Seismic Loading* - Pacific Earthquake Engineering Research Center, PEER Report 2007/04.
- Gazetas G. (1991) - *Foundation vibrations*. Foundation Engineering Handbook, 2nd edition, Van Nostrand Reinhold, 553-593.
- Gazetas G. (1991) - *Formulas and charts for impedance of surface and embedded foundations* - Journal of Geotechnical Engineering, ASCE, vol. 117, no. 9, pp. 1363-1381.
- Gazetas G., Mylonakis G. (2001) - *Soil structure interaction effects on elastic and inelastic structures* - Proceedings of the 4th international conference on recent advances in geotechnical earthquake engineering and soil dynamics; paper no. SOAP – 2, San Diego.CA.
- Ghobarah A. (2004) - *On drift limits with different damage levels* - Proceeding of International Workshop on Performance-based seismic design concepts and implementation, Bled, Slovenia, June 28th – July 1st.
- Gu Q., Conte J.P., Elgamal A., Yang Z. (2009) - *Finite element response sensitivity analysis of multi-yield-surface J2 plasticity model by direct differentiation method* - Computer Methods in Applied Mechanics and Engineering, vol. 198, no. 30-32, pp. 2272-2285.
- Harden C., Hutchinson T., Martin G.R., Kutter B.L. (2005) - *Numerical Modeling of the Nonlinear Cyclic Response of Shallow Foundations* - Pacific Earthquake Engineering Research Center, PEER Report 2005/04.
- Harden C.W., Hutchinson T.C. (2009) - *Beam-on-Nonlinear-Winkler-Foundation Modeling of Shallow, Rocking-Dominated Footings* - Earthquake Spectra, Volume 25, No. 2, pages 277–300.
- Iervolino I., Galasso C., Cosenza E. (2009) - *REXEL: computer aided record selection for code-based seismic structural analysis* - Bulletin of Earthquake Engineering, vol.8, no. 2, pp. 339-362.

- Iguchi, M. and Luco, J.E. (1982) - *Vibration of flexible plate on viscoelastic medium* - J. Engrg. Mech., ASCE, 108(6), 1103-1120.
- Jennings, P.C. and Bielak, J. (1973) - *Dynamics of building-soil interaction* - Bull. Seism. Soc. Am., 63, 9-48.
- Joyner W.B., Chen A.T.F. (1975) - *Calculation of nonlinear ground response in earthquakes* - Bulletin of the Seismological Society of America, vol. 65, no. 5, pp. 1315-1336.
- Karapetrou S.T. (2015) – *Seismic Vulnerability of Reinforced Concrete Buildings Considering Aging and Soil-Structure Interaction Effects* - PhD Thesis, Aristotle University of Thessaloniki
- Karatzizou A., Ptilakis D. (2012) – *Performance Based Concepts of Compliant Soil-Foundation-Structure Systems* – Paper No.12.05 - 2nd International Conference on Performance Based Design in Earthquake Geotechnical Engineering, May 28-30, 2012 – Taormina (Italy)
- Karsan I., Jirsa J. (1969) - *Behavior of concrete under compressive loadings* - ASCE J Struct. Div. 95:2543–2563
- Kausel, E. (1974) - *Forced vibrations of circular foundations on layered media* - Rpt. No. R74 - 11, Dept. of Civil Engrg., MIT, Cambridge, Mass.
- Kramer S.L. (1996) - *Geotechnical Earthquake Engineering* - Prentice-Hall Inc., Upper Saddle River, New Jersey.
- Kwok A.O.L., Stewart J.P., Hashash Y.M., Matasovic N., Pyke R., Wang Z., Yang Z. (2007) - *Use of exact solutions of wave propagation problems to guide implementation of nonlinear seismic ground response analysis procedures* - Journal of Geotechnical Engineering, vol. 133, no. 11, pp. 1385-1398.
- Lee H., Mosalam K.M. (2014) - *Effect of Vertical Acceleration on Shear Strength of Reinforced Concrete Columns* - Pacific Earthquake Engineering Research Center, PEER Report 2014/04.

- Liou, G.S. and Huang, P.H. (1994) - *Effect of flexibility on impedance functions for circular foundations* - J. Engrg. Mech., ASCE, 120(7), 1429-1446.
- Luco, J.E., and Westmann, R.A. (1971) - *Dynamic response of circular footings* - Journal of Engineering Mechanics, Vol. 97, No. 5, pp. 1381-1395.
- Lysmer J., Kuhlemeyer R.L. (1969) - *Finite dynamic model for infinite media* - Engineering Mechanics, vol. 95, pp. 859-877.
- Lysmer J. (1978) - *Analytical procedures in soil dynamics* - University of California at Berkeley, Earthquake Engineering Research Center, Richmond, Report No. UCB/EERC- 78/29, 1978, CA.
- Mahaney J.A., Freeman S.A., Paret T.F., Kehoe B.E. (1993) - *The capacity spectrum method for evaluating structural response during the Loma Prieta earthquake* - Proceedings of National Earthquake Conference, Memphis, 1993, pp. 501-510.
- Maravas A., Mylonakis G., Karabalis D.L. (2007) - *Dynamic Characteristics of Structures on Piles and Footings* - 4th ICEGE. June 25-28, 2007 Paper No. 1672.
- Martinelli E., Faella C. (2015) - *Nonlinear static analyses based on either inelastic or elastic spectra with equivalent viscous damping: A parametric comparison* - Engineering Structures, 88 (2015) 241-250.
- Masing, G. (1926) - *Eigenspannungen and verfertigung beim messing* - Proc. 2nd Int. Congress on Applied Mech., Zurich, Switzerland
- Mazzoni S., McKenna F., Scott M.H., Fenves G.L. (2009) - *Open system for earthquake engineering simulation user command-language manual* - Pacific Earthquake Engineering Research Center, Berkeley, CA
- Meyerhof, G. G. (1963) - *Some recent research on the bearing capacity of foundations* - Canadian Geotechnical Journal, 1(1), 16–26.

- Moehle J.P., Ghannoum W., Bozorgnia Y. (2006) – *Collapse of Lightly Confined Reinforced Concrete Frames during Earthquakes* - S.T. Wasti and G. Ozcebe (eds.), *Advances in Earthquake Engineering for Urban Risk Reduction*, 317-332. 2006 Springer. Printed in the Netherlands.
- Mylonakis G., Gazetas G. (2000) – *Seismic Soil-Structure Interaction: Beneficial or Detrimental?* - *Journal of Earthquake Engineering*, Vol. 4, No. 3 (2000) 277-301
- Naeim, F., Tilelyioglu, S., Alimoradi, A., and Stewart, J.P., 2008 - *Impact of foundation modeling on the accuracy of response history analysis of a tall building* - Proceedings, SMIP2008 Seminar on Utilization of Strong Motion Data, California Strong Motion Instrumentation Program, Sacramento, California, pp. 19-55.
- NIST GCR 12-917-21 (2012) - *Soil Structure Interaction for Building Structures. NEHRP Consultants Joint Venture. A partnership of the Applied Technology Council and the Consortium of Universities for Research in Earthquake Engineering*
- Ostadan F., Deng N., Roesset J.M. (2004) - *Estimating Total System Damping for Soil-Structure Interaction Systems* - Proceedings Third UJNR Workshop on Soil-Structure Interaction, March 29-30, 2004, Menlo Park, California, USA.
- Pais, A., and Kausel, E. (1988) - *Approximate formulas for dynamic stiffnesses of rigid foundations* - *Soil Dynamics and Earthquake Engineering*, Vol. 7, No. 4, pp. 213-227.
- Paulay, T., Prestley, M.J.N (1991) - *Seismic design of reinforce concrete and masonry buildings* – John Wiley and Sons, Inc.
- Pérez Rocha L.E., Aviles J. (2004) – *Site and Interaction dependent strength reduction factors* - 13th World Conference on Earthquake Engineering Vancouver, B.C., Canada August 1-6, 2004 – Paper No. 1059
- Pitilakis D., Clouteau D. (2010) - *Equivalent linear substructure approximation of soil–foundation–structure interaction: model presentation and validation* - *Bull Earthquake Eng* (2010) 8:257–282

- Pitilakis D., Moderessi-Farahmand-Razavi A., Clouteau D. (2013) - *Equivalent-Linear Dynamic Impedance Functions of Surface Foundations* - Journal of Geotechnical and Geoenvironmental Engineering, vol. 139, no. 7, pp. 1130-1139. doi: 10.1061/(ASCE)GT.1943-5606.0000829.
- Pitilakis D., Lamprou D., Manakou M., Rovithis E., Anastiadis A. (2014) – *System Identification of Soil-Foundation Structure Systems by means of Ambient Noise Records: the case of EuroProteas model structure in EUROSEISTEST* – Second European Conference on Earthquake Engineering and Seismology, Istanbul, Aug. 25-29, 2014.
- Pitilakis K., Pitilakis D., Karatzizou A. (2010) – *Demand Spectra and SFSI for the Performance Based Design* - 7th International Conference on Urban Earthquake Engineering (7CUEE) & 5th International Conference on Earthquake Engineering (5ICEE)- March 3-5, 2010, Tokyo Institute of Technology, Tokyo, Japan
- Pitilakis K., Anastasiadis A., Pitilakis D., Rovithis E. (2013) – *Full-Scale Testing of a Model Structure in EUROSEISTEST to Study Soil-Foundation-Structure Interaction* - COMPDYN 2013 4th ECCOMAS Thematic Conference on Computational Methods in Structural Dynamics and Earthquake Engineering - Kos Island, Greece, 12–14 June 2013
- Pitilakis K.D., Karapetrou S.T., Fotopoulou S.D. (2014) - *Consideration of aging and SSI effects on seismic vulnerability assessment of RC buildings* - Bulletin of Earthquake Engineering, vol.12, no. 4, pp. 1755-1776
- Powell, G.H. (2006) - *Static pushover methods – explanation, comparison and implementation* - Proceedings, 8th U.S. National Conference on Earthquake Engineering, San Francisco, California.
- Prévost J.H. (1985) - *A simple plasticity theory for frictional cohesionless soils* - Soil Dynamics and Earthquake Engineering, vol. 4, pp. 9–17.
- Priestley M.J.N., Grant D.N. (2005) - *Viscous damping in seismic design and analysis* - Journal of Earthquake Engineering, vol. 9, Special Issue, pp. 229-255

- Raychowdhury P. (2008) – *Nonlinear Winkler-based Shallow Foundation Model for Performance Assessment of Seismically Loaded Structures* – PhD Thesis, University of California, San Diego
- Raychowdhury, P., and Hutchinson, T.C., (2009) - *Performance evaluation of a nonlinear Winkler-based shallow foundation model using centrifuge test results* - Earthquake Engineering and Structural Dynamics, Vol. 38, No. 5, pp. 679-698.
- Rayleigh J.W.S., Lindsay R.B. (1945) - *The theory of sound* - Dover Publications, New York.
- Riggs, H.R. and Waas, G. (1985) - *Influence of foundation flexibility on soil-structure Interaction* - J. Earthquake Engrg. Struct. Dynamics, 13(5), 597-615.
- Roesset, J.M. (1980) - *A review of soil-structure interaction* - in Soil-structure interaction: The status of current analysis methods and research, J.J. Johnson, ed., Rpt. No. NUREG/CR-1780 and UCRL-53011, U.S. Nuclear Regulatory Com., Washington DC, and Lawrence Livermore Lab., Livermore, CA.
- Saez E., Lopez-Caballero F., Modaressi-Farahmand-Razavi A. (2008) - *Effects of nonlinear soil behaviour on the seismic performance evaluation of structures* – Rivista Italiana di Geotecnica 2/2008
- Saez E.R. (2009) - *Dynamic nonlinear soil-structure interaction* - PhD Thesis, Ecole Central, Paris.
- Saez E., Lopez-Caballero F., Modaressi-Farahmand-Razavi A. (2011) - *Effect of the inelastic dynamic soil-structure interaction on the seismic vulnerability assessment* - Structural Safety, vol. 33, pp. 51-63.
- Saez E., Lopez-Caballo F., Modaressi-Farahmand-Razavi A. (2013) - *Inelastic dynamic soil-structure interaction effects on moment-resisting frame buildings* - Engineering Structures, vol. 51, pp. 166-177.
- SeismoSoft, SeismoSignal (2011) - *A computer program for signal processing of strong-motion data* - Available from URL: www.seismosoft.com.

- Sezen, H., and Moehle, J. (2004) - *Shear Strength Model for Lightly Reinforced Concrete Columns* - Journal of Structural Engineering, ASCE, Vol. 130, No. 1692.
- Spacone E., Filippou F.C., Taucer F.F. (1996) - *Fibre beam-column element for nonlinear analysis of R/C frames, Part I: Formulation* - Earthquake Engineering and Structural Dynamics, vol. 25, pp. 711-725.
- Stewart J.P., Seed R.B., Fenves G.L., (1998) - Empirical Evaluation of Inertial Soil-Structure Interaction Effects - Pacific Earthquake Engineering Research Center, PEER Report 1998/07.
- Stewart J.P., Fenves G.L., Seed R.B. (1999) - *Seismic soil-structure-interaction in buildings I: Analytical methods* - ASCE Journal of Geotechnical and Geoenvironmental Engineering, vol. 125, no. 1, pp. 26-37.
- Stewart J.P., Seed R.B., Fenves G.L., (1999) - *Seismic soil-structure-interaction in buildings II: Empirical findings* - ASCE Journal of Geotechnical and Geoenvironmental Engineering, vol. 125, no. 1, pp. 26-37.
- Stewart J.P., Comartin C., Moehle J.P. (2004) - *Implementation of Soil Structure Interaction Models in Performance Based Design Procedures* - 13th WCEE, Vancouver, Canada, Paper No. 1546.
- Stewart J.P., Kwok A., Hashash Y., Matasovic N., Pyke R., Wang Z., Yang A., (2008) - *Benchmarking of nonlinear geotechnical ground response analysis procedures* - Pacific Earthquake Engineering Research Center, PEER Report 2008/04.
- Terzaghi, K. (1943) - *Theoretical Soil Mechanics* - J. Wiley, New York.
- Vamvatsikos D., Cornell C.A. (2002) - *Incremental dynamic analysis* - Earthquake Engineering and Structural Dynamics, vol. 31, no. 3, pp. 491-514.
- Vamvatsikos D., Cornell C.A. (2004) - *Applied incremental dynamic analysis* – Earthquake Spectra, vol. 20, no. 2, pp. 523–553.

- Vamvatsikos D., Cornell C.A. (2005) - *Developing efficient scalar and vector intensity measures for IDA capacity estimation by incorporating elastic spectral shape information* - Earthquake Engineering and Structural Dynamics, vol. 34, no. 13, pp. 1573–1600.
- Vamvatsikos D., Cornell C.A. (2005) - *Direct estimation of the seismic demand and capacity of MDOF systems through Incremental Dynamic Analysis of an SDOF Approximation* - ASCE Journal of Structural Engineering, vol. 131, no. 4, pp. 589-599.
- Veletsos, A.S., and Wei, Y.T. (1971) - *Lateral and rocking vibrations of footings* - Journal of Soil Mechanics and Foundations Division, Vol. 97, No. 9, pp. 1227-1248.
- Veletsos, A.S. and Verbic, B. (1973) - *Vibration of viscoelastic foundations* - J. Earthquake Engrg. Struct. Dynamics, 2(1), 87-102.
- Veletsos A.S., Meek J.W. (1974) - *Dynamic behaviour of building-foundation systems* - Earthquake Engineering and Structural Dynamics, Vol.3, 121-138
- Veletsos, A.S. and Nair V.V. (1975) - *Seismic interaction of structures on hysteretic foundations* - J. Struct. Engrg., ASCE 101(1), 109-129.
- Williams M.S., Sexsmith R.G. (1995) - *Seismic damage indices for concrete structures: a state-of-the-art review* - Earthquake Spectra, vol. 11, no. 2, pp. 319-349.
- Wolf J.P. (1985) - *Dynamic Soil–Structure Interaction* - Prentice-Hall: New Jersey.
- Yang Z., Lu J., Elgamal A. (2008) - *OpenSees Soil Models and Solid- Fluid Fully Coupled Elements, User’s Manual, ver. 1.0.* - University of California, San Diego, 2008.
- Zienkiewicz, O. C., Bicanic, N., and Shen, F. Q. (1988) - *Earthquake input definition and the transmitting boundary conditions* - in Advances in Computational Nonlinear Mechanics, Springer-Verlag, pp. 109–138.

Annex A

Foundations Impedances

Below the formulations suggested by *Gazetas* (1991), *Mylonakis* (2006) and *Pais and Kausel* (1988) for the evaluation of the foundation impedances are shown (the tables are extracted from *NIST GCR 12-917-21*).

Table A. 1 - Elastic Solutions for Static Stiffness of Rigid Footings at the Ground Surface (NIST GCR 12-917-21)

Degree of Freedom	Pais and Kausel (1988)	Gazetas (1991); Mylonakis et al. (2006)
Translation along z-axis	$K_{z,sv} = \frac{GB}{1-\nu} \left[3.1 \left(\frac{L}{B} \right)^{0.75} + 1.6 \right]$	$K_{z,sv} = \frac{2GL}{1-\nu} \left[0.73 + 1.54 \left(\frac{B}{L} \right)^{0.75} \right]$
Translation along y-axis	$K_{y,sv} = \frac{GB}{2-\nu} \left[6.8 \left(\frac{L}{B} \right)^{0.65} + 0.8 \left(\frac{L}{B} \right) + 1.6 \right]$	$K_{y,sv} = \frac{2GL}{2-\nu} \left[2 + 2.5 \left(\frac{B}{L} \right)^{0.85} \right]$
Translation along x-axis	$K_{x,sv} = \frac{GB}{2-\nu} \left[6.8 \left(\frac{L}{B} \right)^{0.65} + 2.4 \right]$	$K_{x,sv} = K_{y,sv} - \frac{0.2}{0.75-\nu} GL \left(1 - \frac{B}{L} \right)$
Torsion about z-axis	$K_{t,sv} = GB^3 \left[4.25 \left(\frac{L}{B} \right)^{2.45} + 4.06 \right]$	$K_{t,sv} = GJ_t^{0.75} \left[4 + 11 \left(1 - \frac{B}{L} \right)^{10} \right]$
Rocking about y-axis	$K_{yy,sv} = \frac{GB^3}{1-\nu} \left[3.73 \left(\frac{L}{B} \right)^{2.4} + 0.27 \right]$	$K_{yy,sv} = \frac{G}{1-\nu} (I_y)^{0.75} \left[3 \left(\frac{L}{B} \right)^{0.15} \right]$
Rocking about x-axis	$K_{xx,sv} = \frac{GB^3}{1-\nu} \left[3.2 \left(\frac{L}{B} \right) + 0.8 \right]$	$K_{xx,sv} = \frac{G}{1-\nu} (I_x)^{0.75} \left(\frac{L}{B} \right)^{0.25} \left[2.4 + 0.5 \left(\frac{B}{L} \right) \right]$
Notes:	<p>Axes should be oriented such that $L \geq B$.</p> <p>I_t = area moment of inertia of soil-foundation contact, i denotes which axis to take the surface around.</p> <p>$J_t = I_x + I_y$, polar moment of inertia of soil-foundation contact surface.</p> <p>G = shear modulus (reduced for large strain effects, e.g., Table 2-1).</p>	

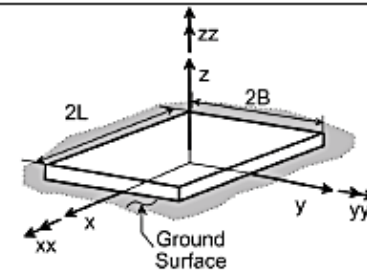


Table A. 2 - Embedment Correction Factors for Static Stiffness of Rigid Footings (NIST GCR 12-917-2)

Degree of Freedom	Pais and Kausel (1988)	Gazetas (1991); Mylonakis et al. (2006)
Translation along z-axis	$\eta_z = \left[1.0 + \left(0.25 + \frac{0.25}{L/B} \right) \left(\frac{D}{B} \right)^{0.8} \right]$	$\eta_z = \left[1 + \frac{D}{21B} \left(1 + 1.3 \frac{B}{L} \right) \right] \left[1 + 0.2 \left(\frac{A_w}{4BL} \right)^{2/3} \right]$
Translation along y-axis	$\eta_y = \left[1.0 + \left(0.33 + \frac{1.34}{1 + L/B} \right) \left(\frac{D}{B} \right)^{0.8} \right]$	$\eta_y = \left(1 + 0.15 \sqrt{\frac{D}{B}} \right) \left[1 + 0.52 \left(\frac{z_w A_w}{BL^2} \right)^{0.4} \right]$
Translation along x-axis	$\eta_x \approx \eta_y$	Same equation as for η_y , but A_w term changes for $B \neq L$
Torsion about z-axis	$\eta_{\omega} = \left[1 + \left(1.3 + \frac{1.32}{L/B} \right) \left(\frac{D}{B} \right)^{0.9} \right]$	$\eta_{\omega} = 1 + 1.4 \left(1 + \frac{B}{L} \right) \left(\frac{d_w}{B} \right)^{0.9}$
Rocking about y-axis	$\eta_{yy} = \left[1.0 + \frac{D}{B} + \left(\frac{1.6}{0.35 + (L/B)^4} \right) \left(\frac{D}{B} \right)^2 \right]$	$\eta_{yy} = 1 + 0.92 \left(\frac{d_w}{B} \right)^{0.6} \left[1.5 + \left(\frac{d_w}{D} \right)^{1.9} \left(\frac{B}{L} \right)^{-0.6} \right]$
Rocking about x-axis	$\eta_{xx} = \left[1.0 + \frac{D}{B} + \left(\frac{1.6}{0.35 + L/B} \right) \left(\frac{D}{B} \right)^2 \right]$	$\eta_{xx} = 1 + 1.26 \frac{d_w}{B} \left[1 + \frac{d_w}{B} \left(\frac{d_w}{D} \right)^{-0.2} \sqrt{\frac{B}{L}} \right]$

Notes:

d_w = height of effective side wall contact (may be less than total foundation height)

z_w = depth to centroid of effective sidewall contact

A_w = sidewall-solid contact area, for constant effective contact height, d_w , along perimeter.

For each degree of freedom, calculate $K_{emb} = \eta K_{sur}$

Coupling Terms: $K_{emb, rz} = \left(\frac{D}{3} \right) K_{emb, x}$

$K_{emb, ry} = \left(\frac{D}{3} \right) K_{emb, y}$

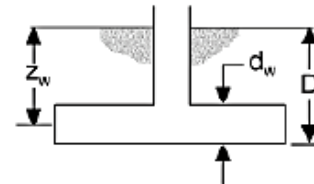


Table A. 3 - Dynamic Stiffness Modifiers and Radiation Damping Ratios for Rigid Footings (NIST GCR 12-917-2)

Degree of Freedom	Surface Stiffness Modifiers	Radiation Damping
Translation along z-axis	$\alpha_z = 1.0 - \left[\frac{\left(0.4 + \frac{0.2}{L/B}\right) a_0^2}{\left(\frac{10}{1+3(L/B-1)}\right) + a_0^2} \right]$	$\beta_z = \left[\frac{4\psi(L/B)}{(K_{z,svr}/GB)} \right] \left[\frac{a_0}{2\alpha_z} \right]$
Translation along y-axis	$\alpha_y = 1.0$	$\beta_y = \left[\frac{4(L/B)}{(K_{y,svr}/GB)} \right] \left[\frac{a_0}{2\alpha_y} \right]$
Translation along x-axis	$\alpha_x = 1.0$	$\beta_x = \left[\frac{4(L/B)}{(K_{x,svr}/GB)} \right] \left[\frac{a_0}{2\alpha_x} \right]$
Torsion about z-axis	$\alpha_{zz} = 1.0 - \left[\frac{\left(0.33 - 0.03\sqrt{L/B-1}\right) a_0^2}{\left(\frac{0.8}{1+0.33(L/B-1)}\right) + a_0^2} \right]$	$\beta_{zz} = \left[\frac{(4/3) \left[(L/B)^3 + (L/B) \right] a_0^2}{(K_{zz,svr}/GB^3) \left[\left(\frac{1.4}{1+3(L/B-1)^{0.7}}\right) + a_0^2 \right]} \right] \left[\frac{a_0}{2\alpha_{zz}} \right]$
Rocking about y-axis	$\alpha_{yy} = 1.0 - \left[\frac{0.55a_0^2}{\left(0.6 + \frac{1.4}{(L/B)^3}\right) + a_0^2} \right]$	$\beta_{yy} = \left[\frac{(4\psi/3)(L/B)^3 a_0^2}{\left(\frac{K_{yy,svr}}{GB^3}\right) \left[\left(\frac{1.8}{1+1.75(L/B-1)}\right) + a_0^2 \right]} \right] \left[\frac{a_0}{2\alpha_{yy}} \right]$
Rocking about x-axis	$\alpha_{xx} = 1.0 - \left[\frac{\left(0.55 + 0.01\sqrt{L/B-1}\right) a_0^2}{\left(2.4 - \frac{0.4}{(L/B)^3}\right) + a_0^2} \right]$	$\beta_{xx} = \left[\frac{(4\psi/3)(L/B) a_0^2}{(K_{xx,svr}/GB^3) \left[\left(2.2 - \frac{0.4}{(L/B)^3}\right) + a_0^2 \right]} \right] \left[\frac{a_0}{2\alpha_{xx}} \right]$
Notes:	<p>Orient axes such that $L \geq B$.</p> <p>Soil hysteretic damping, β_s, is additive to foundation radiation damping, β.</p> <p>$a_0 = \omega B / V_s$; $\psi = \sqrt{2(1-\nu)/(1-2\nu)}$; $\psi \leq 2.5$</p>	

Table A. 4 - Dynamic Stiffness Modifiers and Radiation Damping Ratios for Embedded Footings (NIST GCR 12-917-2)

Degree of Freedom	Radiation Damping
Translation along z-axis	$\beta_z = \left[\frac{4[\psi(L/B) + (D/B)(1+L/B)]}{(K_{z,emb}/GB)} \right] \left[\frac{a_0}{2\alpha_z} \right]$
Translation along y-axis	$\beta_y = \left[\frac{4[L/B + (D/B)(1+\psi L/B)]}{(K_{y,emb}/GB)} \right] \left[\frac{a_0}{2\alpha_y} \right]$
Translation along x-axis	$\beta_x = \left[\frac{4[L/B + (D/B)(\psi + L/B)]}{(K_{x,emb}/GB)} \right] \left[\frac{a_0}{2\alpha_x} \right]$
Torsion about z-axis	$\beta_{\omega_z} = \left[\frac{(4/3) \left[3(L/B)(D/B) + \psi(L/B)^3(D/B) + 3(L/B)^2(D/B) + \psi(D/B) + (L/B)^3 + (L/B) \right] a_0^2}{\left(\frac{K_{\omega_z,emb}}{GB^3} \right) \left[\left(\frac{1.4}{1+3(L/B-1)^{0.7}} \right) + a_0^2 \right]} \right] \left[\frac{a_0}{2\alpha_{\omega_z}} \right]$
Rocking about y-axis	$\beta_{\omega_y} = \left[\frac{(4/3) \left[\left(\frac{L}{B} \right)^3 \left(\frac{D}{B} \right) + \psi \left(\frac{D}{B} \right)^3 \left(\frac{L}{B} \right) + \left(\frac{D}{B} \right)^3 + 3 \left(\frac{D}{B} \right) \left(\frac{L}{B} \right)^2 + \psi \left(\frac{L}{B} \right)^3 \right] a_0^2 + \left(\frac{4}{3} \right) \left(\frac{L}{B} + \psi \right) \left(\frac{D}{B} \right)^3}{\left(\frac{K_{\omega_y,emb}}{GB^3} \right) \left[\left(\frac{1.8}{1+1.75(L/B-1)} \right) + a_0^2 \right]} + \frac{\left(\frac{K_{\omega_y,emb}}{GB^3} \right)}{\left(\frac{K_{\omega_y,emb}}{GB^3} \right)} \right] \left[\frac{a_0}{2\alpha_{\omega_y}} \right]$
Rocking about x-axis	$\beta_{\omega_x} = \left[\frac{(4/3) \left[\left(\frac{D}{B} \right) + \left(\frac{D}{B} \right)^3 + \psi \left(\frac{L}{B} \right) \left(\frac{D}{B} \right)^3 + 3 \left(\frac{D}{B} \right) \left(\frac{L}{B} \right) + \psi \left(\frac{L}{B} \right) \right] a_0^2 + \left(\frac{4}{3} \right) \left(\psi \frac{L}{B} + 1 \right) \left(\frac{D}{B} \right)^3}{\left(\frac{K_{\omega_x,emb}}{GB^3} \right) \left[\left(\frac{1.8}{1+1.75(L/B-1)} \right) + a_0^2 \right]} + \frac{\left(\frac{K_{\omega_x,emb}}{GB^3} \right)}{\left(\frac{K_{\omega_x,emb}}{GB^3} \right)} \right] \left[\frac{a_0}{2\alpha_{\omega_x}} \right]$
Notes:	Soil hysteretic damping, β_s , is additive to foundation radiation damping, β_r . $\alpha_{emb} = \alpha_{sur}$; from Table 2-3a $a_0 = \omega B / V_s$; $\psi = \sqrt{2(1-\nu)/(1-2\nu)}$; $\psi \leq 2.5$

Annex B

Ground Motions

Below the acceleration records and the corresponding response spectra of the earthquakes which were used for the parametric analyses performed in Chapter 4 are shown.

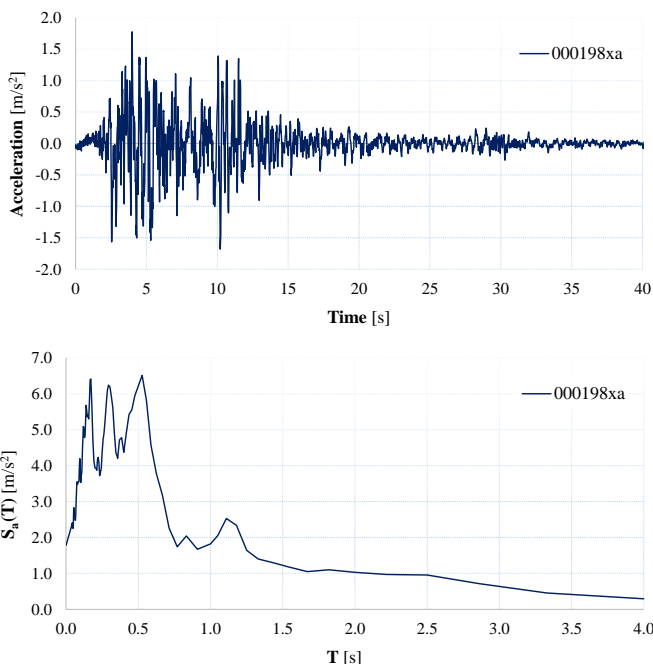


**Figure B. 1 - Group 1 – GM1: Montenegro 15/04/1979
PGA = 1.77m/s² – Mw = 6.9 – R = 21 km**

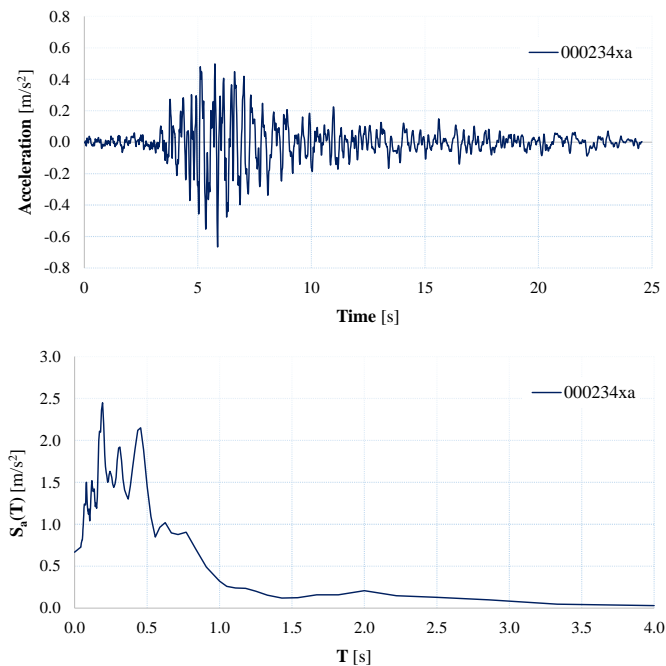


**Figure B. 2 - Group 1 – GM2: Montenegro (aftershock) 24/05/1979
PGA = 0.67 m/s² – Mw = 6.2 – R = 30 km**

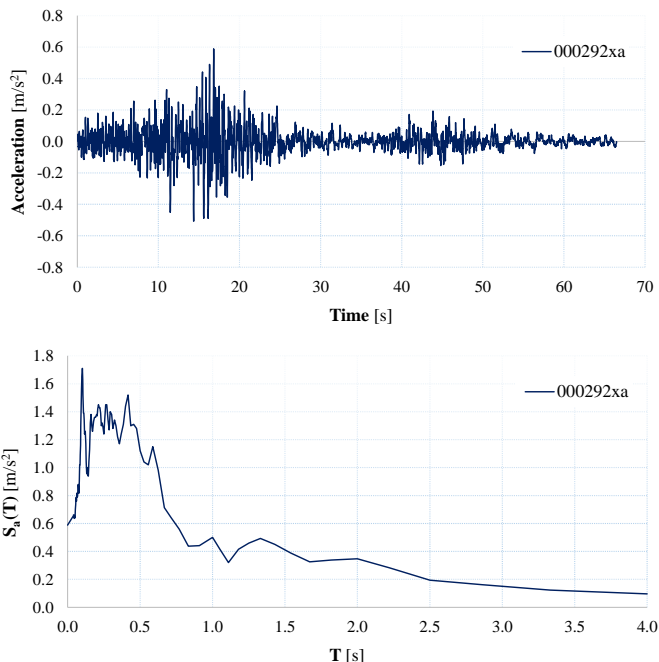


Figure B. 3 - Group 1 – GM3: Campano Lucano 23/11/1980
PGA = 0.59 m/s² – M_w = 6.9 – R = 25 km

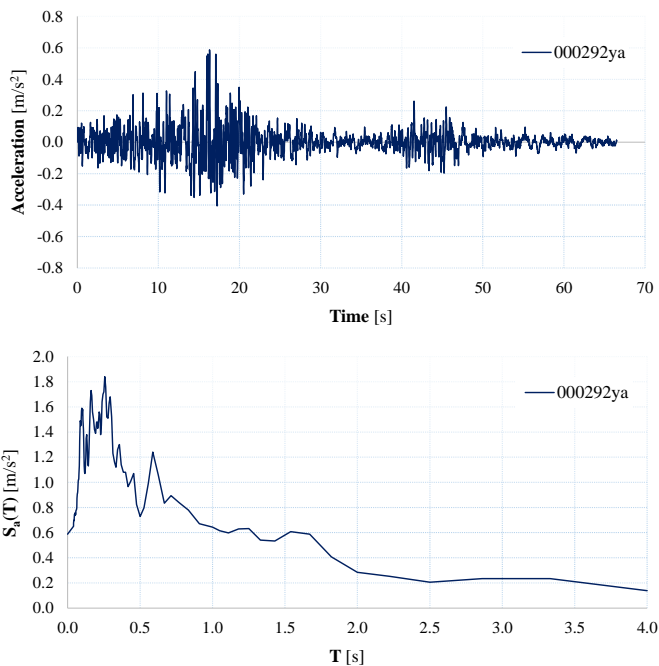


Figure B. 4 - Group 1 – GM4: Campano Lucano 23/11/1980
PGA = 0.59 m/s² – M_w = 6.9 – R = 25 km

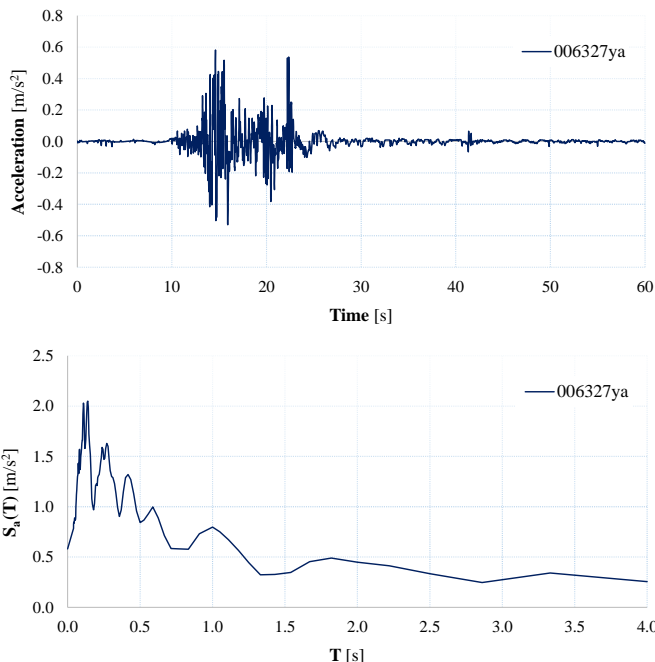


Figure B. 5 - Group 1 – GM5: South Iceland (aftershock) 21/06/2000
PGA = 0.58 m/s² – M_w = 6.4 – R = 24 km

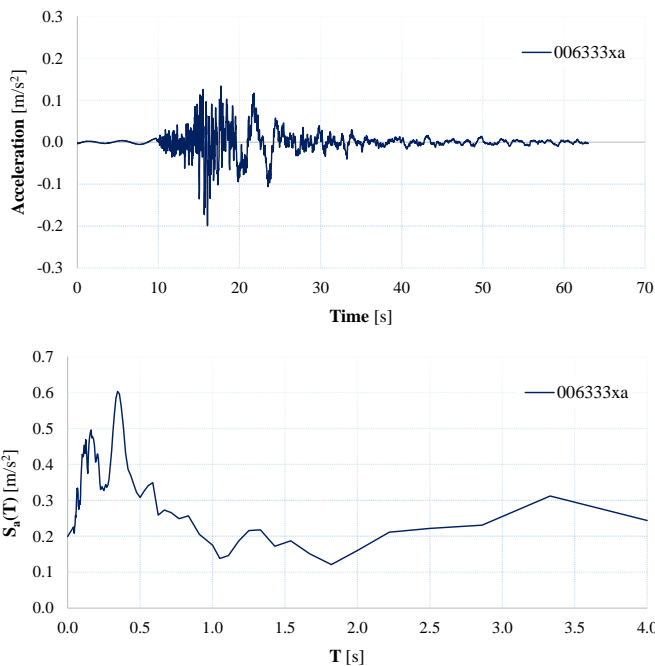


Figure B. 6 - Group 1 – GM6: South Iceland (aftershock) 21/06/2000
PGA = 0.20 m/s² – M_w = 6.4 – R = 28 km

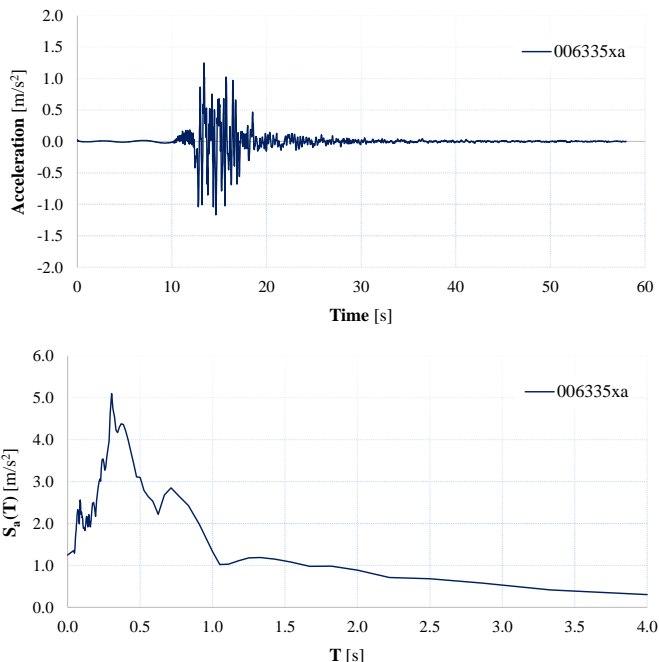


Figure B. 7 - Group 1 – GM7: South Iceland (aftershock) 21/06/2000
PGA = 1.25 m/s² – M_w = 6.4 – R = 15 km

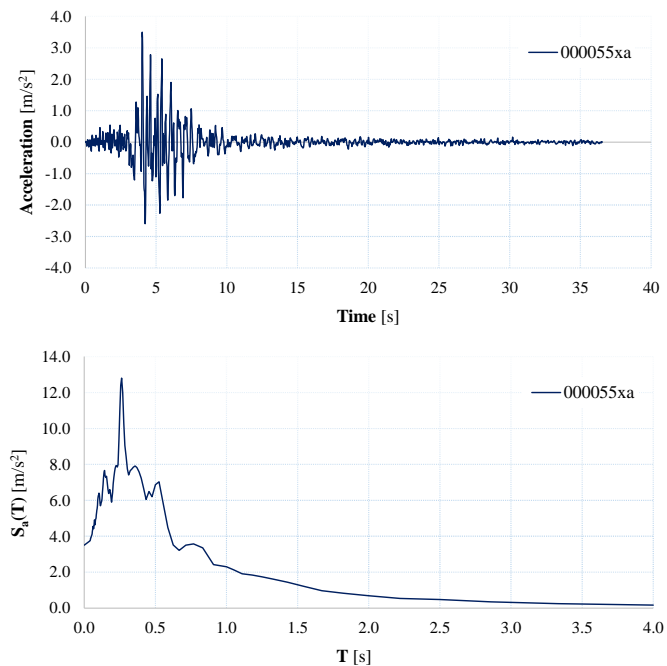


Figure B. 8 - Group 2 – GM1: Friuli 06/05/1976
PGA = 3.50 m/s² – M_w = 6.5 – R = 23 km

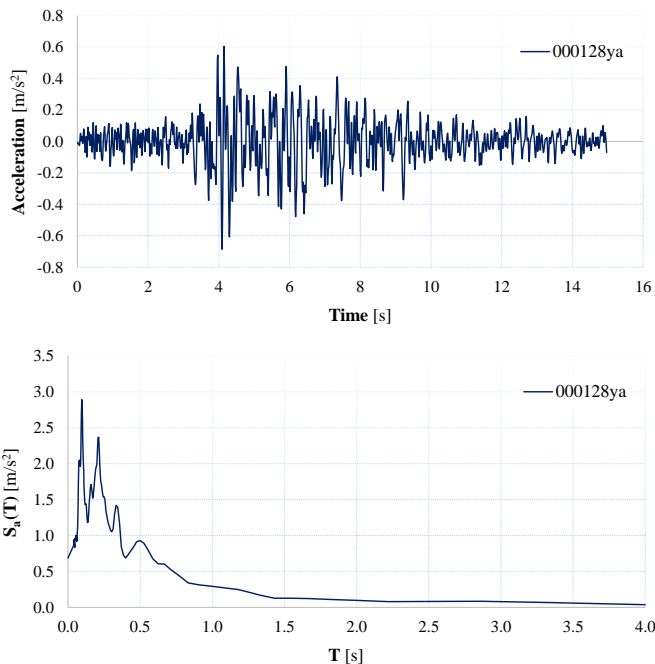


Figure B. 9 - Group 2 – GM2: Friuli (aftershock) 15/09/1976
PGA = 0.69 m/s² – M_w = 6.0 – R = 28 km

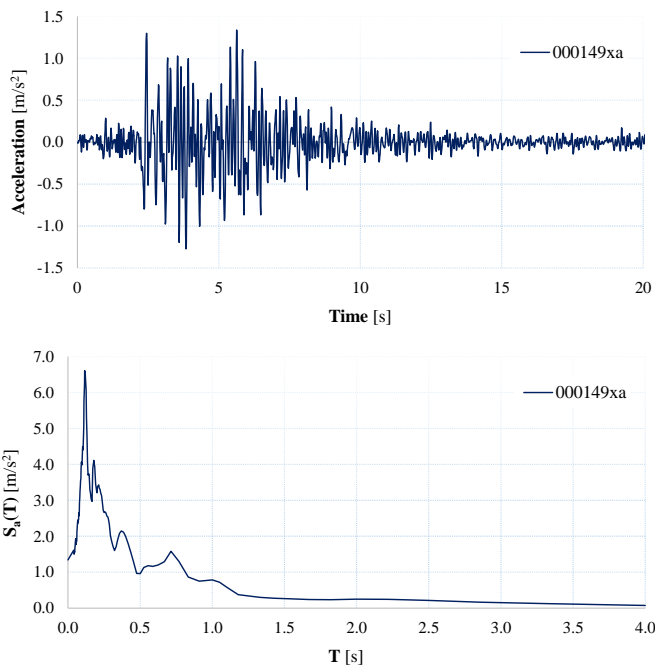


Figure B. 10 - Group 2 – GM3: Friuli (aftershock) 15/09/1976
PGA = 1.34 m/s² – M_w = 6.0 – R = 12 km

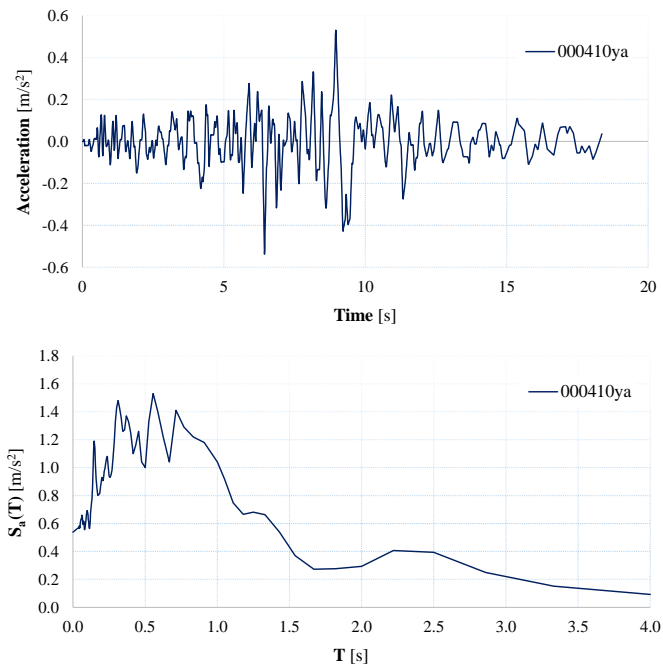


Figure B. 11 - Group 2 – GM4: Golbasi 05/05/1986
PGA = 0.54 m/s^2 – M_w = 6.0 – R = 29 km

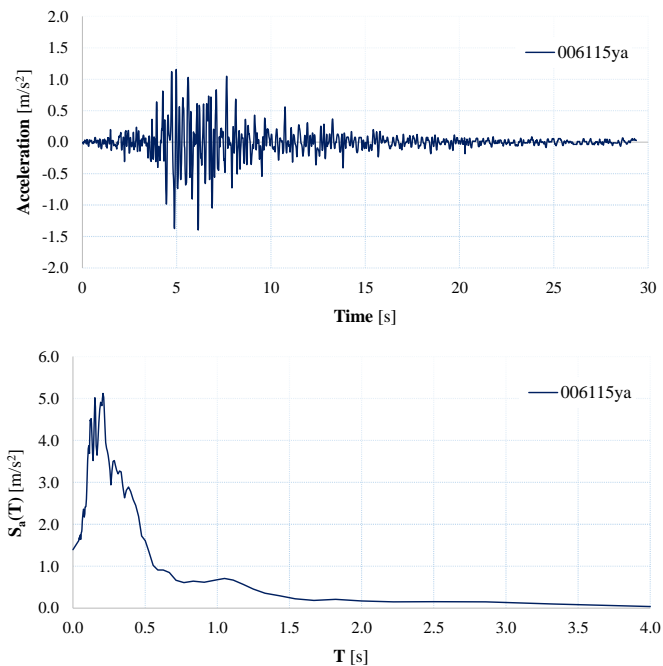


Figure B. 12 - Group 2 – GM5: Kozani 13/05/1995
PGA = 1.40 m/s^2 – M_w = 6.5 – R=17 km

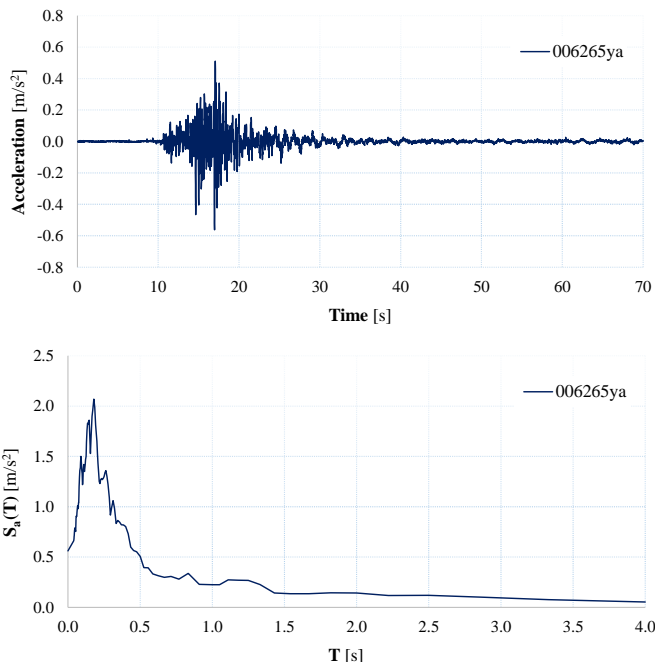


Figure B. 13 - Group 2 – GM6: South Iceland 17/06/2000
PGA = 0.56 m/s² – M_w = 6.5 – R = 29 km

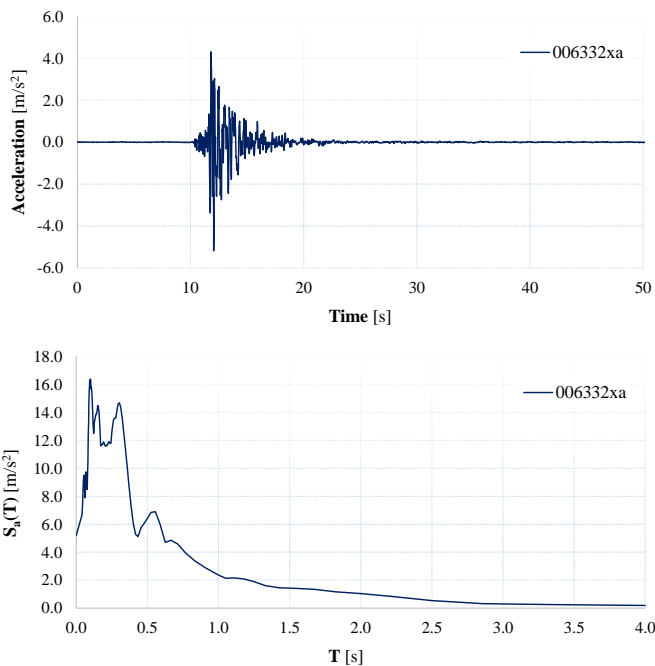
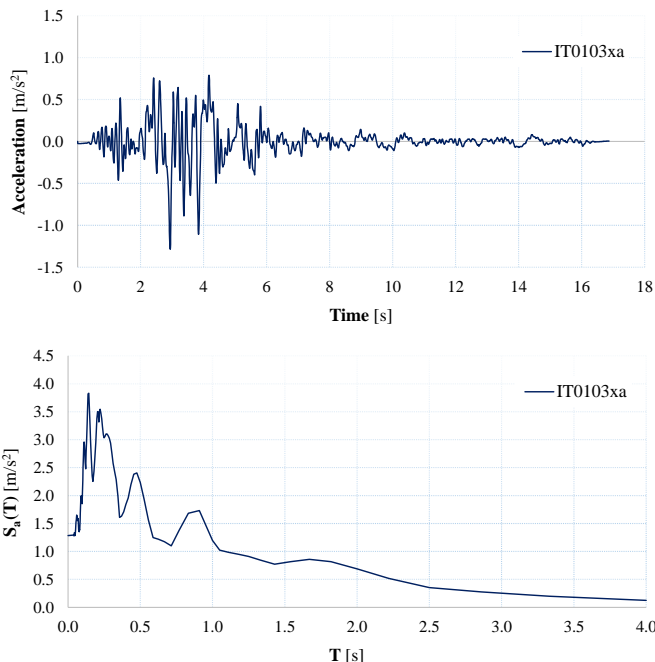
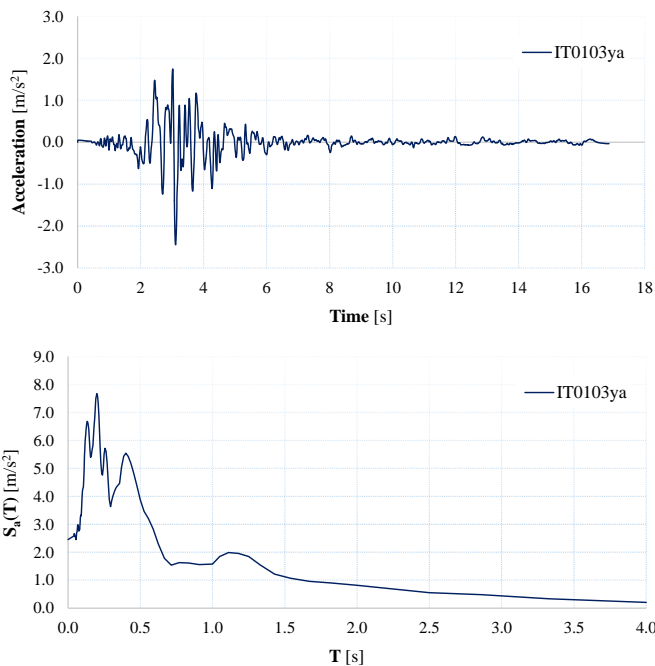


Figure B. 14 - Group 2 – GM7: South Iceland (aftershock) 21/06/2000
PGA = 5.19 m/s² – M_w = 6.4 – R = 6 km



**Figure B. 15 - Group 3 – GM1: Friuli Earthquake 4th shock 15/09/1976
PGA = 1.29 m/s² – M_w = 5.9 – R = 16 km**



**Figure B. 16 - Group 3 – GM2: Friuli Earthquake 4th shock 15/09/1976
PGA = 2.45 m/s² – M_w = 5.9 – R = 16 km**

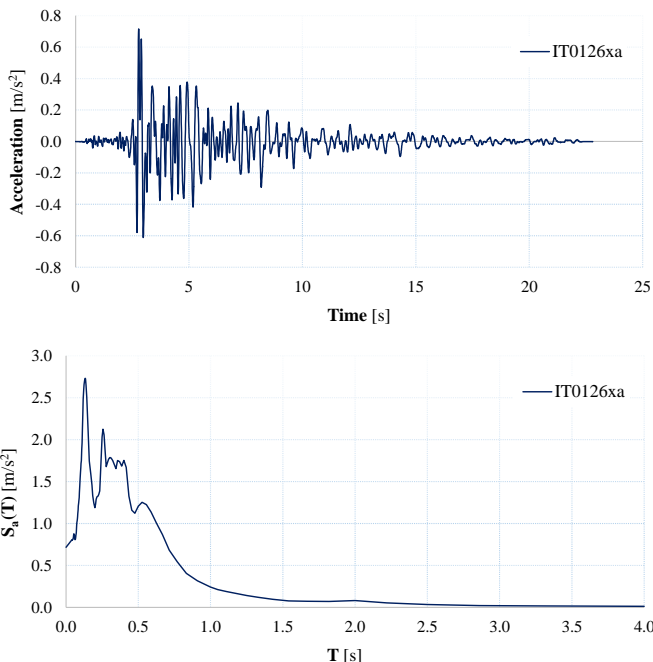


Figure B. 17 - Group 3 – GM3: Ferruzzano 11/03/1978
PGA = 0.72 m/s² – M_w = 5.2 – R = 9 km

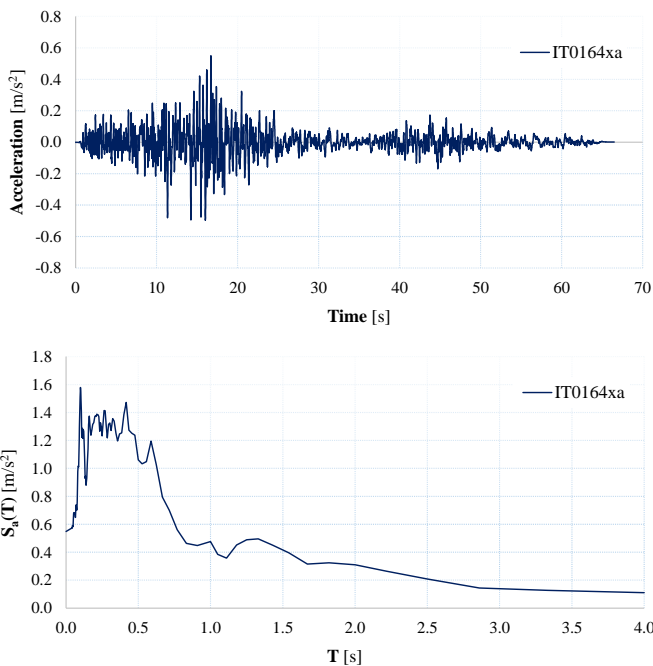


Figure B. 18 - Group 3 – GM4: Irpinia Earthquake 23/11/1980
PGA = 0.55 m/s² – M_w = 6.9 – R = 24 km

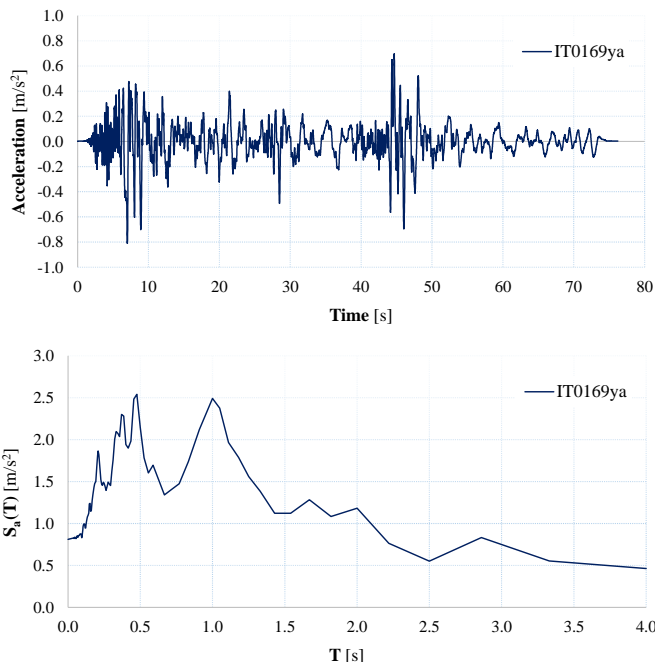


Figure B. 19 - Group 3 – GM5: Irpinia Earthquake 23/11/1980
PGA = 0.81 m/s² – M_w = 6.9 – R = 28 km

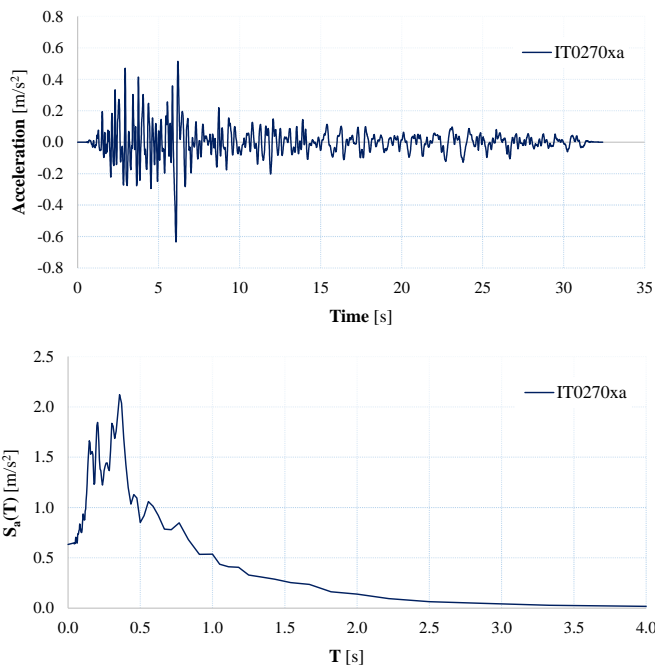
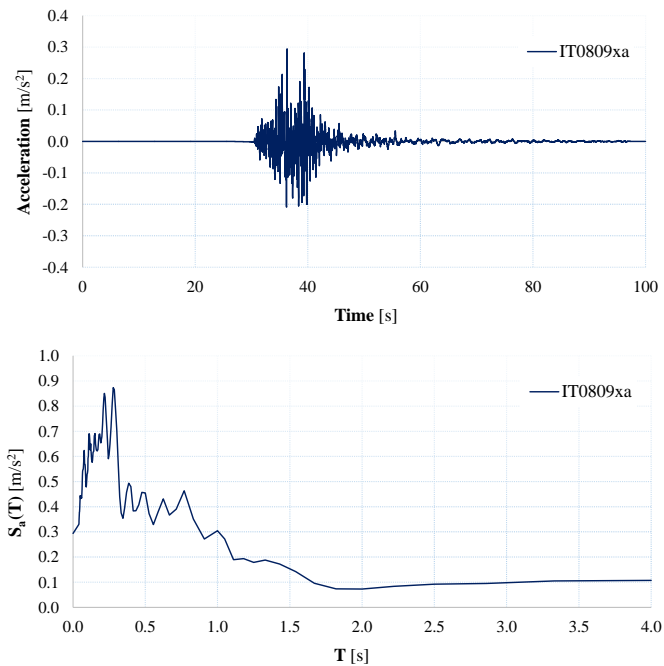


Figure B. 20 - Group 3 – GM6: Val Comino Earthquake 07/05/1984
PGA = 0.63 m/s² – M_w = 5.9 – R = 27 km



**Figure B. 21 - Group 3 – GM7: L'Aquila Mainshock 06/04/2009
PGA = 0.29 m/s² – Mw = 6.3 – R = 23 km**

Parametric Analyses Results

Below the results of all the parametric analyses performed for the four moment resisting frames introduced in Chapter 4 are shown.

The results are shown in terms of maximum base shear and maximum inter-storey drift ratio and are grouped based on the group of records considered for the analyses (see Chapter 4, section 4.3).

In each graph the results obtained for a fixed-base model (blue lines) are compared with those obtained for a flexible-base model (i.e. taking into account the soil-structure interaction).

Two modelling approaches were considered for taking into account the soil-structure interaction: a Complete FEM model (red lines) and a Beam on Non-linear Winkler Foundation model (green lines).

The single lines refers to the results obtained for a specific record of the group, while the bold-dotted lines refers to the average results.

Note 1: The single record curves were stopped to the last PGA level that did not caused the structural collapse.

Note 2: The average curves were stopped to a PGA level for which at least 3 values of structural response were obtained.

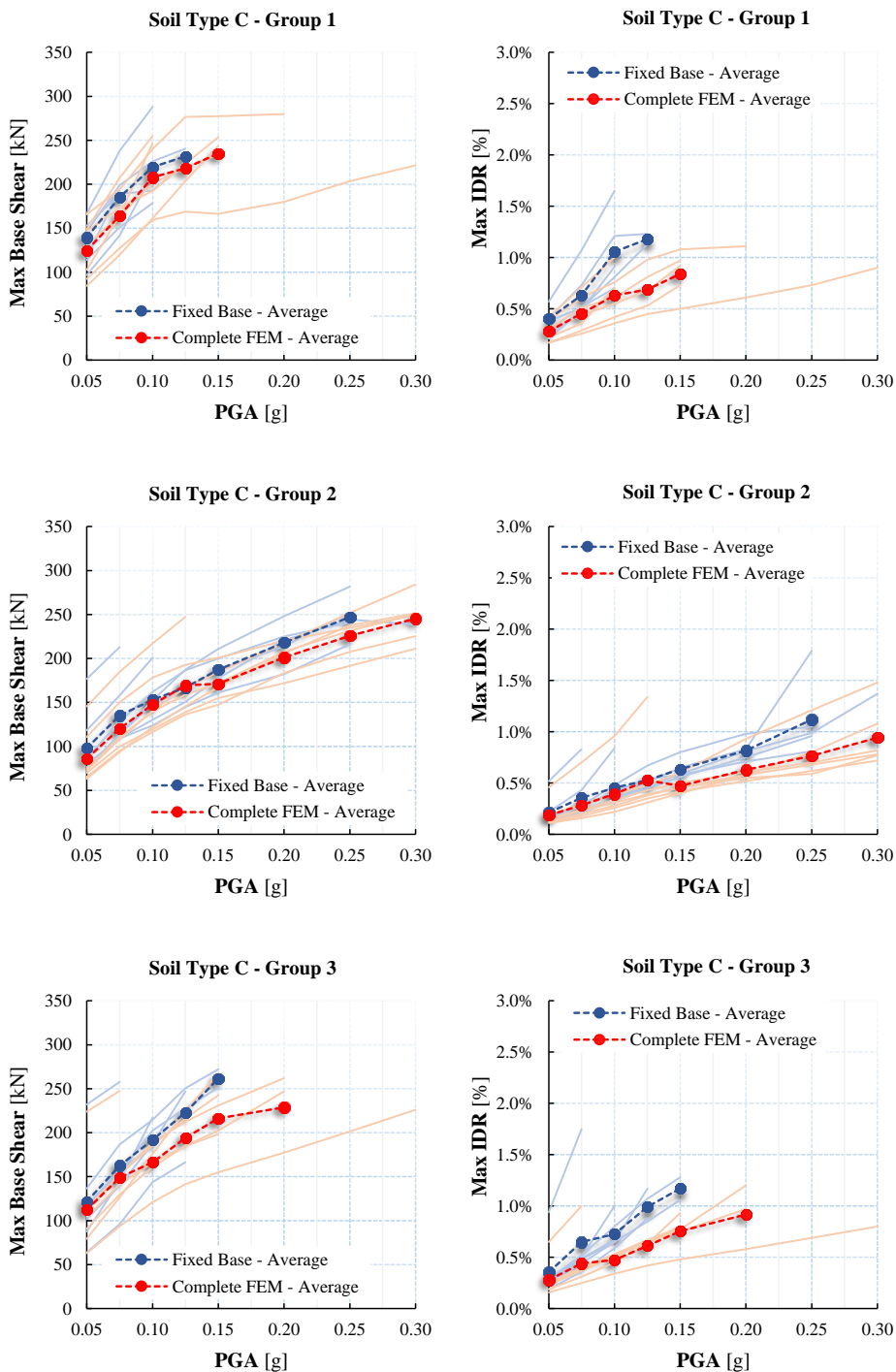


Figure C. 1 - 4 Floors Pre-Code – Soil Type C – Fixed Base VS Complete FEM

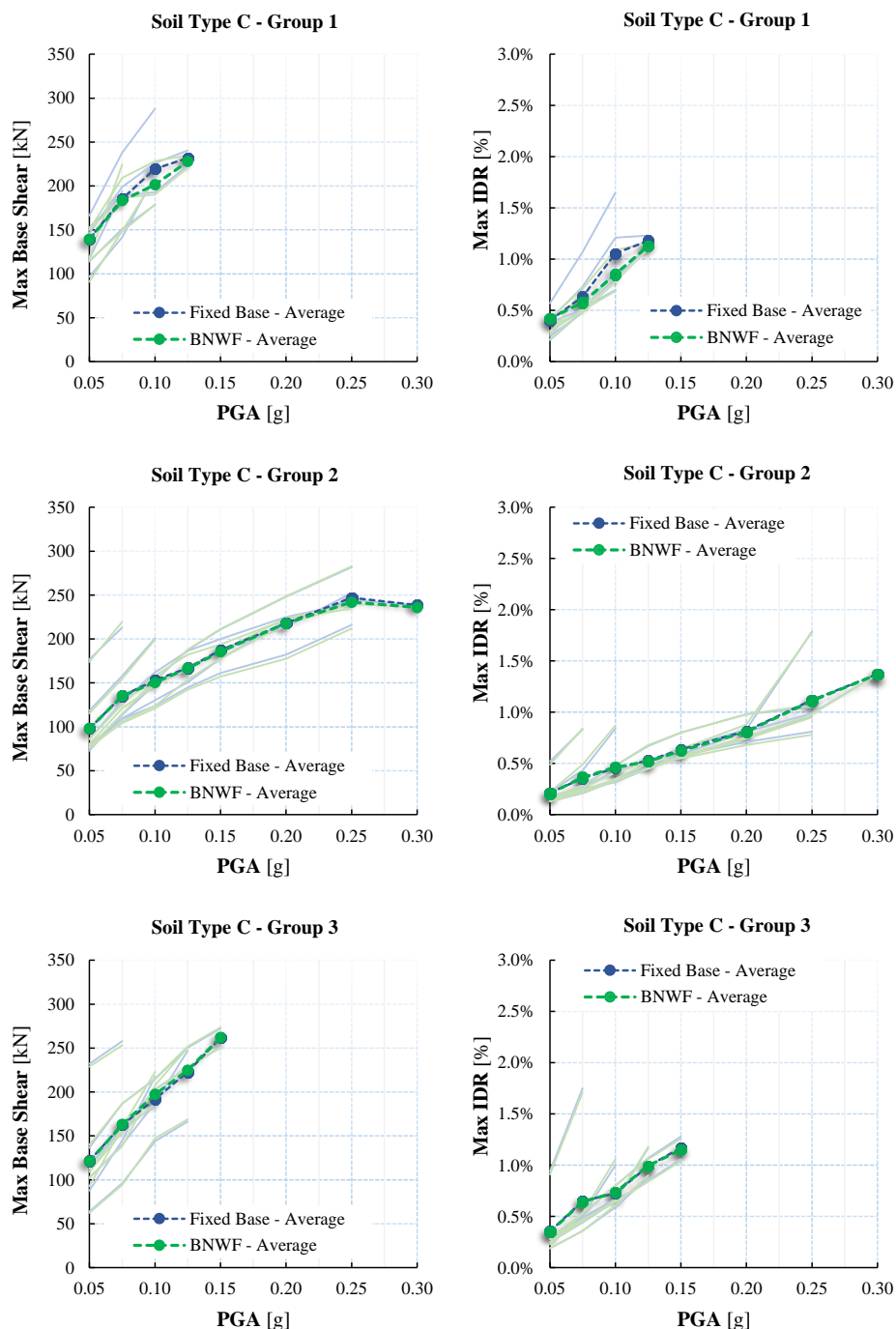


Figure C. 2 - 4 Floors Pre-Code – Soil Type C – Fixed Base VS BNWF

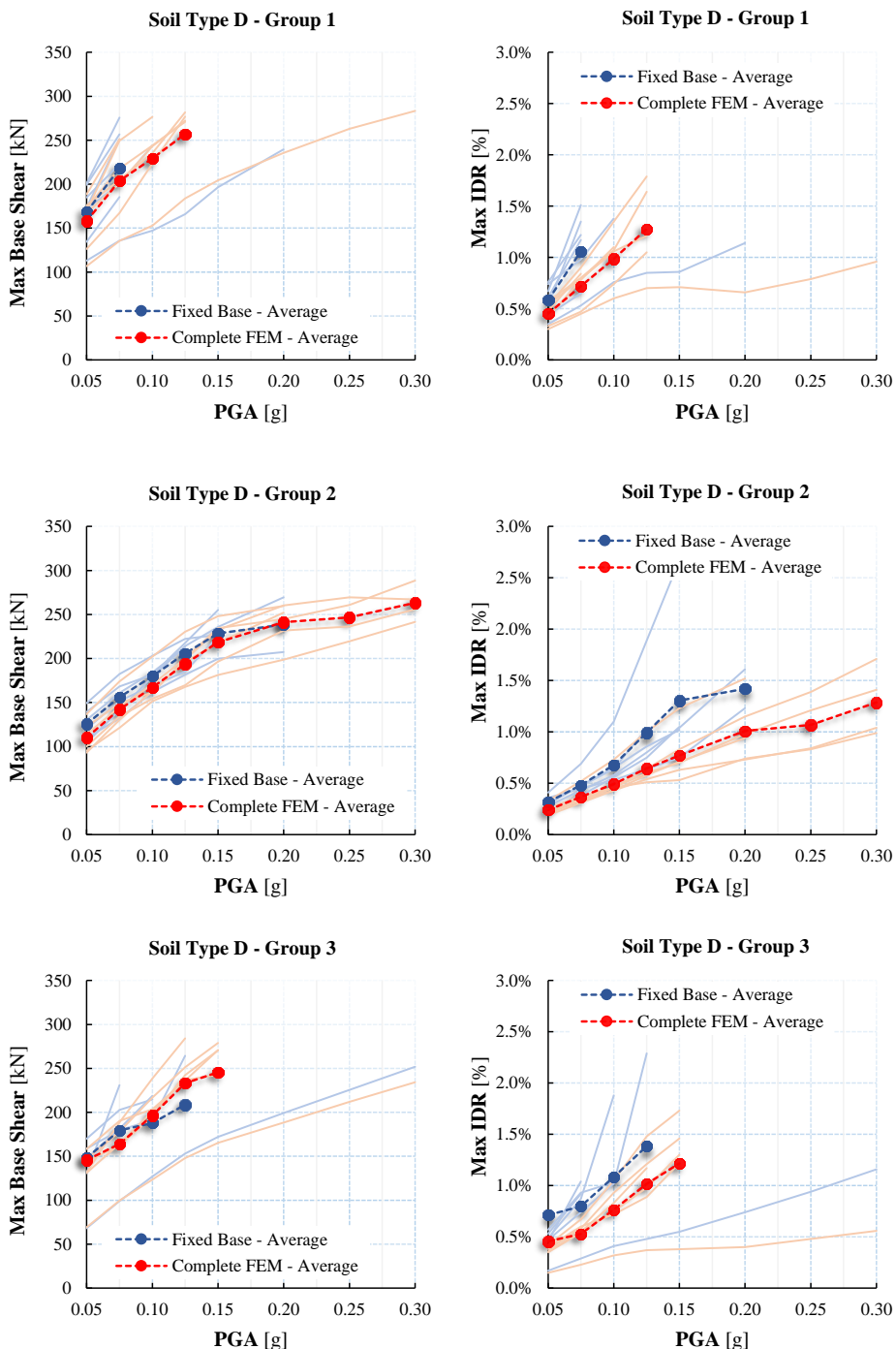


Figure C. 3 - 4 Floors Pre-Code – Soil Type D – Fixed Base VS Complete FEM

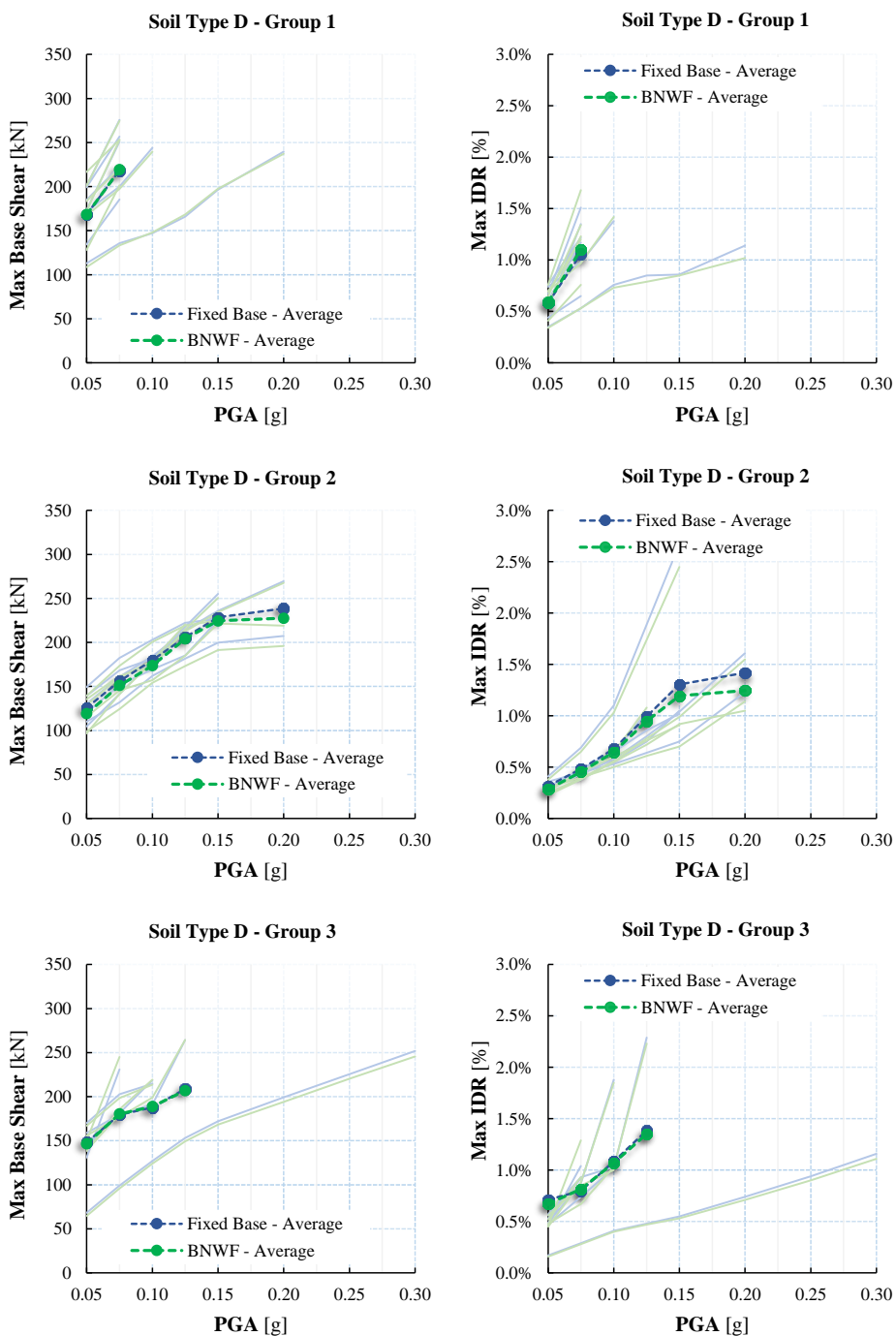


Figure C. 4 - 4 Floors Pre-Code – Soil Type D – Fixed Base VS BNWF

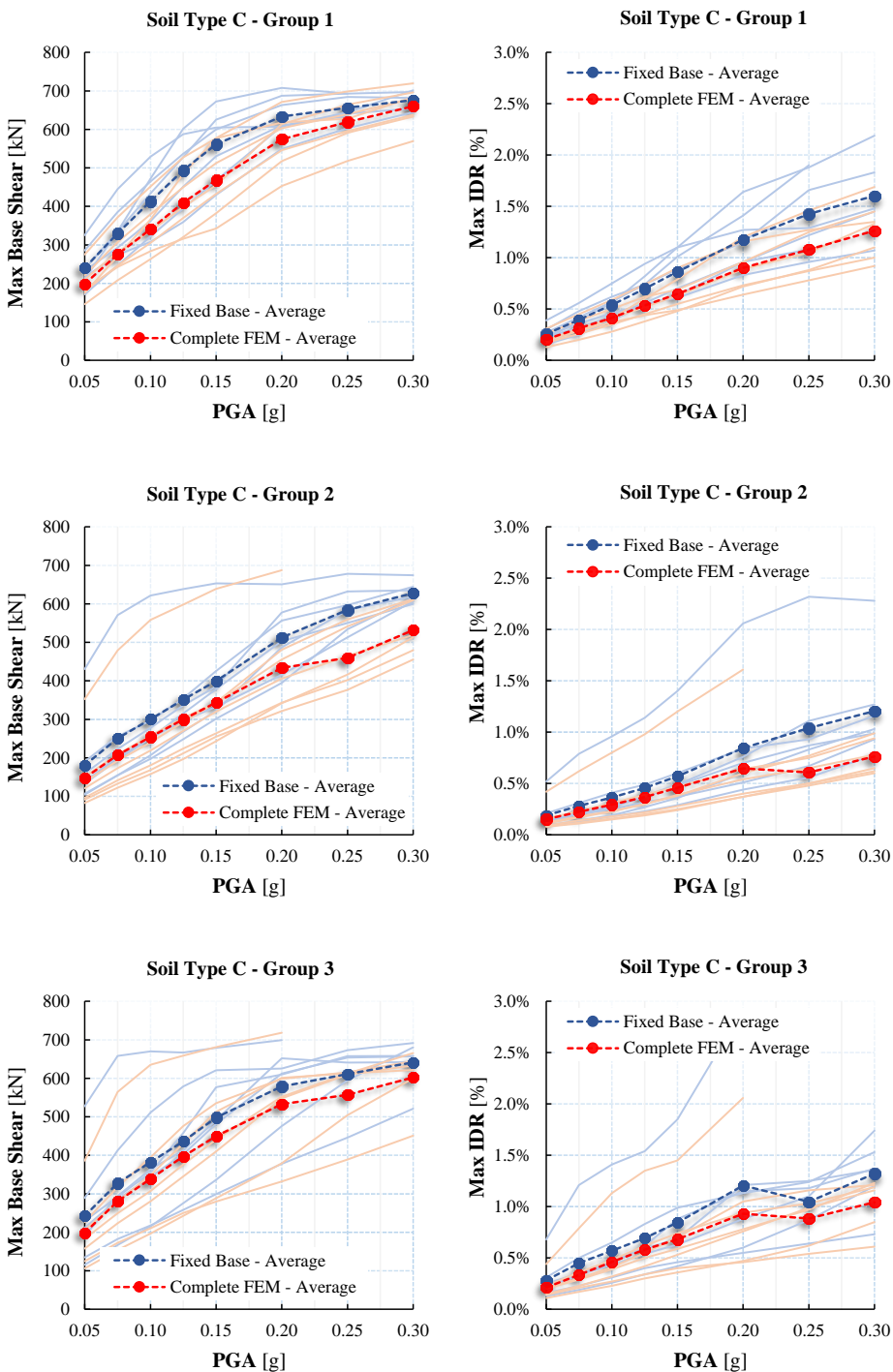


Figure C. 5 - 4 Floors Code compliant – Soil Type C – Fixed Base VS Complete FEM

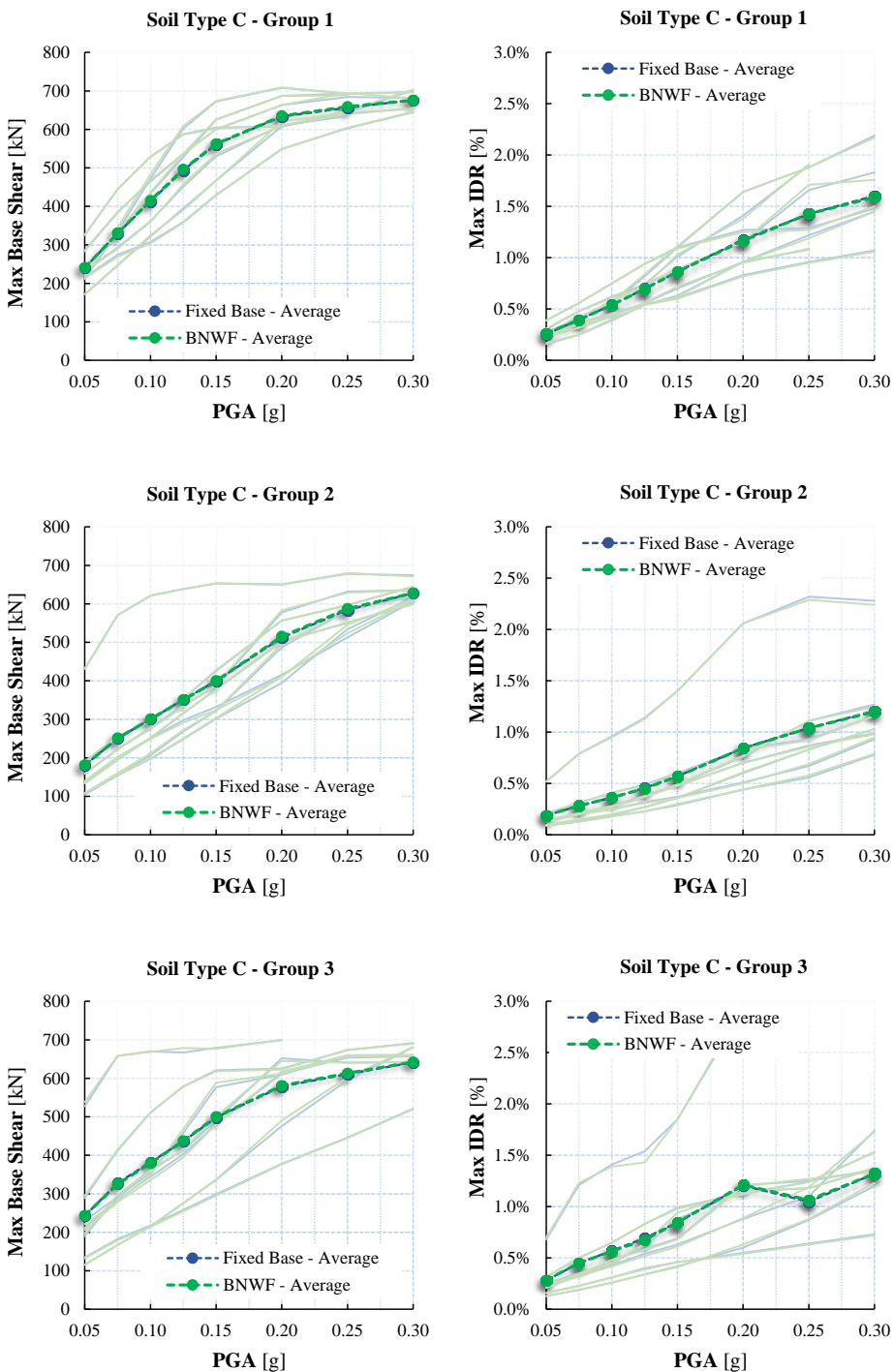


Figure C. 6 - 4 Floors Code compliant – Soil Type C – Fixed Base VS BNWF

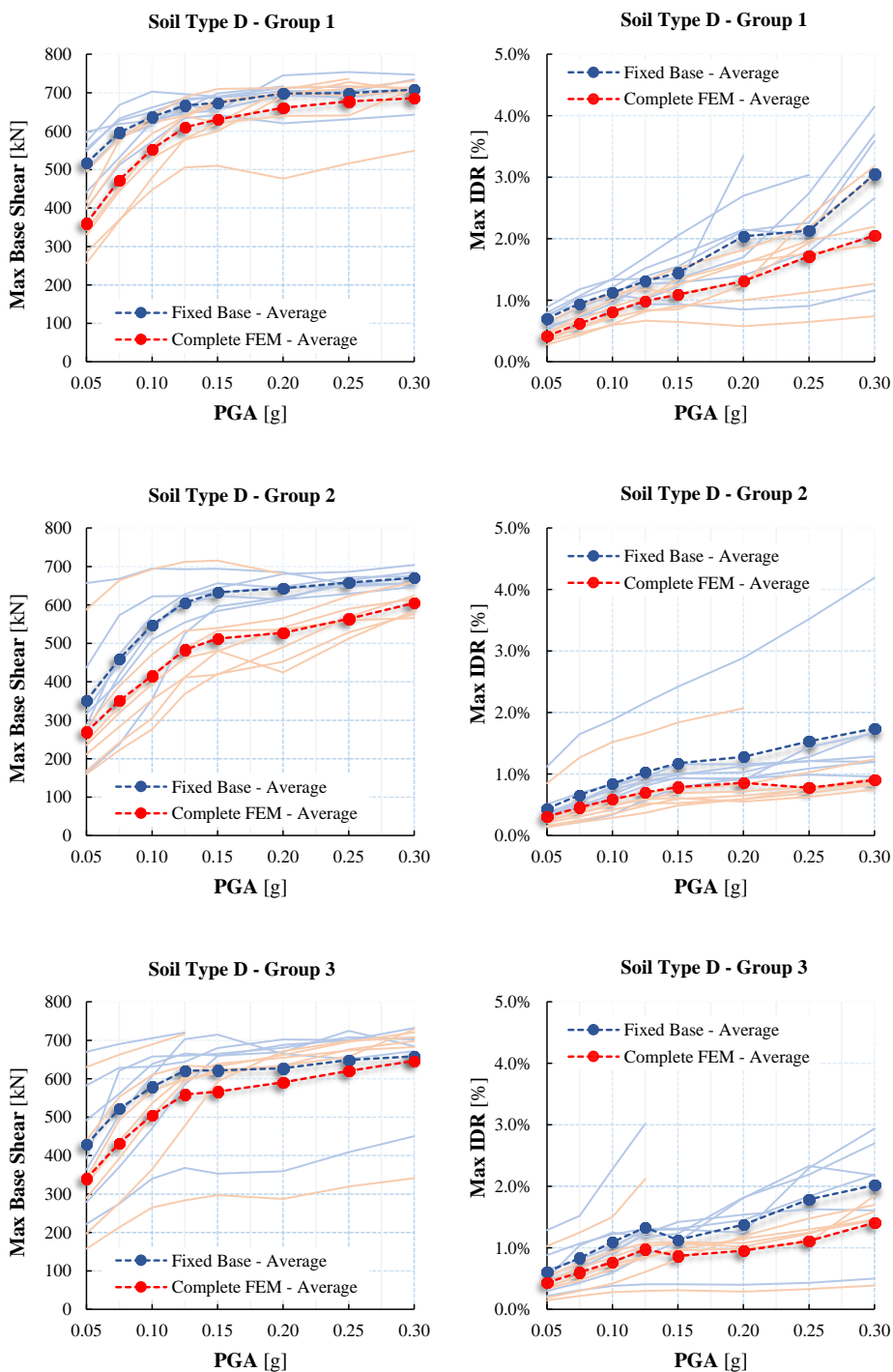


Figure C. 7 - 4 Floors Code compliant – Soil Type D – Fixed Base VS Complete FEM

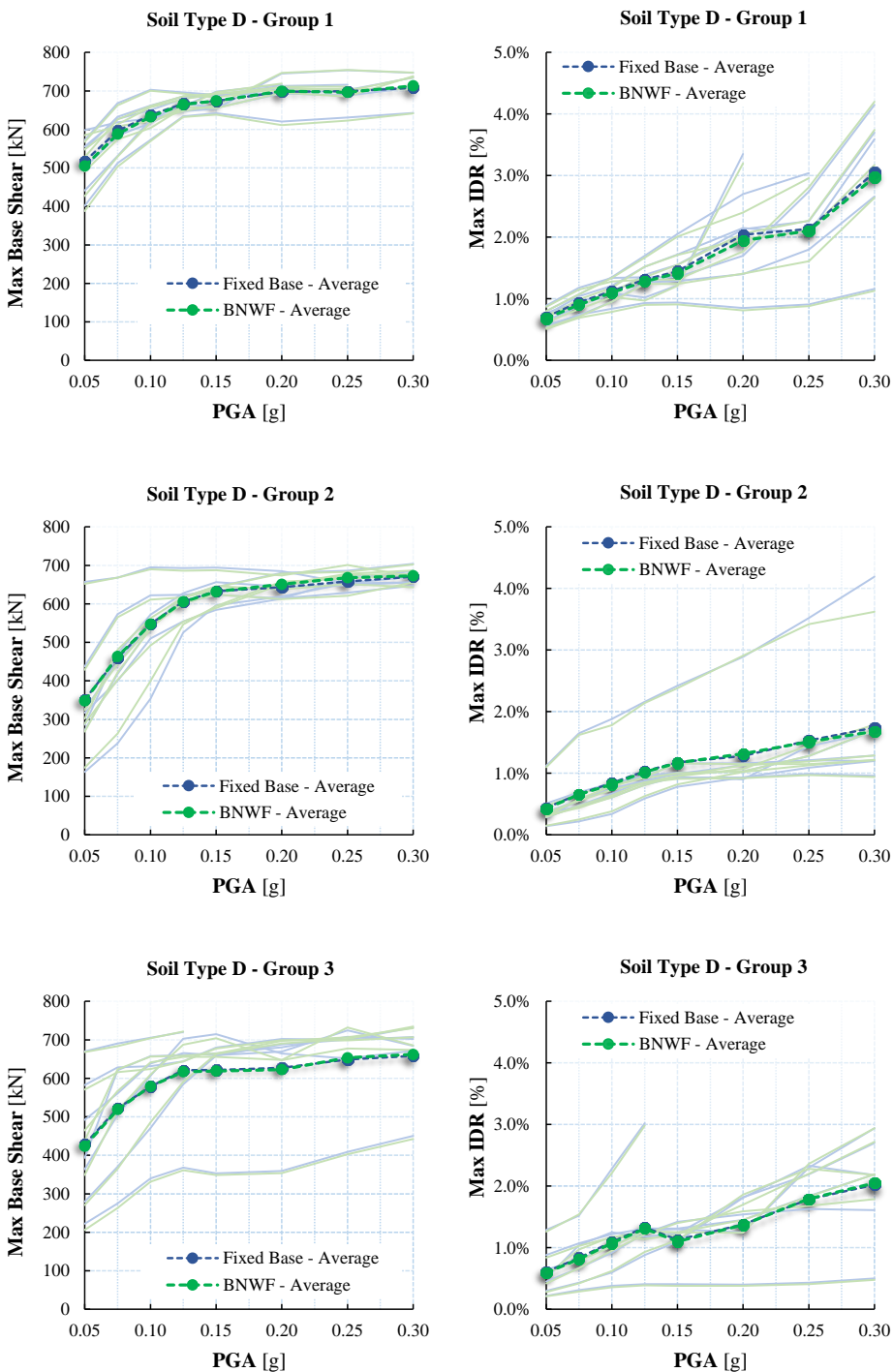


Figure C. 8 - 4 Floors Code compliant – Soil Type D – Fixed Base VS BNWF

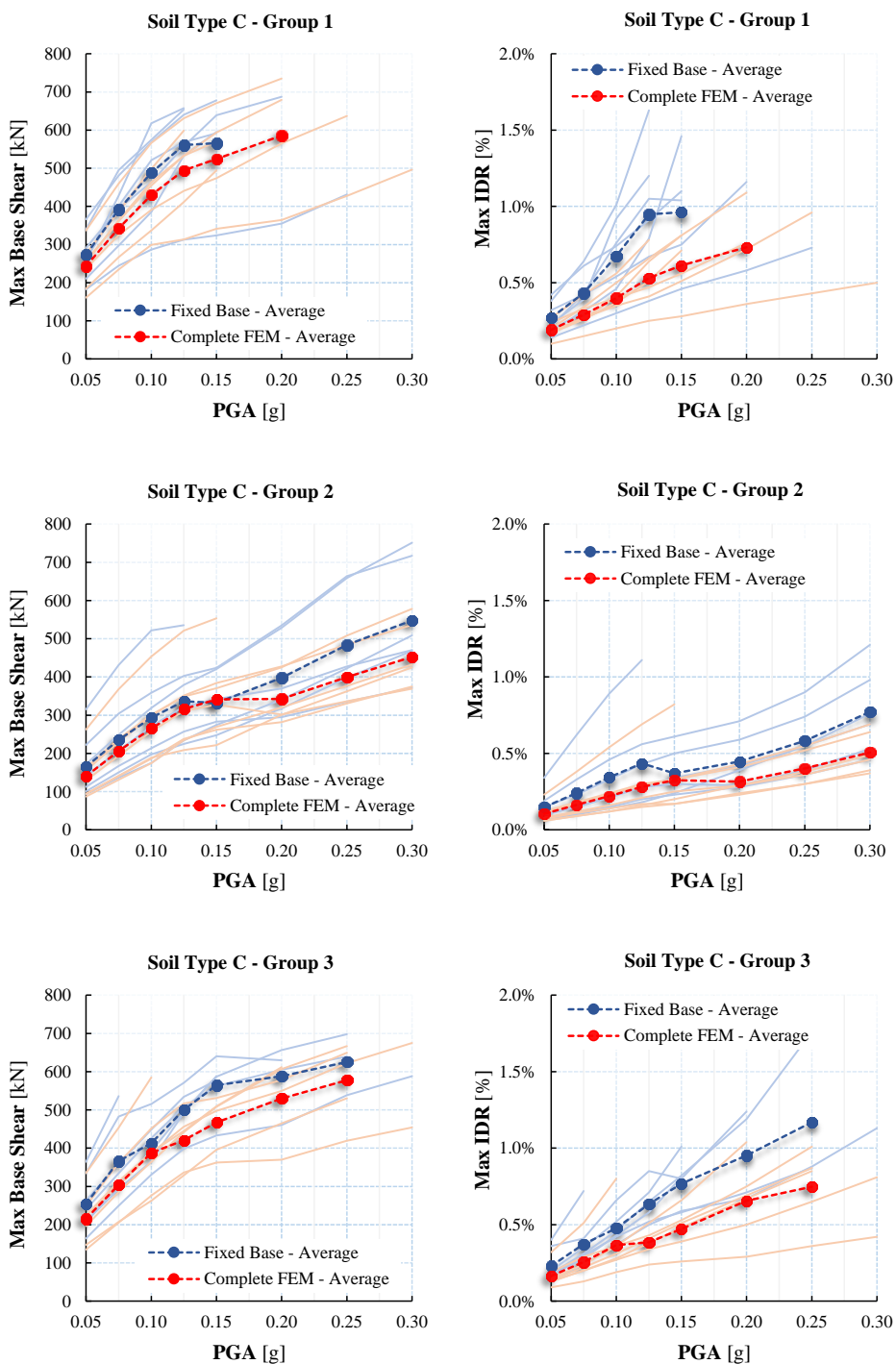


Figure C. 9 - 8 Floors Pre-Code – Soil Type C – Fixed Base VS Complete FEM

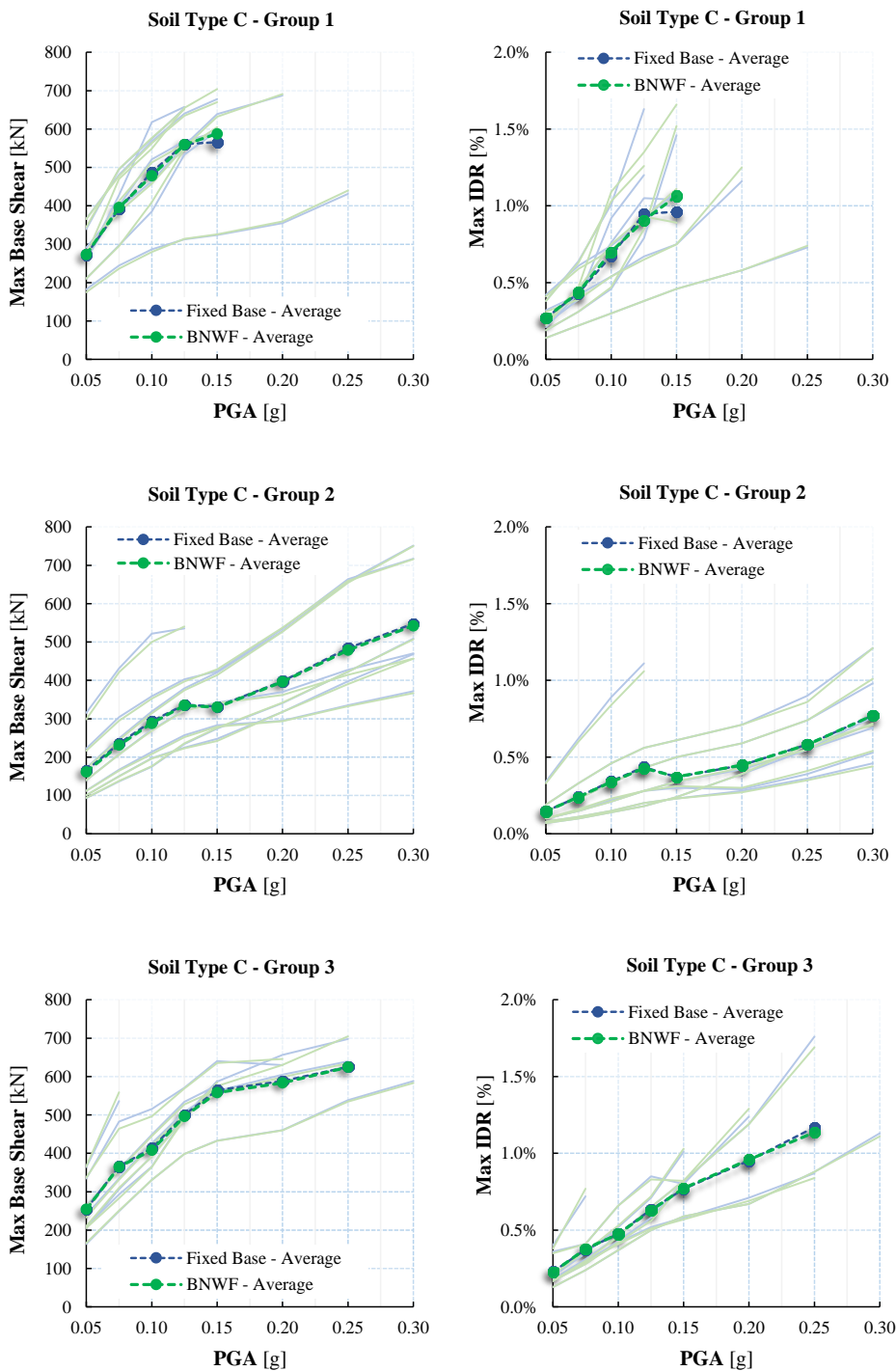


Figure C. 10 - 8 Floors Pre-Code – Soil Type C – Fixed Base VS BNWF

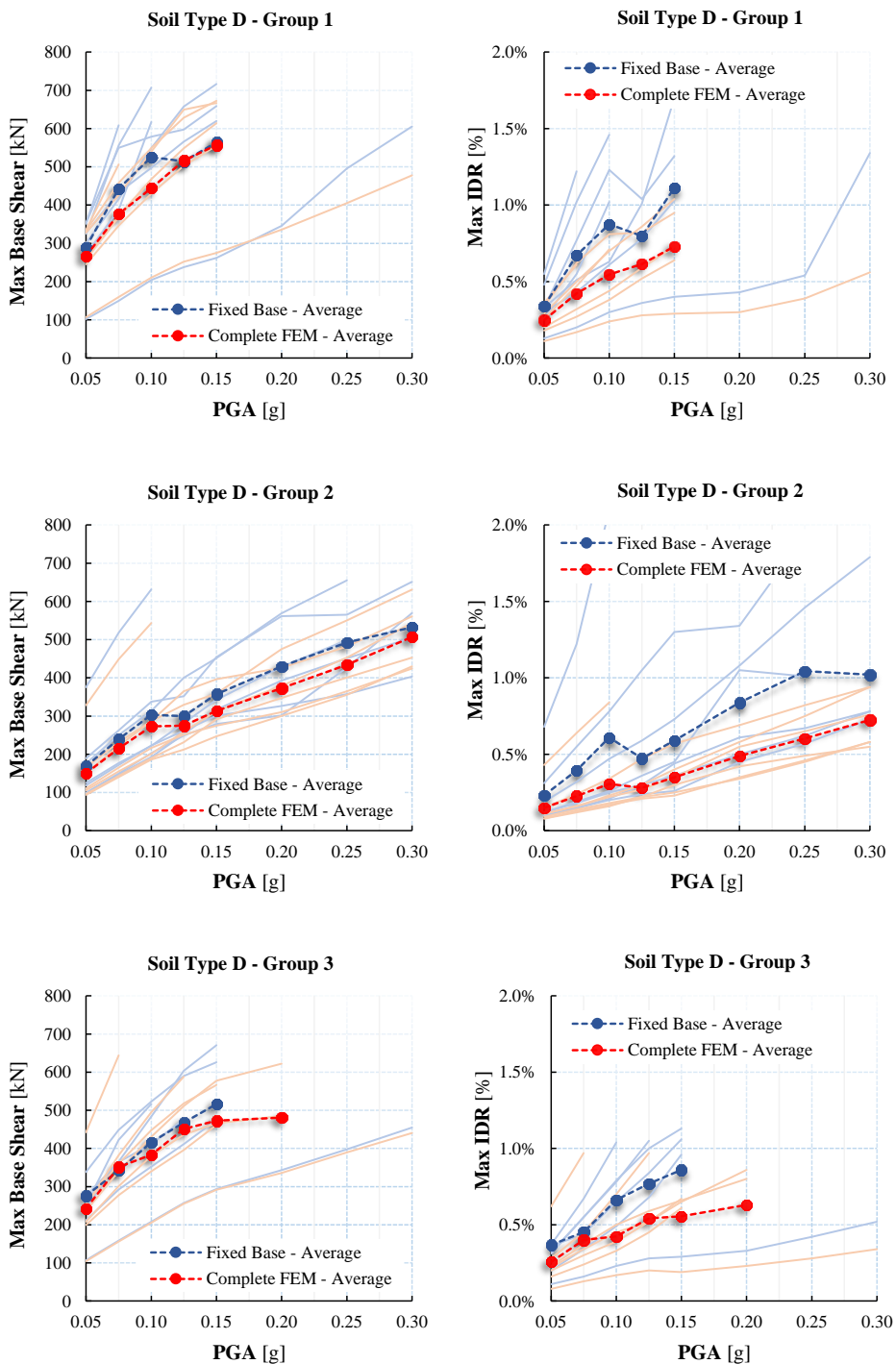


Figure C.11 - 8 Floors Pre-Code – Soil Type D – Fixed Base VS Complete FEM

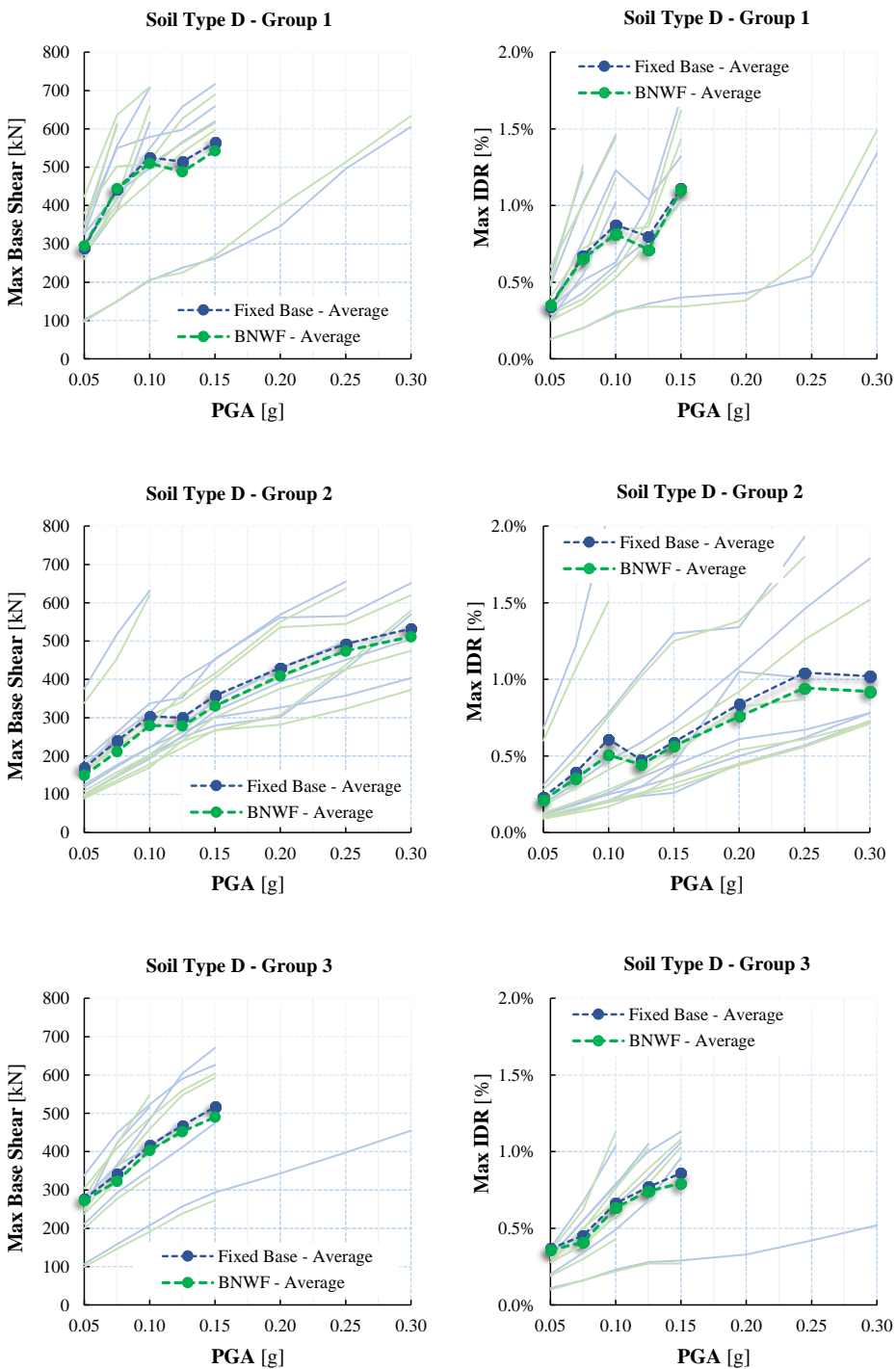


Figure C. 12 - 8 Floors Pre-Code Soil Type D – Fixed Base VS BNWF

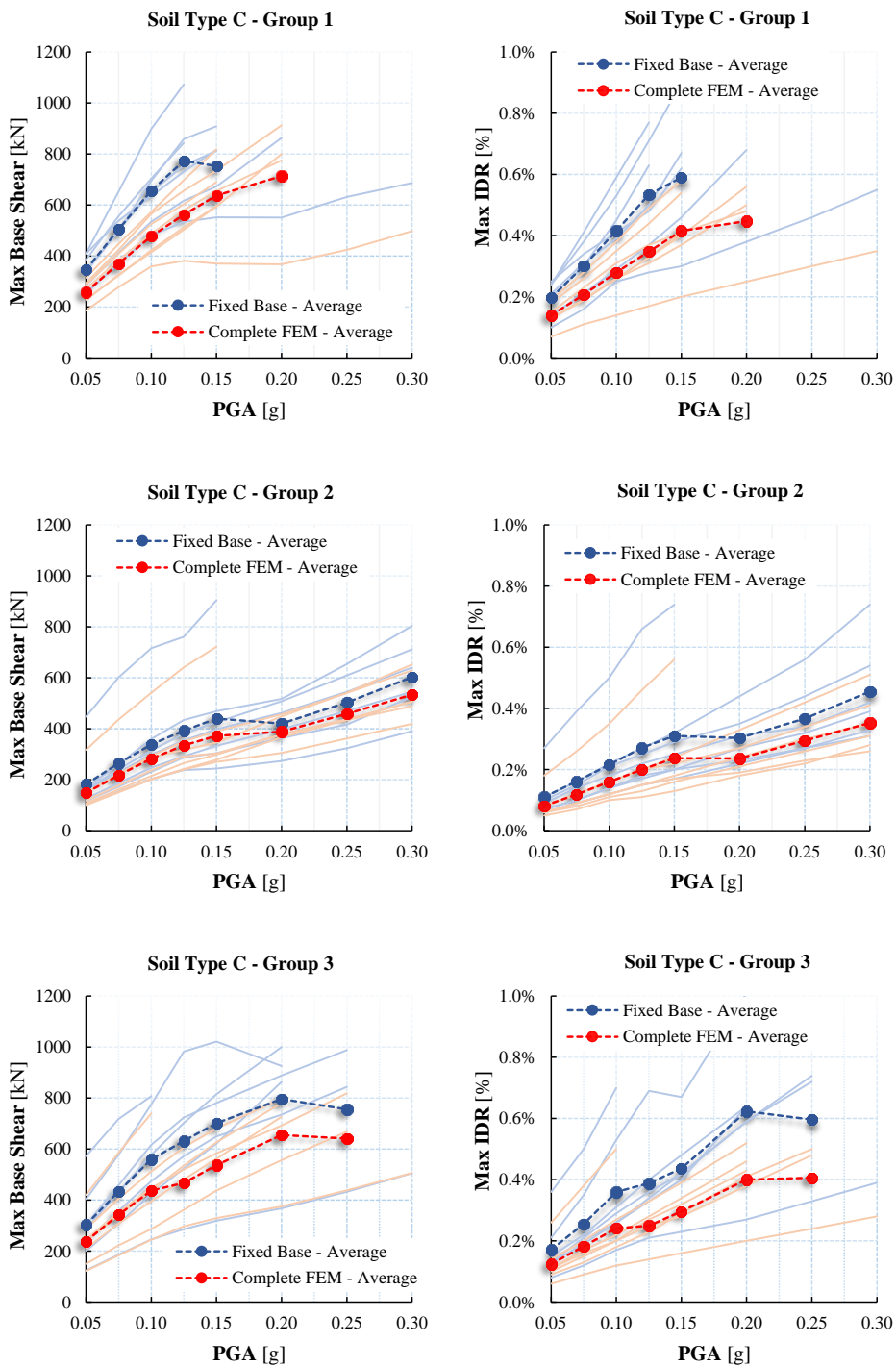


Figure C. 13 - 8 Floors Code compliant – Soil Type C – Fixed Base VS Complete FEM

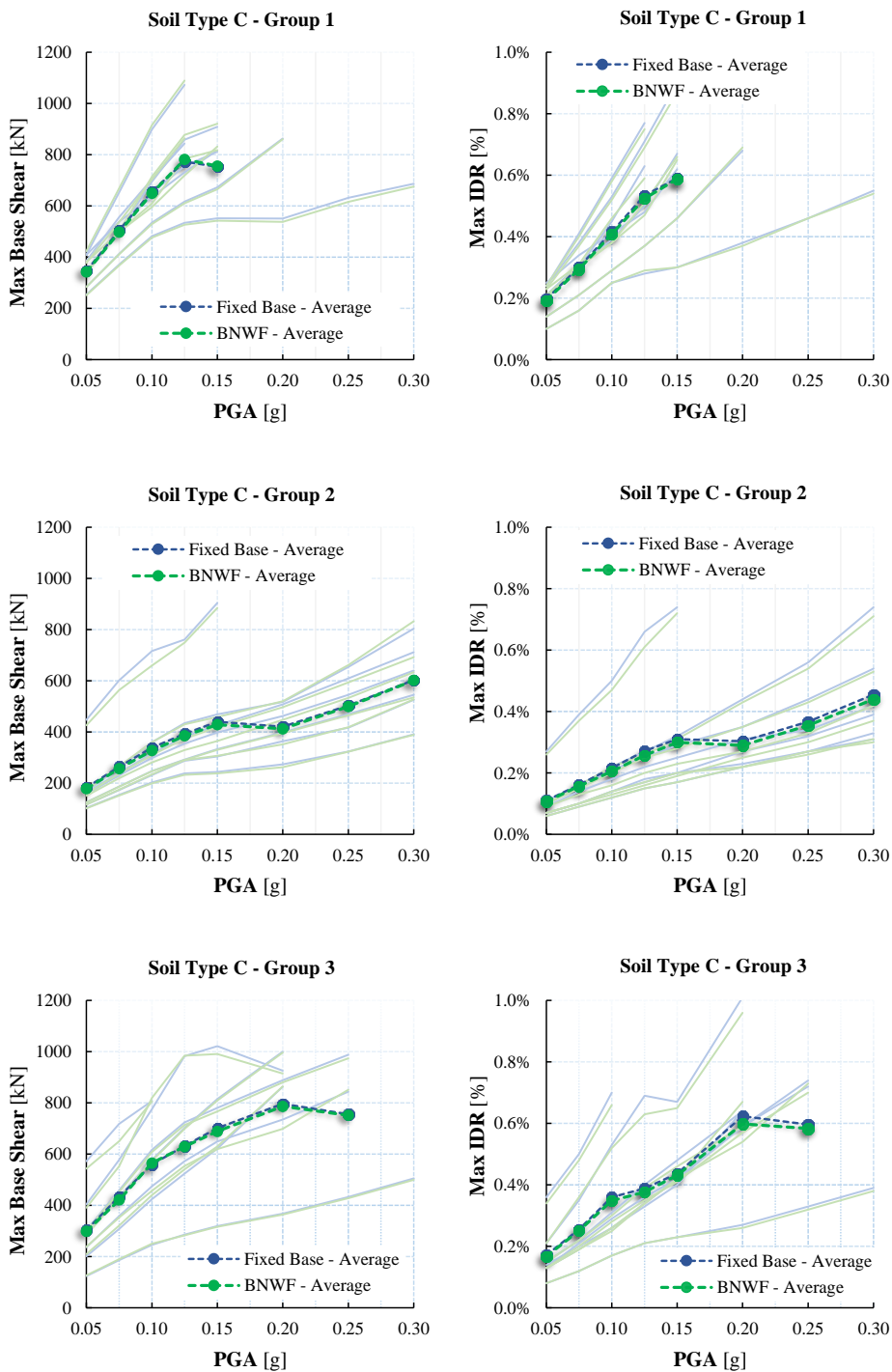


Figure C. 14 - 8 Floors Code compliant – Soil Type C – Fixed Base VS BNWF

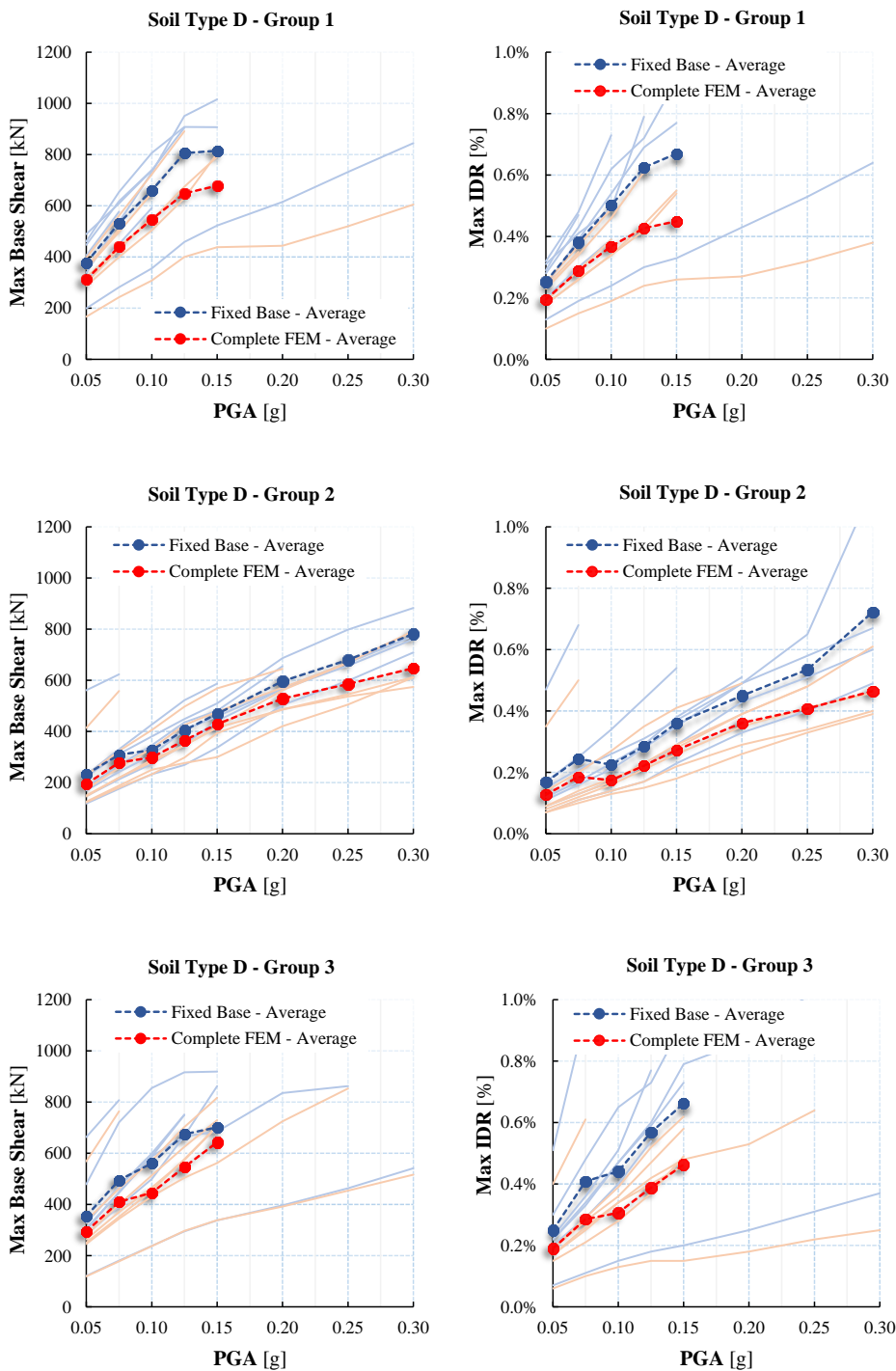


Figure C. 15 - 8 Floors Code compliant – Soil Type D – Fixed Base VS Complete FEM

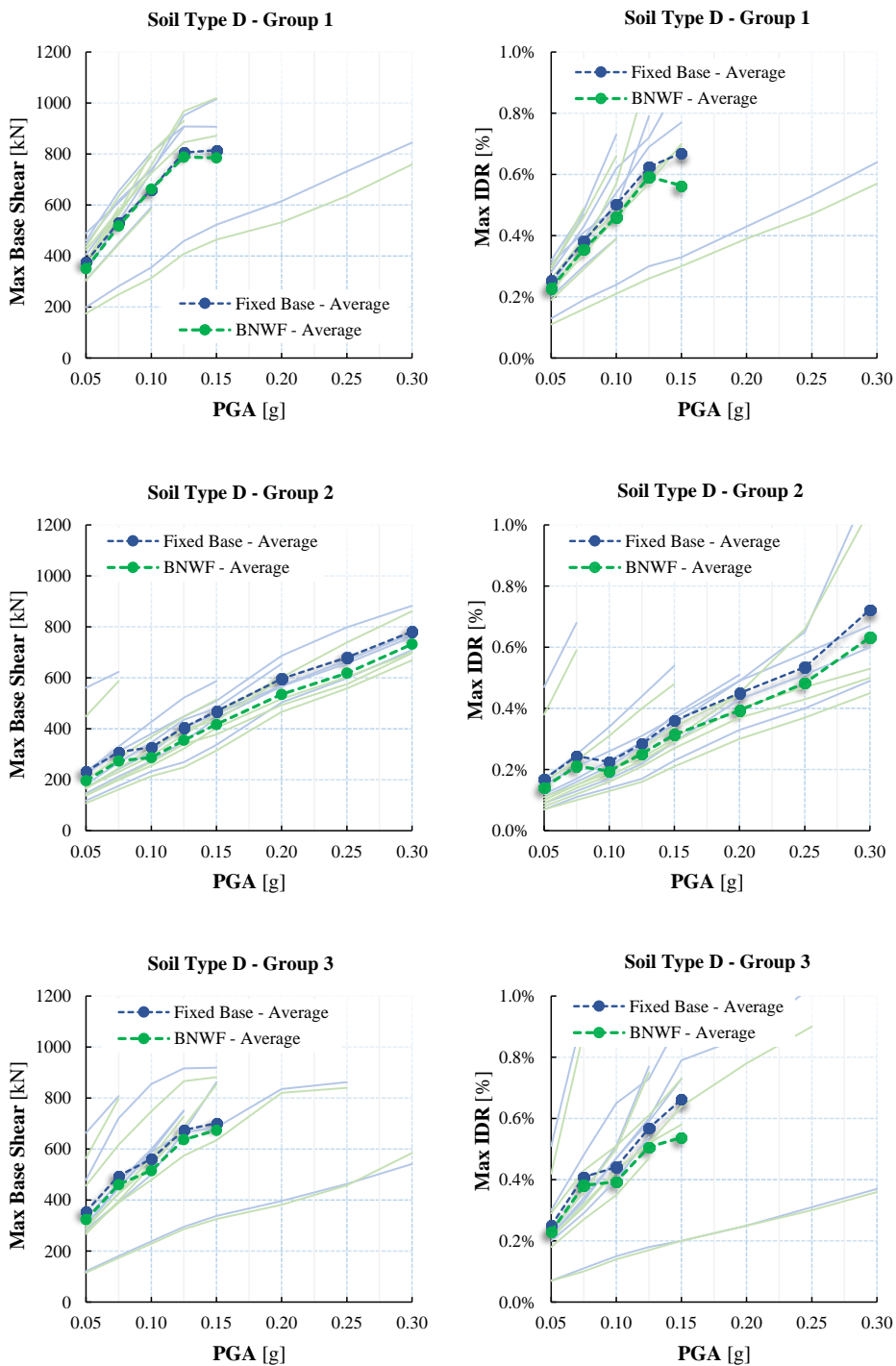


Figure C. 16 - 8 Floors Code compliant – Soil Type D – Fixed Base VS BNWF